Bourne Leisure Ltd

Hafan y Môr Holiday Park '2030 Vision' Masterplan

Modelling study to inform the coastal defence design and assessment

November 2018




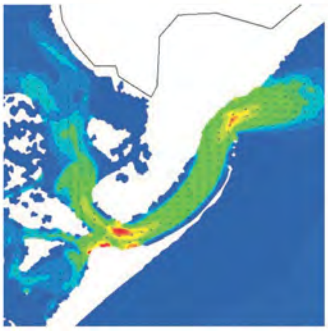


Innovative Thinking - Sustainable Solutions

Page intentionally left blank

Hafan y Môr Holiday Park '2030 Vision' Masterplan

Modelling study to inform the coastal defence design and assessment

November 2018

Document Information

Document History and Authorisation		
Title	Hafan y Môr Holiday Park '2030 Vision' Masterplan	
	Modelling study to inform the coastal defence design and assessment	
Commissioned by	Bourne Leisure Ltd	
Issue date	November 2018	
Document ref	R.3056	
Project no	R/4604/2	
Date	**Version**	**Revision Details**
30/10/2018	1	Issued for client review
19/11/2018	2	Issued for client review
		Accepted as Issued for Client Use

Prepared (PM)	Approved (QM)	Authorised (PD)
R E White	C R Scott	D O'Brien

Suggested Citation

ABPmer, (2018). Hafan y Môr Holiday Park '2030 Vision' Masterplan, Modelling study to inform the coastal defence design and assessment, ABPmer Report No. R.3056. A report produced by ABPmer for Bourne Leisure Ltd, November 2018.

ABPmer
Quayside Suite, Medina Chambers, Town Quay, Southampton, Hampshire SO14 2AQ
T: +44 (0) 2380 711844 W: http://www.abpmer.co.uk/

Non-Technical Summary

Haven Leisure Ltd. is working towards their '2030 vision masterplan' for their Hafan y Môr Holiday Park near Pwllheli (on the Llŷn Peninsula in North Wales, Gwynedd). An integral part of this proposal involves upgrading the coastal defences for the eastern frontage. The marine elements of the proposed work comprise of the following elements:

- A net landward realignment of the shoreline by excavation of the existing land form;
- Five rock fishtail shaped rock-armour groynes (approximately 50 m long, 10 m wide and with an alongshore separation of around 75 m) to provide sheltering to help maintain new beaches; and
- Addition of beach recharge material at interspersed sections between the groynes. The recharge material will be of similar grade to the existing beach material, however the beach will be re-profiled to allow for a retreat of Mean High Water Spring elevations.

These proposed scheme elements are designed to improve protection from ongoing coastal erosion while enhancing the amenity value of the upper-shore sections of the beach frontage.

All elements of the scheme are high in the tidal frame, mainly constrained to areas which presently lie above the elevation of Mean High Water Springs. The tails of the structures sit between Mean High Water Neaps and Mean High Water Springs, which under normal conditions limits tidal inundation to approximately 30 % and 2% of the time respectively. Wave run-up and meteorological conditions will influence water levels, but even taking this into account the majority of the scheme will not be subject to tides and waves for more than 98% of the time. The position of the structures high in the tidal frame inherently reduces the impact the scheme will have on adjacent areas and littoral processes.

Bourne Leisure Ltd have commissioned ABPmer to undertake numerical modelling studies to assess the baseline conditions at the proposed development site with respect to waves, flows and sediment transport and to report on how these conditions are affected by the proposed scheme. Given the small scale of the development and its location high in the tidal frame, the effects of the scheme are anticipated to be minimal. Therefore, it is considered appropriate to demonstrate the effects on more extreme conditions (e.g. greater than 1:1 year events) and to conclude by inference the negligible effect on more frequently occurring conditions.

A suite of modelling tools have been developed using the Danish Hydraulic Institute's (DHI) MIKE21 Flexible Mesh (FM) software. These tools include:

- A regional hydrodynamic model of Cardigan Bay to provide boundary conditions for a local area model;
- A regional spectral wave model run in hindcast mode to simulate wave conditions over the 37 year period between 1979 and 2015). An extremes analysis was applied to model results to identify conditions for a range of return period events. Four conditions were identified for consideration during the assessment of the scheme impact. These include a 1 in 35 year wave from the southwest, a 1 in 35 year wave form the southeast, a 1 in 1 year wave from the southwest and a 1 in 1 year wave from the southeast. Wave parameters were extracted from the regional wave model at times when the defined wave conditions occurred and were used to drive the boundaries in a local area model;

- A dynamically coupled hydrodynamic, spectral wave and sediment transport model of the local area has been developed to simulate extreme conditions. In addition to providing an assessment of the scheme on the local wave, flow and sediment transport conditions, outputs from this model were used as boundary conditions for application in a profile evolution tool; and
- A profile evolution tool to assess the beach drawdown on the proposed beaches.

The key findings from the study are:

- Coastal modelling tools have been constructed to a high standard to support the assessment and have been shown to calibrate and verify with available data;
- The scheme is high in the tidal frame and is only tidally inundated on some tides and for limited periods (over high water);
- Tidally driven flows in the study area are weak and are not expected to contribute directly to sediment transport;
- Waves from the southwest are typically longer in period than those from the southeast and therefore contribute most to sediment transport along the foreshore at Hafan y Môr;
- Wave driven flows are predominantly to the east, especially along the western section of the frontage;
- Even for extreme conditions, the effects of the scheme on flows (combined wave and tide) are highly localised, with changes of more than 0.1 m/s constrained to within approximately 50 m of the groynes in an offshore direction. Further, any changes will only occur during the short periods when the scheme is submerged;
- The groynes provide sheltering to the new beach areas and reduce alongshore transport on the upper foreshore. Even during storm periods, changes to alongshore sediment transport will be limited and at distances of more than 50 m offshore of the groynes are negligible;
- Estimates of beach drawdown obtained from the profile evolution tool are relatively small for the storms simulated when compared to the amounts of beach recharge material; and
- Estimates of wave run up indicate that not all of the beach gets inundated even during extreme wave and water level events.

The main objectives of this modelling study were to enhance the understanding of the present day coastal processes at Hafan y Môr and to provide an assessment of the likely impacts of the proposed coastal defence scheme on these processes. The design itself has wider objectives:

- Ensure that there is negligible alongshore impact of the scheme;
- Identify the expected sand losses during the service life (20 years) of the scheme; and
- Ensure that the geometry and spacing of the groynes is optimised.

The modelling study has supported these objectives as follows:

- *Ensure that there is negligible alongshore impact of the scheme*. The modelling assessments strongly indicate that the scheme has limited impact on adjacent areas. Its design, high in the tide frame, inherently limits the impact it would have on existing littoral processes.
- *Identify the expected sand losses during the service life (20 years) of the scheme*. The modelling studies have assessed beach draw-down for a limited number of storm conditions. Whilst this does not quantify sand losses during its service life, the simulations show that for individual storm events, draw-down is relatively small compared to the amount of beach recharge material.
- *Ensure that the geometry and spacing of the groynes is optimised*. Extensive model simulations have been completed to support the proposed scheme's development, including one alternative layout.

Contents

Appendices

Tables

Figures

1 Introduction

Haven Leisure Ltd. is working towards their '2030 vision masterplan' for their Hafan y Môr Holiday Park near Pwllheli (on the Llŷn Peninsula in North Wales, Gwynedd). An integral part of this proposal involves upgrading the coastal defences for the eastern frontage. This proposed development is designed to provide ongoing coastal erosion protection and to enhance the amenity value of the upper-shore sections of the beach front.

Hafan y Môr is in Tremadoc Bay on the Llŷn Peninsula (see Figure 1). The fronting intertidal area is internationally designated as a Special Area of Conservation (SAC). To minimise any direct impacts of the coastal defence work, the design incorporates a planned recession (realignment) of the shoreline. To provide a greater understanding of the baseline processes and to evaluate the proposed design layout prior to consultation with NRW, ABPmer has been commissioned to undertake numerical wave, flow and sediment transport modelling of the area. The results from this modelling are also required to support the Environmental Statement (ES) and consenting process and include an assessment of the potential impact on the designated area.

This modelling report provides an assessment of the baseline conditions at the development site, with respect to waves, flows and sediment transport and how these conditions are likely to be affected by the proposed scheme. Further, a modelling assessment of the beach profile response to the proposed scheme has been undertaken.

Where practical, the modelling results are presented in a manner which supports the coastal processes and design assessment work (which is being undertaken by a third party).

The report is structured as follows:

Section 2: Scheme overview. Details the key design features of the proposed coastal defence scheme;

Section 3: Modelling Approach. Describes the methodology used in the study and provides details on the modelling tools developed;

Section 4: Baseline understanding. Provides an overview of the present day conditions at the development site with respect to tide, wave and sediment transport; and

Section 5: Scheme Assessment. Results from the modelling study are presented in this section which includes a comparison baseline and scheme conditions for four wave scenarios.

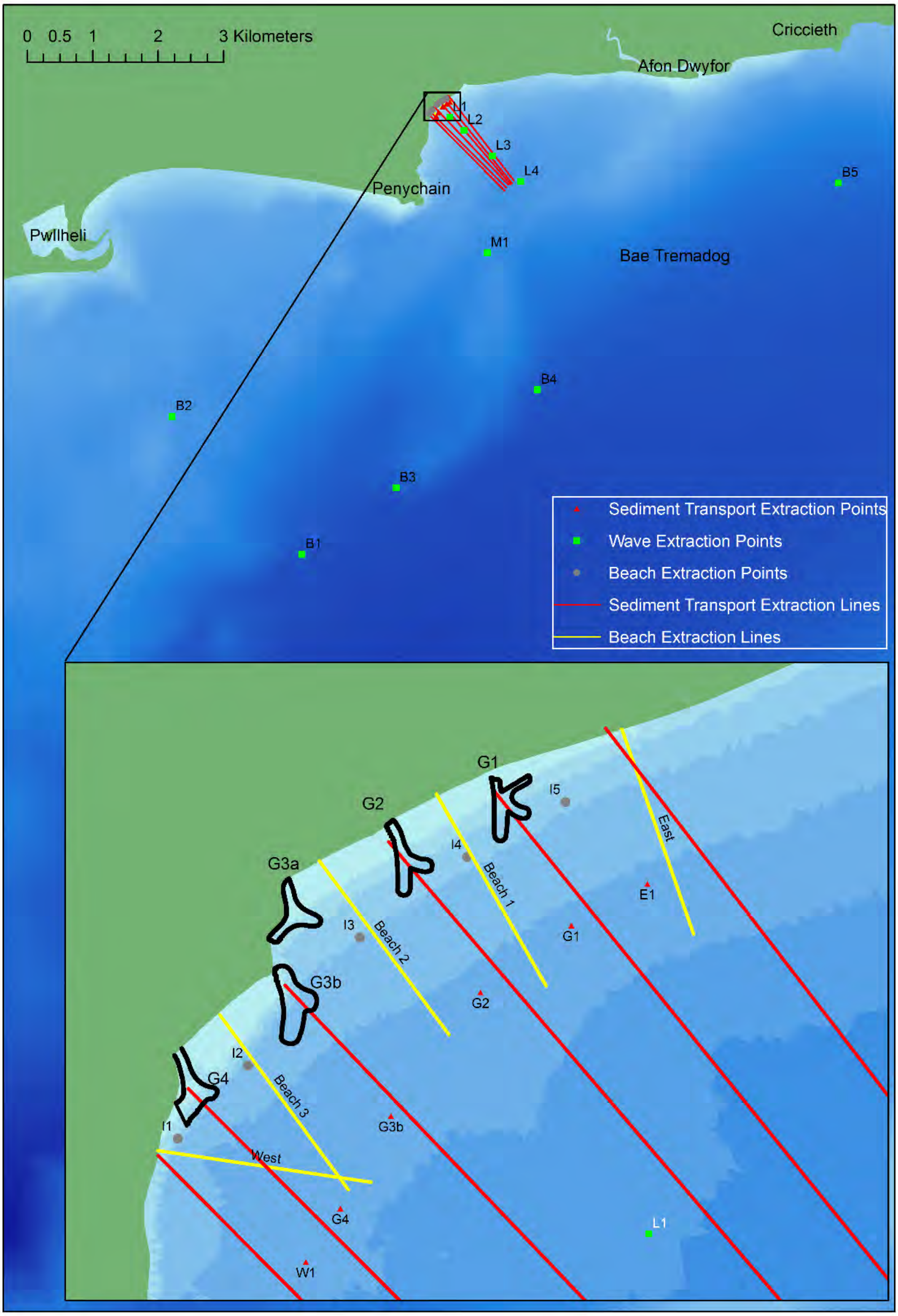

Figure 1. Location map with extraction locations overlaid

2 Scheme Overview

The proposed sea defence scheme at Hafan y Môr involves a net landward realignment of the shoreline by excavation of the existing landform; this will create a shallow beach profile (approximately 1 in 10) and allow for a retreat of the Mean High-Water Spring position in some areas. Five 'fish-tail' shaped rock-armour groynes will be placed on the excavated foreshore, along with interspersed sections of beach recharge. The beach recharge material will be of a similar grade to the current beach material (i.e. sand and shingle). This proposed approach is designed to minimise the extent of intertidal habitat losses and any coastal process effects as well as providing room for sea level rise in the future.

A cross section showing the proposed changes across the beaches (at the mid-way point between the groynes) is shown in Figure 2 while map plots showing the plan view of the baseline and scheme bathymetry are shown in Figure 3.

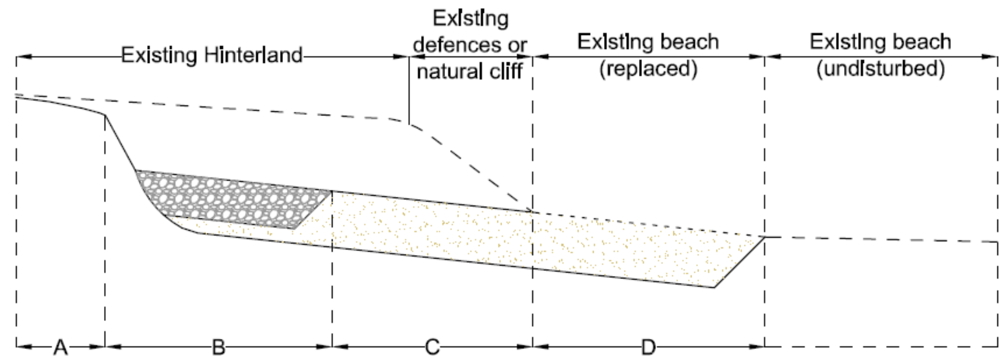

Zones

A: Recessed shoreline, new location with local landscaping to tie in with existing ground levels

B: New shingle beach, variable depth to facilitate public access to the beach overlying new sand beach, 0.5m depth

C: New sand beach, 1.5m depth within existing hinterland

D: New sand beach, 1.5m depth replacing existing beach at similar slope levels

Provided by the Client

Figure 2. Cross section showing the changes to the existing beach for the proposed scheme

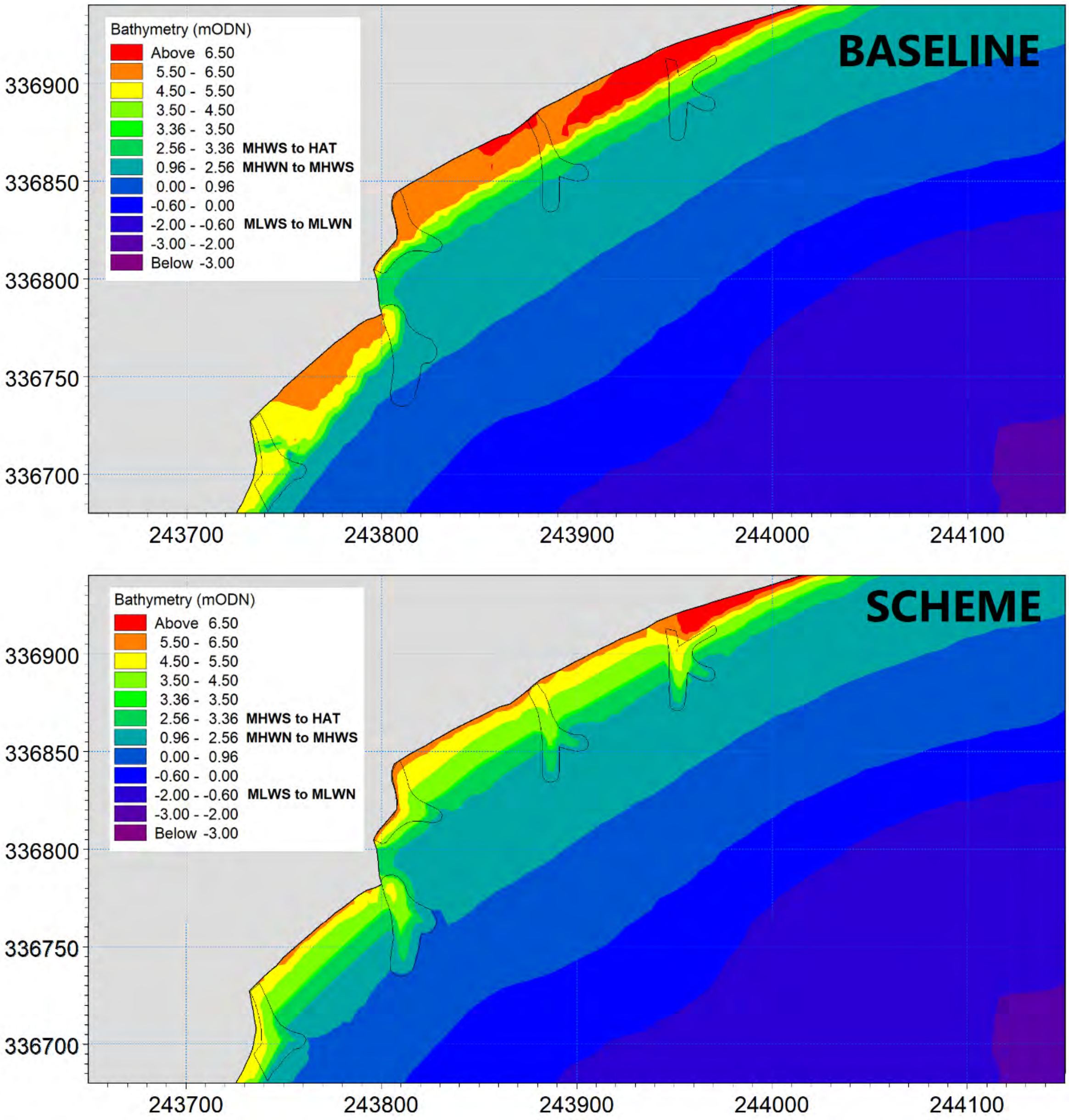

Figure 3. The baseline (upper) and scheme (lower) bathymetry

3 Modelling Approach

To assess the baseline conditions in respect to wave, flows and sediment, and the impact of the proposed scheme on these conditions, a suite of modelling tools have been developed. These tools have been configured using the using the MIKEFM software developed by the Danish Hydraulic Institute (DHI).

The MIKEFM modelling software undergoes continuous development with updates regularly released by the Danish Hydraulic Institute (DHI). This project used the most up to date version of the software available at the time of project commencement (MIKE 2018, Service Pack 2).

The modelling tools developed include:

- A regional flow model, developed to provide boundary conditions for the local area model;
- A regional wave model, developed to provide a definition of the wave climate at the site and to provide boundary conditions for the local area model;
- A local area model in which the MIKEFM hydrodynamic (HD), Spectral Wave (SW) and Sand Transport (ST) modules are dynamically linked so that the effect of waves on flows and the effects of flows on waves are accounted for; and
- MIKEFM profile evolution tool for drawdown assessment on beach cross sections (for sand).

Further details on the setup of these model tools is provided in the following subsections.

3.1 Regional flow model

A regional flow model was developed to provide tidal boundary conditions to drive the coupled local area model. The regional flow model was verified against TotalTide predictions to ensure that the simulated water levels (both in absolute terms and with respect to tidal variations) and tidal flows were suitable to apply as boundary conditions in the local flow model.

3.1.1 Model setup

The mesh for the regional flow model extends over the entirety of Cardigan Bay to Highest Astronomical Tide (HAT) and across the Irish Sea between Ramsey Island (UK coast) and Rosslare (Irish coast) at its southern extent and between Holyhead (UK coast) and Rush (Irish coast) at its northern extent.

The mesh is made up of triangular flexible elements, enabling spatial variations in resolution. The mesh resolution is highest (approximately 200 m) in the area around Hafan y Môr. The mesh resolution reduces away from the site, with a resolution of 1500 m or less across Tremadoc Bay and 4 km or less across Cardigan Bay. To facilitate fast computational run times the mesh resolution reduces to around 11 km in the deeper area of the Irish Sea.

The regional flow model mesh is shown in Figure 4. The model bathymetry is based on data from a range of sources including:

- Project specific bathymetric survey data
- LiDAR data
- MMO survey data of Tremadoc Bay
- EMODnet data

The high resolution of the project specific bathymetry allows key features in the shallow waters around Hafan y Môr to be resolved and hence significantly improves the accuracy of the model in this region.

The model bathymetry is shown in Figure 4, and the extent of these surveys is shown in Figure 5,

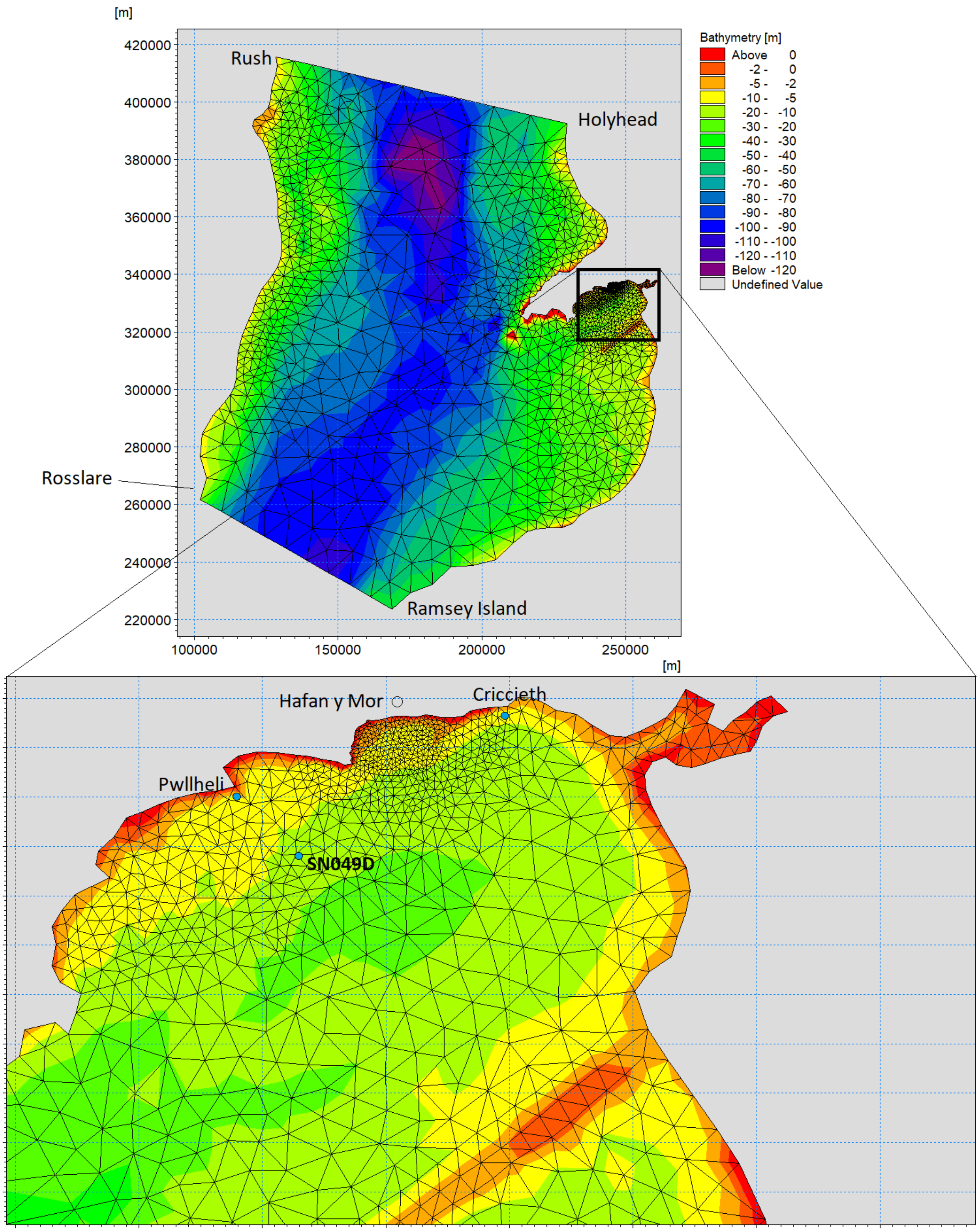

Figure 4. Regional flow model mesh and bathymetry

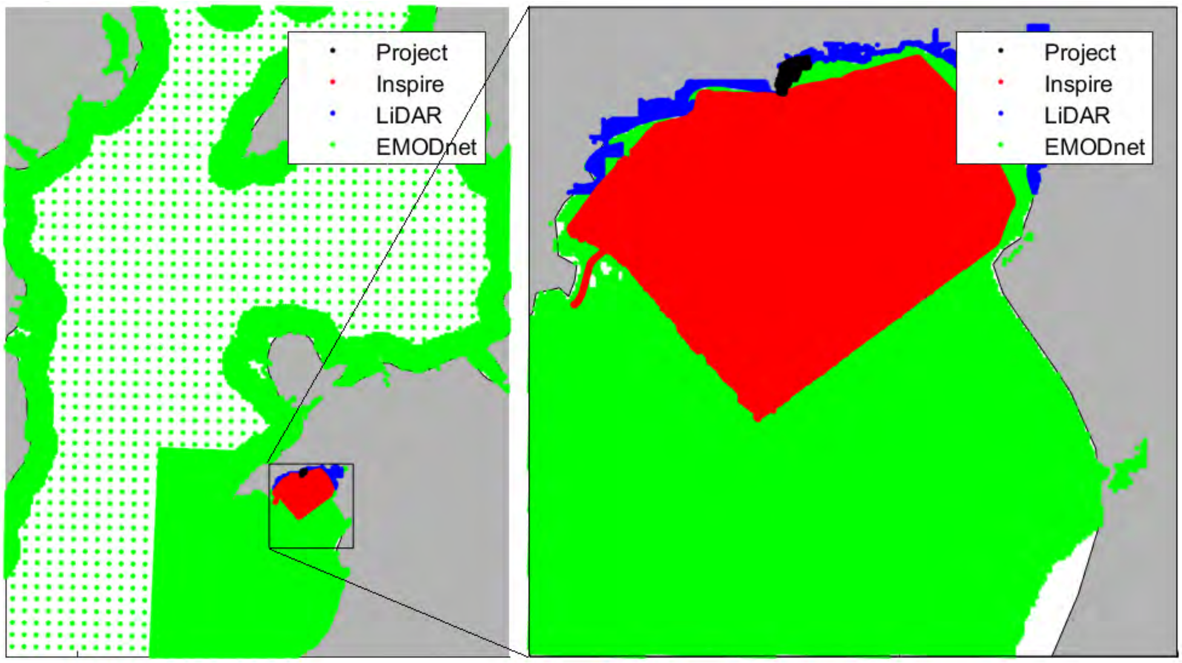

Figure 5. Bathymetric data sets

The regional hydrodynamic model is driven by timeseries of water levels extracted from ABPmer's Tide and Surge model (ABPmer, 2017). To ascertain the performance of the regional model, the model was ran for an eight day period in March 2007. The simulation spans a series of large range spring tides during the first four days of the model run, before tidal ranges reduce towards a neap tide at the end of the eight day period.

3.1.2 Model verification

The model was verified against admiralty predictions of water levels and flows at locations near Hafan y Môr. These included water levels at Criccieth and Pwllheli and a tidal diamond approximately 4 km offshore of Pwllheli in water depths of 13 m ODN (see Figure 4 for locations). Comparisons of modelled and measured water levels and flows are shown in Figure 6 to Figure 8 The model was found to replicate the key features of the tide, capturing the levels and timing of low and high water at both Criccieth and Pwllheli. The model also replicated the variation in tidal levels with the progression from spring range to neap range tides suitably captured. The model also replicated the tidal flow variations at the tidal diamond location, capturing the spring and neap flow variations and the dominant flow axis. Some differences in the flow direction occur around the periods of slack flow with the model showing a more gradual rotation of the flow axis as the tide turns than indicated by the tidal diamond. This difference is most likely a result of a discrepancy between what the Tidal Diamond provides (surface flows) and what the model simulates (depth average flows). Based on the good level of agreement between modelled levels and flows against the admiralty predictions, it is considered that the model provides a suitable tool to assess the effects of the proposed coastal defence scheme on coastal processes.

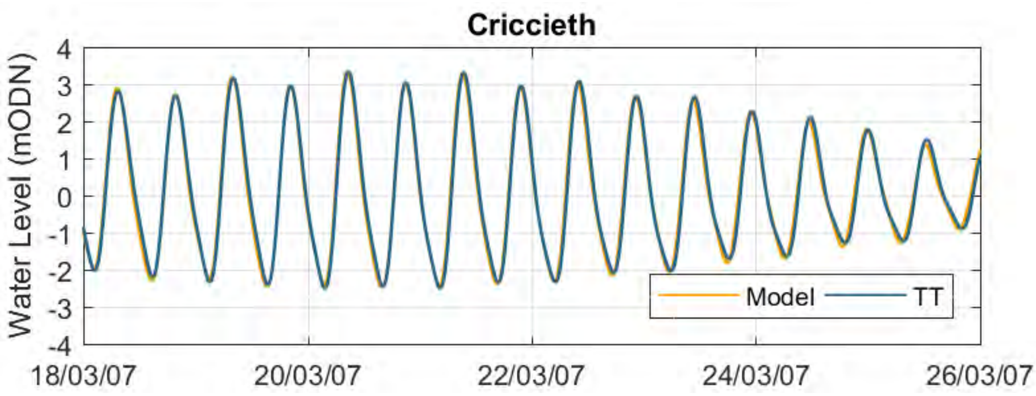

Figure 6. **Time series of modelled water levels at Criccieth against admiralty (TotalTide) predictions**

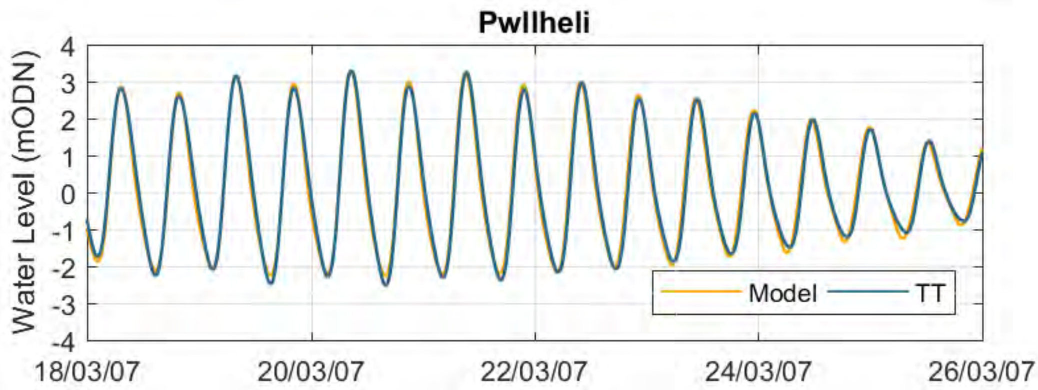

Figure 7. **Time series of modelled water levels at Pwllheli against admiralty (TotalTide) predictions**

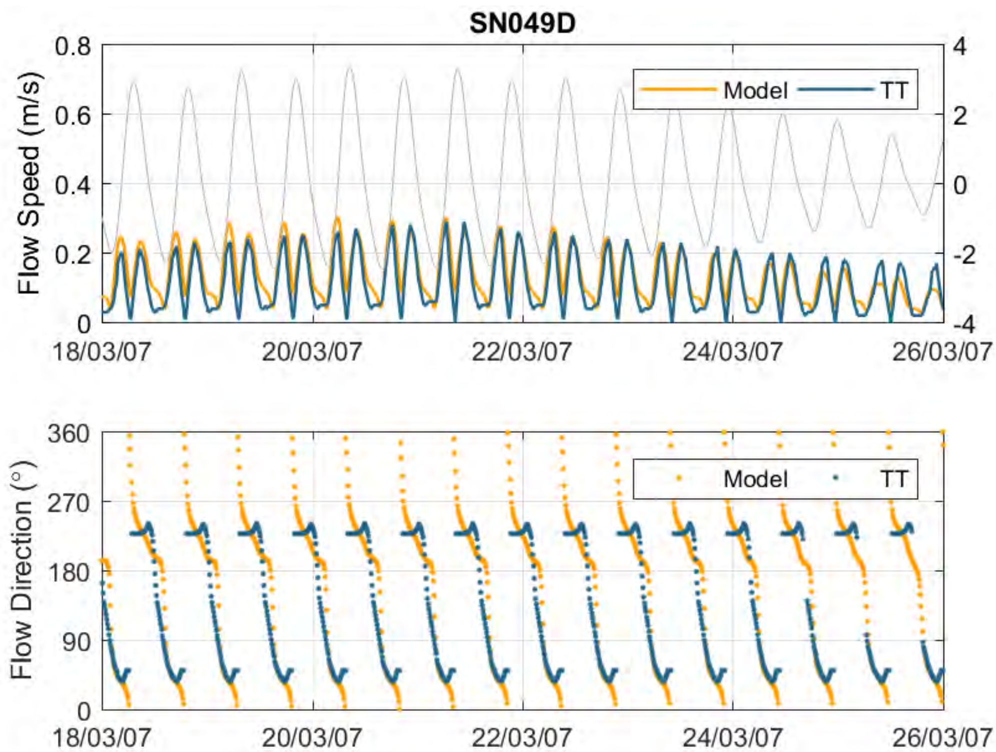

Figure 8. **Time series of modelled flows near Hafan y Môr (at tidal diamond A on admiralty chart 1971) against admiralty (TotalTide) predictions**

Flow vector plots at two hours either side of HW (equating to close to peak flood and peak ebb) are shown in Figure 9. In the deeper offshore areas, the flows are aligned with the bathymetry, while the inshore flows exhibit more complex patterns. At the headland of Penychain there is a flow divergence on the flood tide and a flow convergence on the ebb. The slow tidal flows are generally insufficient to transport any sediment, this is discussed in more detail in Section 4.3.

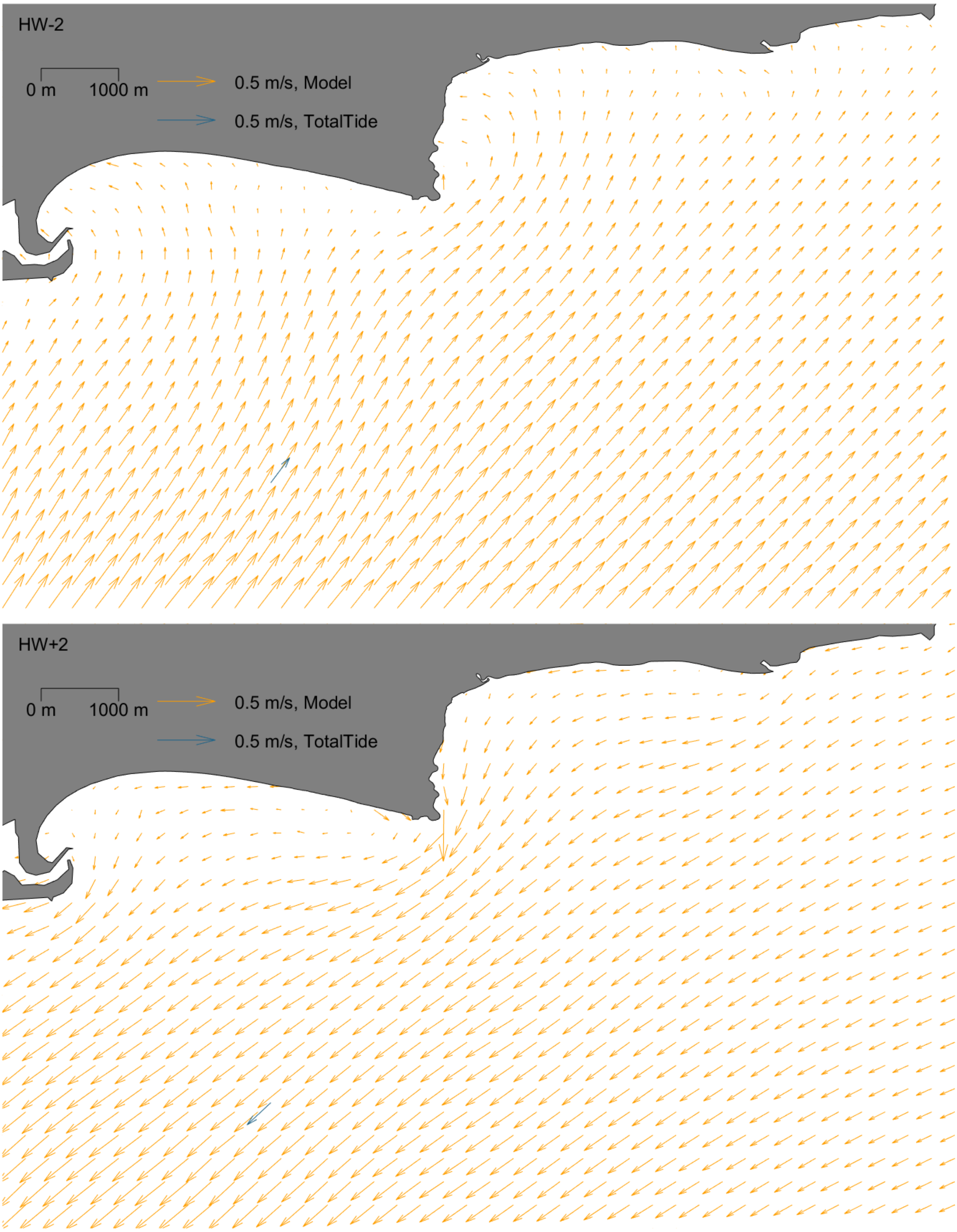

Figure 9. Tidal flows close to Hafan y Môr on the flood tide 2 hours before HW (upper panel) and on the ebb tide 2 hours after HW (lower panel)

3.1.3 Conditions used for local area model

The hydrodynamic model was run used to simulate water levels and tidal flows during a Highest Astronomical Tide (HAT). HAT occurs approximately once per year and as such is a relatively extreme event. HAT was considered in this study due to the high positioning of the proposed scheme in the tidal frame. Water level and flow boundary conditions were extracted from the HAT model simulation and used to drive the local area model (see Section 3.3).

3.2 Regional wave model

A regional hindcast model was developed to simulate the wave climate in Tremadoc Bay. The hindcast model extends across Cardigan Bay over an area of approximately 70 km by 40 km (see Figure 10). The grid resolution varies from 4 km at the offshore boundary and reduces to 200 m close to Hafan y Môr. The hindcast model was driven by a time-series of wave parameters from ABPmer's SEASTATES hindcast at the boundary across the entrance of Cardigan Bay (ABPmer, 2013). These parameters included significant wave height, peak wave period, mean wave direction and directional standard deviation (which provides an indication of wave spreading) for both wind-sea and swell parameters.

The hindcast was run for the 37-year period between 1979 and 2015 inclusive to simulate the wave climate in Cardigan Bay and the propagation of waves inshore as they approach Hafan y Môr. The model was run in fully spectral formulation with twenty-six 10 degree directional bins between 40 and 300 degrees.

The wave conditions were extracted from the 37 year hindcast at ten locations; five of which are used to examine the nearshore wave climate and the propagation of waves across the intertidal at Hafan y Môr, whilst the other five are used to provide offshore boundary conditions for the local area model (see Section 3.3). The extraction locations are shown in Figure 11 and tabulated in Table 1.

Table 1. Extraction location for wave analysis

Extraction Point Name	Easting (m OSGB)	Northing (m OSGB)
M1	244622	334539
L1	244051	336607
L2	244268	336411
L3	244701	336019
L4	245133	335627
B1	241792	329930
B2	239809	332037
B3	243230	330947
B4	245387	332446
B5	249985	335607

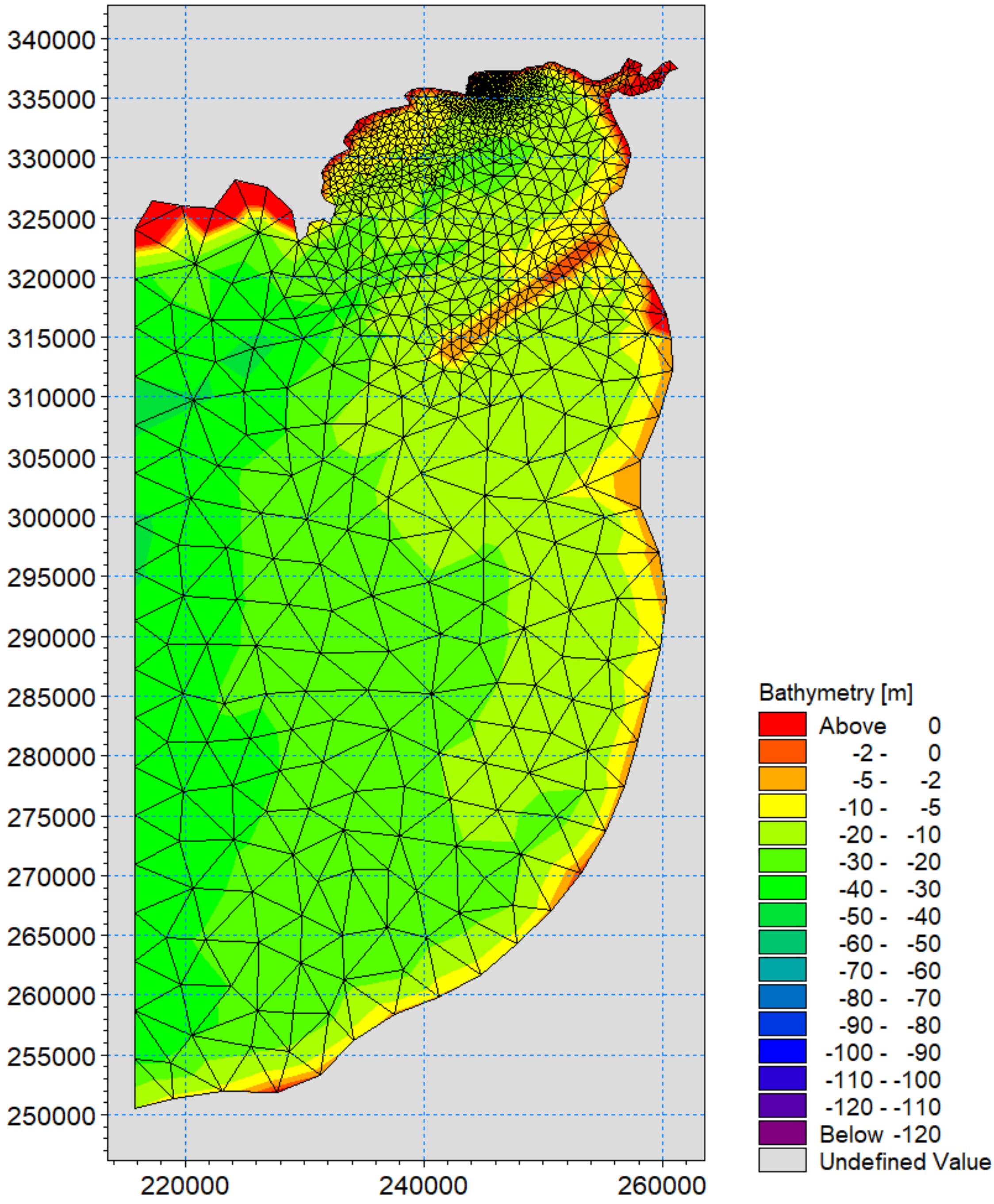

Figure 10. Hindcast SW model mesh and bathymetry

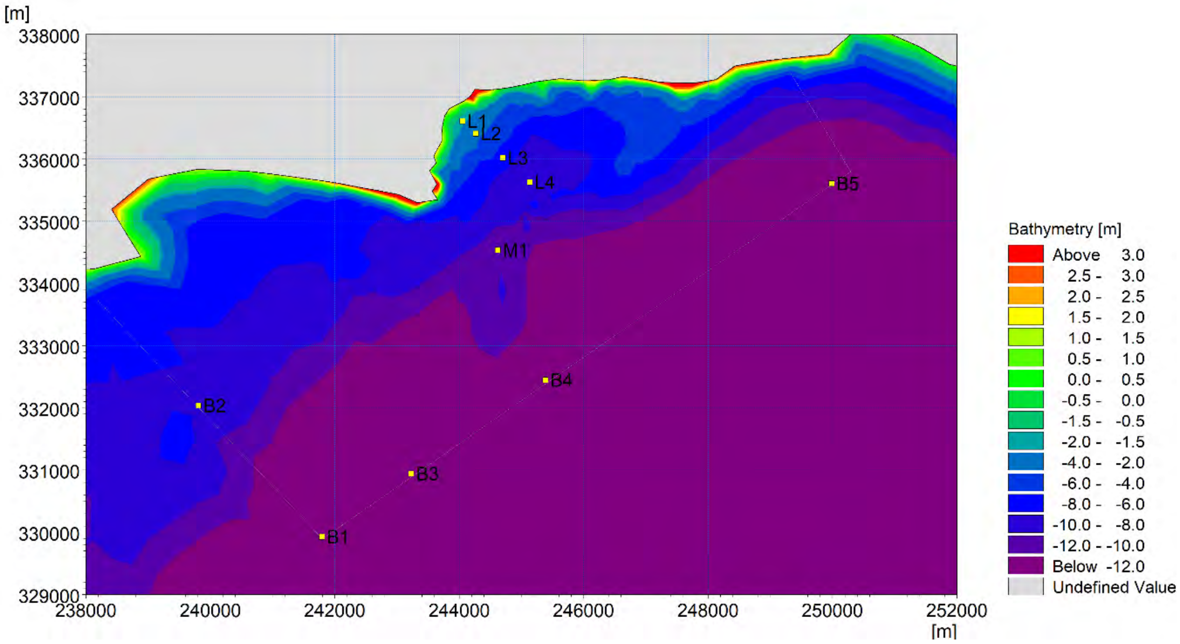

Figure 11. Extraction locations

Frequency wave roses at extraction points M1 and L1 to L4 are shown in Figure 12 to Figure 16. These plots demonstrate the manner in which waves refract as they propagate inshore. The numbers within the roses indicate the numbers of hours per year for each sector/bin.

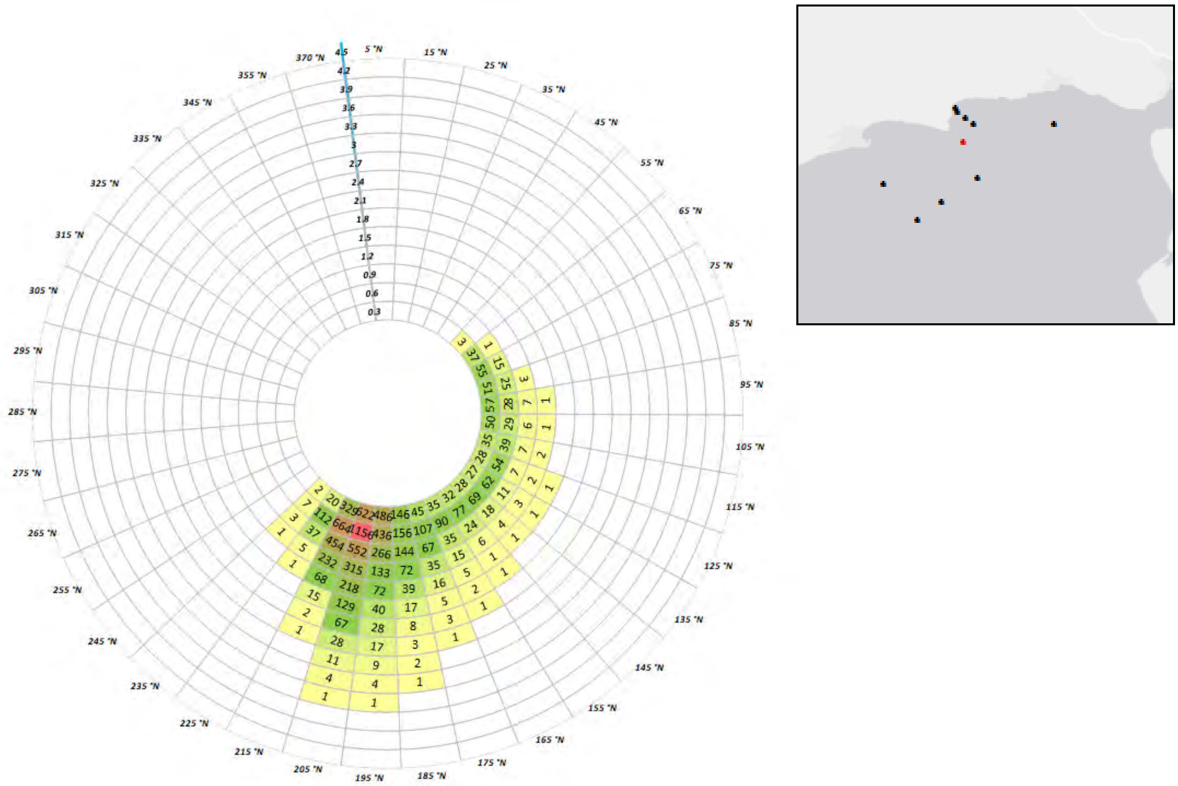

Figure 12. Annualised wave rose at M1, values indicate the number of hours per year

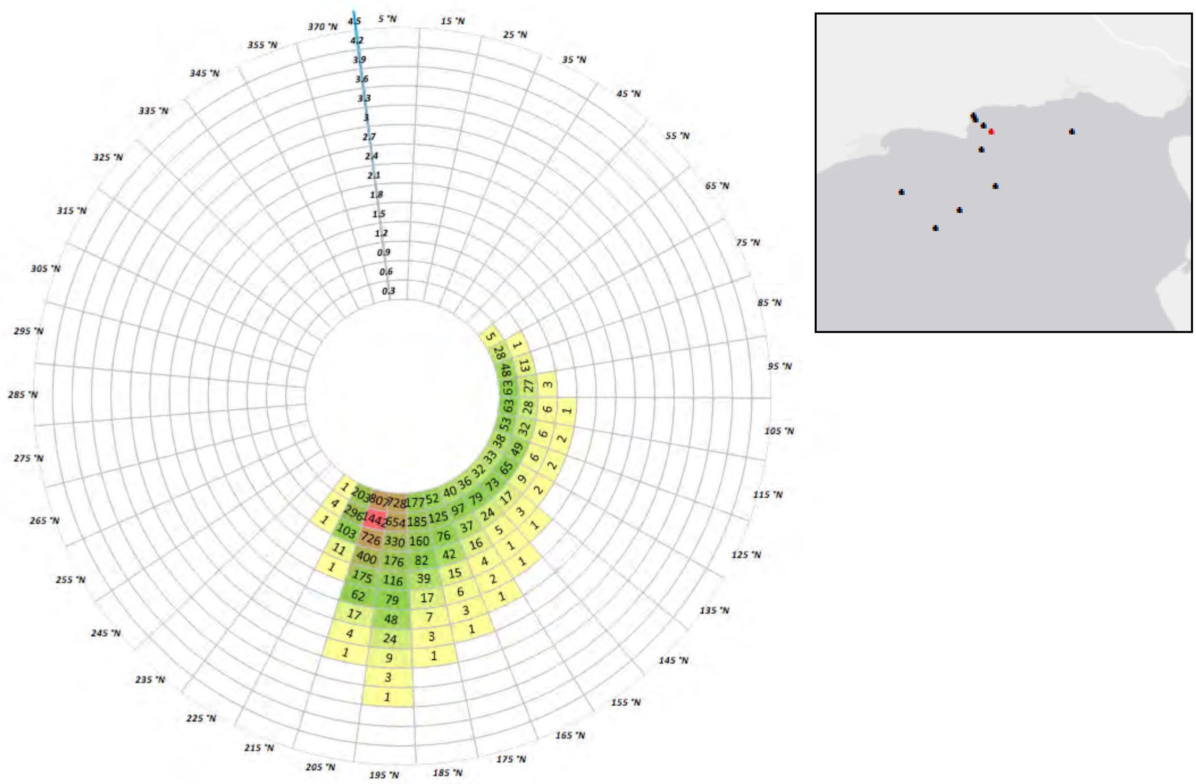

Figure 13. Annualised wave rose at L4, values indicate the number of hours per year

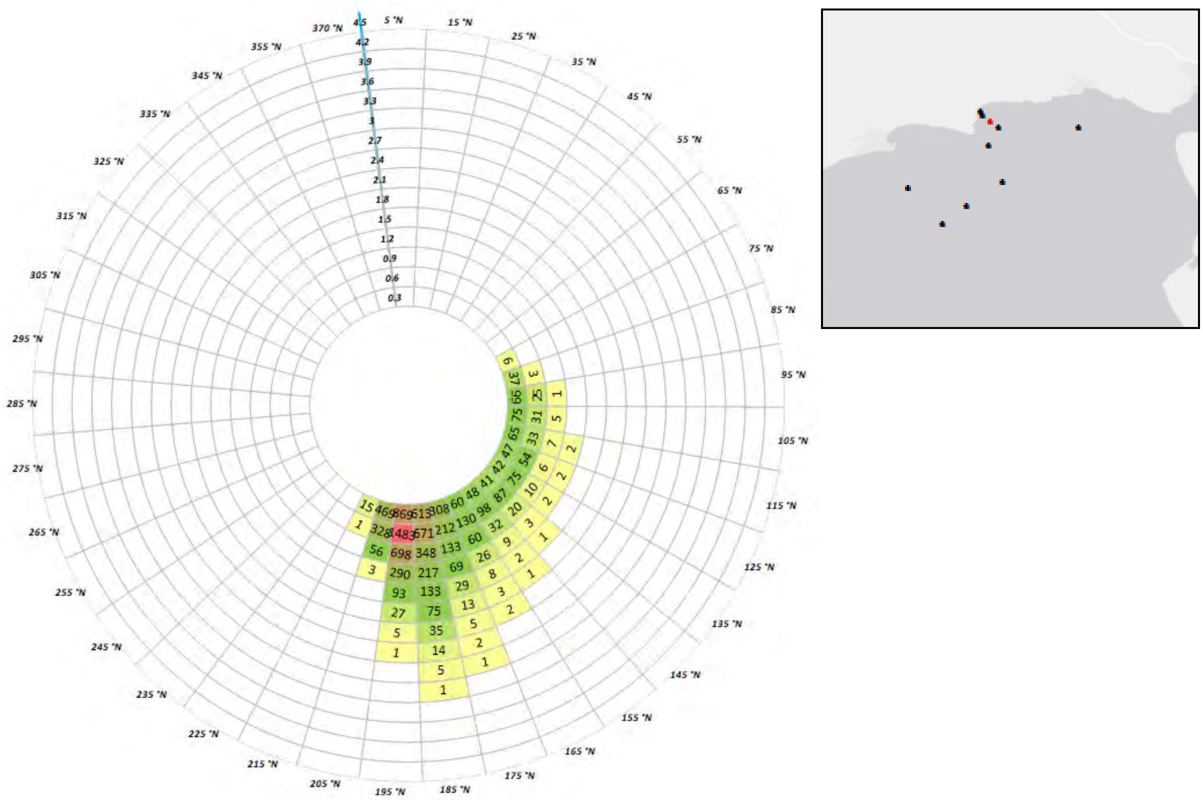

Figure 14. Annualised wave rose at L3, values indicate the number of hours per year

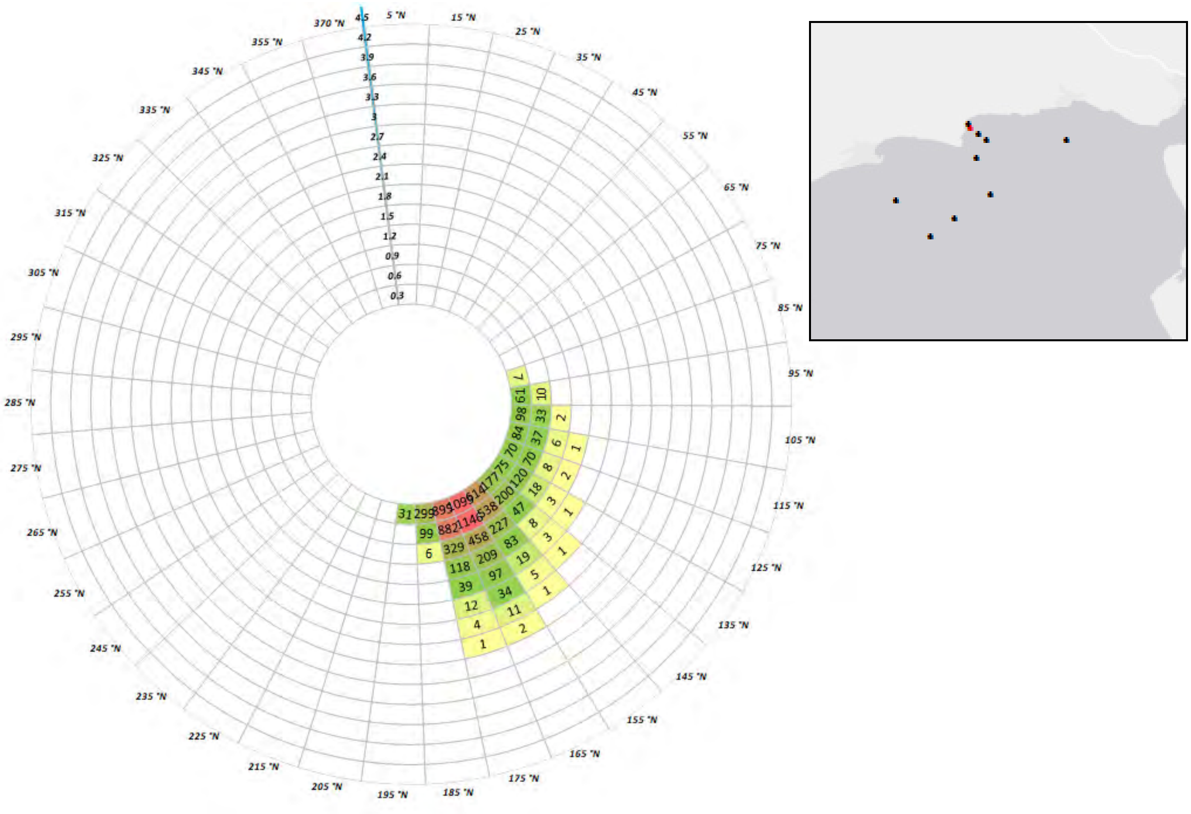

Figure 15. Annualised wave rose at L2, values indicate the number of hours per year

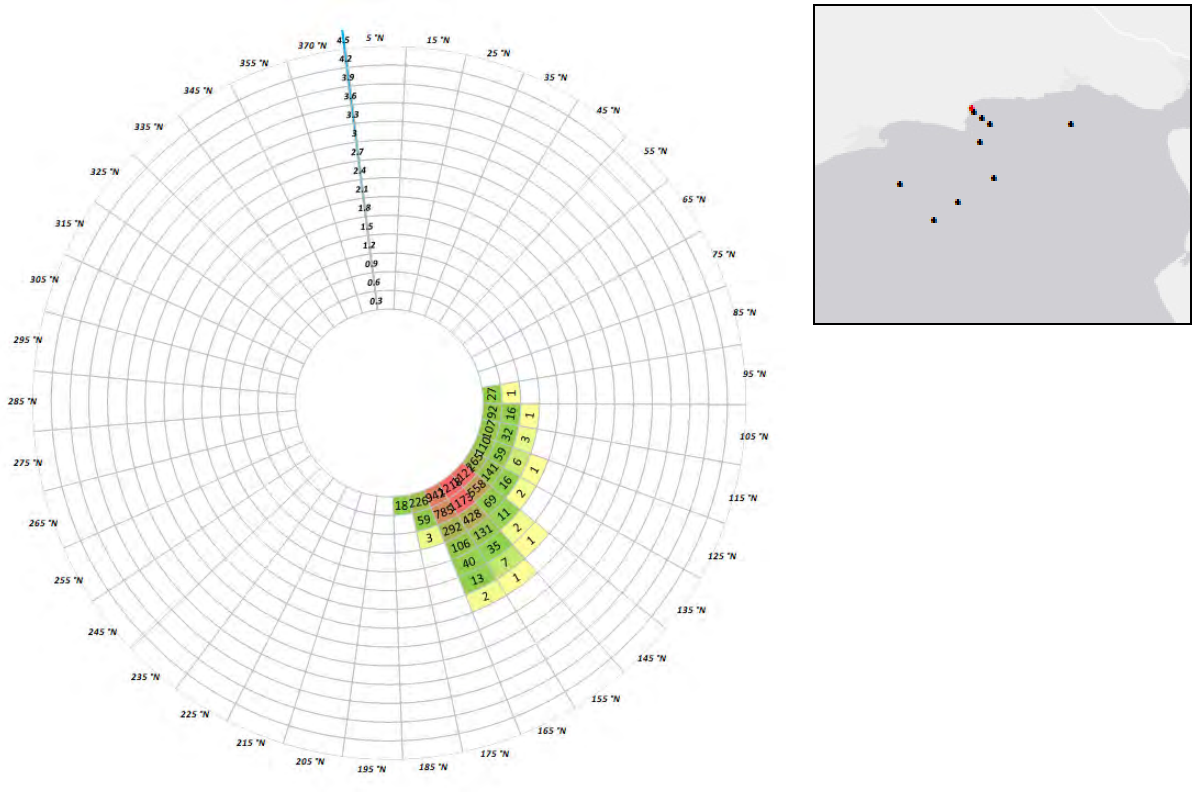

Figure 16. Annualised wave rose at L1, values indicate the number of hours per year

To provide an indication of inter-annual variability, the number of storm events in each year with a peak significant wave height above 1.8 m is shown in Figure 17. The stormiest year in the hindcast was 2015 with 18 events while the calmest year was 2001, with only three events. To include an assessment of the duration of the storm events, the number of hours of storms events are also shown. The year 2015 remains the stormiest with a total of 450 hours of storms (equivalent to 19 days) and 2001 the least stormy. The proposed coastal defence works are situated relatively high in the tidal frame and as such storms are only likely to reach the development during periods when the water level is above 1.5 m ODN (which is approximately 0.5 m above Mean High Water Neap). The hours of storms when water levels are above 1.5 m ODN are therefore also shown Figure 17.

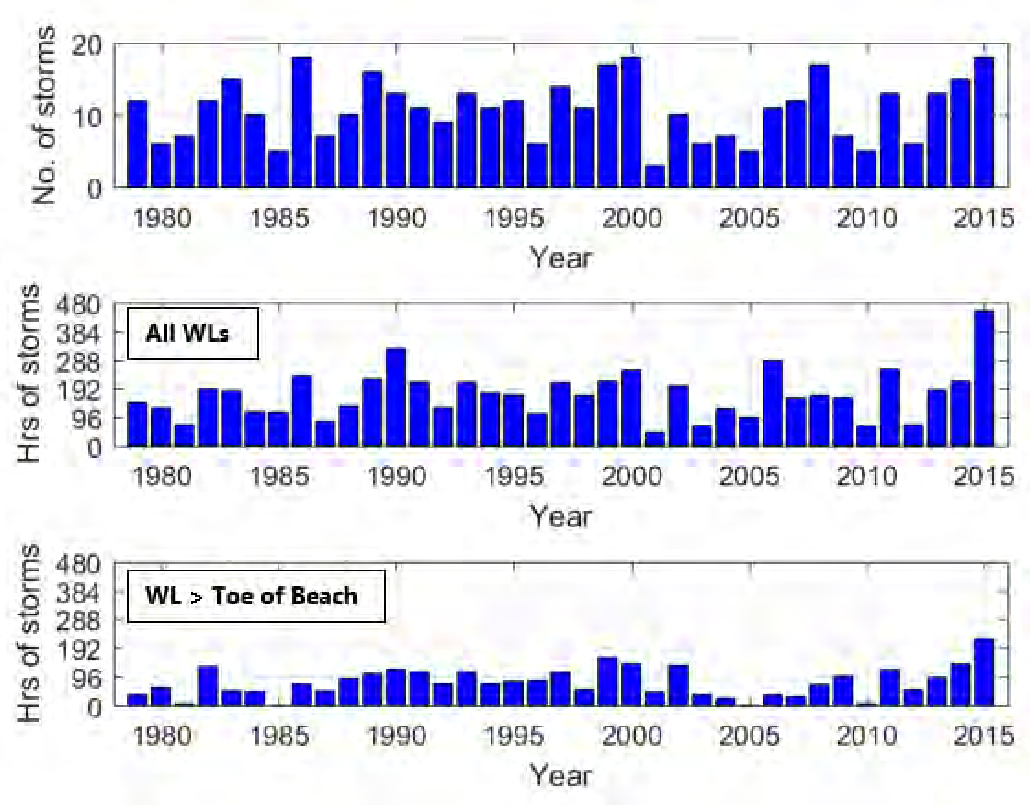

Figure 17. Number of storms (Upper), Hours of storms (Middle) and Hours of storms where WL > toe of beach (Lower) with significant waves over 1.8 m in each year based on waves extracted at M1.

For 2015 this reduces the periods of storms from almost 19 days to around nine days. The year with the minimum number of storm hours when all water levels are considered was 2001; when only water levels reaching the development are considered the minimum number of storm hours occurred in 2005. Statistics of the maximum, minimum and mean number of storm hours per year are provided in Table 2.

An extremes analysis of the modelled waves at M1 has been undertaken to provide a characterisation of wave conditions for a range of return periods for consideration in the local area model. In the analysis waves from the Southwest (180 to 270 degrees) and the southeast (90 to 170) were considered separately. The results from the extremes analysis are provided in Table 3. The wave conditions are characterised by the significant wave height (Hs) and the zero upcrossing wave period (Tz). Waves from the southwest are larger than those from the southeast due to the longer fetch length from the southwest sector. The significant wave height at M1 for a 10 in 1 year wave (return period of 0.1) is 2.09 m for waves from the southwest, while southeasterly waves for this return period have a significant wave height of less than 0.4 m. Comparatively 1 in 35 year wave conditions have a significant wave height of 3.7 m and 2.6 m for waves from the southwest and southeast, respectively. Additionally, waves from the southwest have a longer period than those from the southeast. Longer period waves will 'feel' the bed in shallower waters than shorter period waves and have a greater potential to result in sediment transport.

Table 2. Storm hour statistics based on waves extracted at M1.

Statistic	All storms with Hs>1.8 m		Storms with Hs>1.8 m and WL> toe of beach	
	Hours	Year	Hours	Year
Max. hours of storms in one year (and year of occurrence)	454	2015	223	2015
Min. hours of storms in one year (and year of occurrence)	45	2001	0	1985 and 2005
Average hours of storms in one year	172	-	77	-

Table 3. Extremes analysis of waves at M1

Return Period	Waves from Southwest		Waves from Southeast	
	Hs (m)	Tz (s)	Hs (m)	Tz (s)
0.1	2.09	4.3	<0.4	<2
1	3.10	5.3	1.42	3.6
2	3.27	5.4	1.77	4.0
5	3.47	5.6	2.12	4.4
10	3.59	5.7	2.32	4.6
35	3.7	5.8	2.6	4.8
Tz is estimated from the mean wave steepness				

To provide an indication of spatial variations in the wave climate in Cardigan Bay, map plots of significant wave height are provided in Figure 18. The plots show conditions on 2 March 1997 when wave conditions were typical of a 1 in 1 year return period event for waves from the southwest and on 12 January 2010 when wave conditions were typical of a 1 in 1 year return period event for waves from the southeast. The waves within Tremadoc Bay are smaller than elsewhere in Cardigan Bay, with significant sheltering provided by the headlands of the Llŷn Peninsula to the west. Waves from the east are limited by the short fetch length in this direction. The shallower region of the North Shoals to the southeast of Tremadoc Bay also act to modify the waves climate locally.

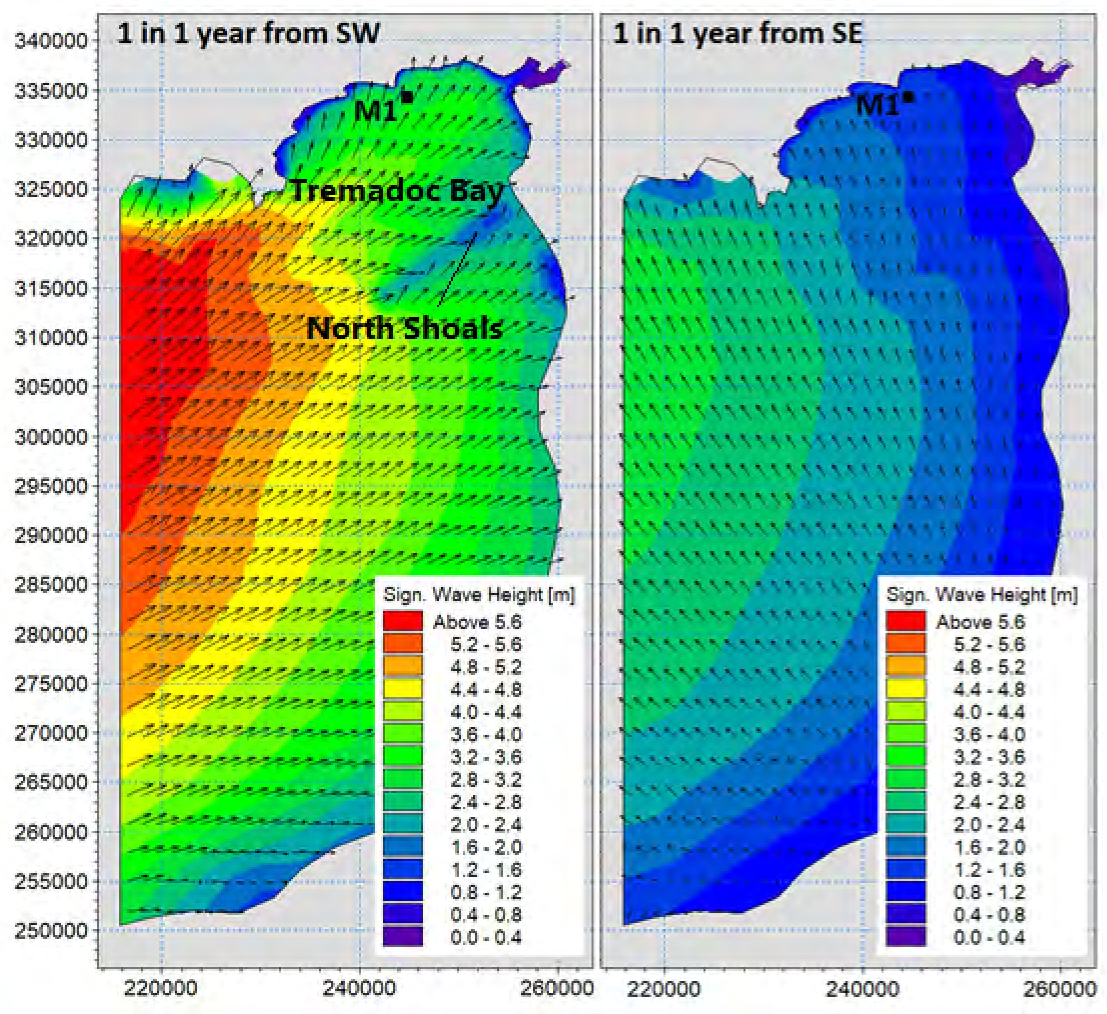

Figure 18. Map plots of wave conditions in Cardigan Bay for a 1 in 1 year wave condition

3.3 Local area model

To assess the impacts of the proposed coastal defence scheme, a detailed area model which simulates tides, waves and sand transport has been developed in the MIKE 21 FM modelling software. The individual modules are dynamically coupled so the effects of waves on tidal flow and the effects of tidal flow on waves are accounted for. The model is driven by tidal conditions from the regional flow model and wave conditions from the regional wave model.

The detailed area model extends approximately 6 km west to 5 km east of Hafan y Môr. The offshore model boundary is located approximately 4 km offshore into water depths of more than 12 m ODN. The model mesh has a resolution of around 3-5 m along the coast at Hafan y Môr to enable detailed resolution of the proposed fish tail groynes. The detailed area model mesh is shown in Figure 19.

A temporally varying water level condition is applied on the western boundary and temporally and spatially varying flow boundary is applied on the southern and eastern boundaries. The model run period has been selected to coincide with March equinox tides; high waters during the run period peak at 3.31 mODN at Pwllheli according to TotalTide values; Highest Astronomical Tide (HAT) at this location is 3.36 mODN, Mean High Water Springs (MHWS) is 2.56 mODN and Mean High Water Neaps (MHWN) is 0.96 mODN. The consideration of HAT is expected to provide an assessment of the scheme when sediment mobility has the potential to occur when tides and waves reach the scheme which is located high up in the tidal frame. An adjustment was applied to the flows on the eastern boundary to allow wave driven flows to exit the model domain.

The wave module applies a spatially varying and temporally constant wave condition on the western and southern boundaries while a closed boundary (which absorbs any waves) is applied on the eastern boundary. The wave boundary conditions (including significant wave height, peak wave period and mean and peak wave directions) were extracted at locations along the boundary of the local area model from the 37-year period hindcast for a period when the selected wave events occurred. Details on the selected wave events are provided in Section 4.2.1 (baseline understanding). A spatially constant wind forcing coincident with the identified wave events was also applied as a spatially and temporally constant value.

The SW module is run in fully spectral formulation to ensure that the wind-wave generation process is included. Eighteen spectral bins between 90 and 270 degrees were applied. Both water levels and flows from the HD simulation were considered within the wave module although it should be noted that tidal flows are not expected to significantly alter the wave field in this region (since tidal flows are typically less than 0.2 m/s on spring tides).

To simulate the effects of the proposed coastal defence scheme, a shallower beach profile (approximately 1 in 10) has been modelled by altering the bathymetry at Beach 1, 2 and 3. The five 'fish-tail' shaped rock armour groynes have been included in the model as bathymetric features. Individual rock pieces forming the fishtail groynes will be of typical diameters of between 0.6 m and 1 m. The surfaces of the groyne structure is therefore likely to result in a relatively significant enhancement to roughness and source of energy dissipation across the structure. The enhanced roughness associated with the groynes is not accounted for in the model.

In addition to the scheme design above, a sensitivity test has been performed without groyne 2. This is referred to as Scheme 2.

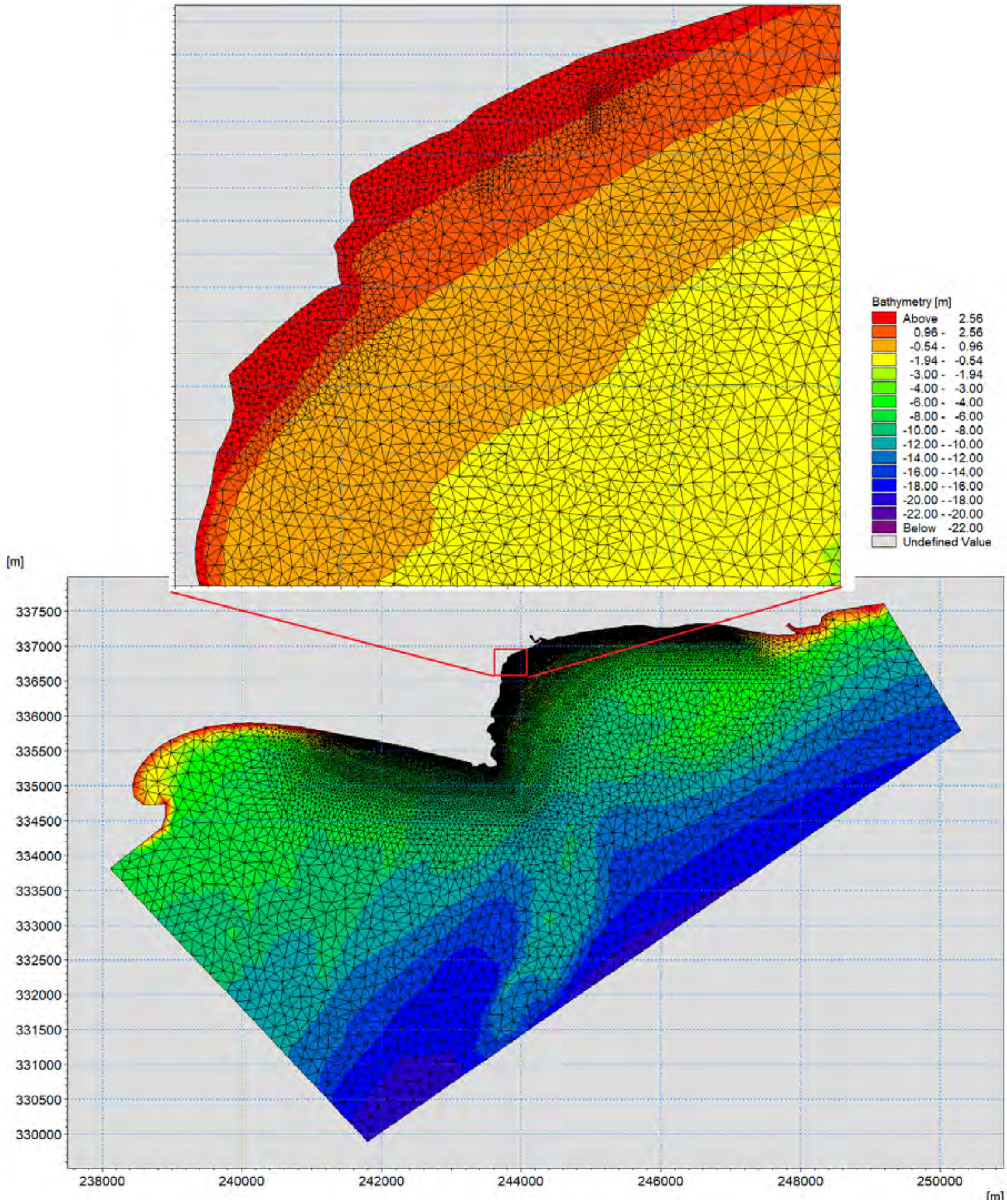

Figure 19. Detailed area model mesh

3.4 Profile evolution modelling

The profile evolution tool in MIKE 21 has been applied to simulate the beach drawdown across the new beaches (Beach 1, Beach 2 and Beach 3). Additionally, beach drawdown across the existing foreshore to the west and east of the scheme has also been considered for some wave conditions (see Section 4.2.1 for wave conditions). The location of the beach profiles is shown in Figure 20. Each profile was defined as being 145 m in length. The wave conditions applied to drive the model are defined at the offshore extent of the profile, extracted from the local area model. The model is run only for the period over high tide (from approximately 2.5 hours before to 2.5 hours after High Water) when the offshore limit of the profile is wet.

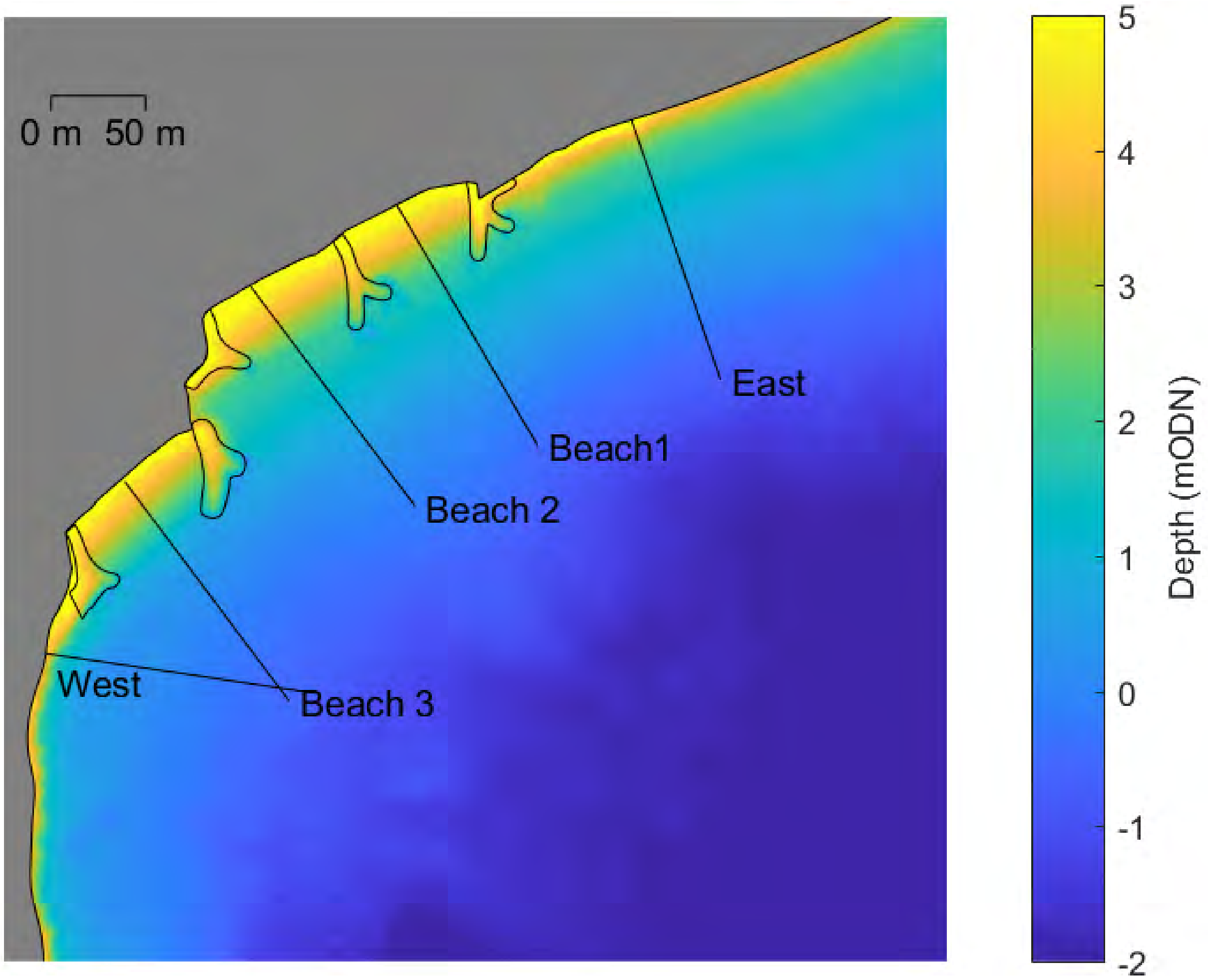

Figure 20. Location of beach profiles

Table 4. Beach drawdown model scenarios

Wave Conditions	Profiles
1 in 35 year southwest	Beach 1, 2, 3, West and East
1 in 35 year southeast	Beach 2 and 3
1 in 1 year southwest	Beach 1, 2 and 3

The model was run with a uniform sediment type along the profile location. A grain diameter of 0.2 mm and a grading of 1.4 was applied. Details on the sediments are provided in Section 4.3.

One of the key tuning parameters in the profile evolution tool is the roughness length. Guideline values range between two and twenty times the sediment grain size. In lieu of any data against which to calibrate the model, three different roughness lengths were tested to provide an indication of the sensitivity of the model output to this calibration parameter. The range of roughness lengths varied from 2.5 times the sediment grain size (shown by dotted line on the plots) to twenty times the sediment grain size (shown by a dashed line on the plots). The main result is shown for ten times the sediment grain size (solid line on the plots). In all cases the dashed line is indiscernible from the solid line, while the dotted line is only discernible for waves from the southwest; this indicates that the results are not particularly sensitive to the range of roughness lengths tested. For waves from the southwest the beach drawdown is slightly increased for the smaller roughness length (because of the reduced energy loss).

4 Baseline Understanding

The coastline around the Hafan y Môr frontage is influenced by the hard geology of the Aberystwyth cliffs and the rock headlands at Penychain and Criccieth. The effects of glaciation have provided a large amount of sediment to the region which, with the oblique wave action across the coastline, has led to the formation of crenulate shaped bays along the south coast of the Llŷn Peninsula. At Borth Fawr, Pwllheli and east of Criccieth, barrier beaches have been created adding natural protection to low lying land behind.

Sediment drift rates across the area are influenced by the presence of the headlands and the shape of the resultant bays. Sediment transport between the bays is generally considered to be low, except for the southern tip of each frontage (Royal Haskoning 2011; Mills 1998). Sediment supply between Pen y chain and Criccieth is limited by the harder, higher foreshore and the influence of the Dwyfor river. Along this coastline the undefended areas have a tendency to roll back at around 0.3 m per year in many areas and this will be significantly affected by sea level rise in the future (Royal Haskoning 2011).

The baseline understanding of the tidal hydrodynamics, wave climate and sediment regime in the study area has been informed by a review of existing information and enhanced with results from the regional wave model and the local area model.

4.1 Tidal hydrodynamics

The tides within Tremadoc Bay exhibit a relatively large tidal range of around 4.5 m on mean spring tides and 1.5 m on neap tides. The levels on mean spring and mean neap tides are given at Pwllheli and Criccieth in Table 5. Levels for Highest Astronomical Tide (HAT) are also provided.

Table 5. Tidal levels ay Pwllheli and Criccieth

Tidal Level	Level at Pwllheli (mODN)	Level at Criccieth (mODN)
Mean Low Water Spring	-1.94	-2.04
Mean Low Water Neap	-0.54	-0.64
Mean High Water Neap	0.96	0.96
Mean High Water Spring	2.56	2.56
Highest Astronomical Tide	3.36	3.36

Despite the large tidal range, tidal flows in Tremadoc Bay are relatively weak. A tidal diamond located offshore of Pwllheli in depths of approximately 13 m ODN indicates peak flows of approximately 0.25 m/s on the flood and ebb of a mean spring tide.

4.2 Wave climate

4.2.1 Wave conditions

An extremes analysis of the 37 year hindcast wave climate at site M1 (see Figure 11 for location) was undertaken (see Table 3). A number of wave conditions were then selected to assess the impact of the scheme on present day flow, wave and sediment conditions. The wave conditions were selected based on the requirement to assess the potential for sand losses during the 20 year service life of the groynes. A 1 in 35 year return period event has a between a 40% and 60 % chance of occurrence during a 20 year period (MAFF, 2000), and is therefore considered a suitable extreme event to analyse to address the study requirement. In addition, a 1 in 1 year wave condition has been selected to provide an indication of the likely effect of the scheme on alongshore transport under more frequent conditions. While a 1 in 1 year event is still a relatively extreme condition, given the small scale of the development and its location high in the tidal frame, the effects of the scheme are anticipated to be minimal. Therefore, it is considered appropriate to demonstrate the negligible effect on more extreme conditions and to conclude by inference the negligible effect on more frequently occurring conditions.

Results from the 37 year hindcast at M1 were examined to identify periods when the selected wave events occurred; where possible waves occurring at a time when water level was close to zero were selected. The parameters from the regional wave model at extraction location M1 are provided in Table 6.

Table 6. Characteristic wave events at M1

	1 in 35 year SW	1 in 35 year SE	1 in 1 year SW	1 in 1 year SE
Date of example event	23/12/1999 20:00	13/12/1981 13:00	02/03/1997 01:00	12/01/2010 17:00
Hs (m)	3.7 (3.7)	2.7 (3.0)	3.12	1.44
Tz (sec)	5.6 (7.0)	4.6 (4.6)	5.2	3.6
Tp (sec)	9.7 (9.9)	6.3 (6.2)	10.0	5.1
Mean wave dir (deg)	196 (191)	165 (166)	202	154
Wind Speed (m/s)	20	18	18.6	11.7
Wind dir (deg)	197	143	214	120

Selected wave conditions were simulated in the Local Area Model for the present day (i.e. baseline condition) and the effect

4.2.2 Coupled tide and wave driven flows

The baseline results from the detailed area model are shown as series of spatial map plots and time series plots at extraction points located offshore of the proposed groyne structures. These extraction locations are shown in Figure 1 and are tabulated in Table 7.

A full set of figures is provided in Appendix B (Figure B1 to Figure B40). Key figures are repeated for ease of reference in this section alongside commentary to aid baseline understanding.

For each wave event (1 in 35 year southwest, 1 in 35 year southeast, 1 in 1 year southwest and 1 in 1 year southeast), the following plots are presented:

- Map plots of significant wave height (Figure B1, Figure B2, Figure B21 and Figure B22);
- Time series of significant wave height, peak wave period and mean wave direction at E1, G1, G2, G3b, G4 and W1 (Figure B3 to Figure B8 and Figure B23 to Figure B28);
- Map plots of wave and tide induced flow at the times of peak flood (one hour before High Water), High Water (HW) and peak ebb (3 hours after HW) (Figure B9 to Figure B12 and Figure B29 to Figure B32);
- Map plots showing combined wave and tide flows and tide only flows (Figure B13, Figure B14, Figure B33 and Figure B34); and
- Time series of water level and flow (combined wave and tide induced flows) at E1, G1, G2, G3b, G4 and W1 (Figure B15 to Figure B20 to Figure B35 to Figure B40).

Peak values of significant wave height and their associated wave period and flow conditions are provided in Table 7.

For the 1 in 35 year waves, wave heights at the site are similar for waves from the south west and from the south east (see Figure 21 and Figure 22), with peak values of around 2 m. Despite differences in the coming direction in deeper water, waves approach the shore from a similar direction for both wave conditions. For example, at location G2 the mean wave direction is 159 ºN and 152 ºN for waves from the southwest and southeast, respectively (Figure 23 and Figure 24). For reference the beach at this location is presently orientated at 60 ºN so that oblique waves are from 150 ºN.

The main difference in wave characteristic for the two coming directions is the wave period, with longer period waves from the southwest and shorter period waves for the waves from the southeast. For example, for the 1 in 35 year wave event the peak period is 10 seconds for waves from the southwest, compared to 6 seconds for waves from the southeast (see Table 7). The longer period waves from the southwest lead to increased energy and hence induce slightly faster flows than the shorter period waves from the southeast. These combined tide and wave driven flows are significantly faster than any tide only driven flows (which peak at less than 0.1 m/s at these locations for the large range tide modelled) and thus the wave driven flow is dominant (see Figure 25).

Compared to waves from the southwest, waves from the southeast drive a more complex flow pattern along the adjacent coastline with areas of convergence and divergence. Convergence occurs offshore of Afon Wen which is possibly due to river interaction. Areas where the southeast waves drive a westward flow in the model reduce the net eastward transport of sediment. Observations show that beaches are wider in these areas which supports the model's predictions.

Despite variations in flow directions away from the site, waves from both the southwest and from the southeast drive a predominantly north-eastward flow along the foreshore at the site. This north-eastward flow is prevalent throughout most of the tide, with only a short duration (around 1 hour for south-easterly waves and around 0.5 hours for south-westerly waves) of much weaker south-westward flows. These periods of south-westward flows coincide with periods of shallow water. On this basis, the analysis of scheme effects on combined tide and wave driven flows is focussed primarily on the time of HW when both inundation and flows are at a maximum. Example time series of wave and tide induced flows are shown at location G2 in Figure 25 and Figure 26 for 1 in 35 year and 1 in 1 year return period wave conditions, respectively.

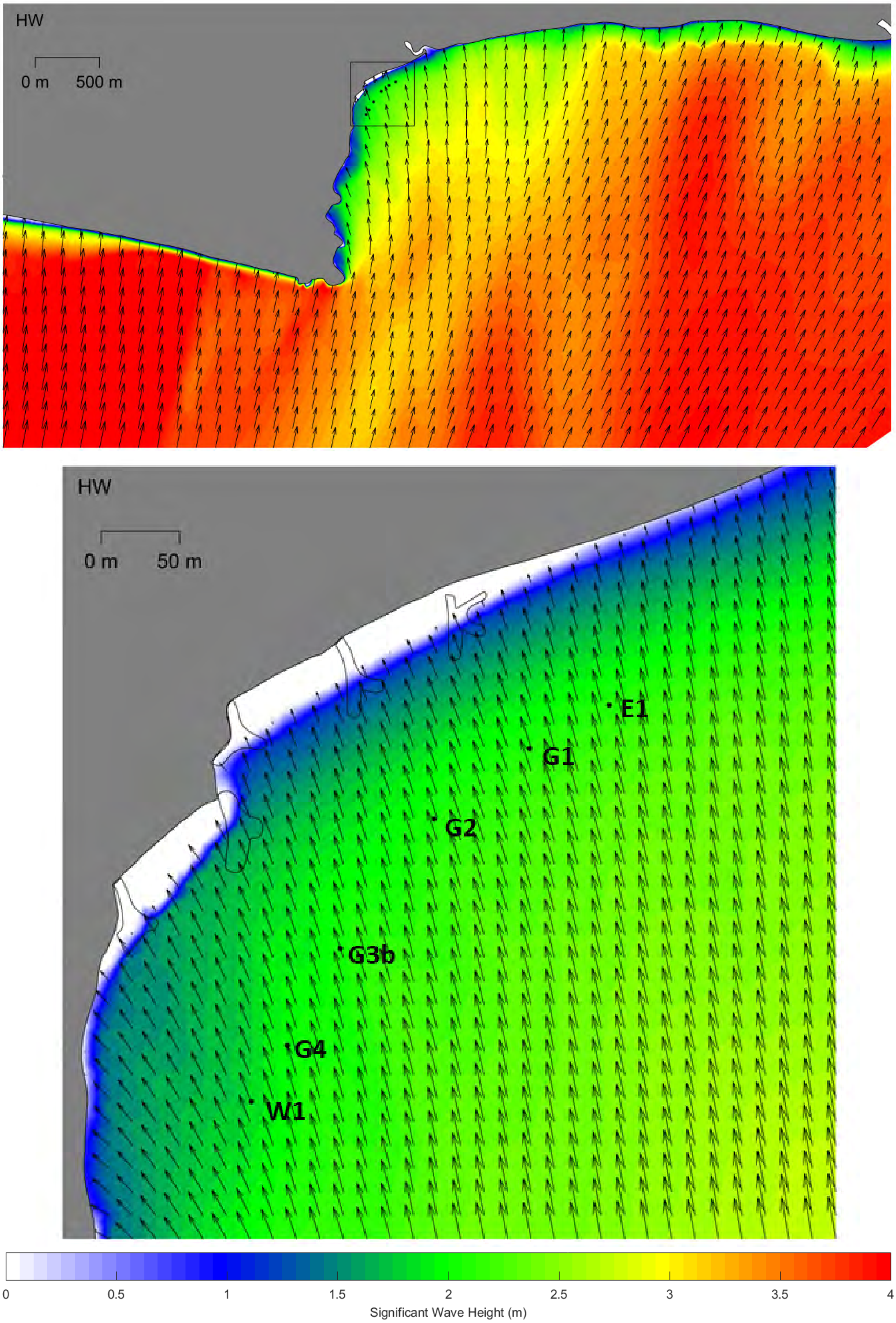

Groynes are not included in the model and shown for indicative purposes

Figure 21. Baseline significant wave height for a 1 in 35 year wave from the southwest

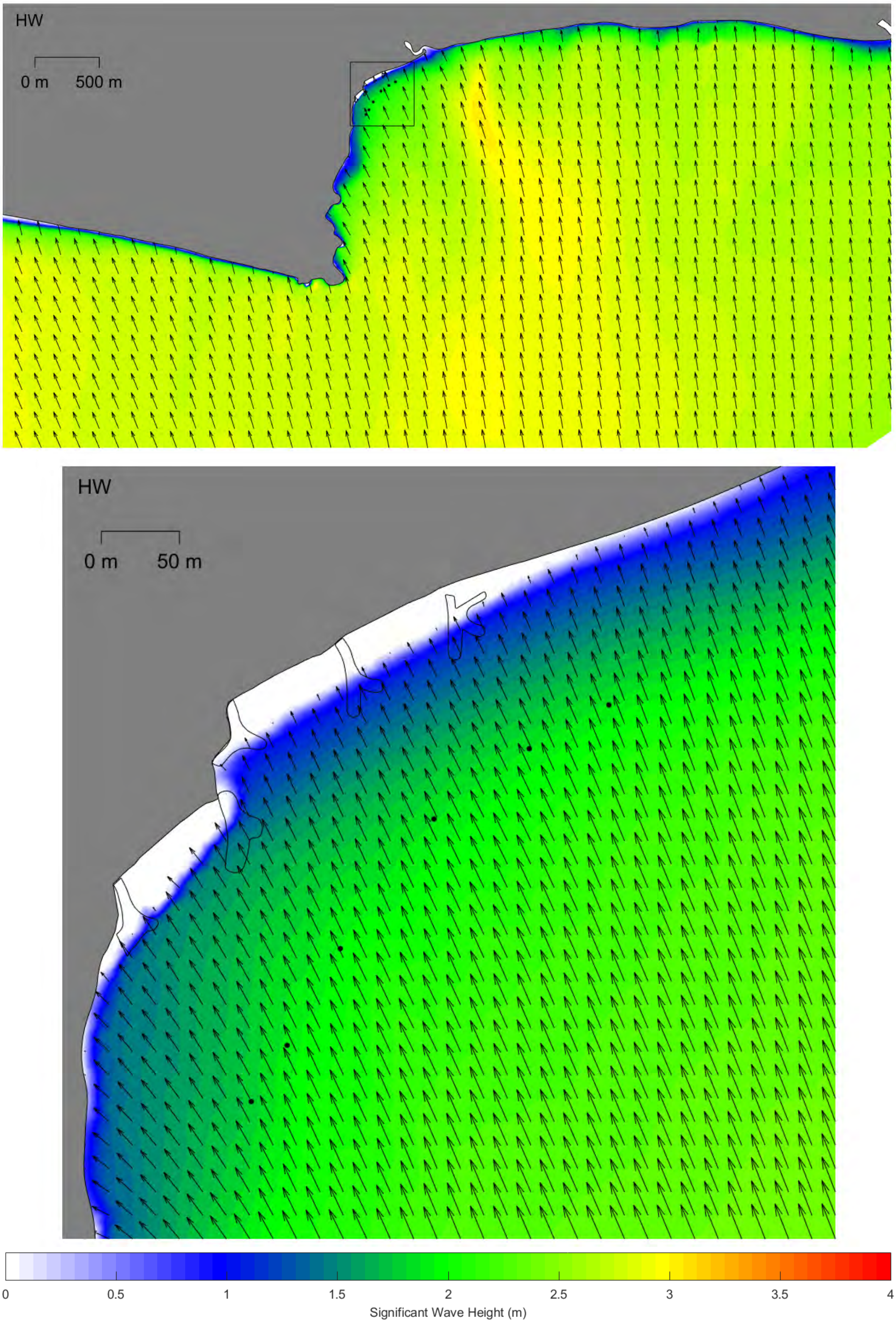

Groynes are not included in the model and shown for indicative purposes

Figure 22. Baseline significant wave height for a 1 in 35 year wave from the southeast

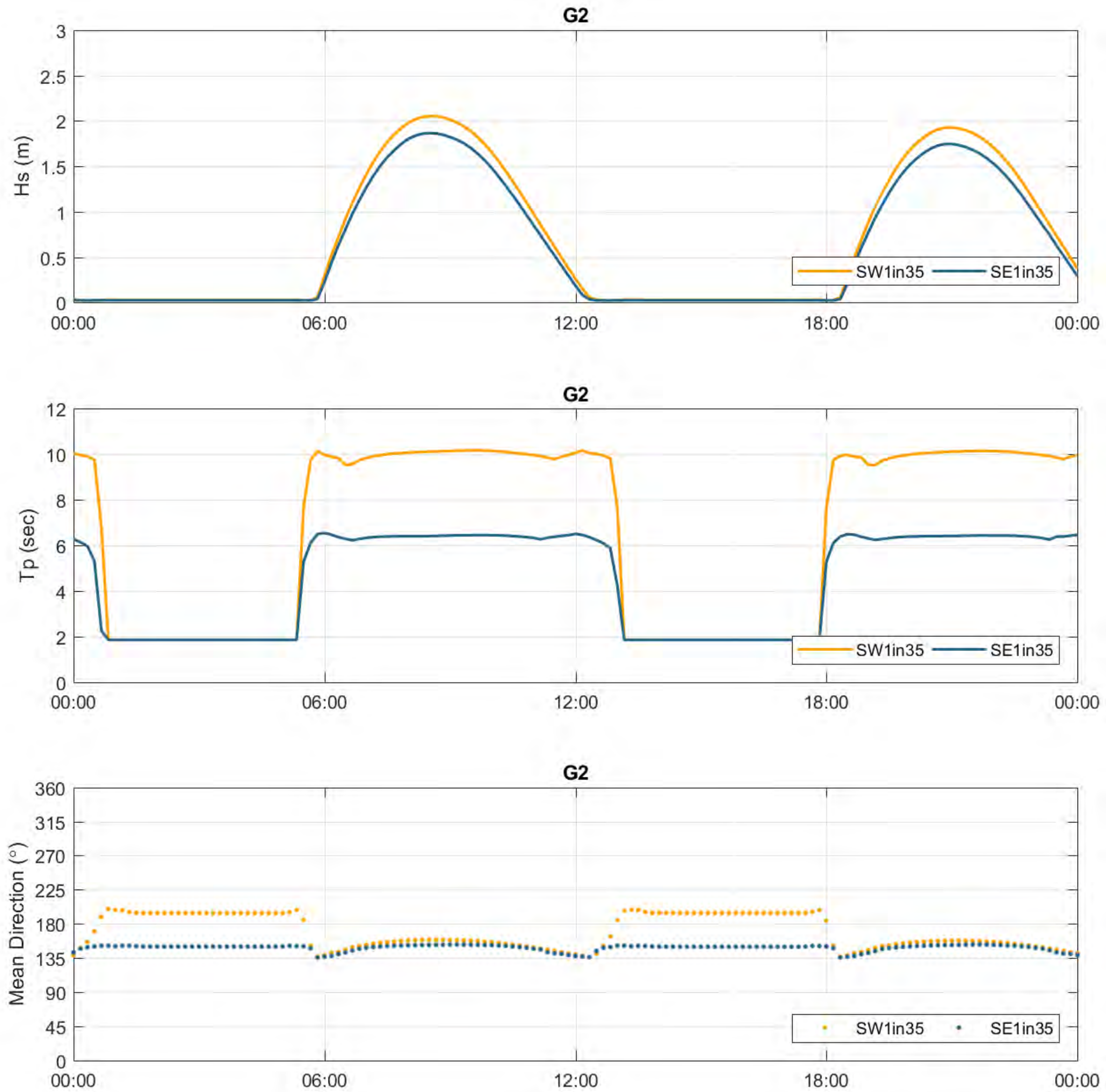

Figure 23. Time series of baseline significant wave height, peak wave period and mean wave direction at G2

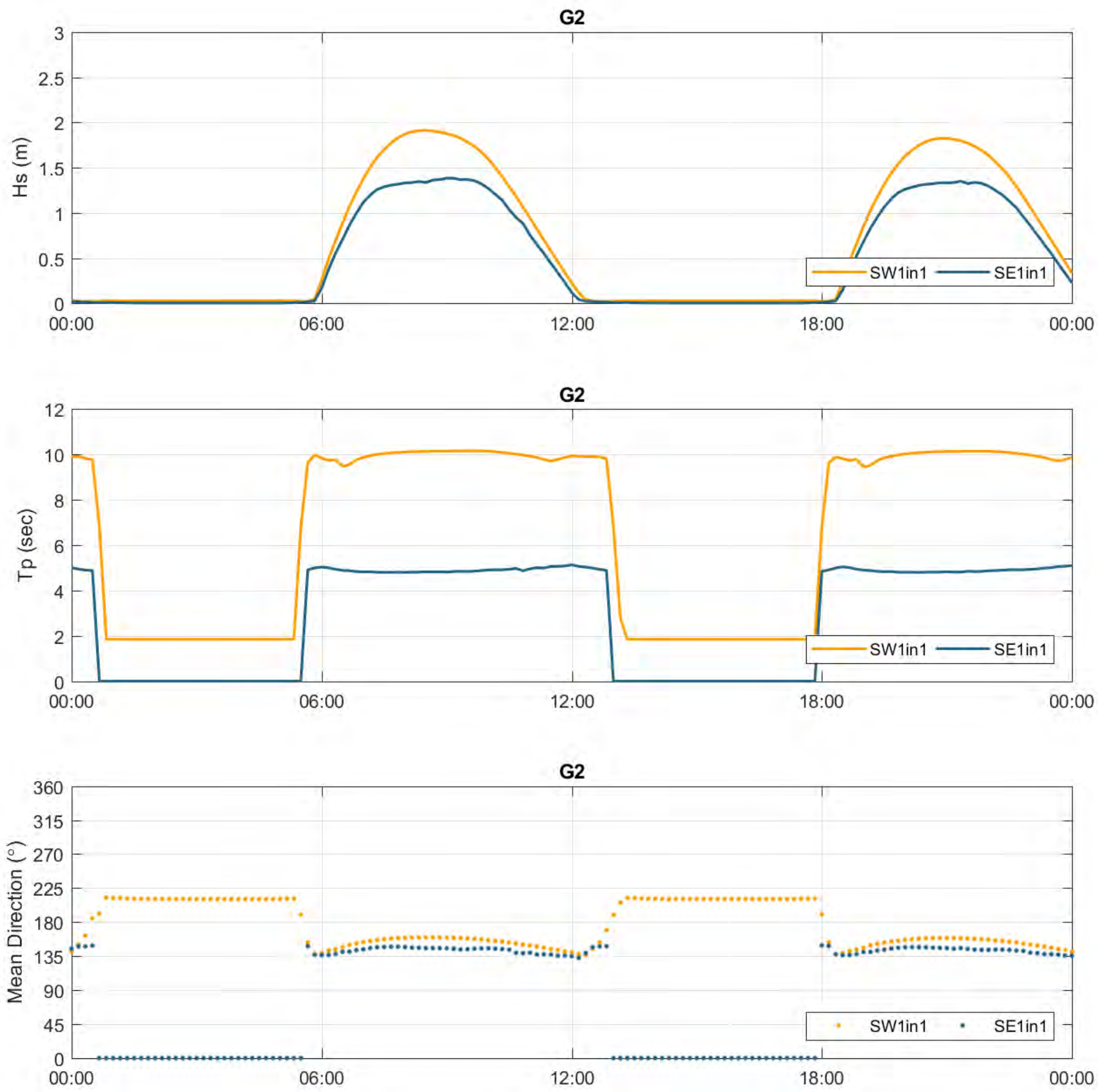

Figure 24. **Time series of baseline significant wave height, peak wave period and mean wave direction at G2 for 1 in 1 year wave event**

Table 7. Extracted peak wave and flow conditions for the simulated wave events

		E1	G1	G2	G3b	G4	W1
Easting (m)		244050	243999	243938	243878	243844	243821
Northing (m)		336842	336814	336769	336686	336624	336588
1 in 35 year wave from SW	Hs (m)	2.1	2.1	2.0	2.0	2.0	1.8
	Tp (sec)	10	10	10	10	10	10
	Wave dir (°)	163	159	159	160	159	157
	Flow (m/s)	0.71	0.70	0.70	0.68	0.68	0.74
	Flow dir (°)	65	57	53	44	29	19
1 in 35 year wave from SE	Hs (m)	1.9	1.9	1.9	1.9	1.9	1.8
	Tp (sec)	6	6	6	6	7	7
	Wave dir (°)	157	153	152	152	152	150
	Flow (m/s)	0.60	0.63	0.67	0.64	0.63	0.69
	Flow dir (°)	71	62	55	45	30	19
1 in 1 year wave from SW	Hs (m)	1.9	1.9	1.8	1.8	1.8	1.6
	Tp (sec)	10	10	10	10	10	10
	Wave dir (°)	164	160	160	160	160	157
	Flow (m/s)	0.60	0.60	0.60	0.54	0.53	0.59
	Flow dir (°)	66	57	53	44	29	18
1 in 1 year wave from SE	Hs (m)	1.3	1.4	1.4	1.4	1.3	1.2
	Tp (sec)	4.8	4.8	4.8	4.8	4.9	4.9
	Wave dir (°)	147	145	144	146	145	144
	Flow (m/s)	0.62	0.62	0.63	0.58	0.57	0.62
	Flow dir (°)	239	182	169	85	46	24
Note that wave direction is coming direction while flow direction is direction to.							

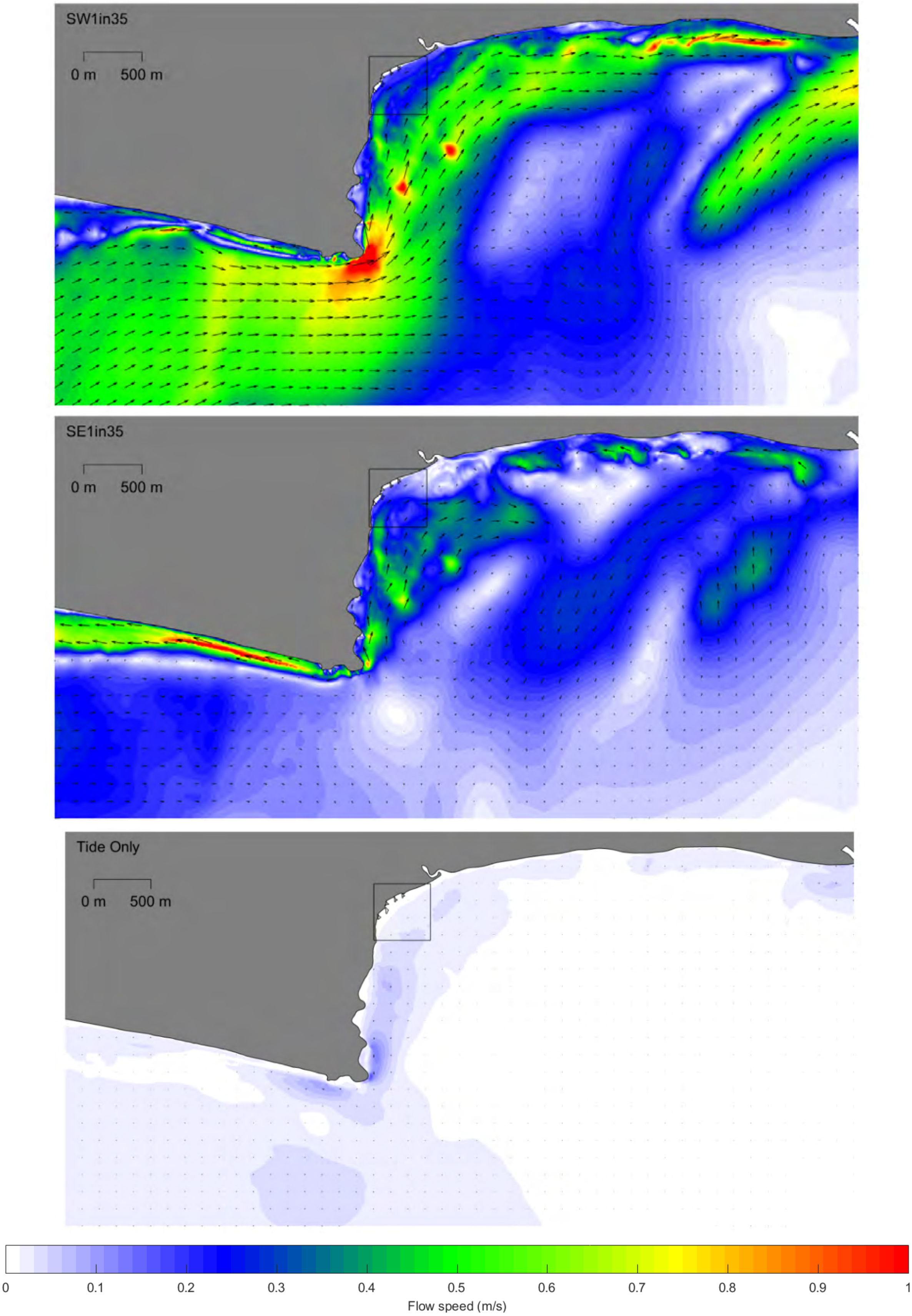

Groynes are not included in the model and are shown only for indicative purposes

Figure 25. Baseline mean wave and tidal flow throughout tidal cycle during 1 in 35 year events

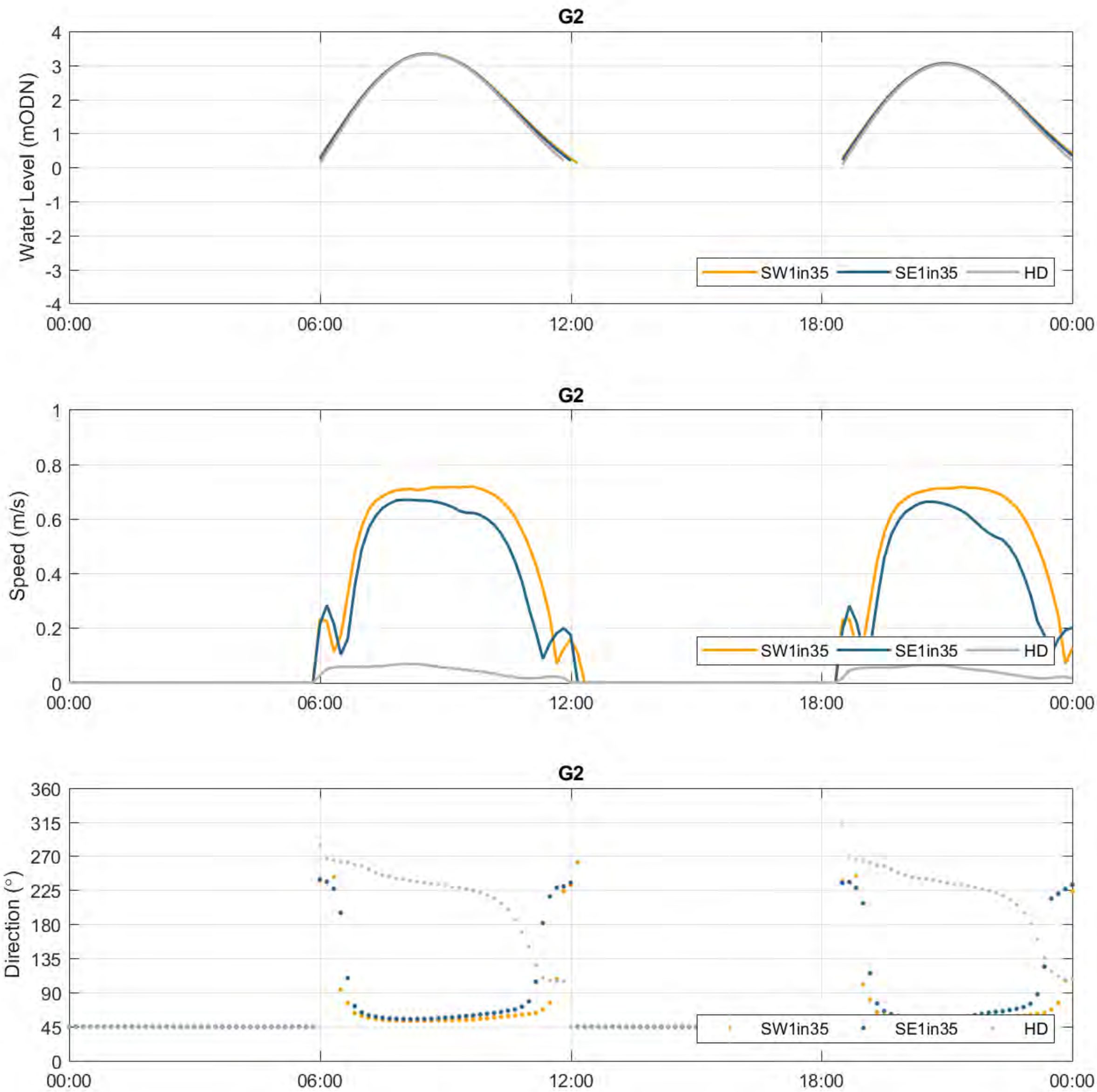

Figure 26. **Time series of baseline water level, flow speed and flow direction at G2 for 1 in 35 year wave event**

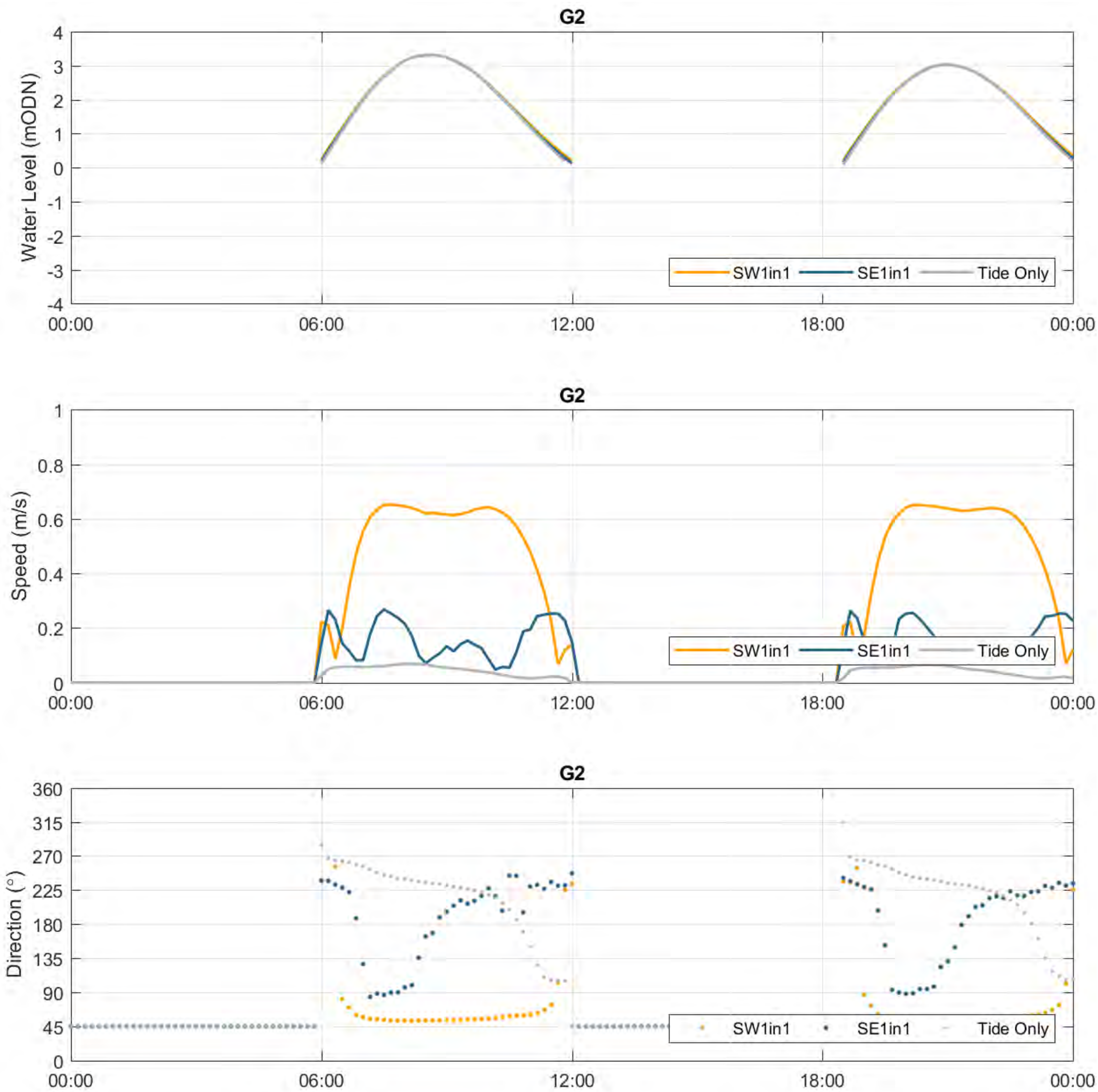

Figure 27. Time series of baseline water level, flow speed and flow direction at G2 for 1 in 1 year wave event

4.3 Sediments

Beach sampling was undertaken as part of a site investigation carried out in August and September 2017 by Murray Rix Geotechnical. From the sediment samples collected it appears that the foreshore fronting the development site is characterised by fine sands (with a median grain size of around 0.2 mm) on the lower foreshore (below approximately Mean Sea Level) and coarser sediments (fine to medium gravels with a median grain size of between 4 mm and 23 mm) on the upper foreshore (at Mean High Water Spring) (see Figure 28). In addition to the offshore fining of sediments, based on the data collected at the sample locations, there appears to be a slight alongshore fining in a west to east direction (i.e. with coarser sediment at Mean High Water Neap at the western edge of the survey area than at the eastern edge of the survey data).

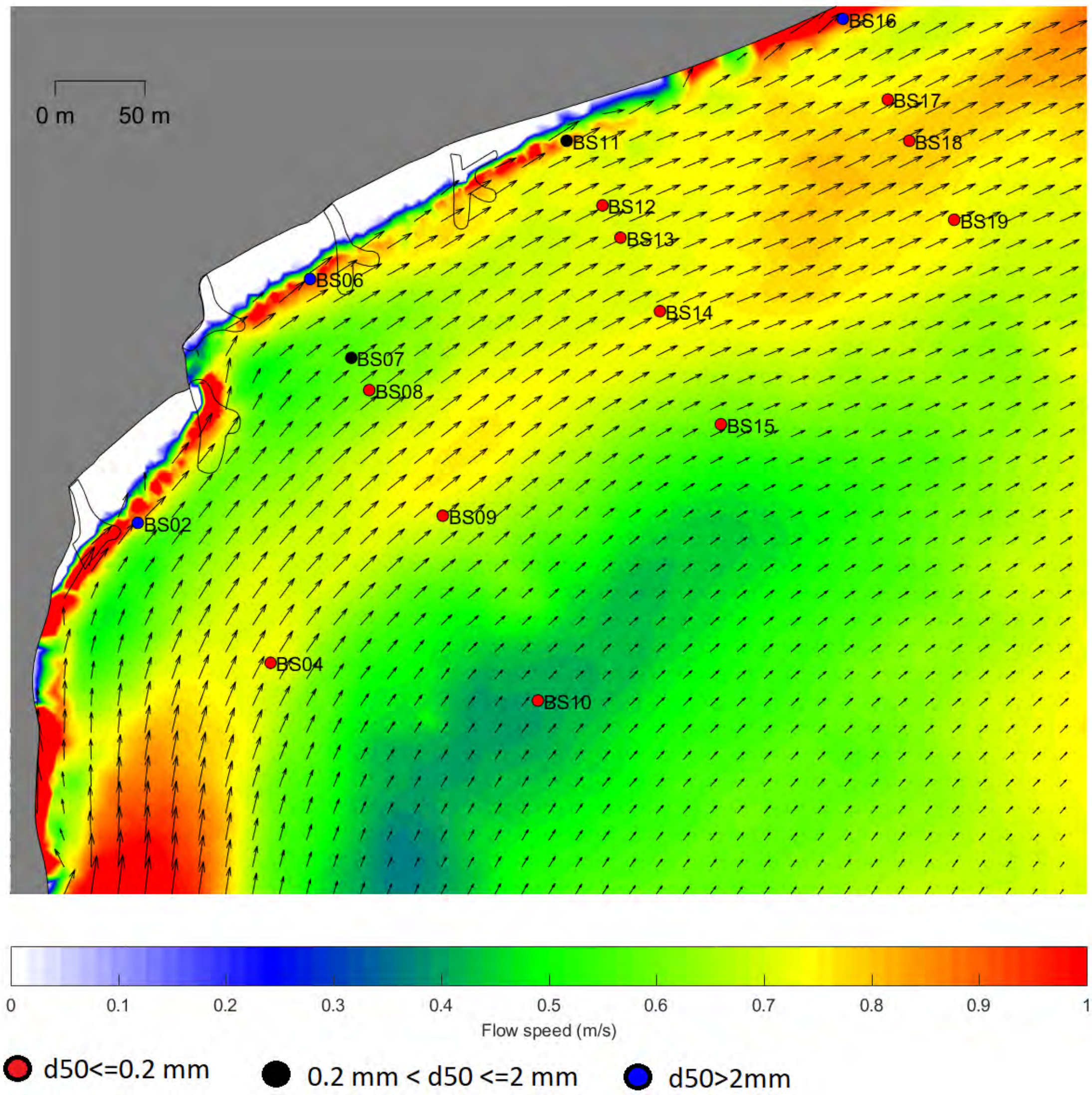

Groynes are not included in the model and are shown only for indicative purposes.

Figure 28. Sediment sample data superimposed on baseline maximum flows for 1 in 35 year wave from the southwest

The Sand Transport (ST) module was applied in the detailed area model to identify the baseline sediment transport characteristics in and around the fronting coastline at Hafan y Môr. The model was run with a uniform sediment grain size of 0.2 mm and includes the dynamically coupled effect of tides and waves.

The baseline sediment transport is shown in Figure 29 at the time of HW (when both inundation and combined tide-wave flows are at a maximum) for a 1 in 35 year wave from the southwest (upper panel) and from the southeast (lower panel). Note that all transport loads are output in solid volumes. The sediment transport for the extreme wave event is generally directed parallel to the coast in an eastward direction, with a slight offshore tendency in the shallowest water around elevations of MHWS. Highest sediment transport occurs for the event from the southwest, consistent with the higher energy associated with waves from this direction. Sediment transport is lower for 1 in 1 year wave conditions (Figure 30) but with a similar pattern for waves from the southwest. For waves from the southeast the sediment transport exhibits a less coherent pattern for the 1 in 1 year wave event (as per the wave driven flows), with areas of converging transport at relatively low rates. Sediment transport for the baseline (and scheme) is quantified across the sections shown in Figure 29 in Section 5.2.

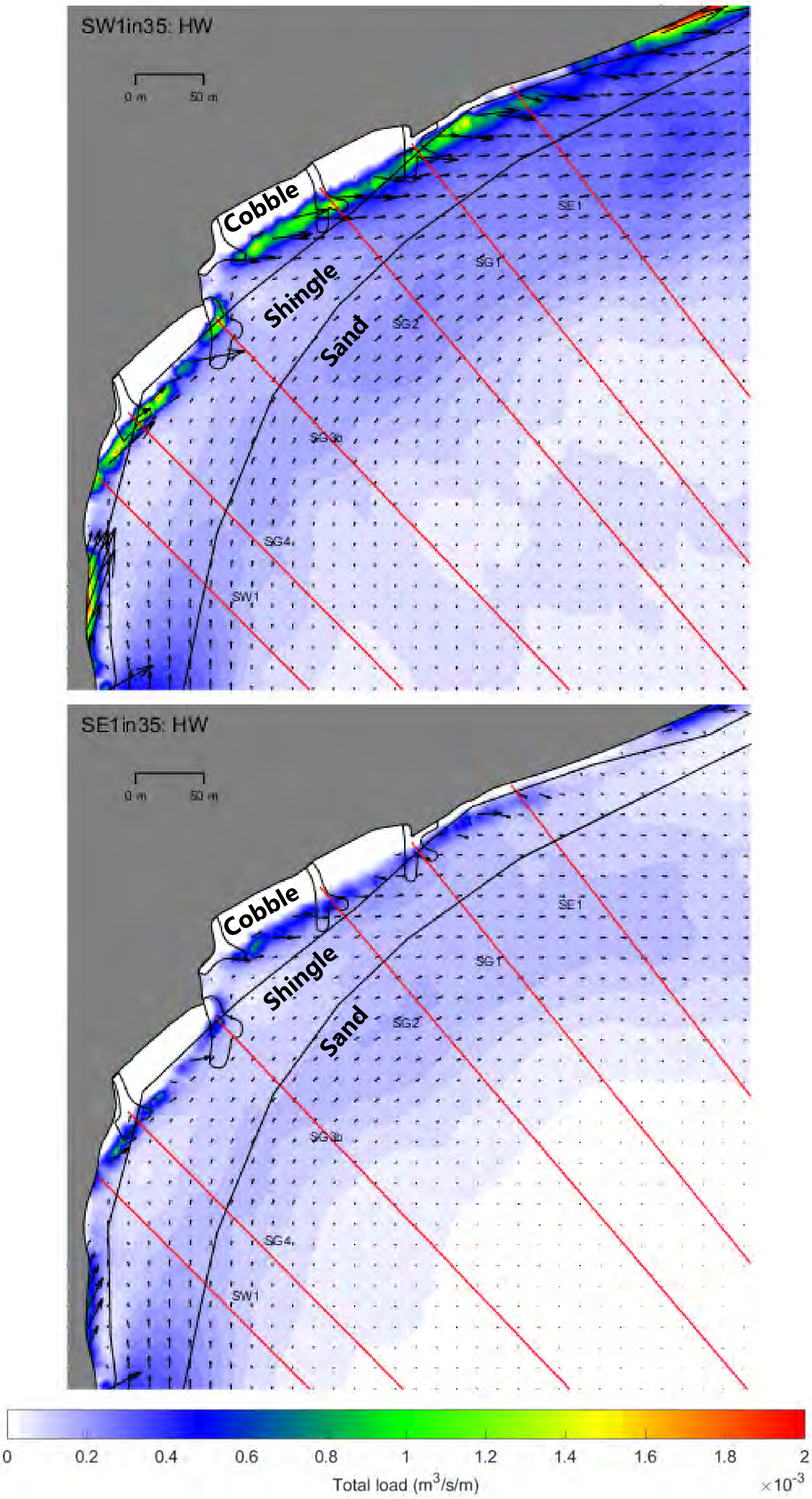

Groynes are not included in the model and are shown only for indicative purposes.
Sediment type i.e. cobbles, shingle and sand are shown for indicative purposes only.
A 0.2 mm sand has been used as the grain size in the model.

Figure 29. Baseline sediment transport for the 1 in 35 year wave from the southwest (upper) and the 1 in 35 year wave from the southeast (lower)

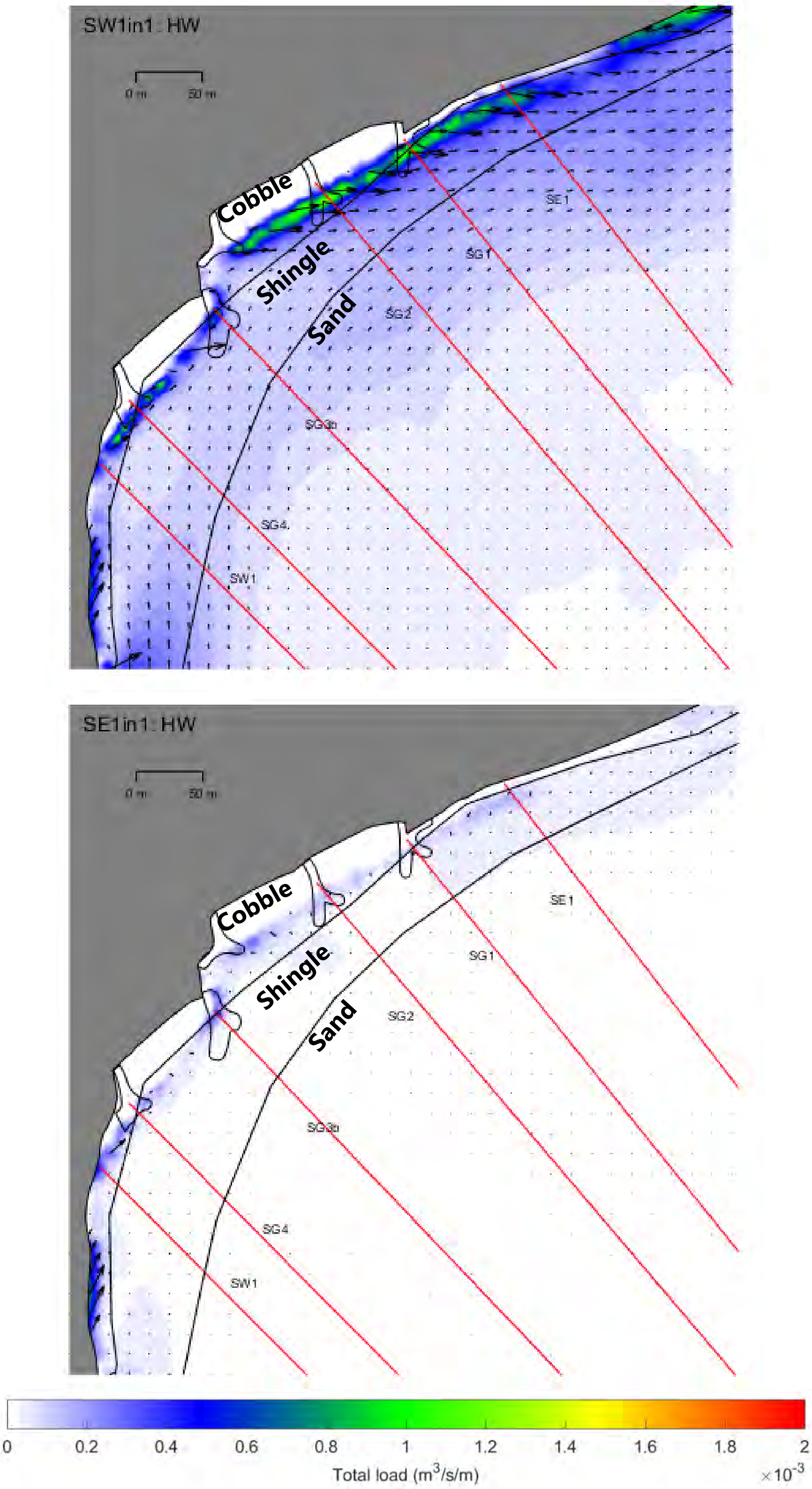

Groynes are not included in the model and are shown only for indicative purposes.
Sediment type i.e. cobbles, shingle and sand are shown for indicative purposes only.
A 0.2 mm sand has been used as the grain size in the model.

Figure 30. Baseline sediment transport for the 1 in 1 year wave from the southwest (upper) and the 1 in 1 year wave from the southeast (lower)

5 Scheme Assessment

To evaluate the scheme design and provide a greater understanding of its likely effects on the wider coastal hydrodynamic and sediment transport processes, the coupled MIKE21 FM model has been used to simulate both the baseline conditions and the modified conditions for the proposed coastal defence scheme.

Through a comparison between results from the baseline and scheme model runs, which capture the tidal variations of a Highest Astronomical Tide (HAT) and the wave scenarios described in Table 6, this section presents an assessment of the proposed coastal defence scheme on hydrodynamics and sediment transport.

It should be noted that the scheme is positioned high in the tidal frame and therefore inherently doesn't impact littoral processes. Therefore, these simulations have been setup to assess rare conditions (that occur during storms) rather than typical conditions, when there will be negligible impact.

For each of the four wave scenarios modelled, the effect of the scheme is considered with respect to flows (combined wave and tides) and sediment transport. The following figures are presented:

- Map plots of peak flows; a comparison between combined wave-induced and tidal flows for the baseline and scheme cases and an enlarged view showing flow details around the groynes. These are shown for the model timestep closest to HW when the inundation is highest and when flows are fastest) (Figure B41 to Figure B48);
- Water level, flow speed and direction time-series over the tidal cycle at extraction locations (see Figure 1 for locations) (Figure B49 to Figure B68); and
- Sediment transport and time series of instantaneous sediment transport across sections (Figure B69 to Figure B116).

In addition, results from the MIKE Profile Evolution model for each wave scenario are also provided. These results are presented as plots of Beach drawdown at Beach 1, Beach 2 and Beach 3 as well as some plots to show the drawdown along profiles to the west and east of the coastal defence scheme (Figure B117 to Figure B126).

Results are also presented for an additional scheme run (scheme 2) in which Groyne 2 (G2 on Figure 1) is removed to provide an assessment of the suitability of the groyne spacing (Figure B127 to Figure B138).

A full set of figures is provided in Appendix B (Figure B41 to Figure B138). Key figures are repeated in this section for ease of reference, alongside commentary to aid understanding.

5.1 Flows

In this section, the term 'flow' refers to the combined tide and wave induced flow.

Map plots of the flows along the area fronting the proposed coastal defence scheme are shown for the baseline and scheme model runs at the time of HW (when flows are fastest and the scheme will have the greatest impact) in Figure 31. Results are shown for a 1 in 35 year wave from the southwest, which is the wave condition with the fastest baseline flows. Results for the other wave conditions modelled are provided in Appendix B; these generally show a similar trend but with a smaller magnitude.

The scheme structures provide sheltering along the lower section of the foreshore and consequently reduce the flows along the new beaches. This flow reduction is most apparent to the northeast of Groyne 3a. Locally, the groyne structures result in some divergence of flows along with a small acceleration in flow over the groynes, most notable at the seaward end of the structures. The model is likely to over predict any acceleration of flow over the groynes since the model roughness has not been modified to account for any increase in roughness associated with the groynes.

The reprofiling of the beaches also results in a divergence of the flows further inshore, this is most notable on Beach 3. For ease of comparison, baseline and scheme vectors are superimposed on the same plot in Figure 32, alongside a flow speed difference plot. The difference plot indicates that the changes in flows are small in magnitude (around 0.5 m/s or less) and are localised (occurring within approximately 50 m of the groynes). Further it should be noted that changes of this magnitude would only occur for a short period around HW and then only on the larger range tides (due to the high positioning of the scheme in the tidal frame).

The areas of flow increase occur in shallow water, mainly in an area which is dry in the baseline case. Given the shallow water depths in these new embayments, the effect on discharge is likely to be relatively small. To demonstrate this effect, the discharge (which considers the combined effect of flow speed and water depth) across three cross shore profiles has been quantified for the baseline and scheme runs and these are plotted in Figure 33 (the location of the cross shore profiles are shown in Figure 32). These show that despite localised flow increases, the net effect of the scheme is a reduction in the volume of water crossing the beach areas.

To provide an indication of how the scheme effect varies throughout the tide, a time series of baseline and scheme flows at location I4 is provided in Figure 34. Results are shown for each wave condition modelled. Location I4 is located in a water depth of approximately 1.9 m above ODN and as such dries out except for a couple of hours either side of high water on a HAT. The impact on flow is largest at the time of fastest baseline flow (i.e. around HW). The effect of the scheme on flows for the 1 in 1 year wave from the southeast does not show a discernible increase or decrease in flow. This is due to the low flows and complex circulation pattern which occurs for this condition.

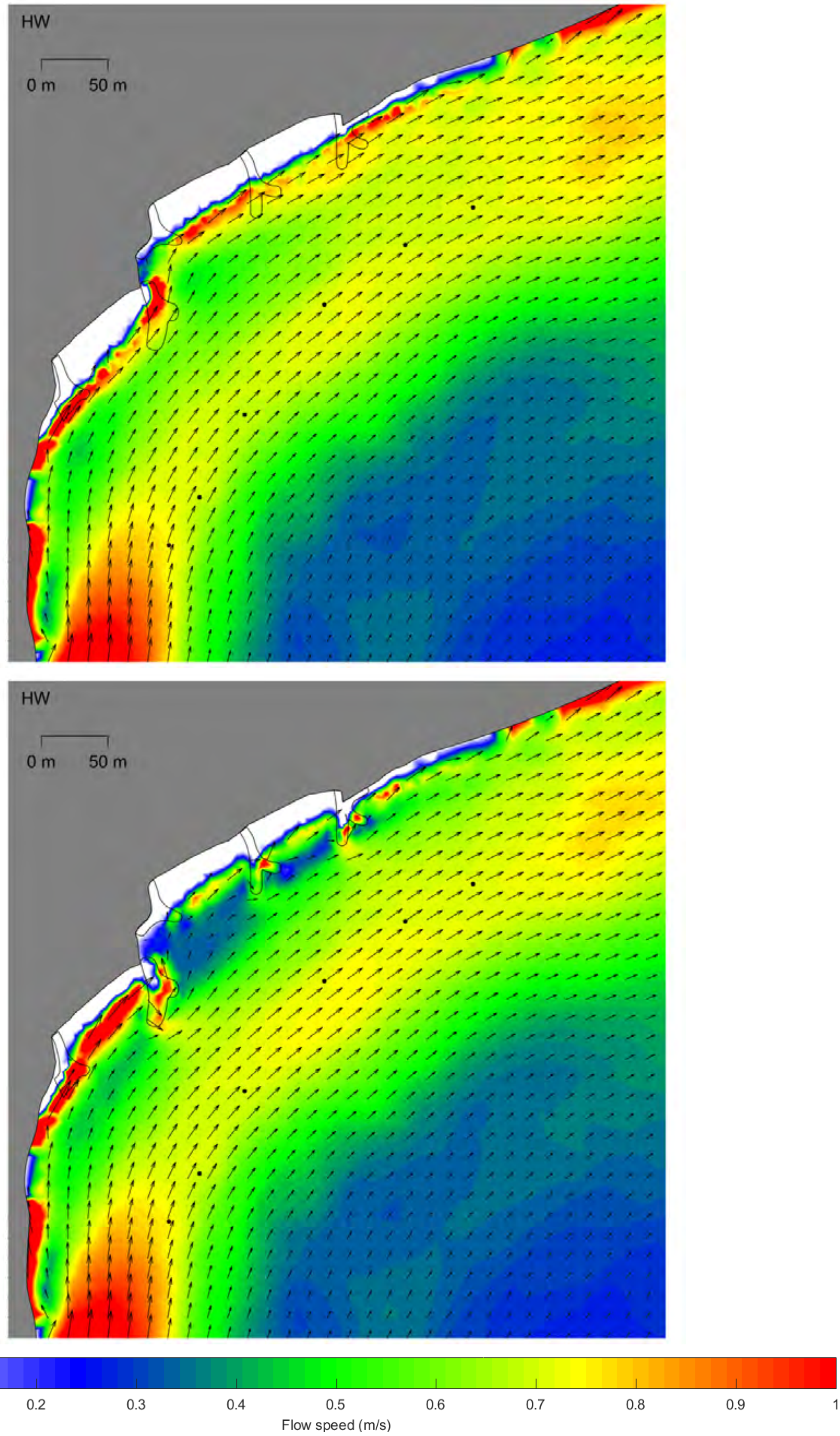

Extraction points are marked for reference but not labelled, see Figure 1 for labels.

Figure 31. The proposed scheme Flows from the 1 in 35 year wave from the southwest for baseline (upper) and scheme (lower)

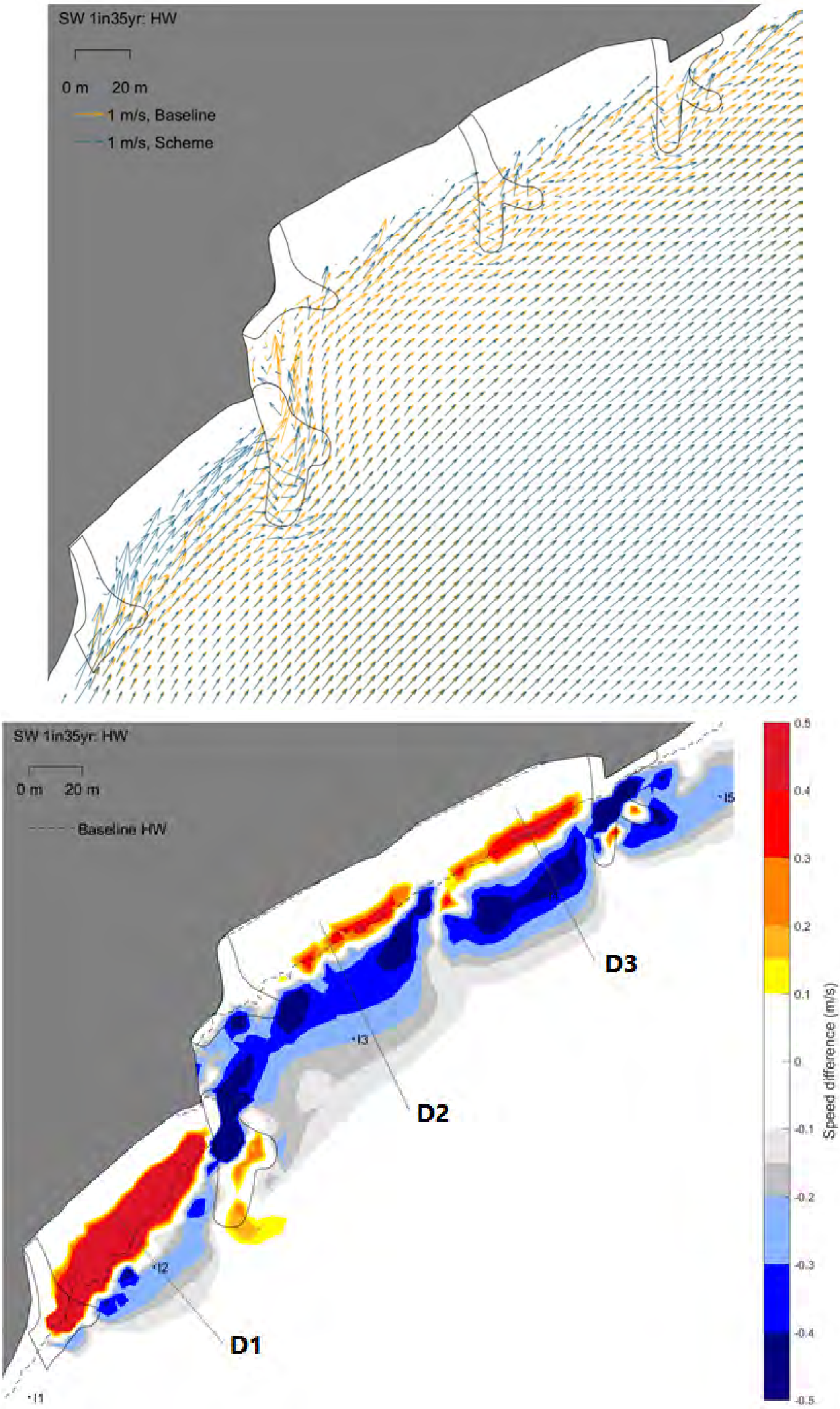

Figure 32. **Baseline and Scheme flows (upper) and the difference in flow (scheme minus baseline) (lower) from the 1 in 35 wave from the southwest**

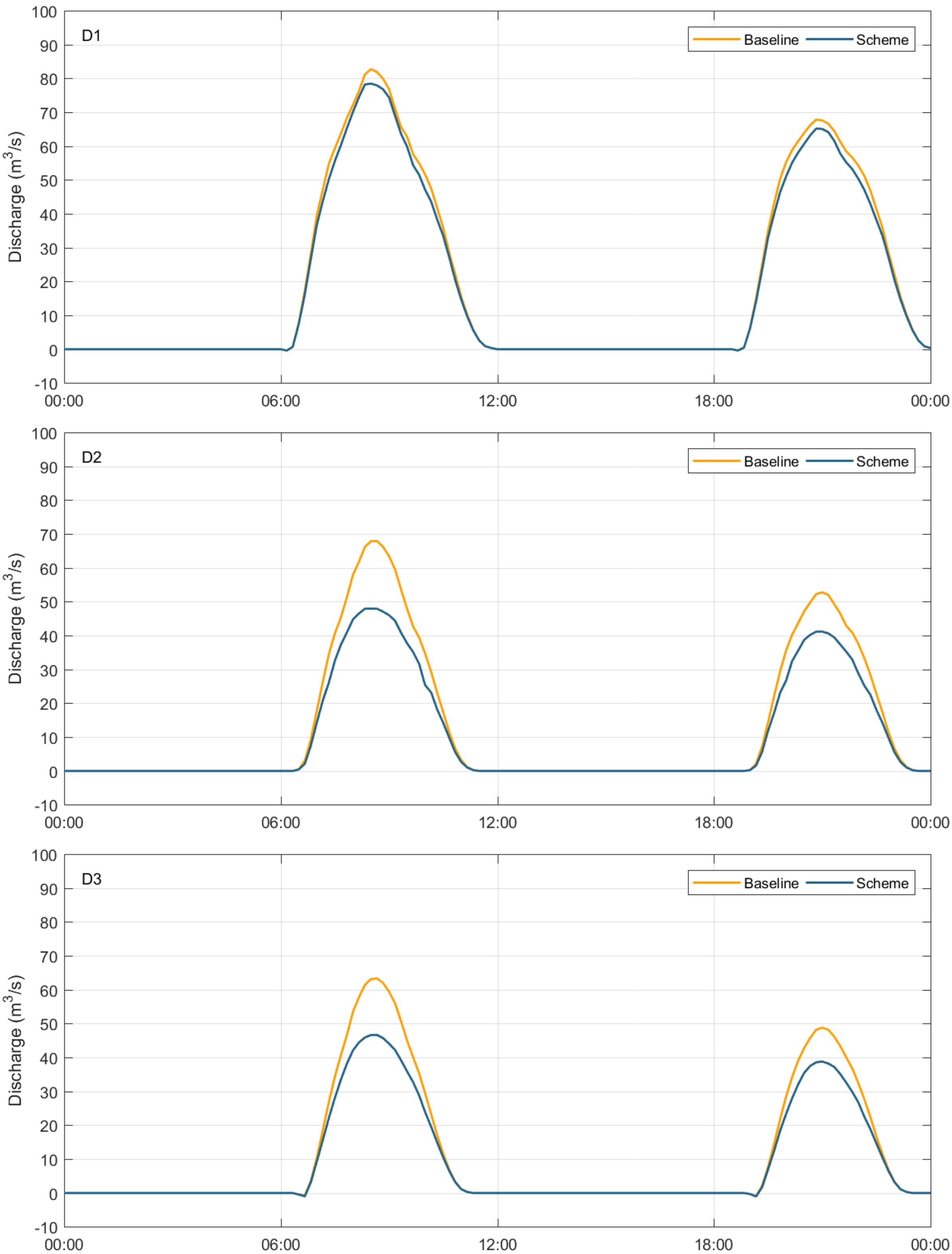

Figure 33. Time series of discharge across D1, D2 and D3 for the 1 in 35 year wave event

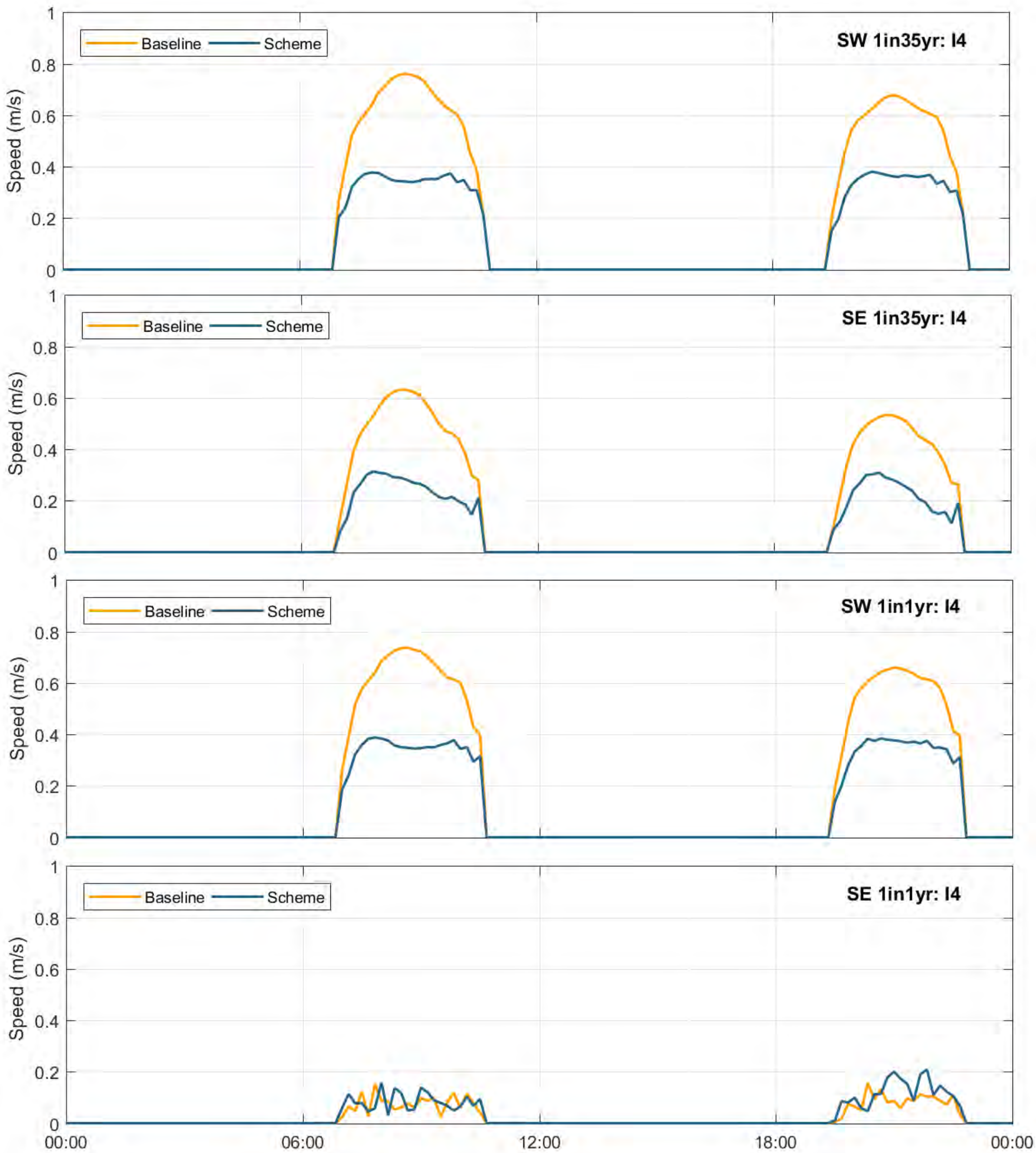

Figure 34. Time series of baseline and scheme flows at location I4 for the four wave conditions modelled

5.2 Sediment transport

To assess the effect of the proposed coastal defence scheme on potential sand transport across Tremadoc Bay, the MIKE ST model has been run coupled with the MIKE HD and SW models. The coupled model has been setup to simulate the sand transport on a HAT for the four wave conditions defined in Table 6. A spatially uniform grain size of 0.2 mm diameter has been applied in the model; in areas where coarser sediments occur the model may therefore over predict the sediment transport rates. Surficial sediments at the seaward end of these sections are known to be presently comprised of cobbles and shingle (see Figure 35 for indicative sediment types). However, beach nourishment between the groynes will comprise of sandy material similar to the lower foreshore, so the model has therefore been setup to represent sand transport.

The sediment transport has been quantified across six longitudinal sections extending in an offshore direction. The locations of the sections are shown in Figure 35. The defined sections include sections to the west (approximately 30 m from Groyne 4) and east (approximately 50 m from Groyne 1) of the scheme footprint and sections extending offshore from each groyne structure (except Groyne 3a).

The net sediment transport across each section has been quantified over a single tidal cycle (for HAT) for each of the wave events modelled. The net transport has been quantified for the total length of the section (which extend more than 1.5 km into the area of zero alongshore transport) and for the inshore 500 m of the section. Results are tabulated in Table 8 to Table 15 and an example of the graphical presentation of the result is shown in Figure 36 to Figure 38. Time series of instantaneous sediment transport have also been generated (see for example Figure 39). A full set of graphs are provided for all sections and wave conditions in Appendix B. All results are solid volumes of sediment and do not account for porosity.

A number of observations can be made from the results presented:

- The net transport across each section is positive indicating a transport from the southwest to the northeast. This is true of all wave conditions for both the present day and post implementation of the coastal defence scheme (and for both the full offshore section and the inshore part of the section), except for the inner part of the easternmost section for a 1 in 1 year wave from the southeast when there is a small net transport to the southwest;
- The effect of the coastal defences on the net sediment transport is a reduction, except across SG4 where there is small increase. This increased transport results from changes at the landward end of the section, where the set back of Beach 3 results in faster flows into the embayment. All the predicted changes in sand transport are small in respect to the net baseline transport which occurs; and
- Even for the extreme events modelled, changes in sediment transport are mainly confined to within 500 m offshore of the groyne structures and are not expected to extend more than 200 m to the west or east of the scheme footprint.

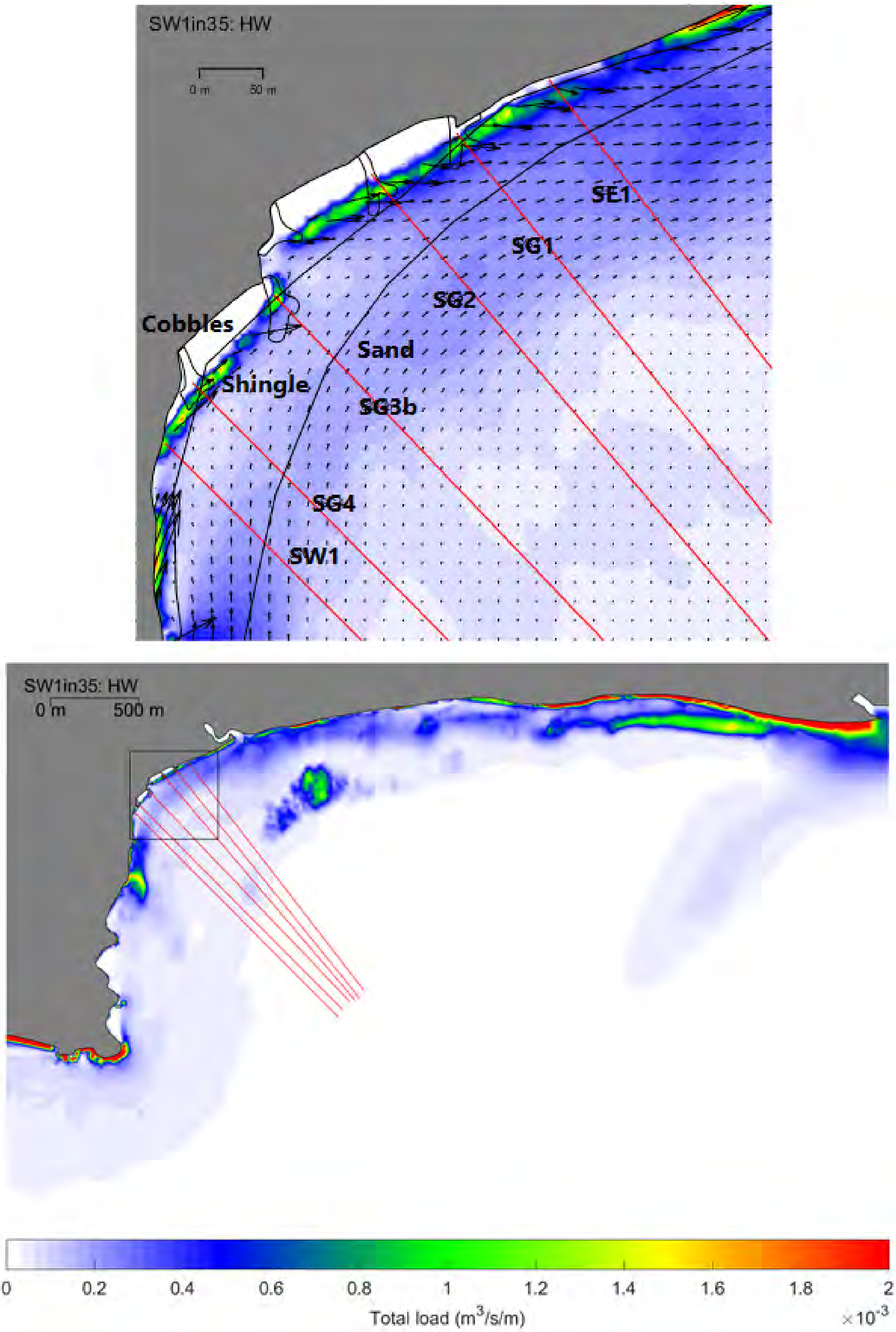

Sediment type i.e. cobbles, shingle and sand are shown for indicative purposes only.
A 0.2 mm sand has been used as the grain size in the model.

Figure 35. Location of the sediment transport sections with baseline surficial sediment zones indicated

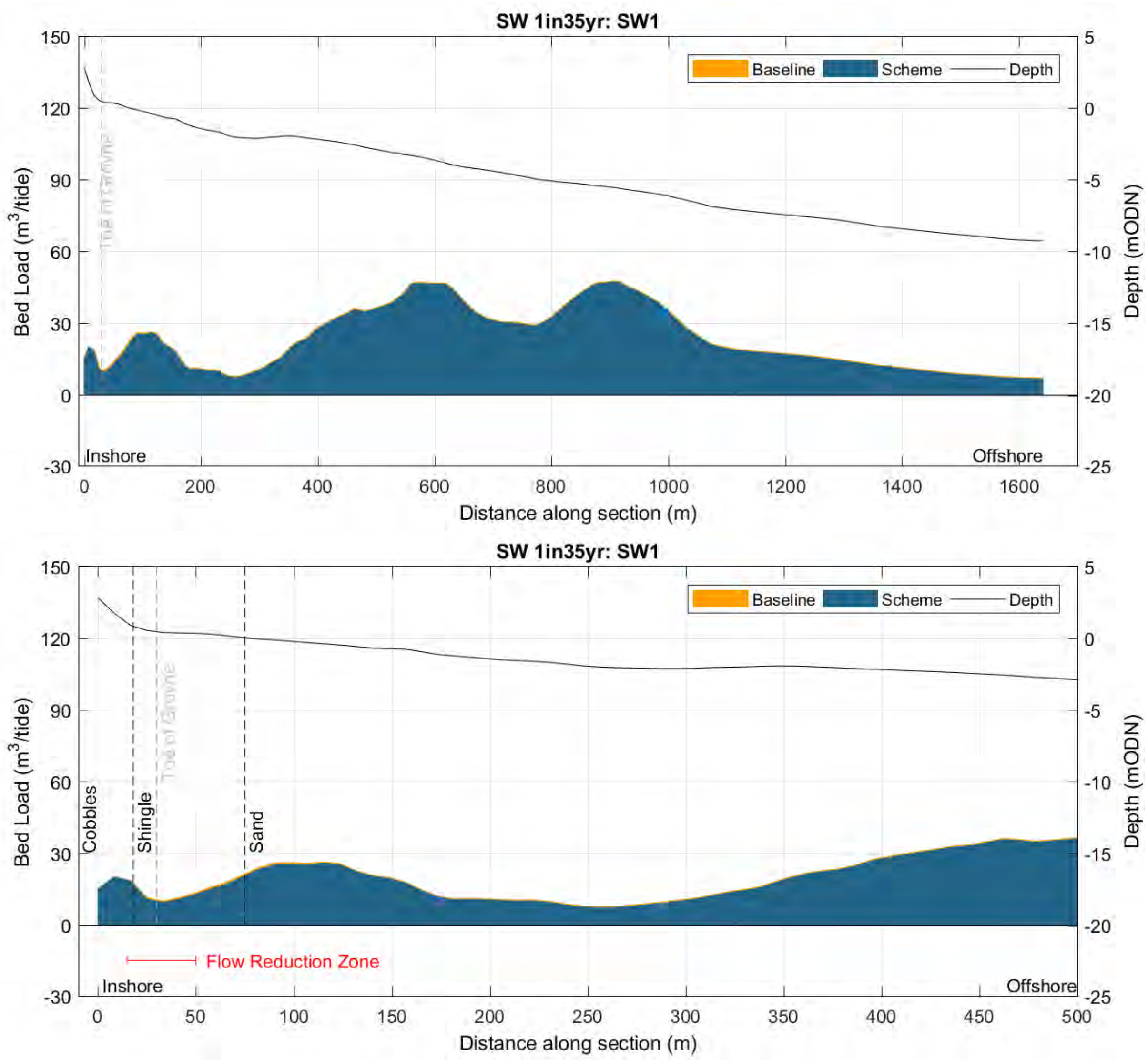

Positive values indicate transport to the northeast and negative values indicated transport to the southwest.
Sediment type i.e. cobbles, shingle and sand are shown for indicative purposes only.
A 0.2 mm sand has been used as the grain size in the model.

Figure 36. Sediment transport across SW1 for 1 in 35 year wave from the southwest

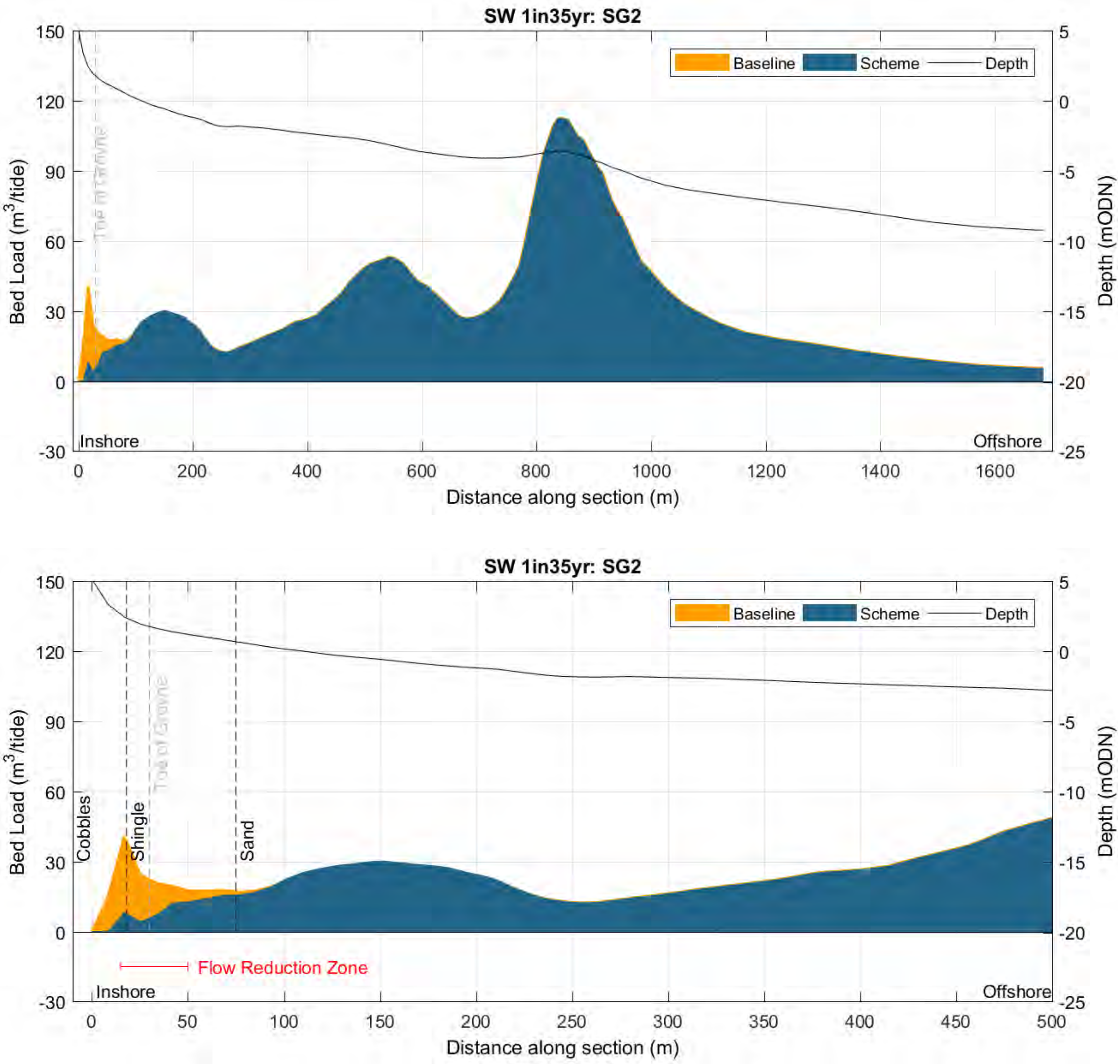

Positive values indicate transport to the northeast and negative values indicated transport to the southwest.
Sediment type i.e. cobbles, shingle and sand are shown for indicative purposes only.
A 0.2 mm sand has been used as the grain size in the model.

Figure 37. Sediment transport across SG2 for 1 in 35 year wave from the southwest

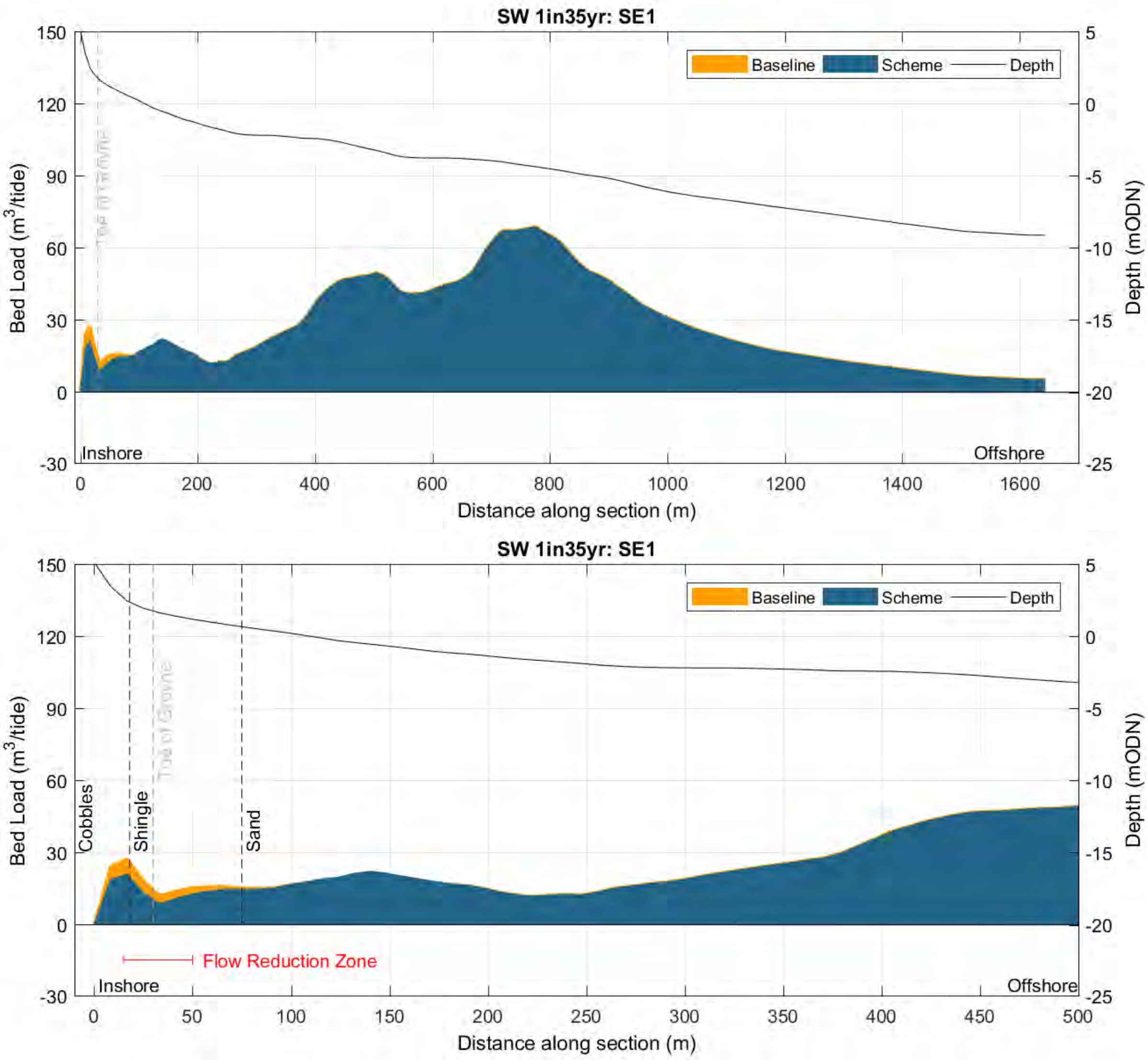

Positive values indicate transport to the northeast and negative values indicated transport to the southwest.
Sediment type i.e. cobbles, shingle and sand are shown for indicative purposes only.
A 0.2 mm sand has been used as the grain size in the model.

Figure 38. Sediment transport across SE1 for 1 in 35 year wave from the southwest

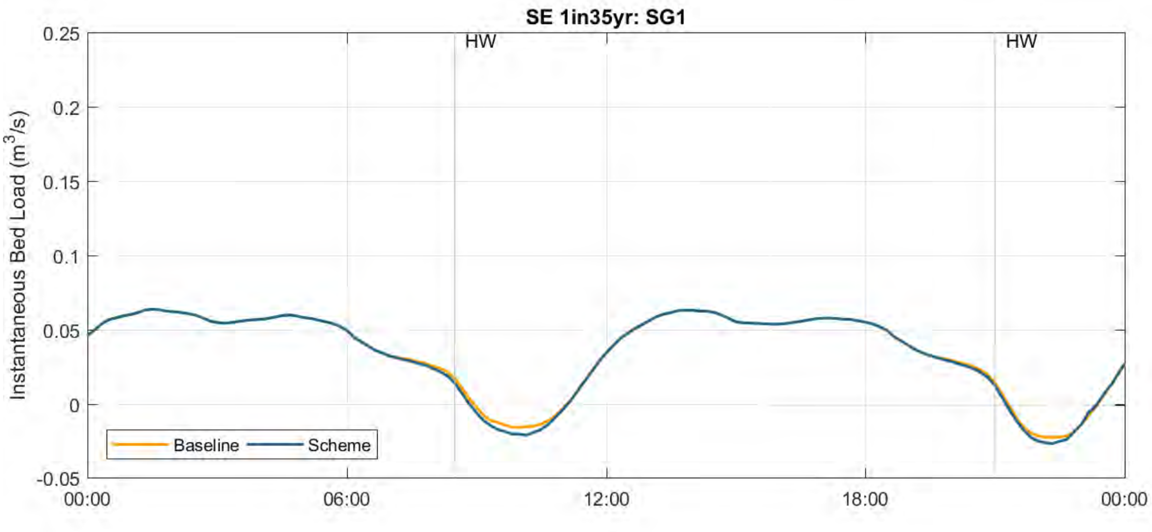

Positive values indicate transport to the northeast and negative values indicated transport to the southwest.

Figure 39. Time series of instantaneous sediment transport across SG1 for 1 in 35 year wave from the southeast

Table 8. Sand transport rates for 1 in 35 year wave event from the southwest

Section	Sand Transport (m^3/tide)		Difference (m^3/tide)	Difference (%)
	Baseline	Scheme		
SW1	4617	4615	-2	0
SG4	5162	5179	17	0
SG3b	7389	7365	-24	0
SG2	6255	6168	-87	-1
SG1	5426	5360	-66	-1
SE1	5551	5526	-25	0

Note that a uniform sediment grain size of 0.2 mm has been applied in the model
Values given are solid volumes and do not account for porosity
Values are for a single extreme tidal cycle (1 in 1 year tide and 1 in 35 year wave)
Differences are scheme minus baseline

Table 9. Sand transport rates for 1 in 35 year wave event from the southwest, survey area only

Section	Sand Transport (m^3/tide)		Difference (m^3/tide)	Difference (%)
	Baseline	Scheme		
SW1	1192	1190	-2	0
SG4	1210	1227	17	-1
SG3b	1480	1456	-24	2
SG2	1539	1452	-87	6
SG1	1396	1330	-66	5
SE1	1498	1474	-25	2

Note that a uniform sediment grain size of 0.2 mm has been applied in the model
Values given are solid volumes and do not account for porosity
Values are for a single extreme tidal cycle (1 in 1 year tide and 1 in 35 year wave)
Differences are scheme minus baseline

Table 10. Sand transport rates for 1 in 35 year wave event from the southeast

Section	Sand Transport (m^3/tide)		Difference (m^3/tide)	Difference (%)
	Baseline	Scheme		
SW1	1878	1875	0	0
SG4	2115	2144	29	1
SG3b	3386	3366	-20	-1
SG2	2423	2375	-48	-2
SG1	1729	1687	-42	-2
SE1	1654	1631	-24	-1

Note that a uniform sediment grain size of 0.2 mm has been applied in the model
Values given are solid volumes and do not account for porosity
Values are for a single extreme tidal cycle (1 in 1 year tide and 1 in 35 year wave)
Differences are scheme minus baseline

Table 11. Sand transport rates for 1 in 35 year wave event from the southeast, survey area only

Section	Sand Transport (m^3/tide)		Difference (m^3/tide)	Difference (%)
	Baseline	Scheme		
SW1	824	819	-5	-1
SG4	805	832	27	3
SG3b	908	885	-23	-3
SG2	737	687	-50	-7
SG1	524	481	-44	-8
SE1	418	392	-26	-6

Note that a uniform sediment grain size of 0.2 mm has been applied in the model
Values given are solid volumes and do not account for porosity
Values are for a single extreme tidal cycle (1 in 1 year tide and 1 in 35 year wave)
Differences are scheme minus baseline

Table 12. Sand transport rates for 1 in 1 year wave event from the southwest

Section	Sand Transport (m^3/tide)		Difference (m^3/tide)	Difference (%)
	Baseline	Scheme		
SW1	3498	3996	-2	0
SG4	3896	3925	29	1
SG3b	5761	5736	-26	0
SG2	4833	4753	-79	-2
SG1	4149	4086	-63	-2
SE1	4255	4233	-22	-1

Note that a uniform sediment grain size of 0.2 mm has been applied in the model
Values given are solid volumes and do not account for porosity
Values are for a single extreme tidal cycle (1 in 1 year tide and 1 in 1 year wave)
Differences are scheme minus baseline

Table 13. Sand transport rates for 1 in 1 year wave event from the southwest, survey area only

Section	Sand Transport (m^3/tide)		Difference (m^3/tide)	Difference (%)
	Baseline	Scheme		
SW1	938	935	-2	0
SG4	944	973	29	3
SG3b	1155	1129	-26	-2
SG2	1192	1113	-79	-7
SG1	1068	1005	-63	-6
SE1	1120	1097	-22	-2

Note that a uniform sediment grain size of 0.2 mm has been applied in the model
Values given are solid volumes and do not account for porosity
Values are for a single extreme tidal cycle (1 in 1 year tide and 1 in 1 year wave)
Differences are scheme minus baseline

Table 14. Sand transport rates for 1 in 1 year wave event from the southeast

Section	Sand Transport (m^3/tide)		Difference (m^3/tide)	Difference (%)
	Baseline	Scheme		
SW1	434	433	-1	0
SG4	417	445	28	7
SG3b	637	625	-12	-2
SG2	348	352	4	1
SG1	212	210	-2	-1
SE1	242	240	-2	-1

Note that a uniform sediment grain size of 0.2 mm has been applied in the model
Values given are solid volumes and do not account for porosity
Values are for a single extreme tidal cycle (1 in 1 year tide and 1 in 1 year wave)
Differences are scheme minus baseline

Table 15. Sand transport rates for 1 in 1 year wave event from the southeast, survey area only

Section	Sand Transport (m^3/tide)		Difference (m^3/tide)	Difference (%)
	Baseline	Scheme		
SW1	298	297	-1	0
SG4	256	283	28	11
SG3b	241	229	-12	-5
SG2	112	116	4	4
SG1	28	27	-2	-5
SE1	-13	-14	-1	-5

Note that a uniform sediment grain size of 0.2 mm has been applied in the model
Values given are solid volumes and do not account for porosity
Values are for a single extreme tidal cycle (1 in 1 year tide and 1 in 1 year wave)
Differences are scheme minus baseline

5.3 Beach drawdown

Wave and water level conditions have been extracted from the local area model and used to drive the profile evolution tool in MIKE 21. The model has been set up to assess the cross shore drawdown for a selection of extreme events, with a particular focus on the new beaches.

The beach drawdown for each of the profiles and for each of the wave scenarios modelled has been quantified in Table 16. Values are given as areas for the cross section (i.e. to obtain an estimate of volume would need to multiply by the along shore extent of the beach). Positive values indicate a drawdown (loss). Beach drawdown areas have also been quantified for the part of the section offshore of the toe of the structures; these values are all negative indicating that material drawn down from higher up the beach has been deposited in this part of the section. For reference, the area of beach nourishment for each section is also provided. The beach drawdown is largest on Beach 3 (which is most exposed to waves) with approximately 15 to 20 % of the beach nourishment material drawn down during a 1 in 35 year wave event (for both waves from the southwest and waves from the southeast) on a HAT. In terms of levels this is a reduction in bed level of around 0.33 m. Comparably, for a 1 in 1 year wave event approximately 5 % of the beach nourishment material was drawn down Beach 3.

Table 16. Beach drawdown for different wave conditions

Parameter		Area of Beach Drawdown Along Section (m^2)		
		Beach 1	Beach 2	Beach 3
Beach nourishment along section (m^2)		33	47	40
Area of drawdown	1 in 35 year wave from southwest	5	6	7
	1 in 35 year wave from southeast	-	4	7
	1 in 1 year wave from southwest	2	2	2
Area of drawdown offshore *	1 in 35 year wave from southwest	-4	-5	-3
	1 in 35 year wave from southeast	-	-2	-2
	1 in 1 year wave from southwest	-1	0	0
* drawdown in area offshore of toe of structures Negative values indicate that sediment is deposited in the offshore area				

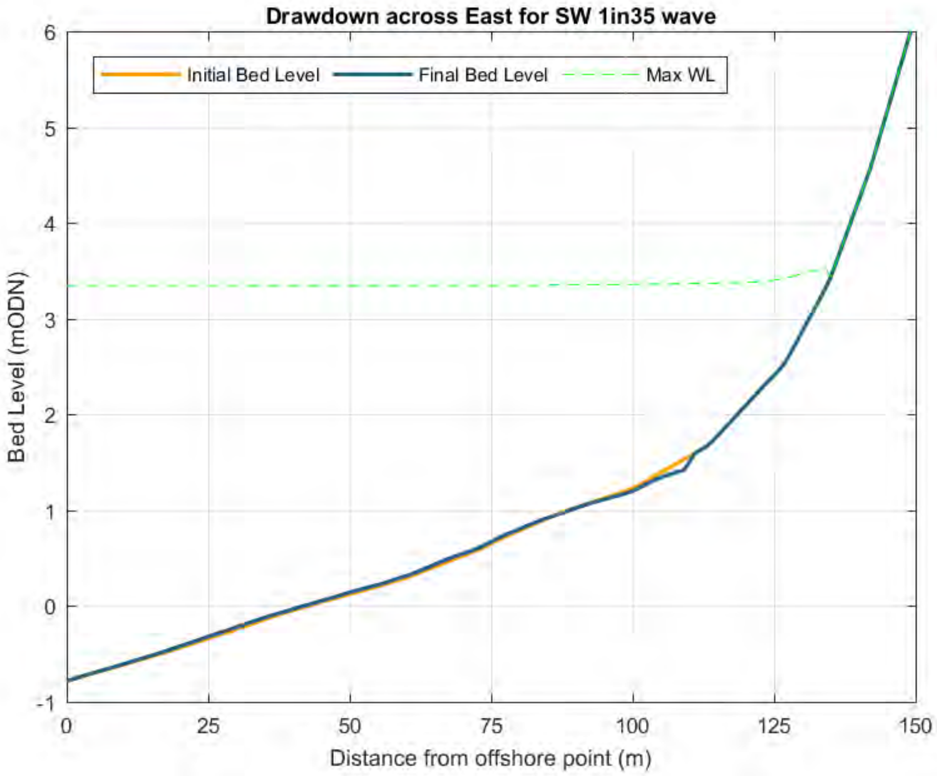

The dotted blue line shows the results for the smaller roughness length

Figure 40. Beach drawdown on East profile during 1 in 35 year wave event from the southwest

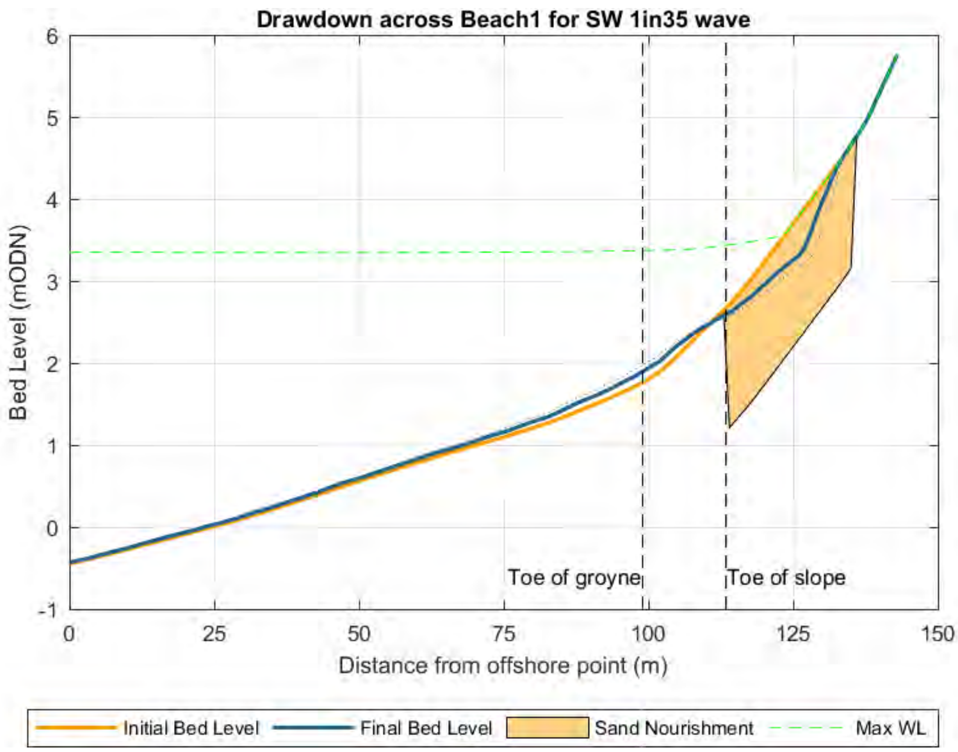

The dotted blue line shows the results for the smaller roughness length.

Figure 41. Beach drawdown on Beach 1 during 1 in 35 year wave event from the southwest

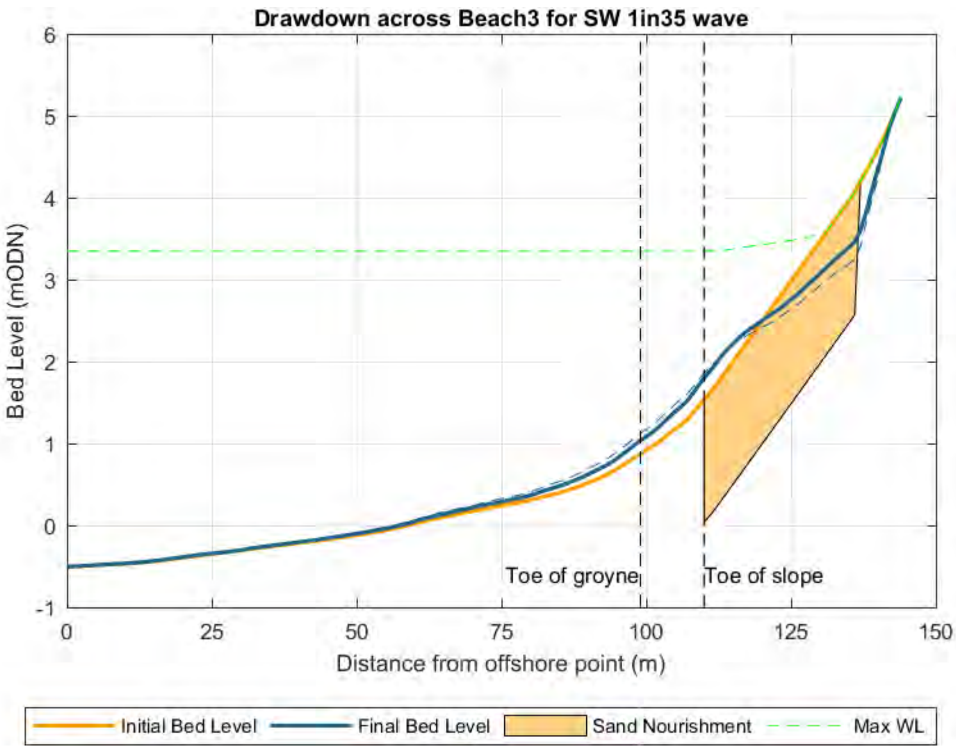

The dotted blue line shows the results for the smaller roughness length.

Figure 42. Beach drawdown on Beach 3 during 1 in 35 year wave event from the southwest

5.4 Sensitivity test

A sensitivity test in which one of the groynes (Groyne 2, refer to Figure 1 for location) was removed has been undertaken. This modified scheme design (referred to as Scheme 2) was considered to help inform an assessment of the suitability of the groyne spacing in the proposed design. The effect of Scheme 2 on flows and sediment transport was modelled for the 1 in 35 year wave from the southwest and the 1 in 35 year wave from the southeast. The effect for 1 in 1 year wave conditions was not considered.

The removal of Groyne 2 from the scheme resulted in a reduction in the sheltering effect of the development on the upper foreshore, therefore yielding faster flows on Beach 1 (see Figure 1 for location) than the original scheme design. However, there is still a reduction in flows relative to the baseline. The flows on Beach 1 at location I4 are shown for the baseline, the original scheme and the updated scheme (scheme 2) in Figure 43 for the wave from the southwest. Flow are reduced from 0.75 m/s for the baseline, to 0.55 m/s for scheme 2 (compared to 0.4 m/s for the original scheme). The subsequent effect of the reduced flow reduction on sediment transport is shown in Figure 44.

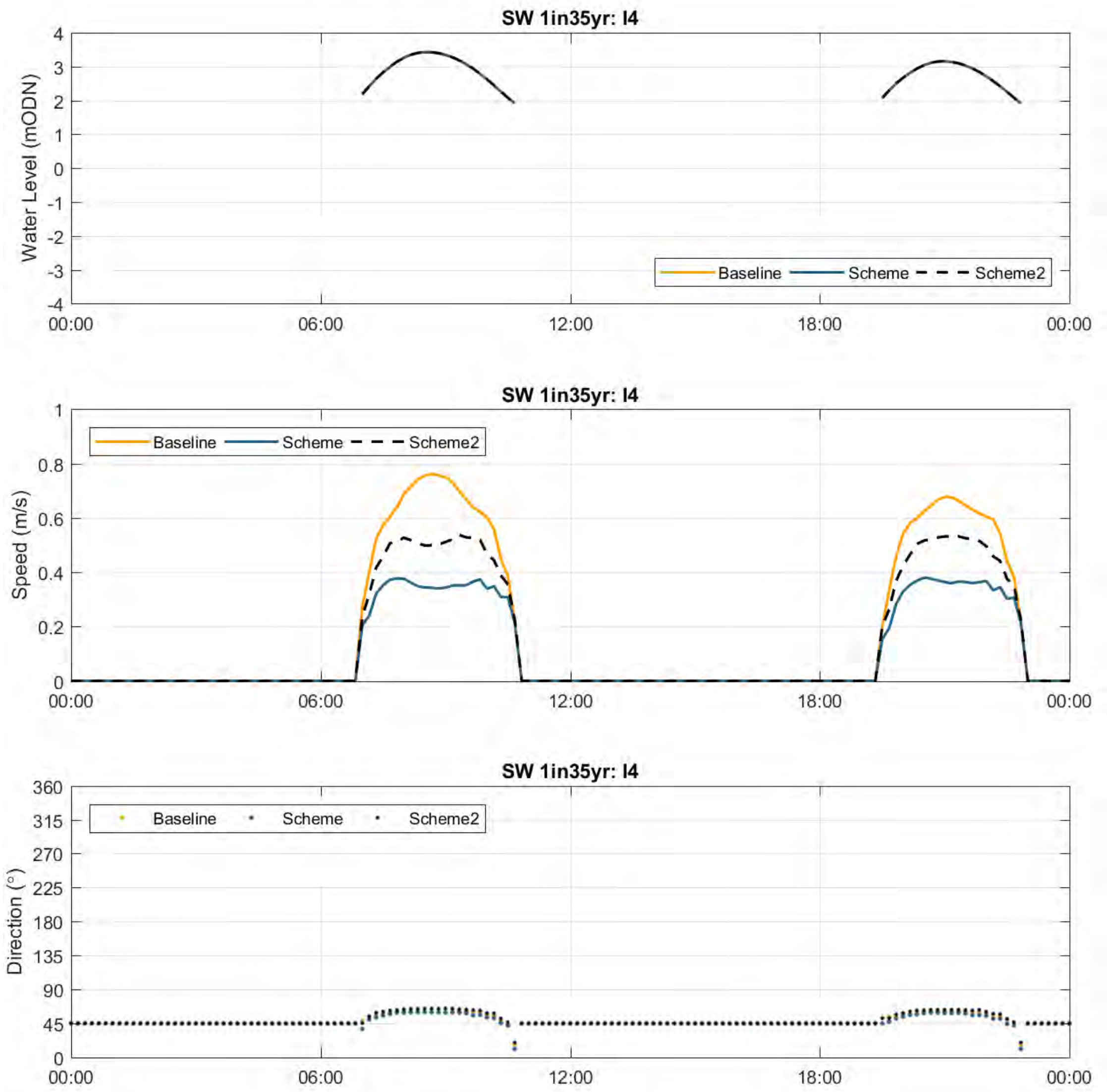

Figure 43. **Time series of water level, flow speed and flow direction at I4 for the baseline and scheme runs for the 1 in 35 year wave from the SW**

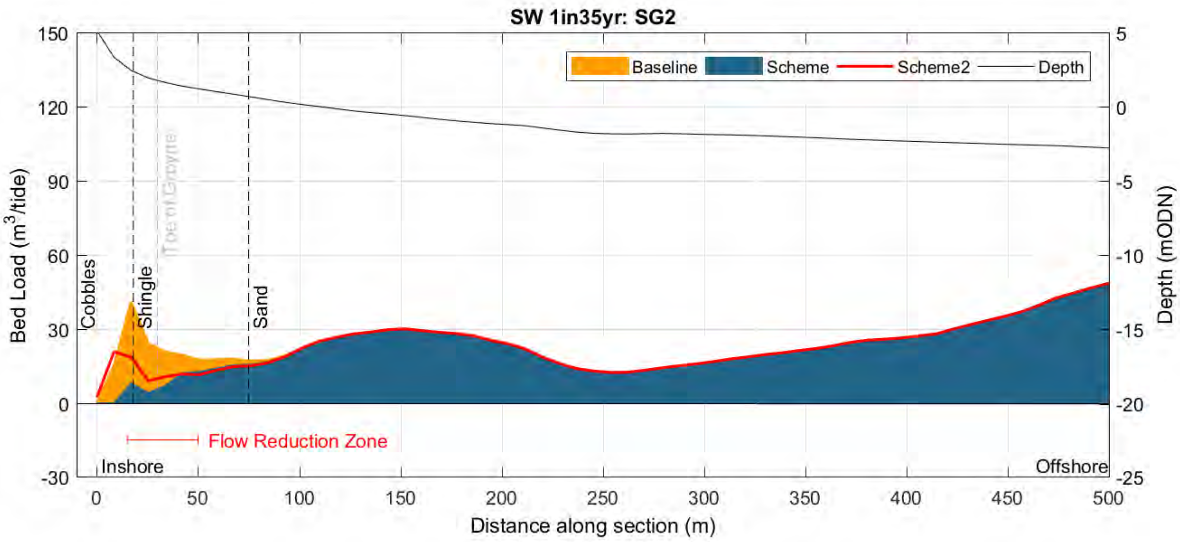

Sediment type i.e. cobbles, shingle and sand are shown for indicative purposes only.
A 0.2 mm sand has been used as the grain size in the model.

Figure 44. Sediment transport across SG2 for 1 in 35 year wave from the southwest

6 Discussion

The proposed Hafan y Môr coastal defences would be located high in the tidal frame and would include the construction of five fishtail shaped rock-armour groynes and a setting back of the existing beach to allow a net landward realignment of the Mean High Water Spring elevation. This realignment would be achieved through excavation of the existing land form and the addition of beach recharge material. ABPmer was commissioned to model this scheme to achieve the following:

- enhance the understanding of the present day coastal processes at Hafan y Môr; and
- assess the likely impacts of the proposed new coastal defence scheme on these processes.

These study objectives were achieved through the development of a set of bespoke modelling tools which simulate tidal variations and the wave climate in the study region, as well as the alongshore and cross-shore sediment transport associated with a number of extreme tide and wave events. Model simulations for both the 'baseline' and the 'scheme' conditions were undertaken. The modelling indicates that tidal flows in the study area are weak and are unlikely to contribute directly to sediment transport. Waves approach the coast from a relatively narrow band, predominantly driving eastward flows along the coast in the study area (particularly in the western section of the frontage). Wave-driven flows during extreme events are sufficient to transport sand material in suspension.

Even for the extreme conditions modelled, the effects of the scheme on flows (combined wave and tide) are highly localised, with changes of more than 0.1 m/s constrained to within approximately 50 m of the groynes in an offshore direction. Given the high elevation of the scheme in the tidal frame, the proposed coastal defence scheme is only inundated on some tides and for limited periods (over high water) and therefore any changes can only occur during these short immersion periods.

The proposed groyne structures provide sheltering of the new beach areas and reduce alongshore transport on the upper foreshore. Even during storm periods, changes to alongshore sediment transport will be limited and negligible at distances of over 50 m down shore of the groynes. Similarly estimates of beach drawdown obtained from the profile evolution tool indicate relatively small cross shore transport for the storms simulated when compared to the amounts of beach recharge material.

In addition to the main objectives of this review, this study has helped inform the following scheme design objectives:

- Ensure that there is negligible alongshore impact of the scheme;
- Identify the expected sand losses during the service life (20 years) of the scheme; and
- Ensure that the geometry and spacing of the groynes is optimised.

The modelling assessments strongly indicate that the scheme has limited impact on adjacent areas. The scheme's situation, high in the tide frame, inherently limits the impact it would have on existing littoral processes. Sand losses during the service life have not directly been assessed by the model but the beach drawdown associated with a limited number of storm conditions has been quantified and this analysis indicate that the drawdown effect during individual storm events is relatively small compared to the amount of beach recharge material. The extensive modelling undertaken for the proposed scheme, along with the modelling of an alternative scheme (with the omission of one of the groynes), provides an indication of the sheltering effect of the groynes which can be used to inform an assessment of their suitability.

7 References

ABPmer. (2000). Climate Change and Coastal Erosion. ABP Marine Environmental Research Ltd, Report No. R.1111.

ABPmer (2013). SEASTATES Wave Hindcast Model: Calibration and Validation Report. ABP Marine Environmental Research Ltd, Report No. R.2145.

ABPmer (2017). SEASTATES North West European Continental Shelf Tide and Surge Hindcast Database Model Validation Report. ABPmer, Report No. R.2784.

DHI (2017). MIKE 21 Spectral Waves FM, Spectral Waves Module, User Guide, 120 pp.

Hedges, T (2010). Wave processes training course: Linear wave theory and nearshore processes. Presented to ABPmer, September 2010.

Le Mehaute, B., R.C.U Koh and L-S Hwang (1968), A synthesis on wave run-up. Journal of waterways and Harbours Division, American Society of Civil Engineers, Vol. 94, No. WW1, February 1968, pp. 77-92.

MAFF (2000). Flood and coastal defence project appraisal guidance. Approaches to risk. A procedural guide for operating authorities. Ministry of Agriculture, Fisheries and Food. FCDPAG4, 2000.

8 Abbreviations/Acronyms

1D	One dimension(al)
2D	Two dimension(al)
ABPmer	ABP Marine Environmental Research Ltd
AOD	Above Ordnance Datum
c.	*Circa*
DHI	Danish Hydraulic Institute
FM	Flexible mesh
HAT	Highest Astronomical Tide
HD	Hydrodynamic
HW	High Water
MHWN	Mean high water neap
MHWS	Mean high water spring
MLWN	Mean low water neap
MLWS	Mean low water spring
NRW	Natural Resources Wales
SAC	Special Area of Conservation
ST	Sediment transport
SW	Spectral Wave
UKHO	United Kingdom Hydrographic Office

Cardinal points/directions are used unless otherwise stated.

SI units are used unless otherwise stated.

9 Nomenclature

A	wave orbital amplitude
Asb	bed load coefficient
Ass	suspended load coefficient
Cd	drag coefficient
D	wave energy dissipation
D_{50}	median grain diameter
D_{90}	grain diameter that 90% of the sediment is finer
D*	dimensionless particle size
Hs	significant wave height
L	wavelength
T_p	peak wave period
U	current speed
U_{rms}	R.M.S. wave orbital speed
U_w	maximum wave orbital velocity
V_a	volume of sediment accreted (XBeach)
V_e	volume of sediment eroded (XBeach)
X	cross-shore distance (zero = + 4 m AOD)
X_b	measured pre-storm beach profile
X_m	measured post-storm beach profile
X_x	predicted post-storm beach profile from XBeach
Y	horizontal alongshore coordinates
c_f	bed friction coefficient
f_{morf}	morphological 'acceleration' term
f_p	peak frequency
f_w	wave friction factor
g	gravitational acceleration
h	water depth
k_s	Nikuradse grain roughness
p	sediment porosity
r	relative roughness
s	ratio of densities between sediment and sea water (~ 2.58)
t	time
u	flow velocity in x-direction
u_{crit}	critical flow velocity for sediment entrainment
$u_{cr,c}$	critical flow velocity for sediment entrainment due to currents only
$u_{cr,w}$	critical flow velocity for sediment entrainment due to waves only
u_m	time and depth-averaged flow velocity
u_{rms}	near-bed short wave orbital motion
v	flow velocity in y-direction
w_s	sediment fall velocity
z	vertical coordinate
z_b	bed level
z_0	bed roughness length

θ	wave direction (degrees N)
β	bed slope
γ	wave breaking calibration parameter
ν	kinematic viscosity
ρ_s	mass density of sand
ρ_w	mass density of water
θ_{ws}	wave skin friction Shields parameter
τ_{crit}	critical skin friction bed shear stress for sediment entrainment
τ_w	wave period-averaged shear stress
τ_{wc}	total (combined wave and current) skin friction bed shear stress
τ_{ws}	wave-only skin friction bed shear stress
ω	wave mobility number

Appendices




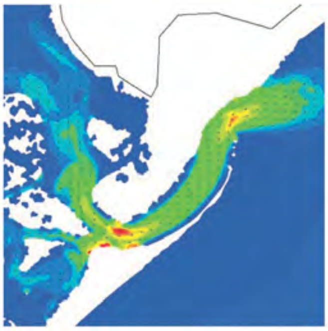


Innovative Thinking - Sustainable Solutions

ABP mer

A Additional Information

This appendix provides additional information requested by the client. This includes additional technical information on the MIKEFM SW model, including its limitations (section A1), Annual wave roses from the regional wave model (section A2), an indication of wave breaking and run up (section A3) and an assessment of wave energy density (section A4).

A.1 The MIKEFM SW Model

Full details on the MIKE FM SW model can be found in DHI (2017).

The MIKE 21 SW model includes the following physical phenomena:

- Wave growth by action of wind
- Non-linear wave-wave interaction
- Dissipation due to white-capping
- Dissipation due to bottom friction
- Dissipation due to depth-induced wave breaking
- Refraction and shoaling due to depth variations
- Wave-current interaction
- Effect of time-varying water depth and flooding and drying

Diffraction and reflection are not included in the model.

One assumption of the MIKE21 SW model is that linear wave theory is applicable. Linear wave theory assumes the following (Hedges, 2010):

- The waves described have heights which are small compared with the wavelength and the water depth $H/L < 0.04$.
- Water is homogeneous and incompressible and so it has a uniform density;
- The water lacks viscosity and surface tension;
- The waves are long-crested;
- The waves are of constant form i.e. they do not change shape as they travel across the water surface;
- The seabed is horizontal and impermeable;
- The waves are propagating on quiescent water i.e. there is no motion of the water apart from that induced by the waves.

The Ursell number provides an indication of which wave theory is most applicable. Figure A1 shows a map of Ursell number for the 1 in 35 southeast wave. Most of the area modelled has an Ursell number less than 40 and hence linear wave theory is well suited. Towards the beaches where the bathymetry is shallower, the Ursell number is higher than 40 and hence Cnodial wave theory becomes more applicable.

In the regions where the Ursell number is higher than 40, the waves crests will become more peaked and troughs become longer and flatter and the assumptions made in linear wave theory start to break down. Despite this, it is broadly accepted that linear wave theory provides a reasonable approximation of the wave conditions, even in regions where the wave theory is not strictly valid with many instances of linear wave theory providing a good level of agreement against measured datasets.

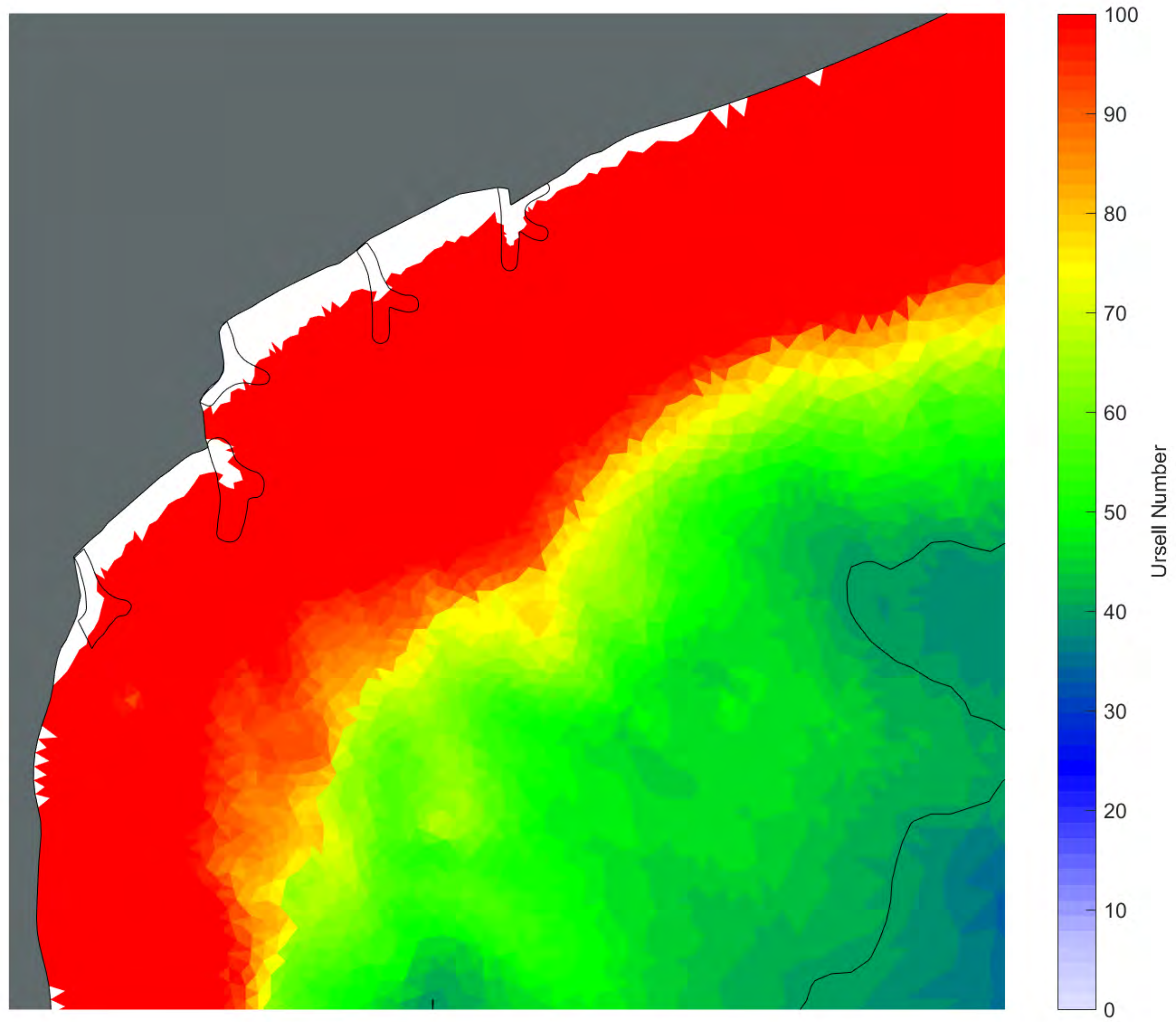

Figure A1. Ursell number for 1 in 35 year wave from the southwest

A.2 Annual Wave Roses at M1

To provide information on how the magnitude and direction of wave conditions varies between years wave roses have been produced for each year in Figure A2 to Figure A5. These wave roses show the conditions at location M1. For directionality, a 10 degree bins size was applied. Only waves with a significant wave height 1.8 m have been considered for this analysis. Waves above 1.8 m occur for approximately 10 storm events per year. The dominant wave directions for larger waves are typically in the 190 to 200° bin and the 200 to 210° bins.

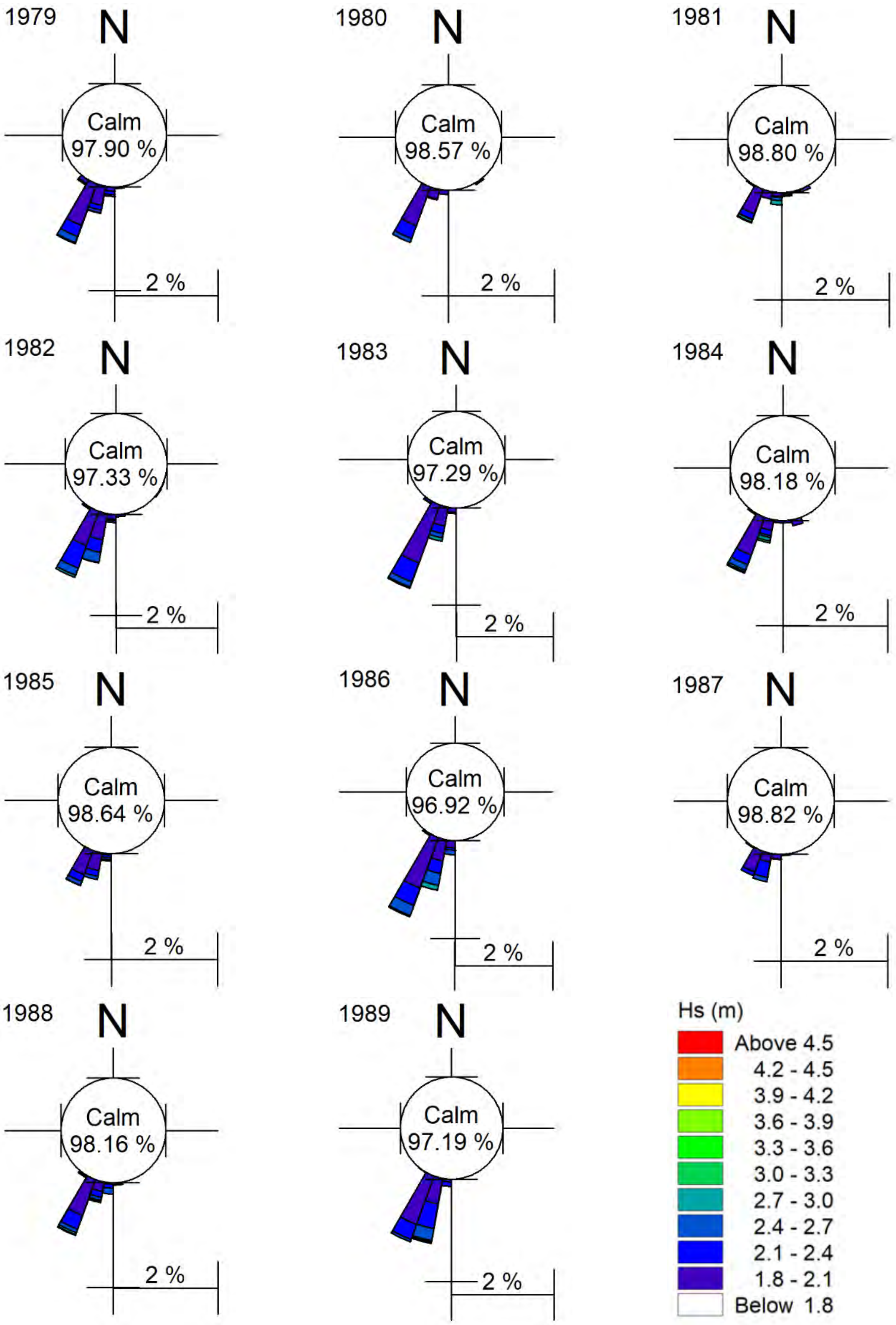

Figure A2. Annual wave roses at M1 for significant wave heights above 1.8 m, 1979-1989

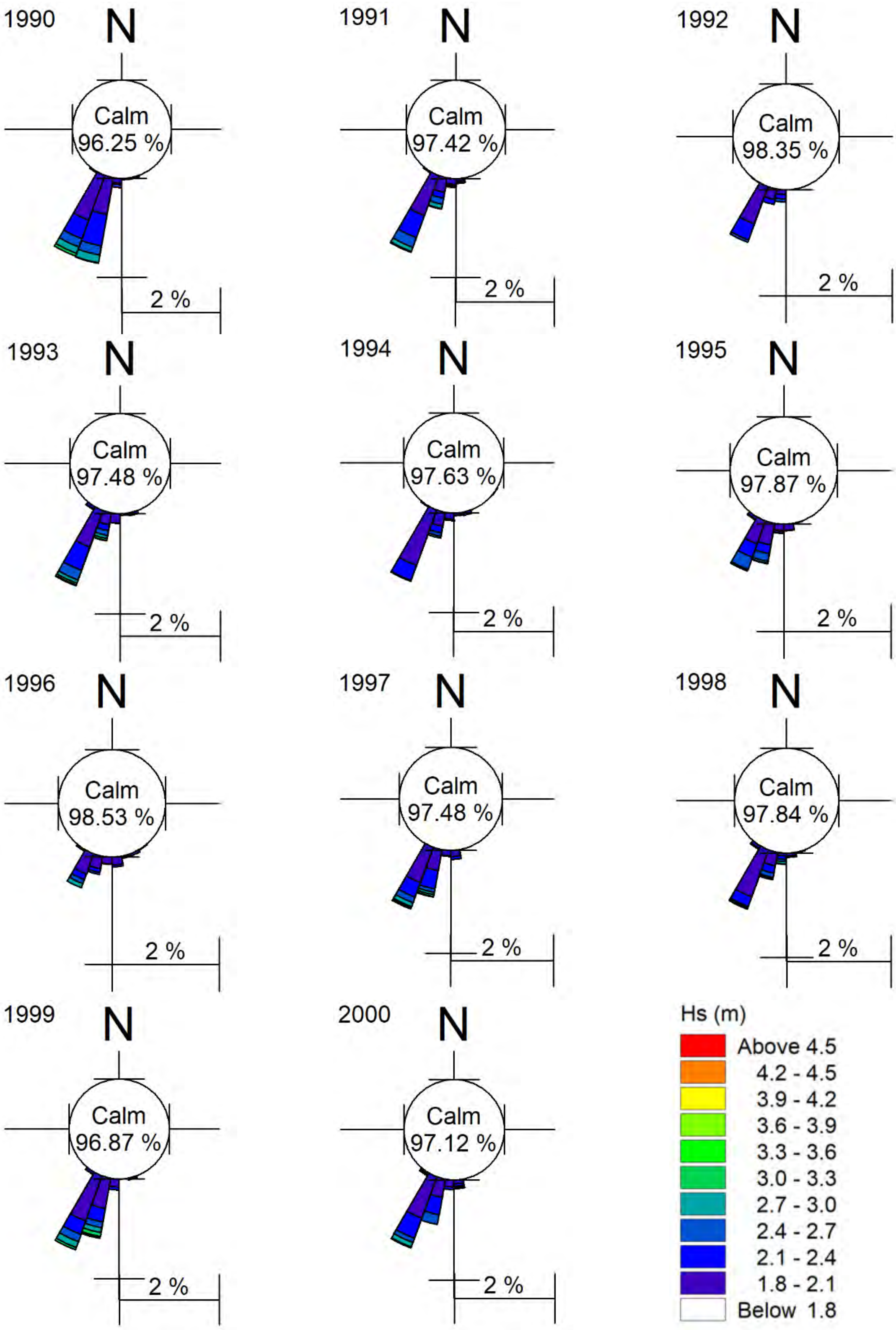

Figure A3. Annual wave roses at M1 for significant wave heights above 1.8 m, 1990-2000

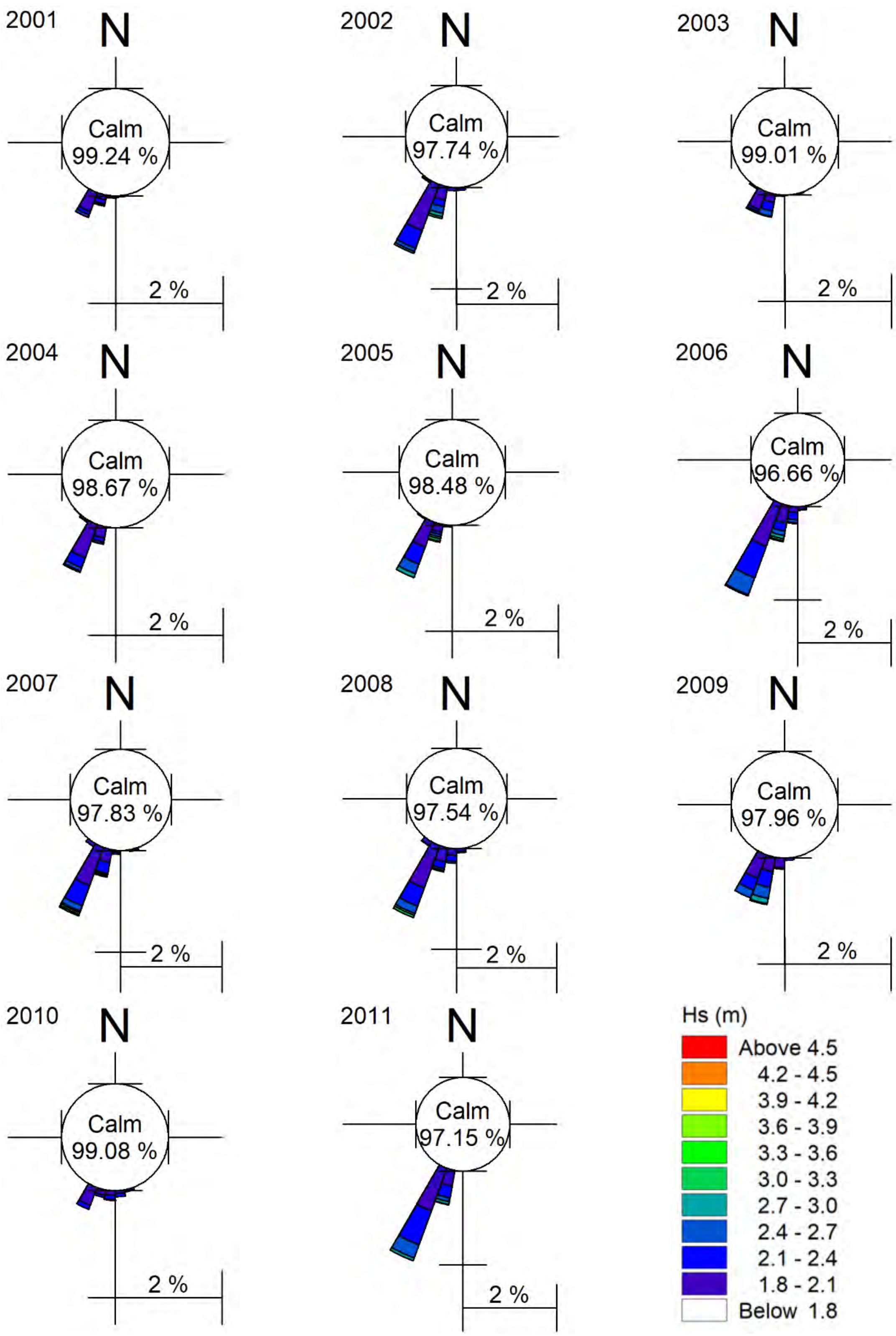

Figure A4. Annual wave roses at M1 for significant wave heights above 1.8 m, 2001-2011

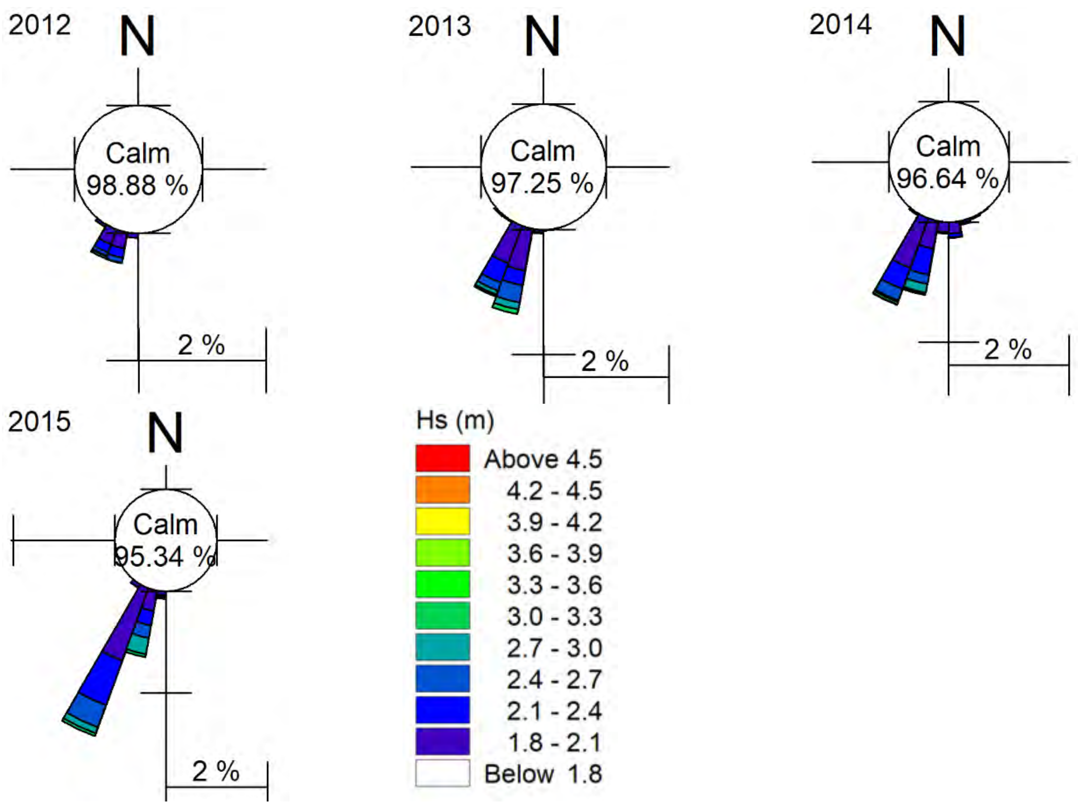

Figure A5. Annual wave roses at M1 for significant wave heights above 1.8 m, 2012-2015

A.3 Wave Breaking and Run Up

Of the various processes to which water waves are subject, wave breaking is one of the most interesting to hydraulic engineers, due to its influence on sediment movement on beaches and the exertion of forces on coastal structures. The process of wave breaking is dependent on the steepness of the waves and the steepness of the slope. Steep waves on gentle slopes will spill water gently from their crests, resulting in little reflection of the incident wave energy. Comparatively long, low waves on steep slopes tend not to break at all and instead will surge up and down the slope with most of the energy being reflected.

The Iribarren number (N_I) is a useful parameter for describing the behaviour of wave on a slope and is given by;

$$N_I = \frac{\tan\beta}{(\frac{H}{L_o})^{1/2}}$$

in which β is the slope angle, wave height *H* is measured at the toe of the slope and L_0 is the wave length.

Values of N_I associated with different types of wave action are shown in Table A1.

Table A1. Iribarren numbers associated with wave types

Wave Parameter	N_I
Spilling	< 0.4
Plunging	0.4 – 2.3
Collapsing	2.3 – 3.2
Surging	>3.2

In general, the maximum wave heights that exist depend on the wave length, the water depth and the sea-bed slope. The maximum wave height is typically referred to as the breaking wave height (H_b). Different formulations have been defined which determine the breaking wave height in deep, intermediate and shallow water depths. The location of wave breaking (i.e. where H_b is greater than Hs) is shown for the HAT tide and for each wave scenario in Figure A6

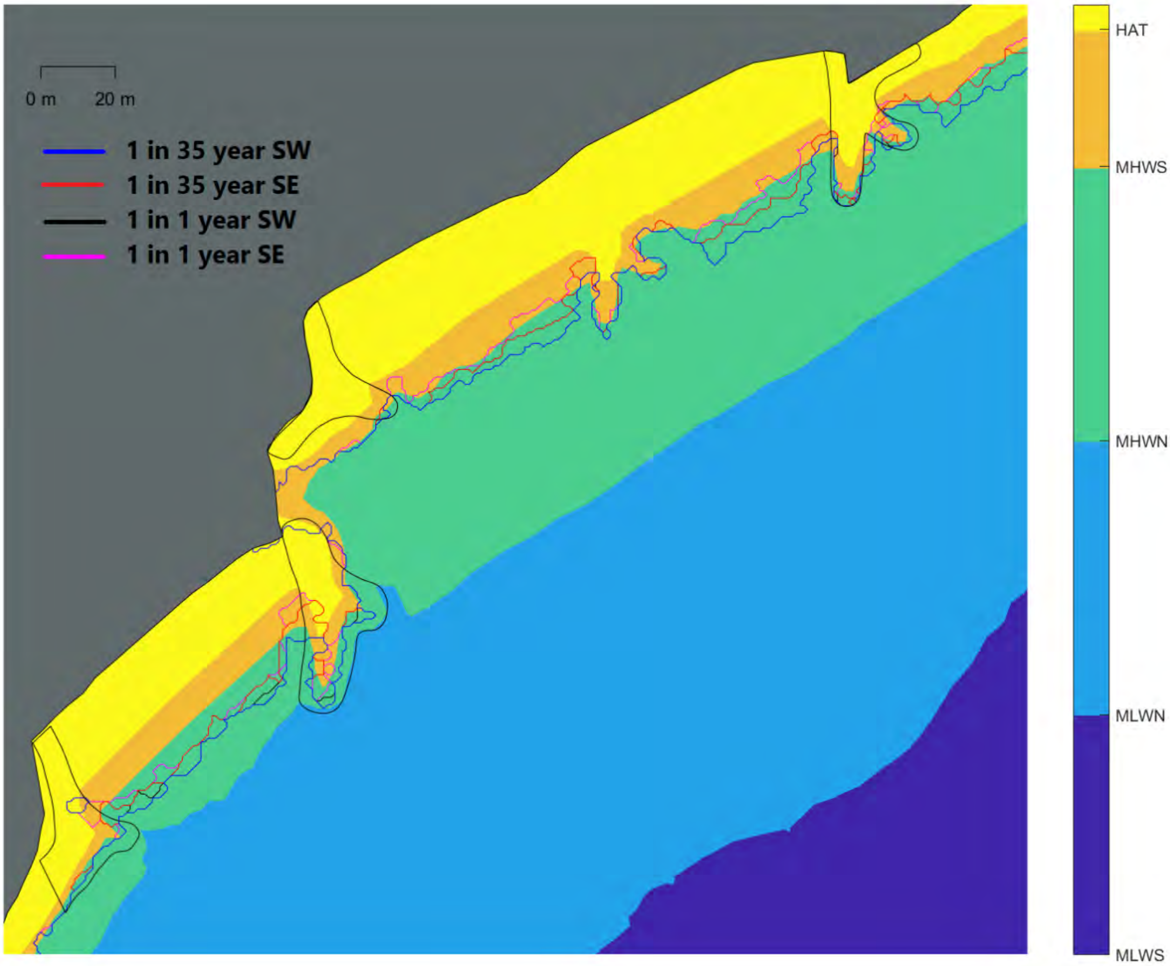

Figure A6. Location of wave breaking

Waves from the southeast break further up the beach and will surge up and down the beach with more energy being reflected. Comparatively the waves from the southwest will be more likely to break further down the slope.

After breaking begins, the wave height continues to reduce as a result of the decreasing water depth, and the mean water level rises. At the shoreline, the mean water level is above the level of the still water. The initial depression of the mean water level is known as wave set-down and the subsequent rise as wave set-up.

The maximum set-up, S_{max}, occurs at the shoreline:

$$S_{max} \approx \frac{3\gamma H_b}{8}$$

Where γ is a empirically derived constant which is between 0.7 to 1.3.

After a wave has broken, much of the wave energy which remains when the mass of water reaches the shoreline is used in driving it up the face of the beach. The run-up (R), is the maximum height above still-water level to which the water rises and it includes the effect of wave-setup. Its value depends upon the slope steepness, roughness and permeability together with the incident wave characteristics. The run-up on a smooth, impermeable slope or maximum run-up, R_{si} may be estimated with Hunt's formula (Le Mehaute *et al*, 1968):

$$\frac{R_{si}}{H} \approx N_I = \frac{\tan\beta}{(\frac{H}{L_o})^{1/2}}$$

for $N_I \leq 2.3$ i.e. for spilling and plunging breakers.

To allow for slope roughness and permeability, R_{si} may be multiplied by a factor $r_R$which has values of about 0.9 to 1.0 for smooth concrete slopes and about 0.5 to 0.7 for slopes armoured with stone:

$R \approx r_R R_{si}$

It should be noted that R cannot be less than S_{max} (since R includes the effect of wave setup).

In this case, a value of 0.8 has been chosen for r_R.to represent the roughness and permeability of the beach.

A summary of key wave parameters is provided for each wave condition modelled in Table A2 (1 in 35 year wave events) and Table A3 (1 in 1 year wave events). These parameters have been extracted from the local area model at the toe of each beach at the time of HW for HAT.

Table A2. Wave parameters for the scheme run (at HW), 1 in 35 year wave events

Wave Parameter	Beach 1		Beach 2		Beach 3	
	SW 1 in 35	SE 1 in 35	SW 1 in 35	SE 1 in 35	SW 1 in 35	SE 1 in 35
H_b (m)	1.41	1.38	1.38	1.35	1.26	1.24
N_I	0.48	0.42	0.50	0.44	0.46	0.39
Breaker type	Plunging	Plunging	Plunging	Plunging	Plunging	Spilling
R_{SI} (m)	0.67	0.50	0.65	0.49	0.69	0.52
S_{max} (m)	0.42	0.41	0.41	0.41	0.38	0.37
R (m)	0.54	0.41	0.52	0.41	0.55	0.42

Table A3. Wave parameters for the scheme run (at HW), 1 in 1 year wave events

Wave Parameter	Beach 1		Beach 2		Beach 3	
	SW 1 in 1	SE 1 in 1	SW 1 in 1	SE 1 in 1	SW 1 in 1	SE 1 in 1
H_b (m)	1.37	1.15	1.34	1.12	1.22	1.04
N_I	0.49	0.38	0.51	0.38	0.47	0.36
Breaker type	Plunging	Spilling	Plunging	Spilling	Plunging	Spilling
R_{SI} (m)	0.65	0.39	0.63	0.38	0.67	0.38
S_{max} (m)	0.41	0.34	0.40	0.34	0.37	0.31
R (m)	0.52	0.34	0.50	0.34	0.54	0.31

The N_I numbers indicate that the waves would be plunging breakers. The run-up (the maximum height above the still water level) varies with the wave conditions modelled, being smallest (around 0.3 m) for the 1 in 1 year wave from the southeast and largest (around 0.55 m) for waves from the southwest.

The extent of wave run up is shown for each wave condition in Figure A7.

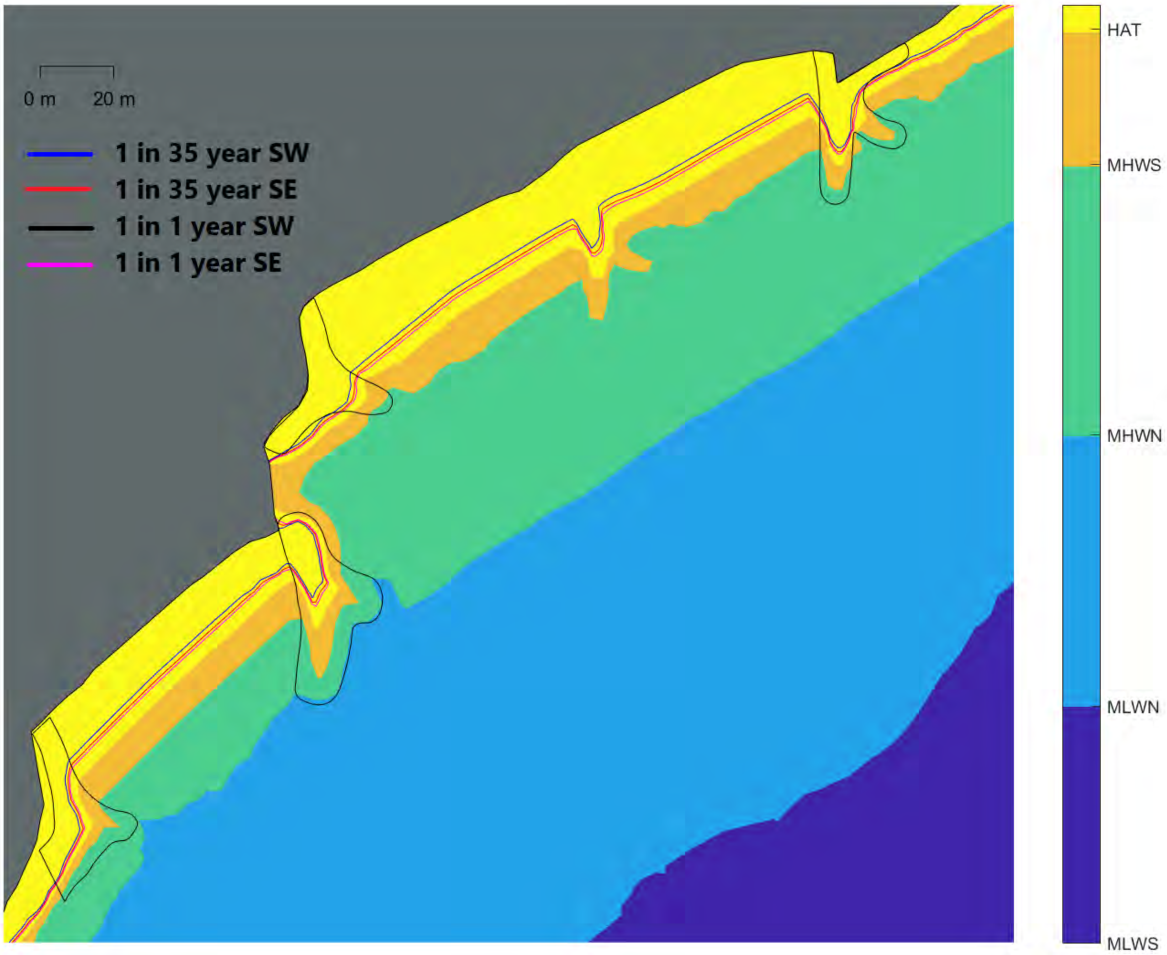

Figure A7. Estimate of wave run up based on results from the local area model and Hunt's formula

A.4 Wave Energy Density

To provide an indication of the effect of tidal flows on the wave field, the wave energy density has been calculated at the time of peak flood (when coming waves move onto a following current) and at the time of peak ebb (when coming waves move onto opposing currents). The calculation does not account for the effect of wave breaking.

These are shown in Figure A8. As expected, based on the low tidal flows in the region, the wave energy density is broadly similar at the time of peak flood and peak ebb, with only minor increases in wave energy density at the time of peak ebb. This energy increase results from the adverse current shortening the waves.

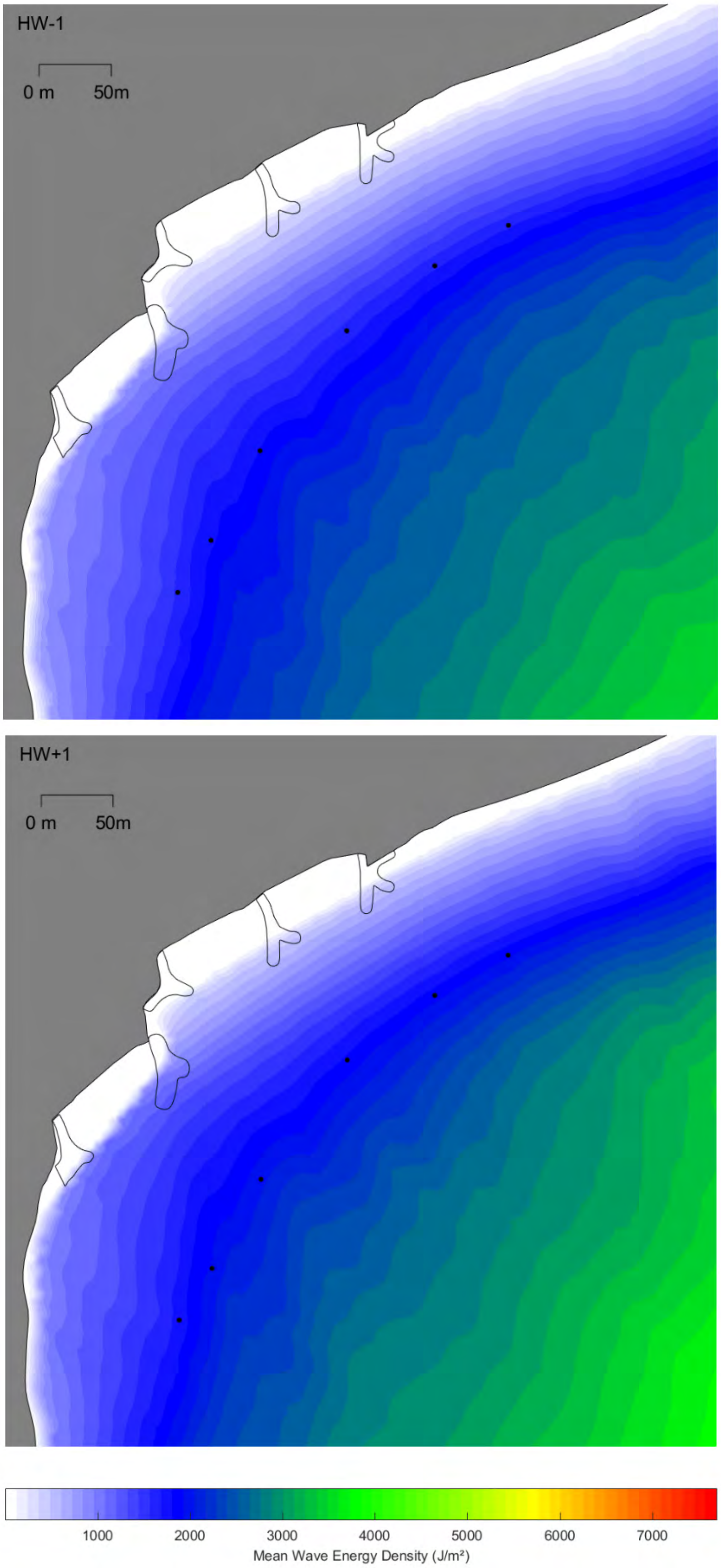

Extraction points are marked for reference but not labelled, see Figure 1.

Figure A8. Example of mean wave energy density at HW-1 (Upper) and HW+1 (Lower) during 1 in 35 year event from southeast

B Additional Figures

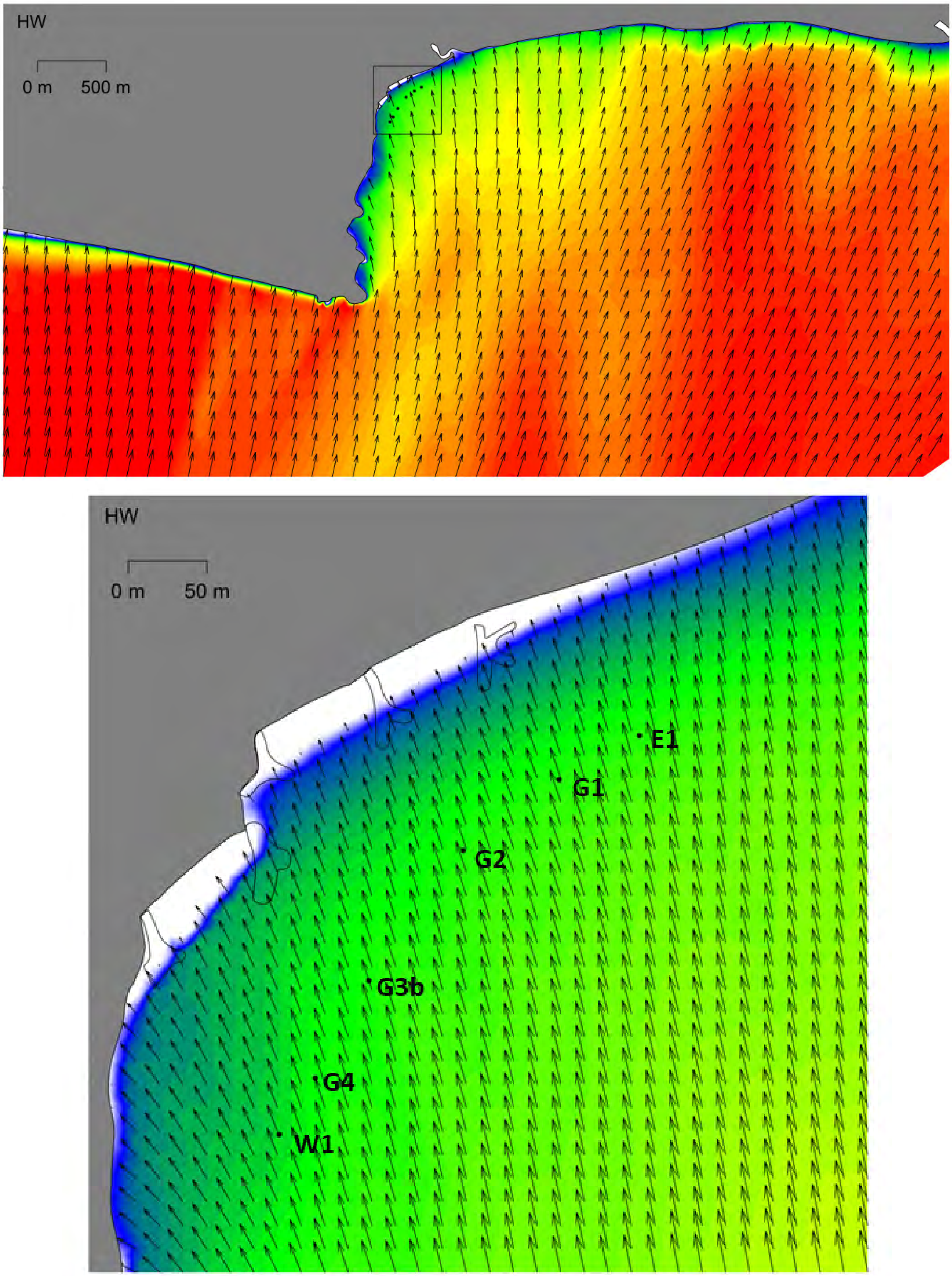

Groynes are not included in the model and are shown only for indicative purposes.

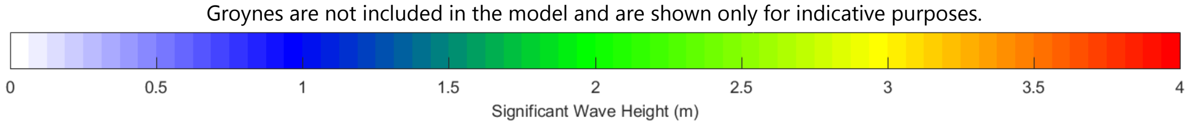

Figure B1. Baseline significant wave height for a 1 in 35 year wave from the southwest

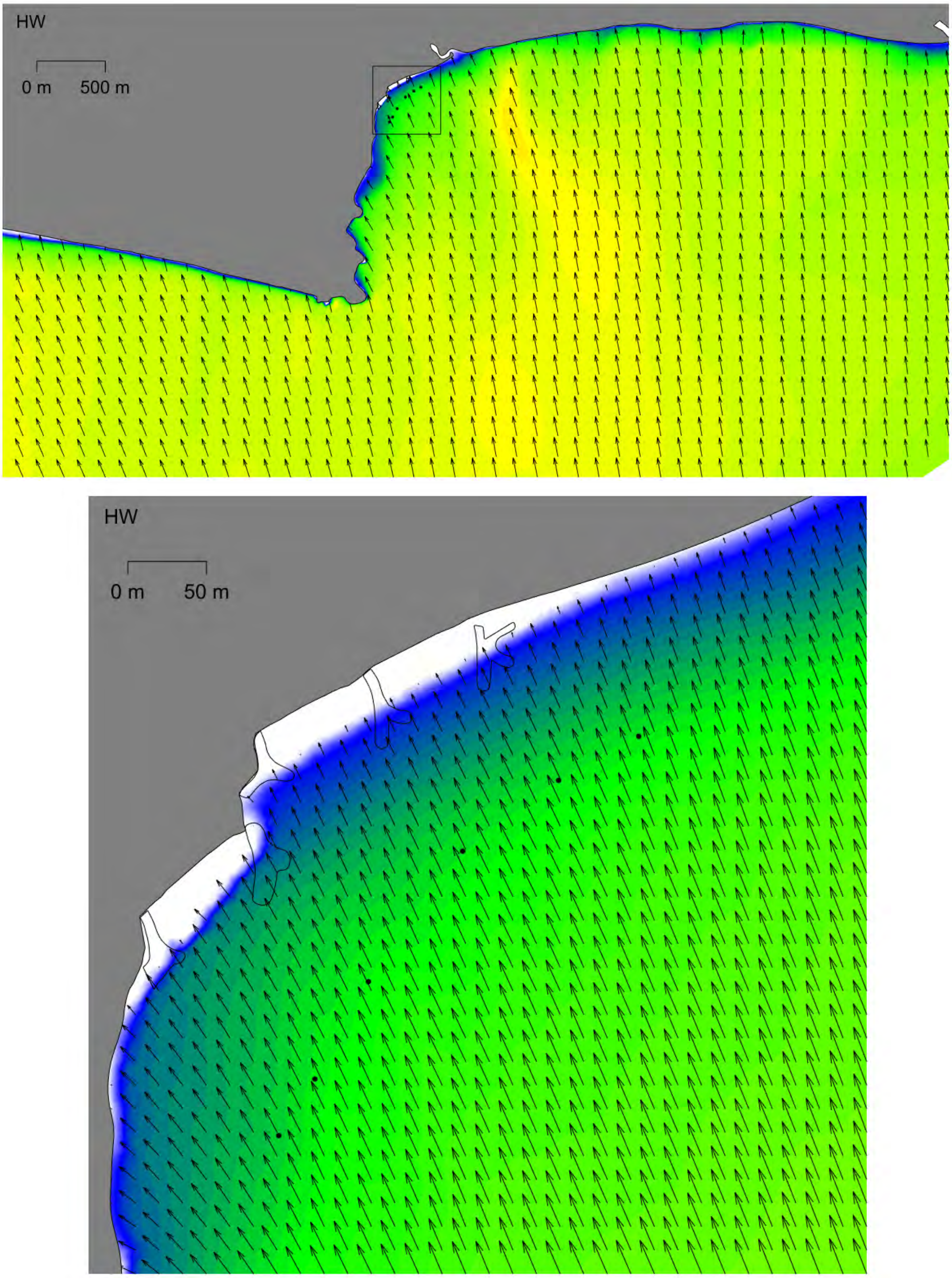

Groynes are not included in the model and are shown only for indicative purposes.
Extraction points are marked for reference but not labelled, see Figure 1.

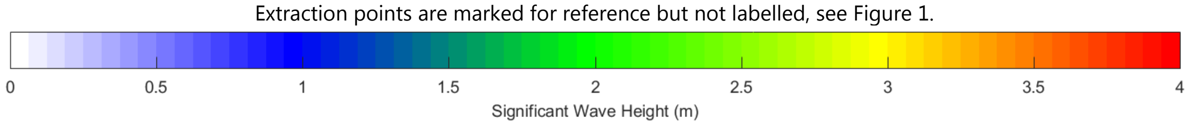

Figure B2. Baseline Significant wave height for a 1 in 35 year wave from the southeast

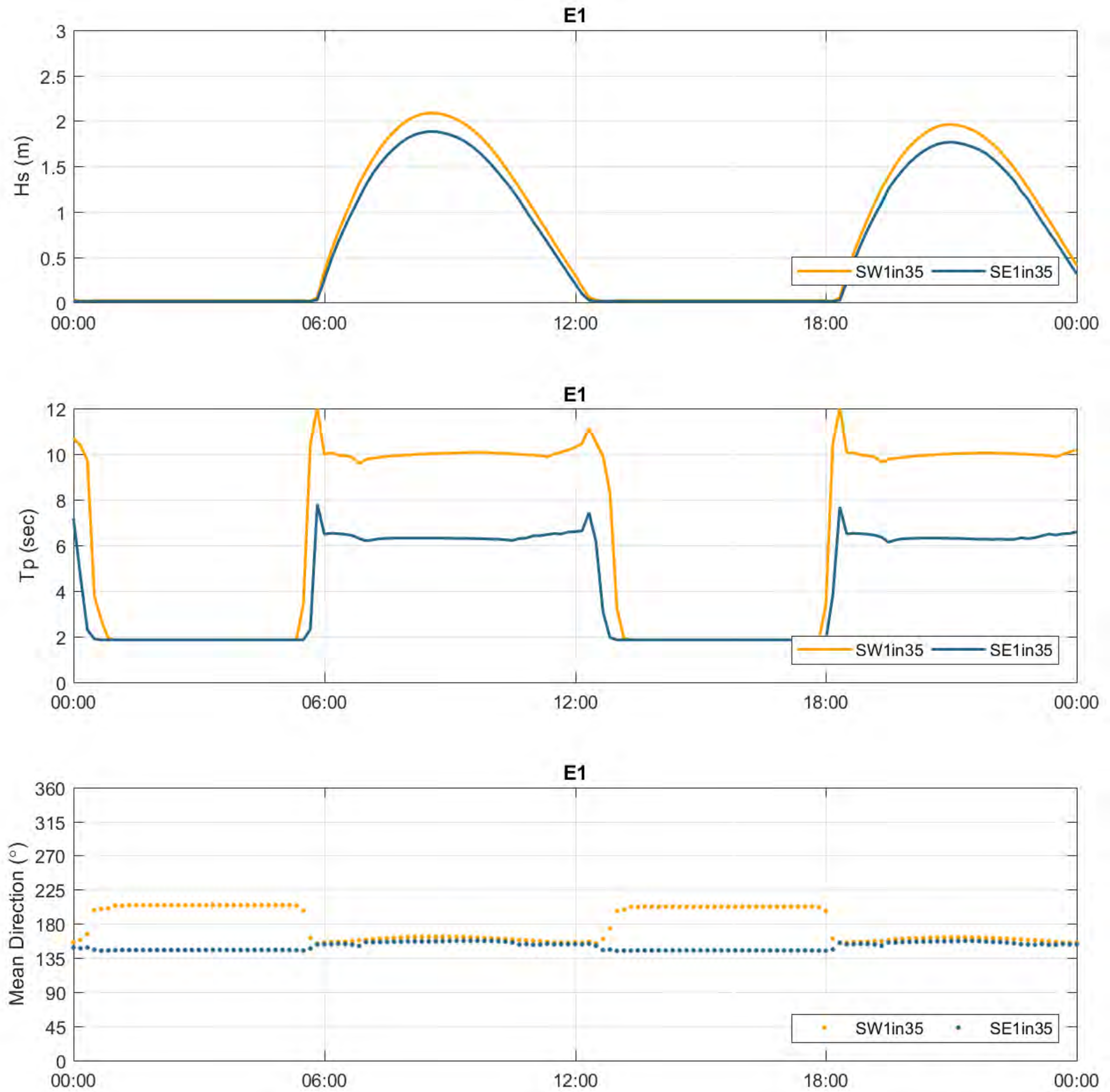

Figure B3. **Time series of baseline significant wave height, peak wave period and mean wave direction at E1 - 1 in 35 year event**

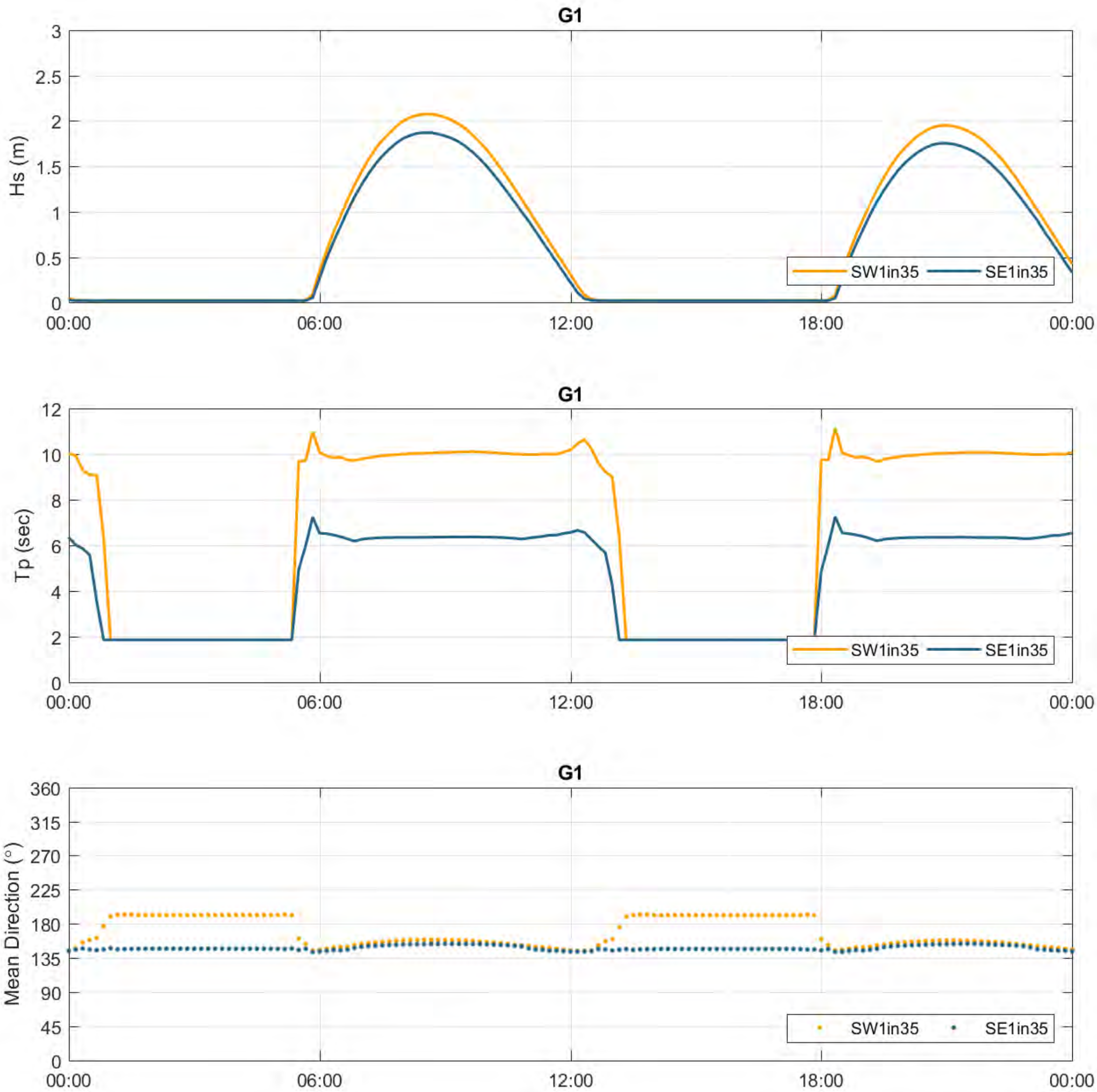

Figure B4. **Time series of baseline significant wave height, peak wave period and mean wave direction 1 at G1 - 1 in 35 year event**

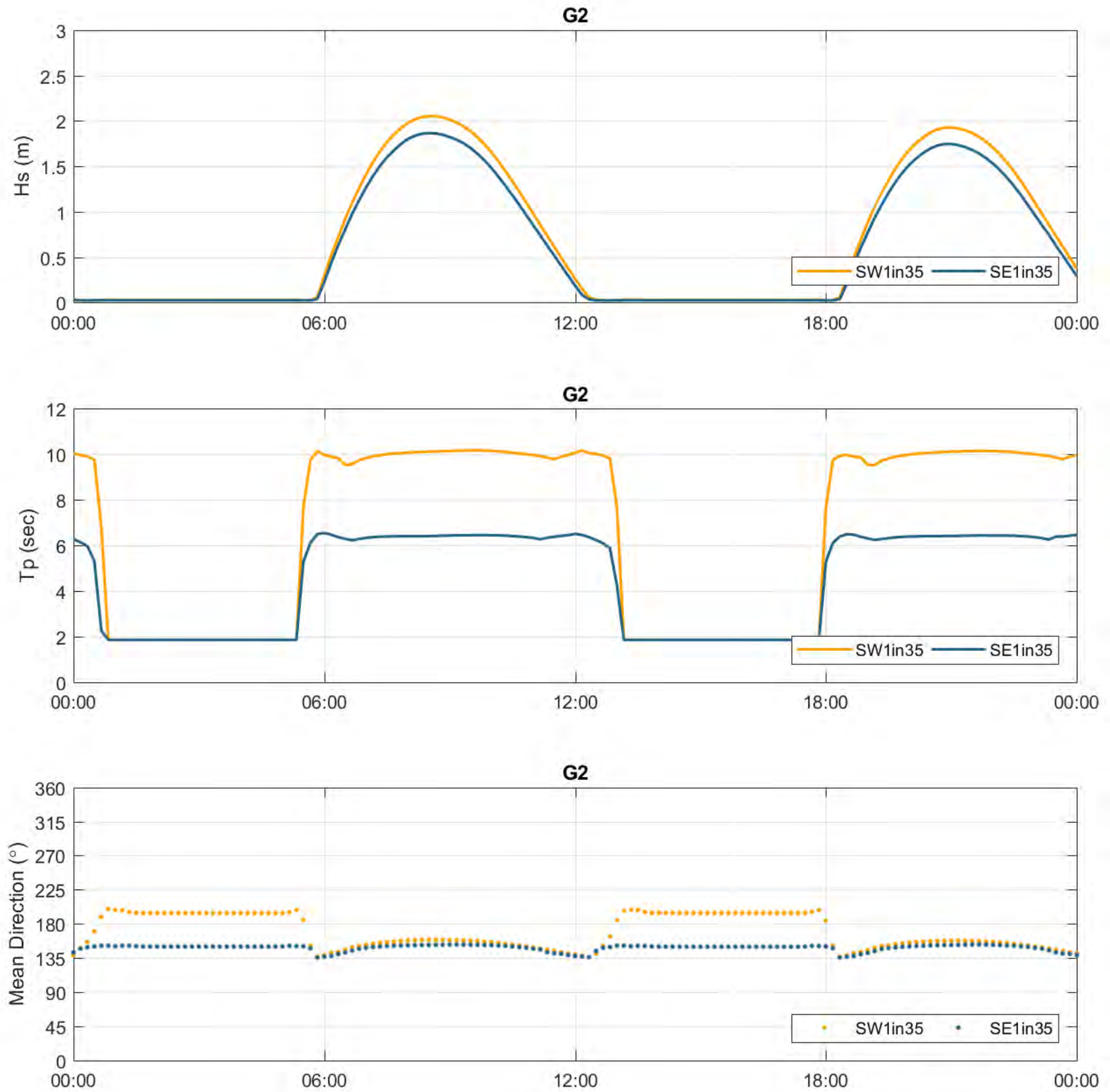

Figure B5. **Time series of baseline significant wave height, peak wave period and mean wave direction at G2 - 1 in 35 year event**

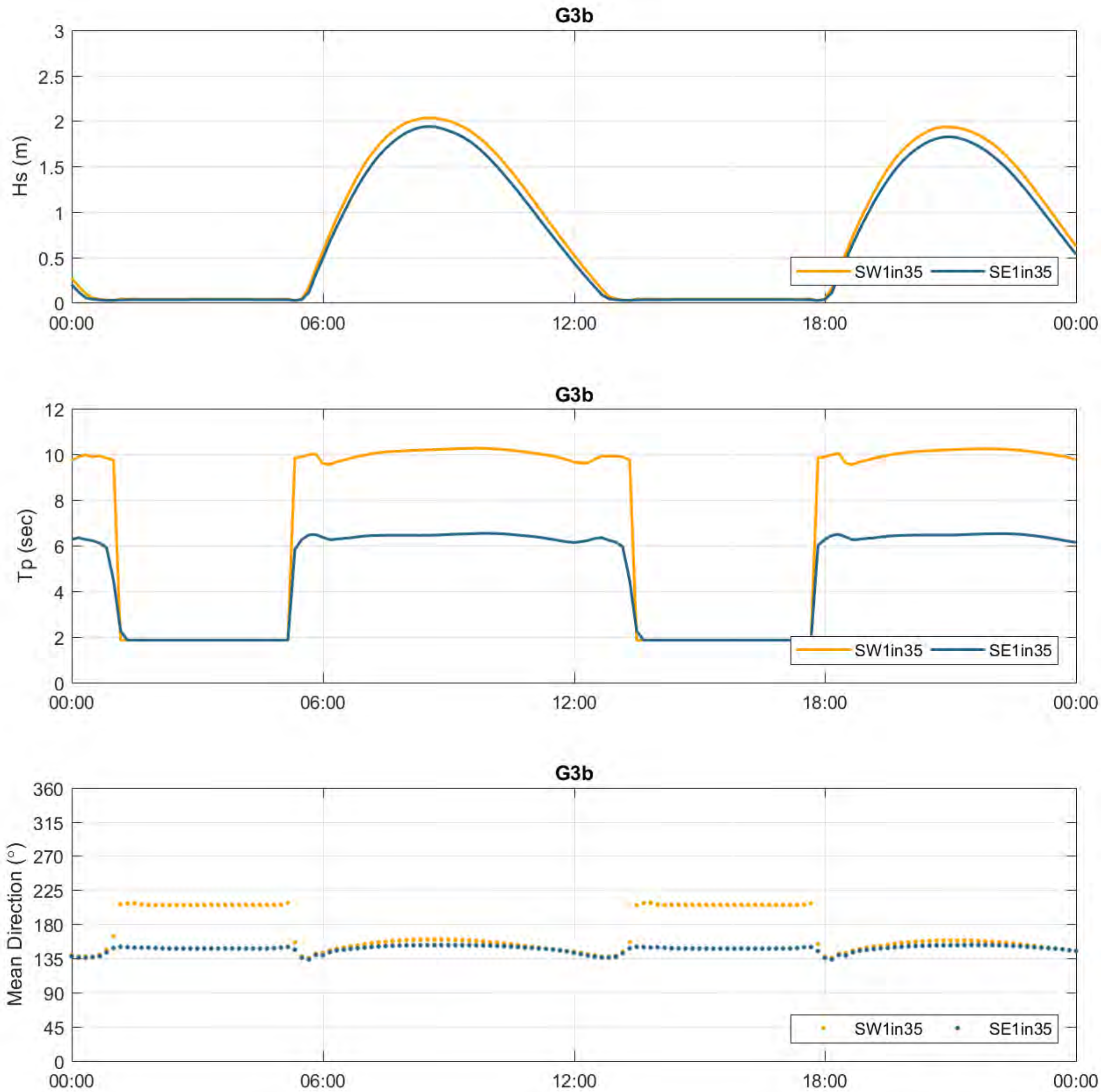

Figure B6. **Time series of baseline significant wave height, peak wave period and mean wave direction at G3b - 1 in 35 year event**

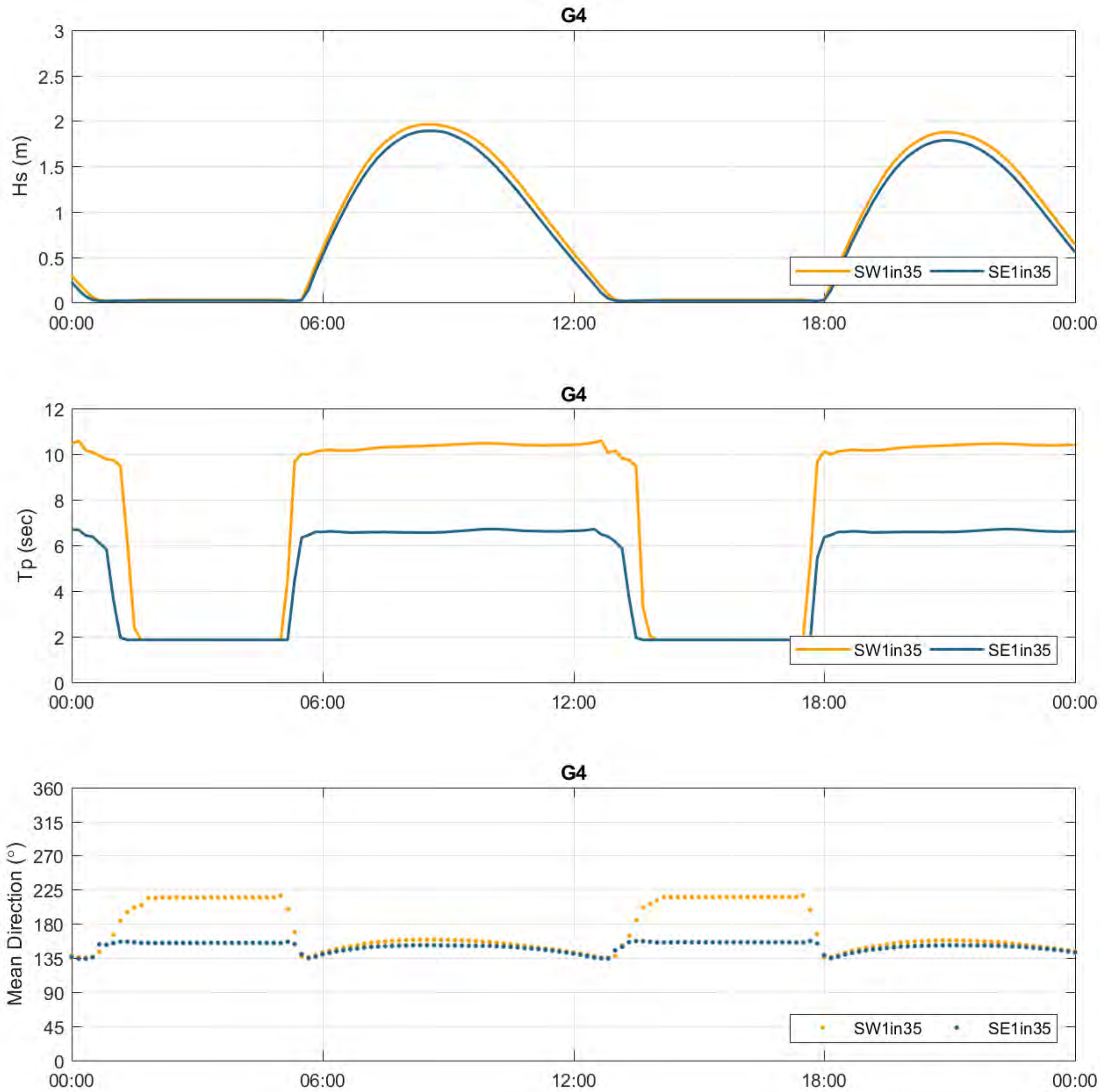

Figure B7. Time series of baseline significant wave height, peak wave period and mean wave direction at G4 - 1 in 35 year event

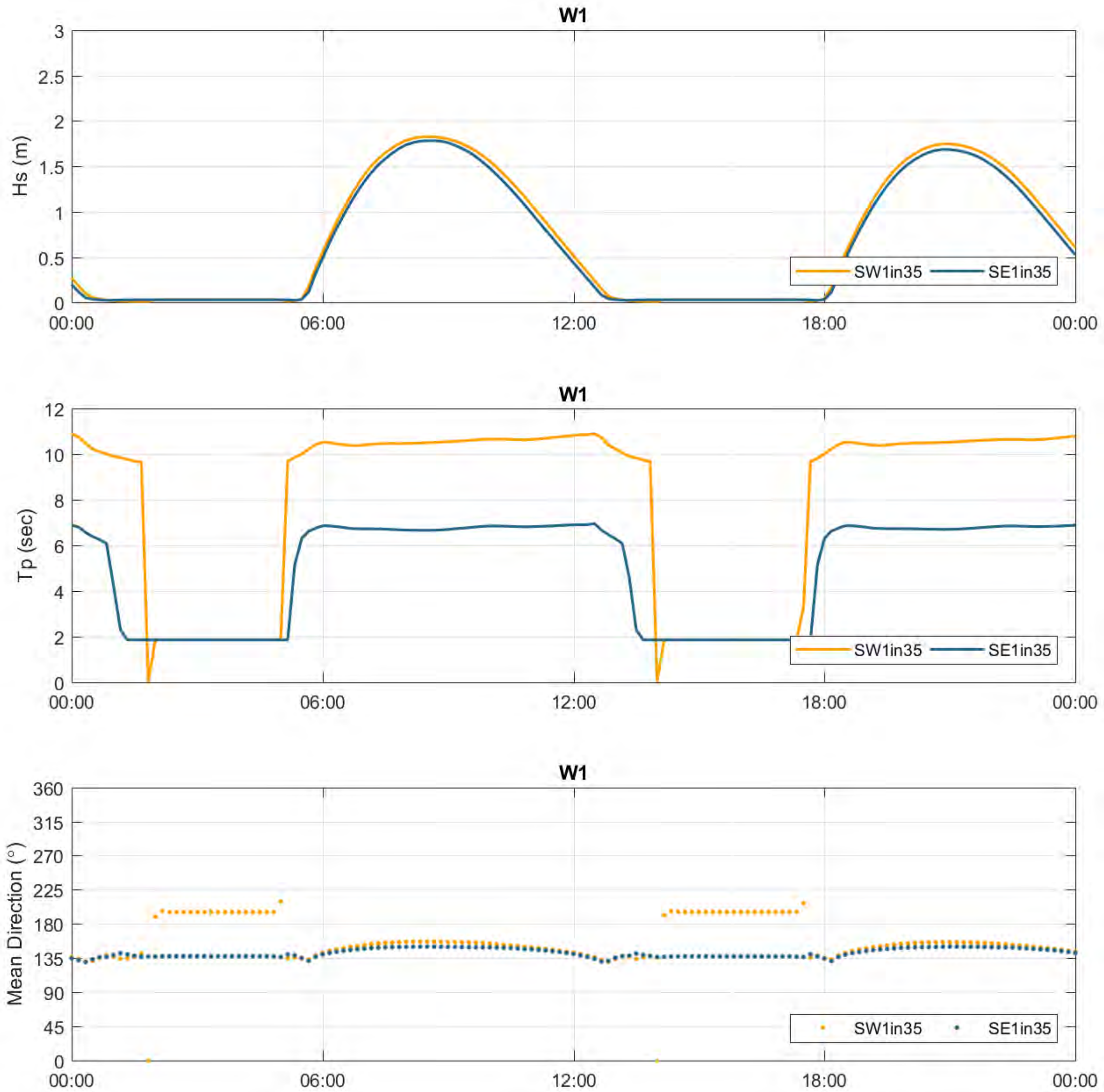

Figure B8. **Time series of baseline significant wave height, peak wave period and mean wave direction at W1 - 1 in 35 year event**

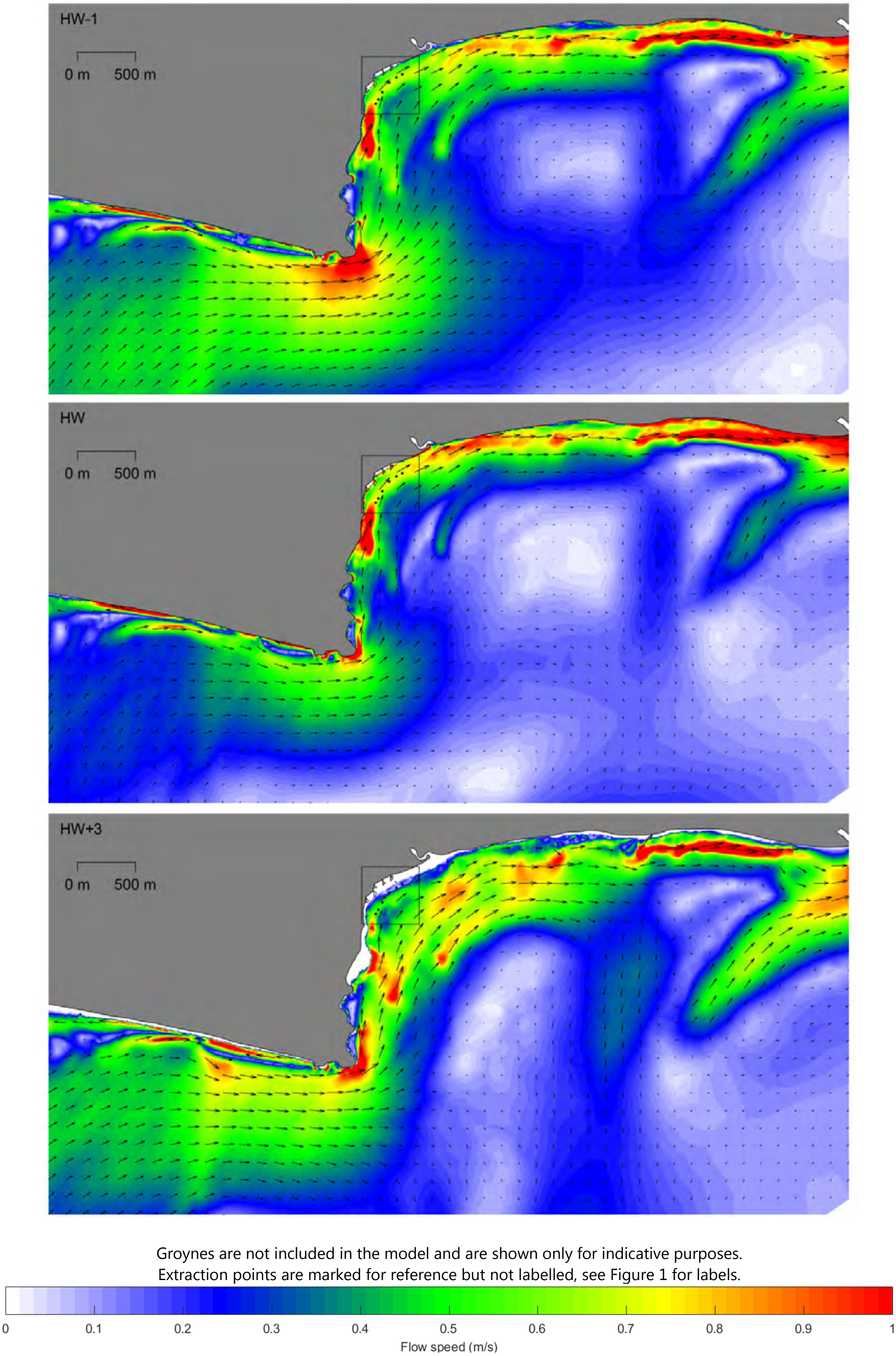

Figure B9. Baseline wave and tidal flow for 1 in 35 year wave from the southwest

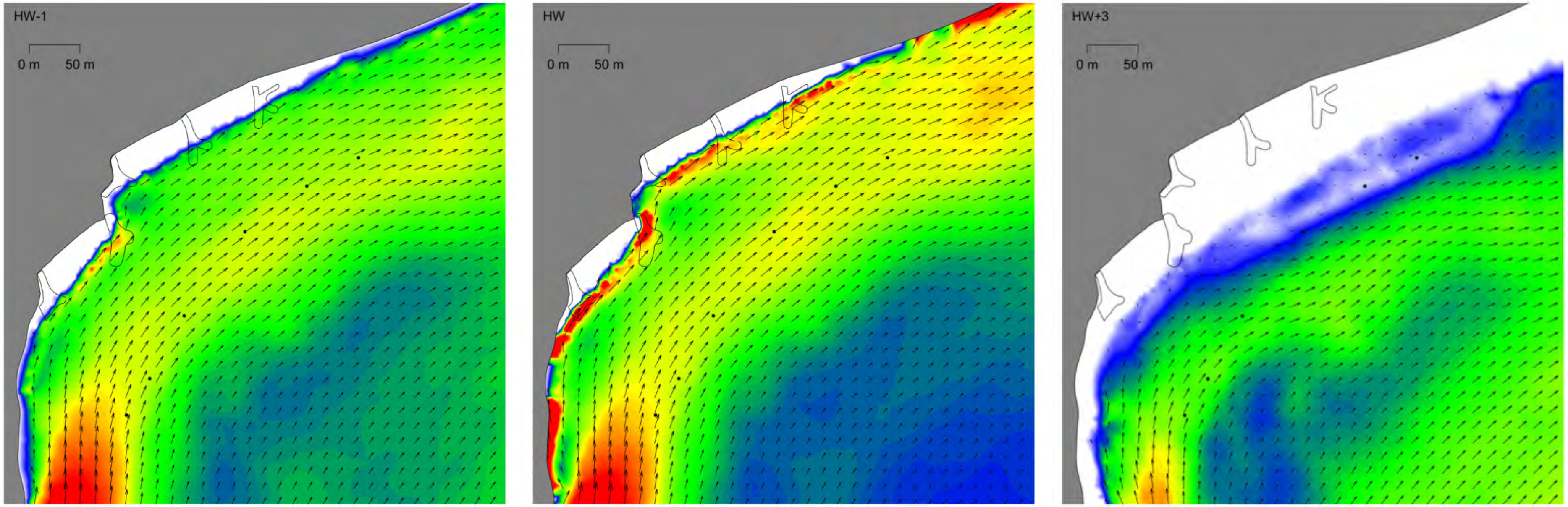

Groynes are not included in the model and are shown only for indicative purposes.
Extraction points are marked for reference but not labelled, see Figure 1 for labels.

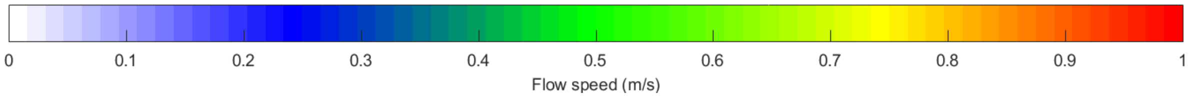

Figure B10. Baseline wave and tidal flow for 1 in 35 year wave from the southwest – local area

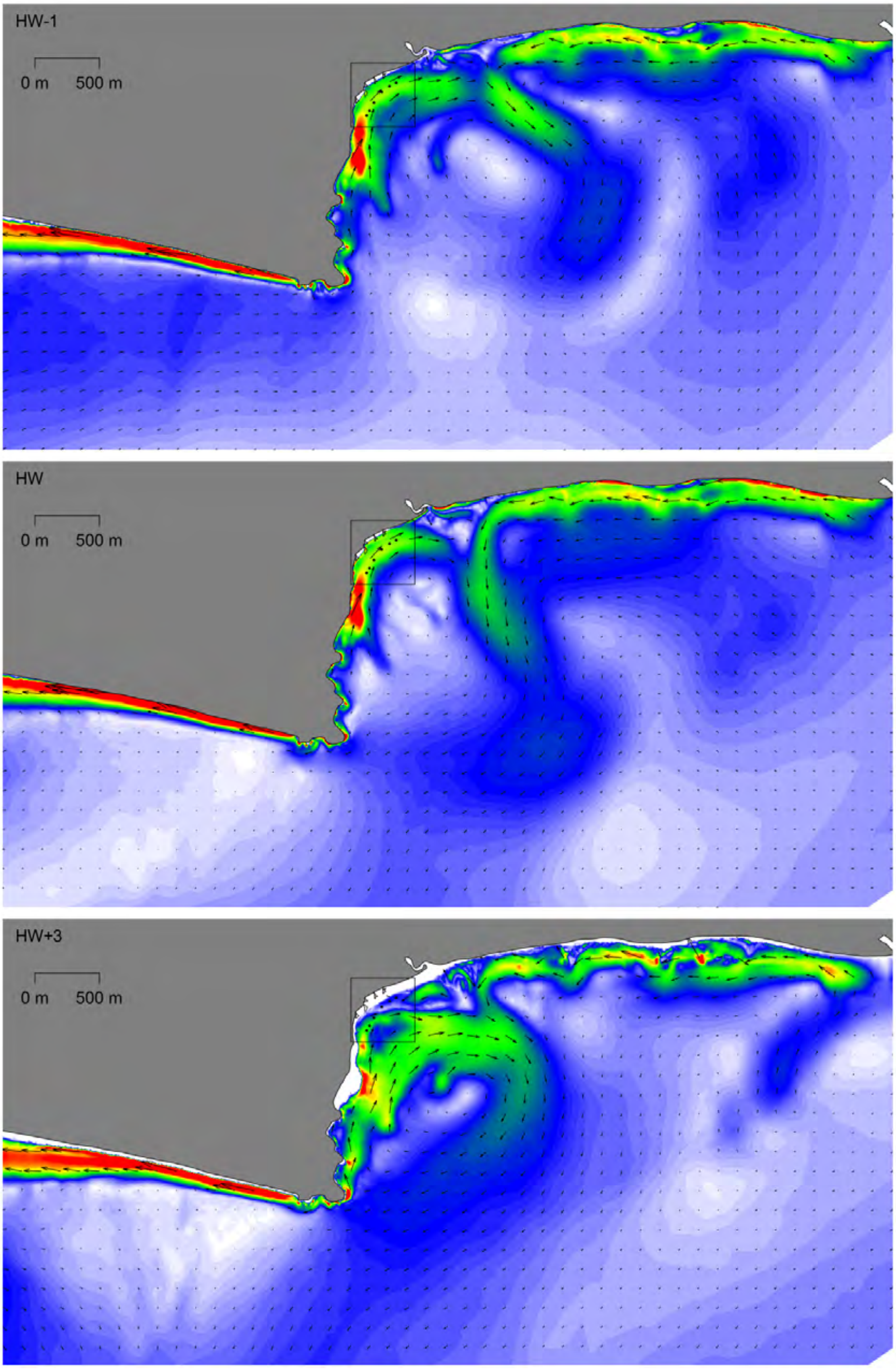

Groynes are not included in the model and are shown only for indicative purposes.
Extraction points are marked for reference but not labelled, see Figure 1 for labels.

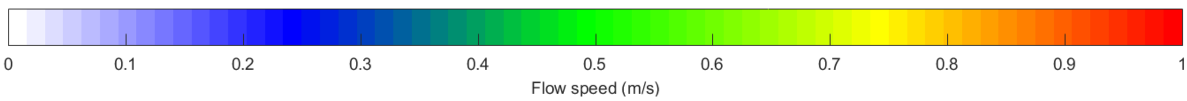

Figure B11. Baseline wave and tidal flow for 1 in 35 year wave from the southeast

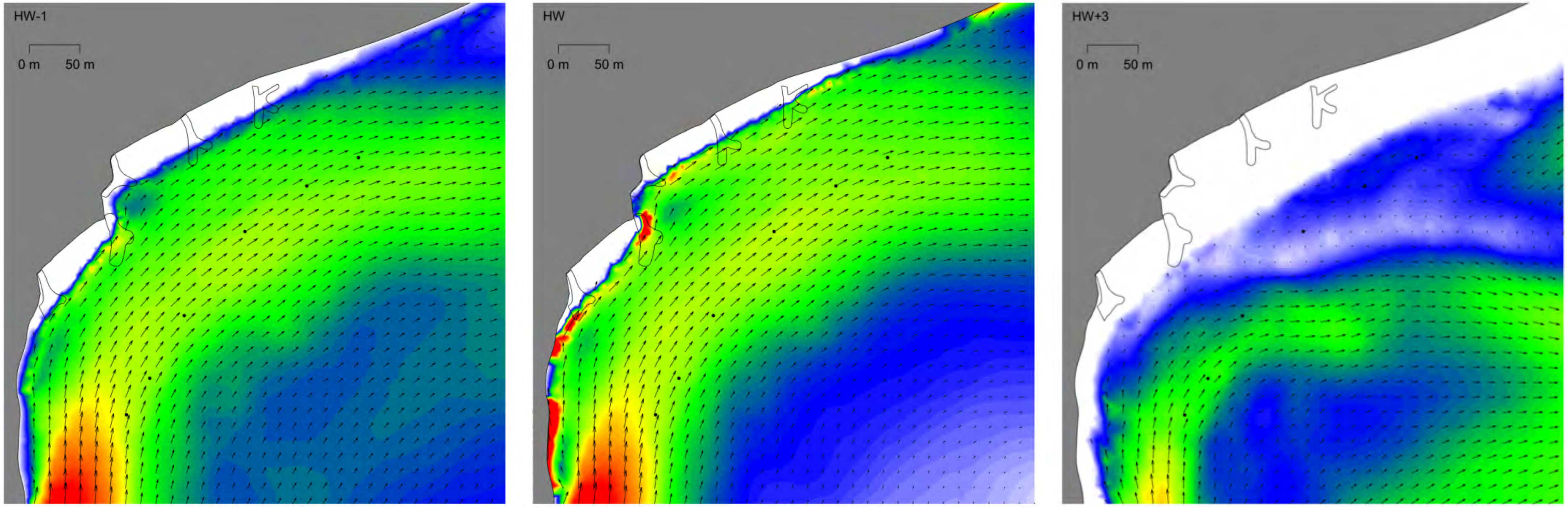

Groynes are not included in the model and are shown only for indicative purposes.
Extraction points are marked for reference but not labelled, see Figure 1 for labels.

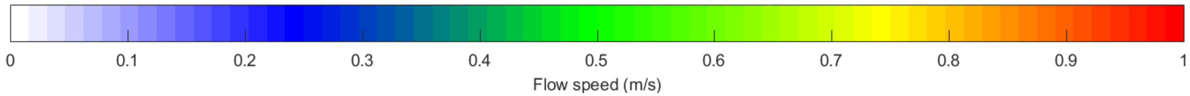

Figure B12. Baseline wave and tidal flow for 1 in 35 year wave from the southeast – local area

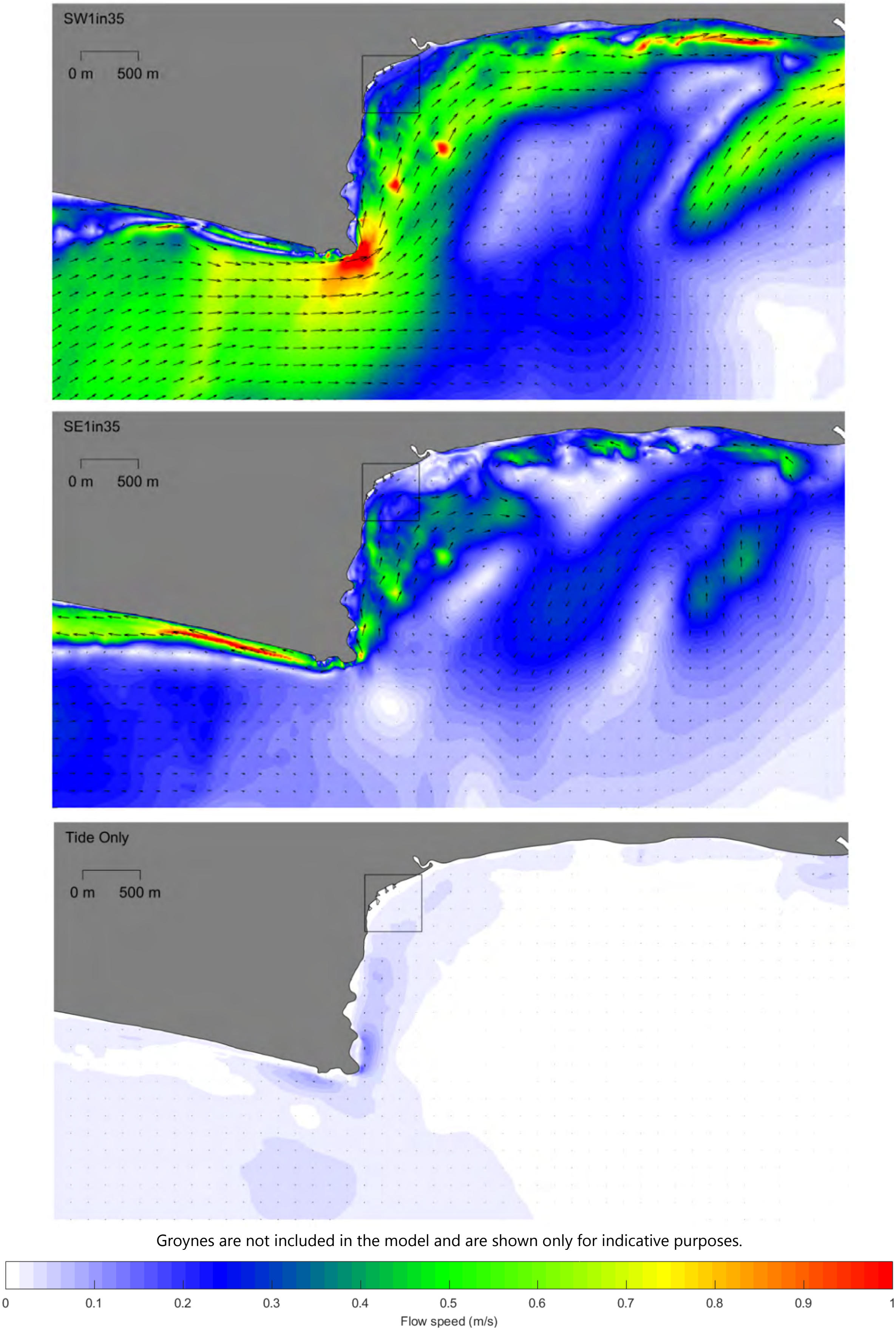

Figure B13. Baseline mean wave and tidal flow throughout a tidal cycle during 1 in 35 year event

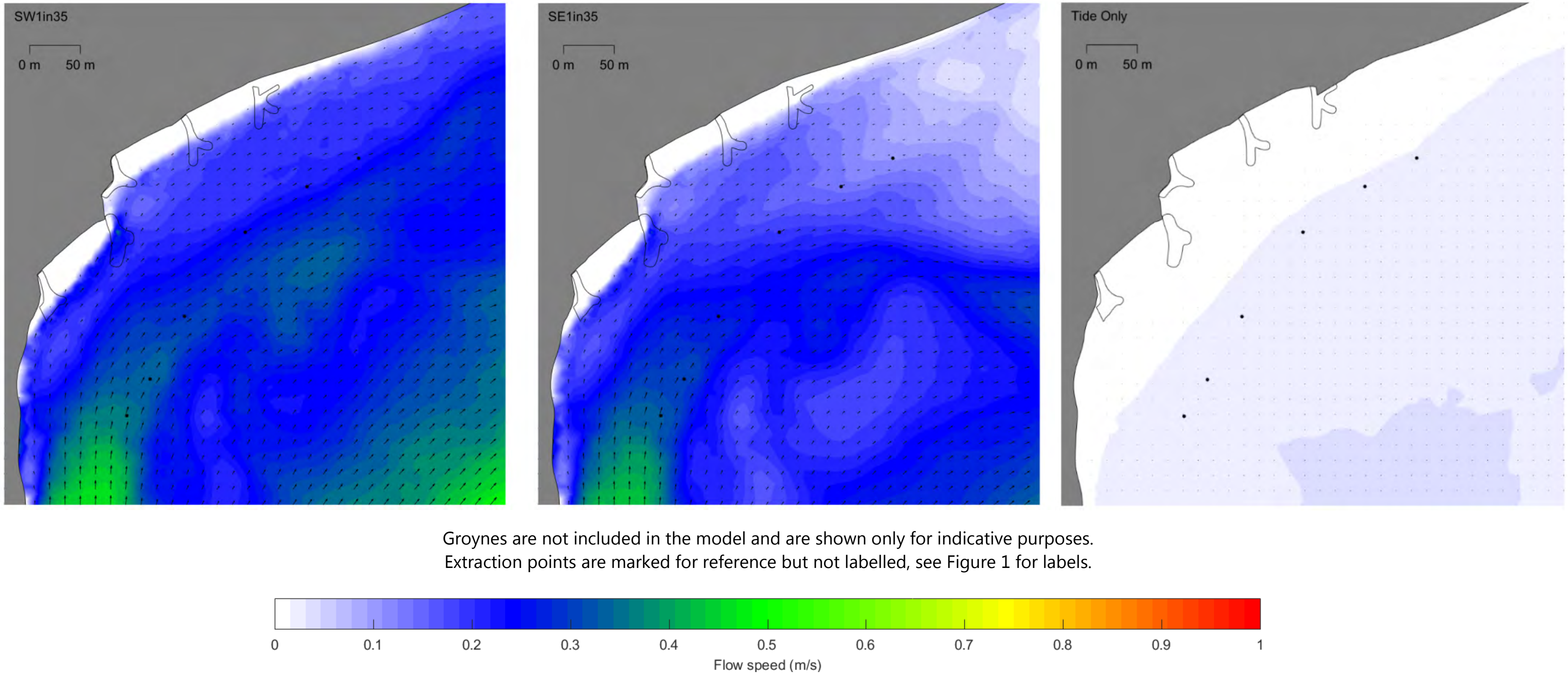

Figure B14. Baseline mean wave and tidal flow throughout a tidal cycle during a 1 in 35 year event – local area

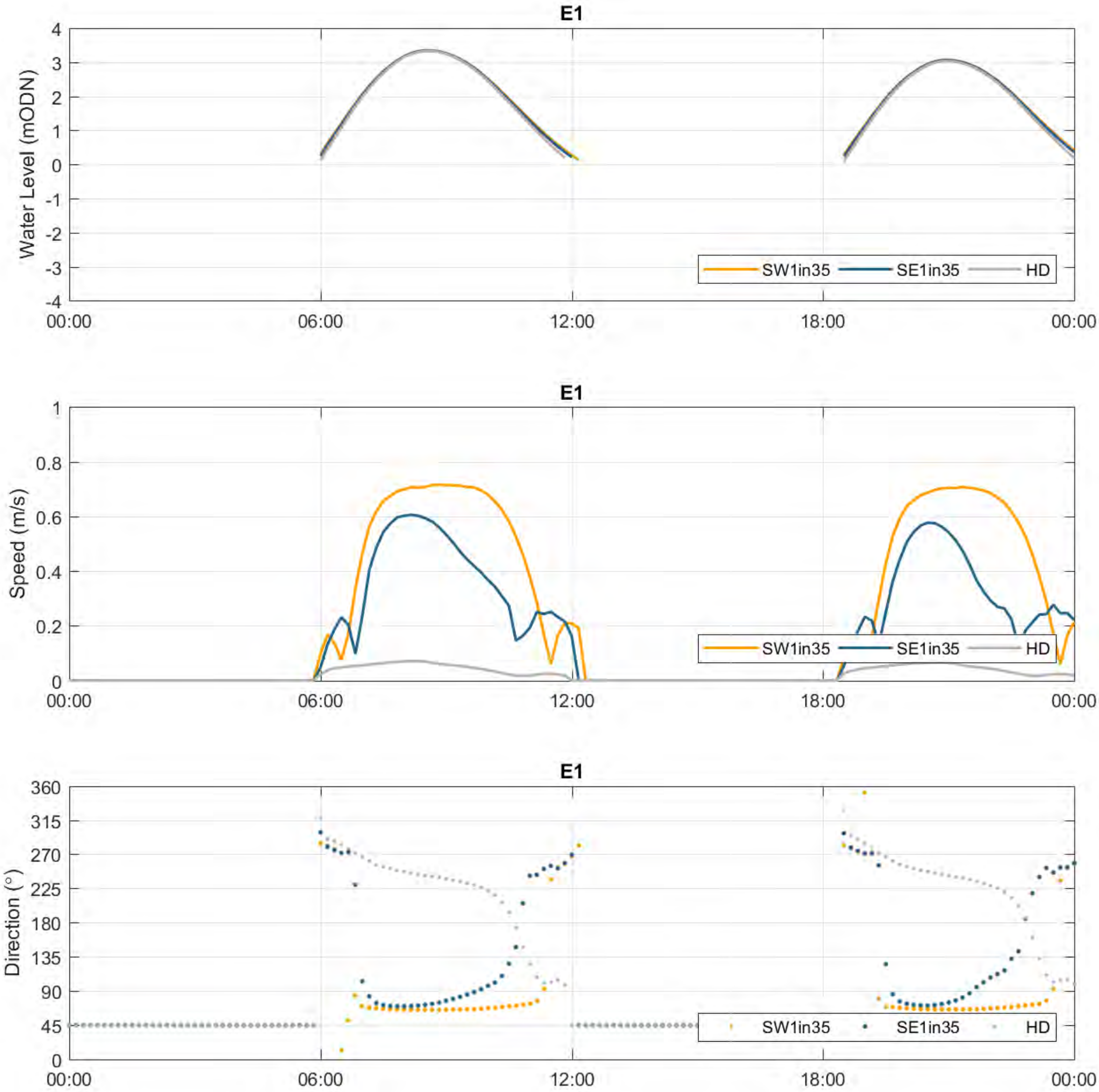

Figure B15. **Time series of baseline water level, flow speed and flow direction at E1 for 1 in 35 year events**

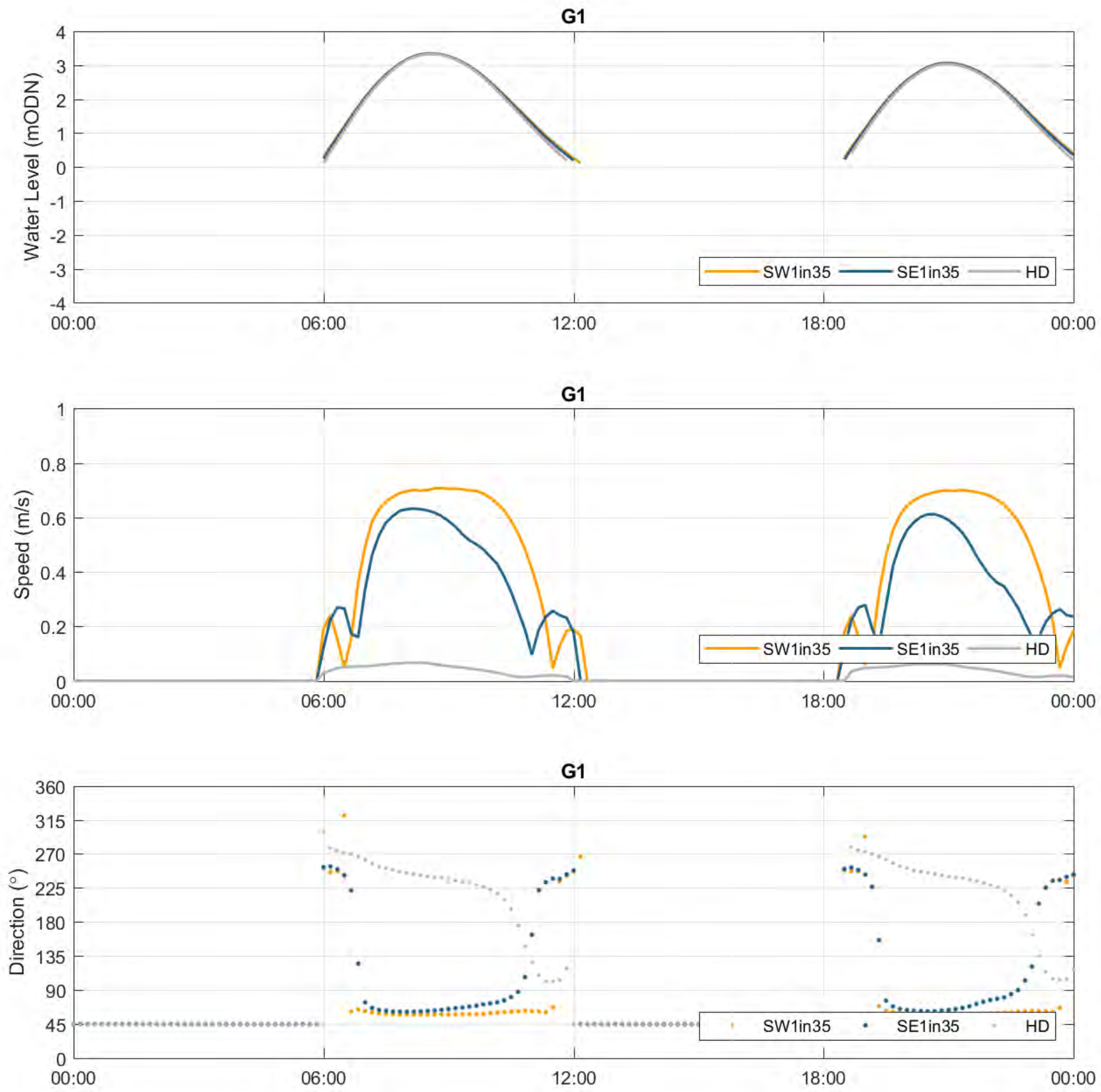

Figure B16. **Time series of baseline water level, flow speed and flow direction at G1 for 1 in 35 year events**

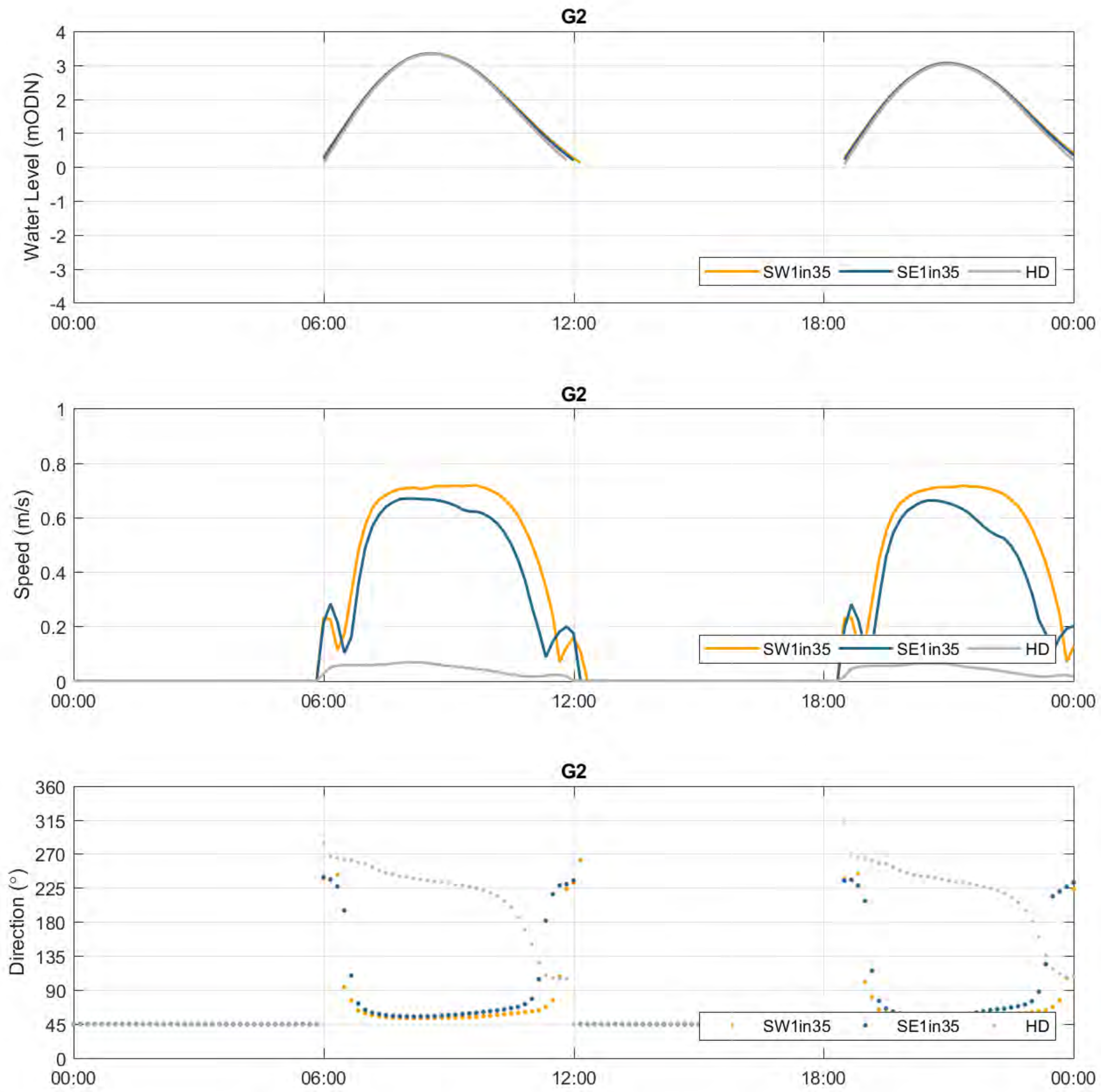

Figure B17. **Time series of baseline water level, flow speed and flow direction at G2 for 1 in 35 year event**

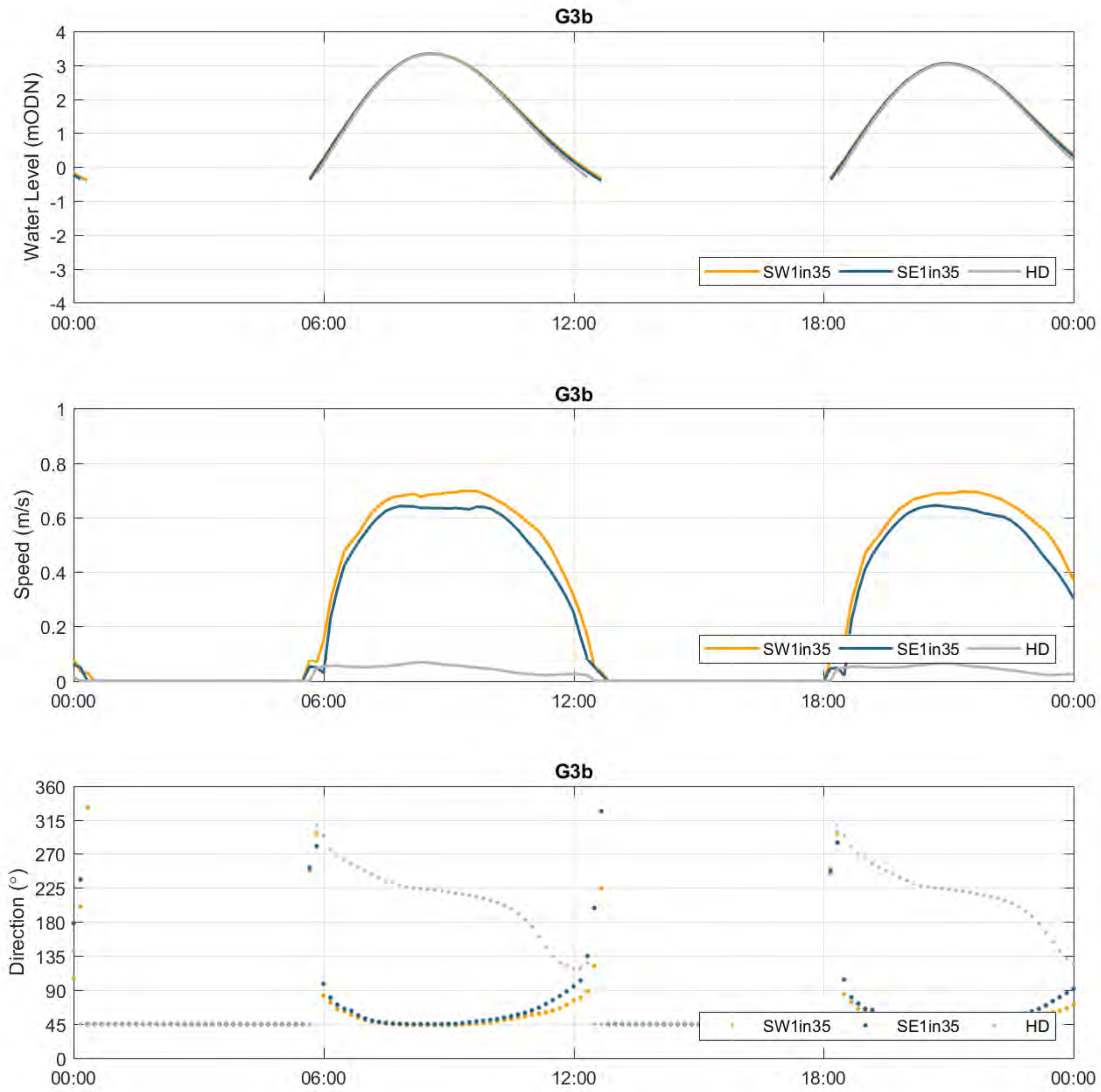

Figure B18. Time series of baseline water level, flow speed and flow direction at G3b for 1 in 35 year events

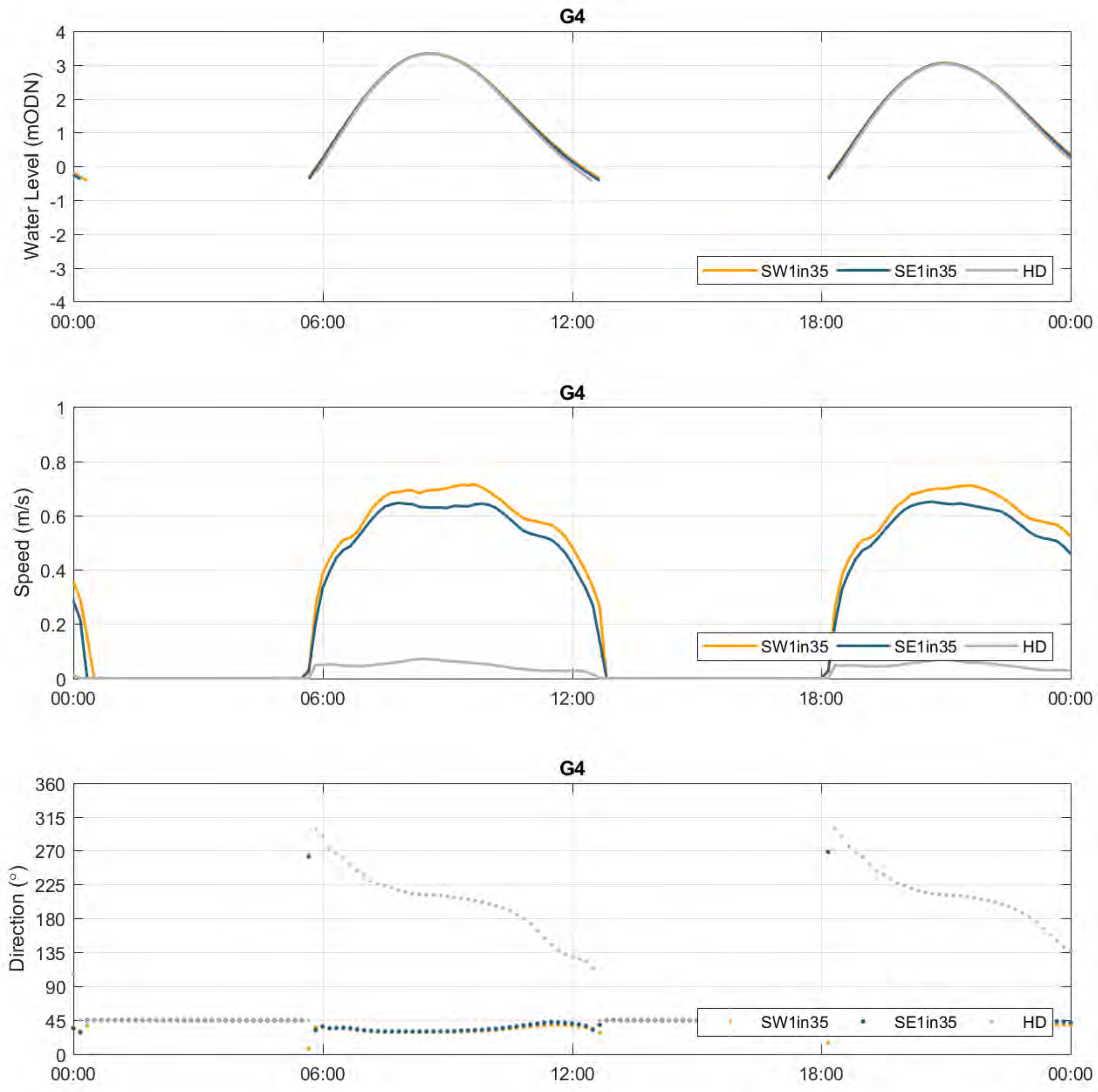

Figure B19. **Time series of baseline water level, flow speed and flow direction at G4 for 1 in 35 year events**

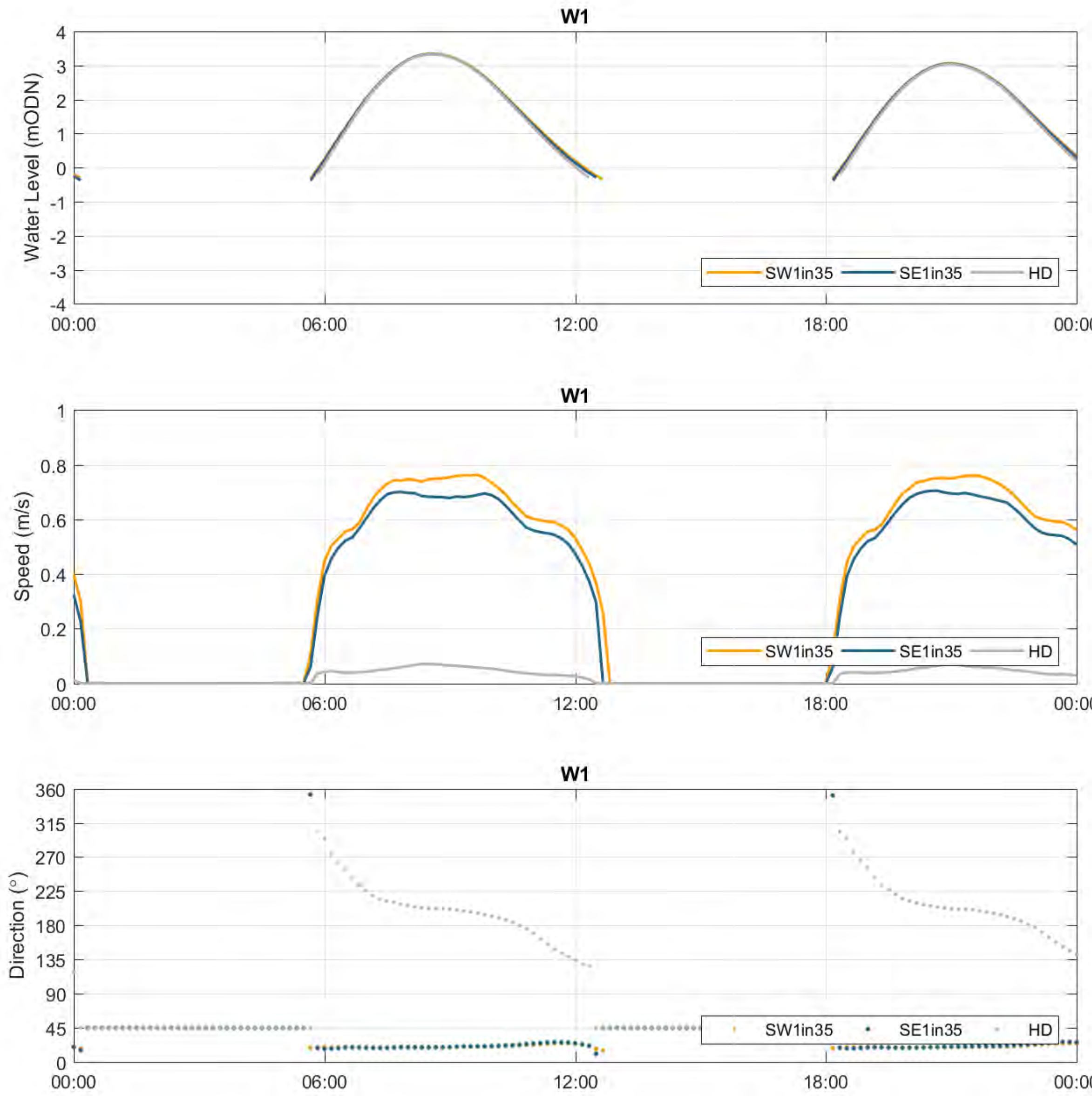

Figure B20. **Time series of baseline water level, flow speed and flow direction at W1 for 1 in 35 year events**

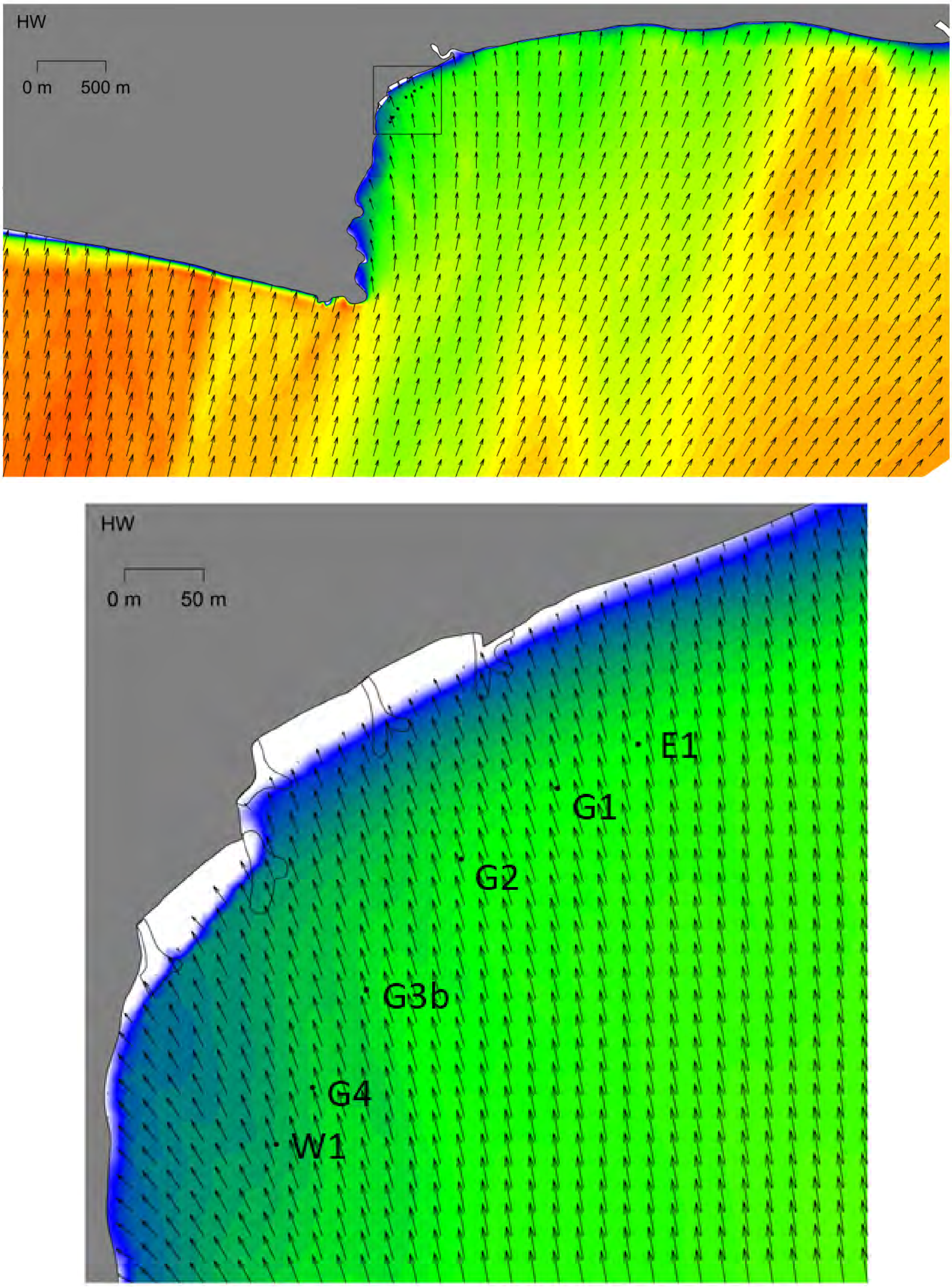

Groynes are not included in the model and are shown only for indicative purposes.

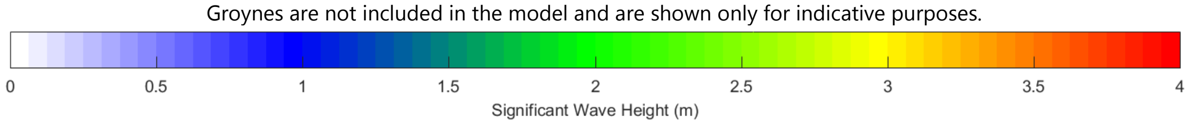

Figure B21. Baseline Significant wave height for a 1 in 1 year wave from the southwest

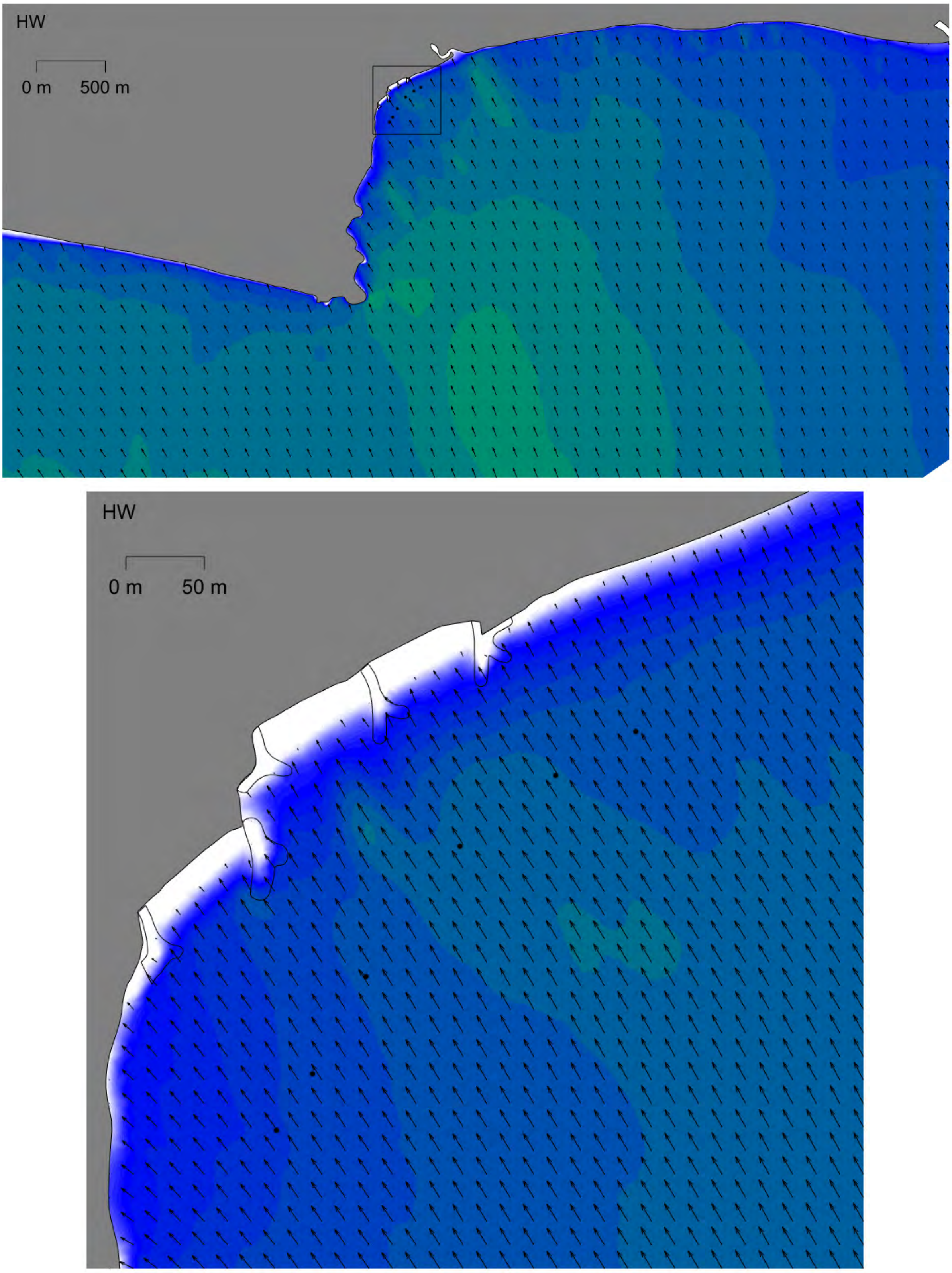

Groynes are not included in the model and are shown only for indicative purposes.
Extraction points are marked for reference but not labelled, see Figure 1 for labels.

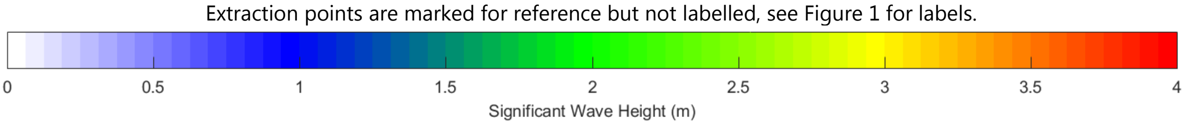

Figure B22. Baseline Significant wave height for a 1 in 1 year wave from the southeast

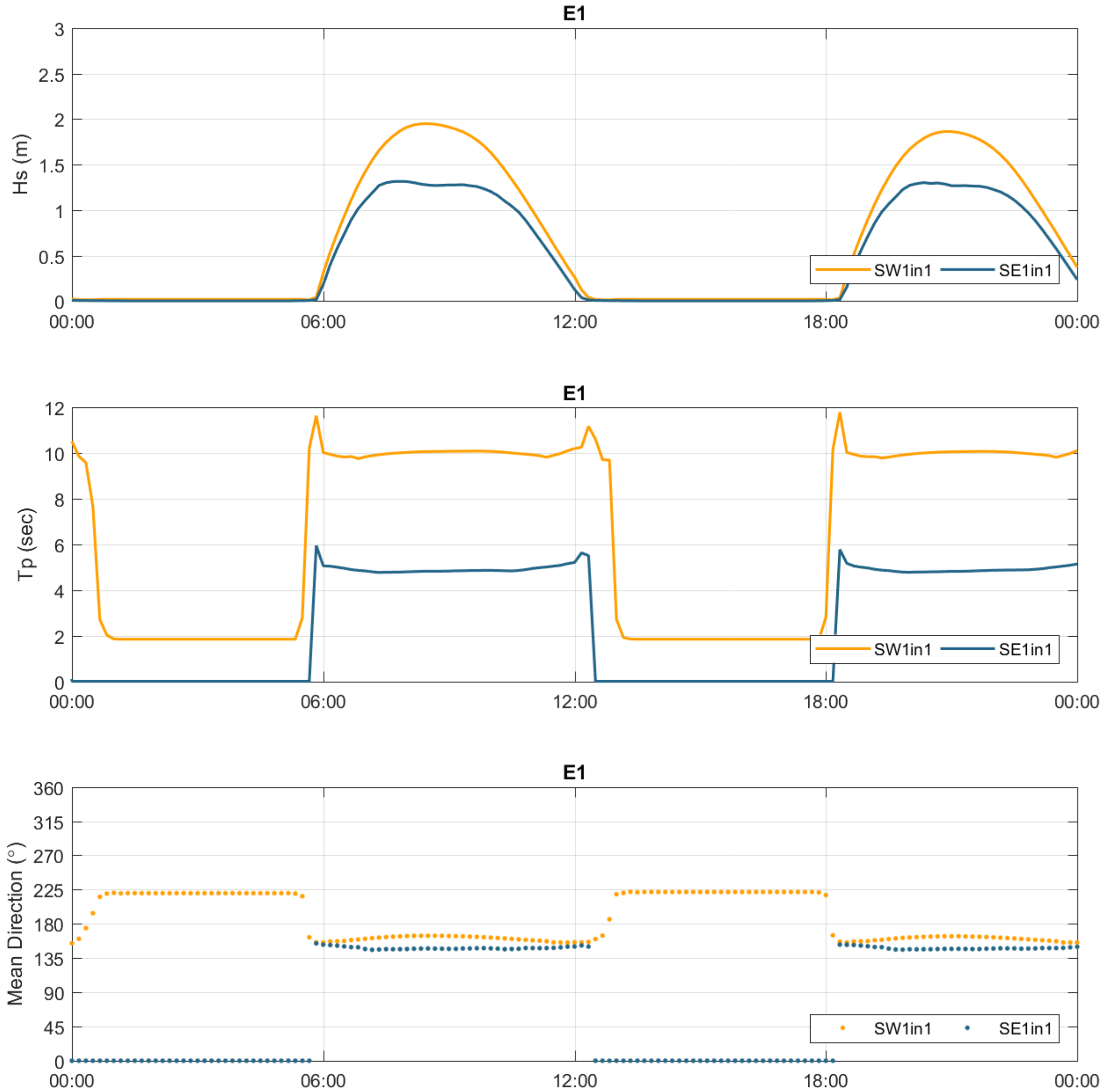

Figure B23. **Time series of baseline significant wave height, peak wave period and mean wave direction at E1 - 1 in 1 year event**

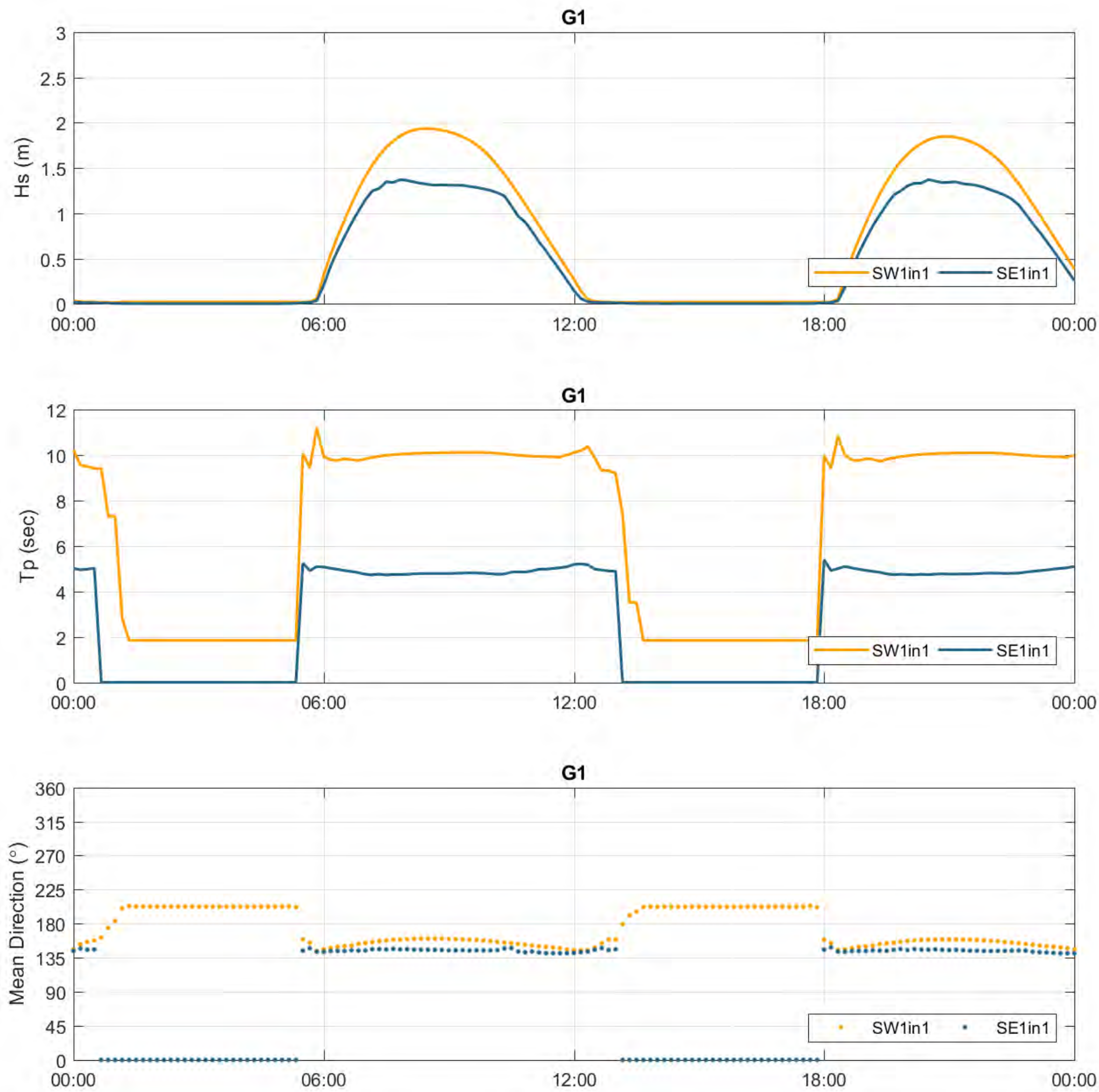

Figure B24. **Time series of baseline significant wave height, peak wave period and mean wave direction at G1 - 1 in 1 year event**

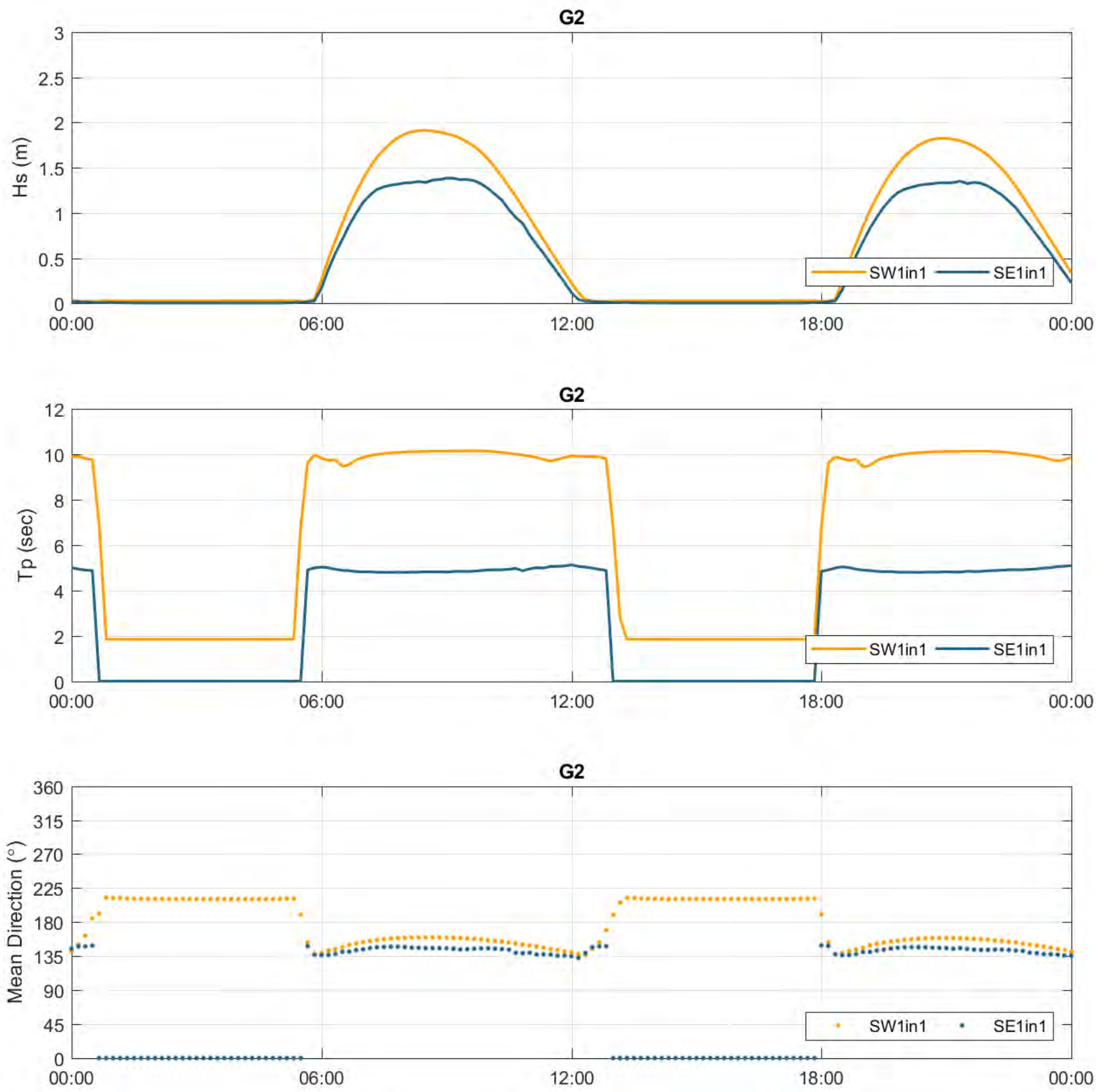

Figure B25. **Time series of baseline significant wave height, peak wave period and mean wave direction at G2 - 1 in 1 year event**

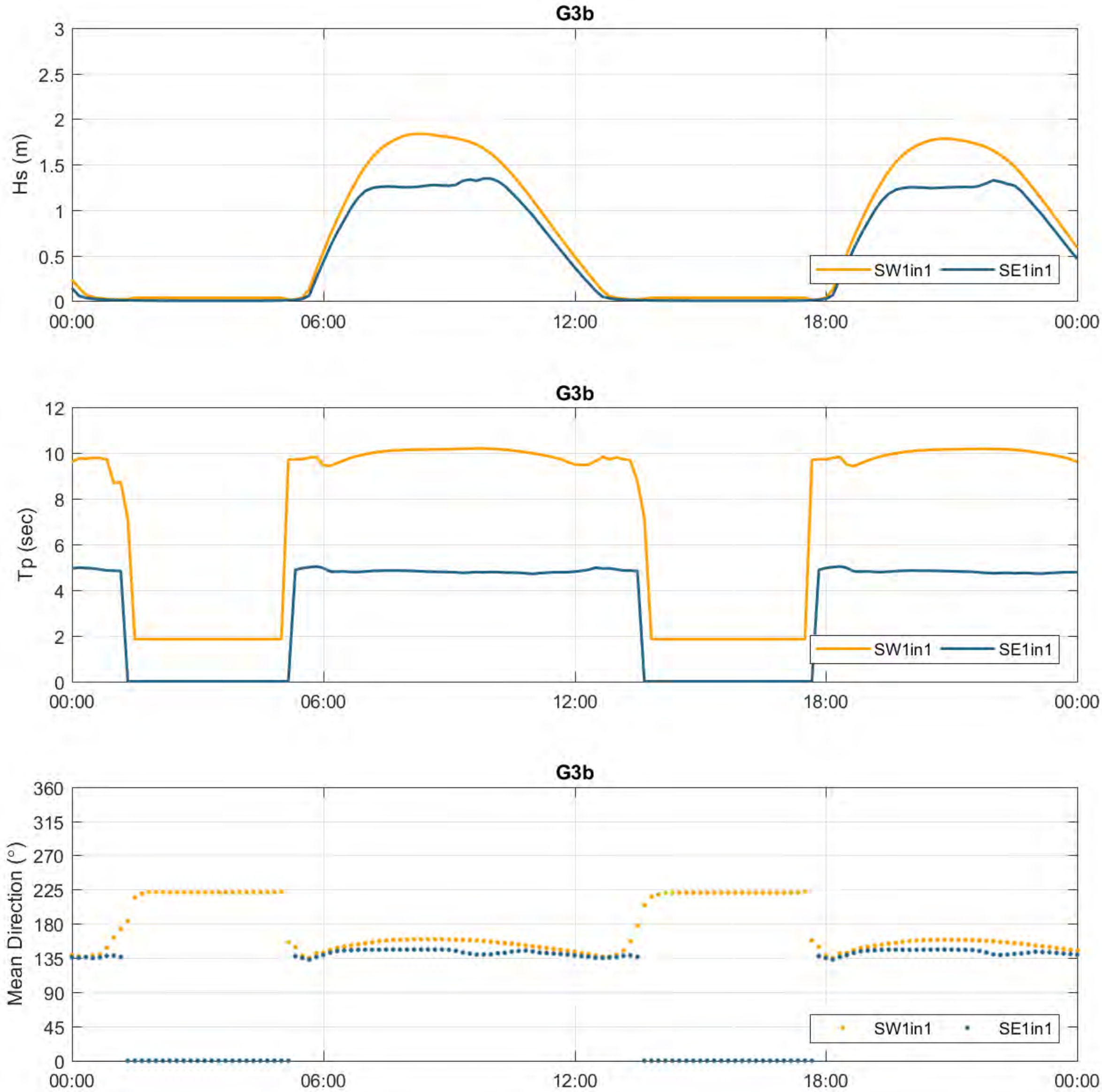

Figure B26. **Time series of baseline significant wave height, peak wave period and mean wave direction at G3b - 1 in 1 year event**

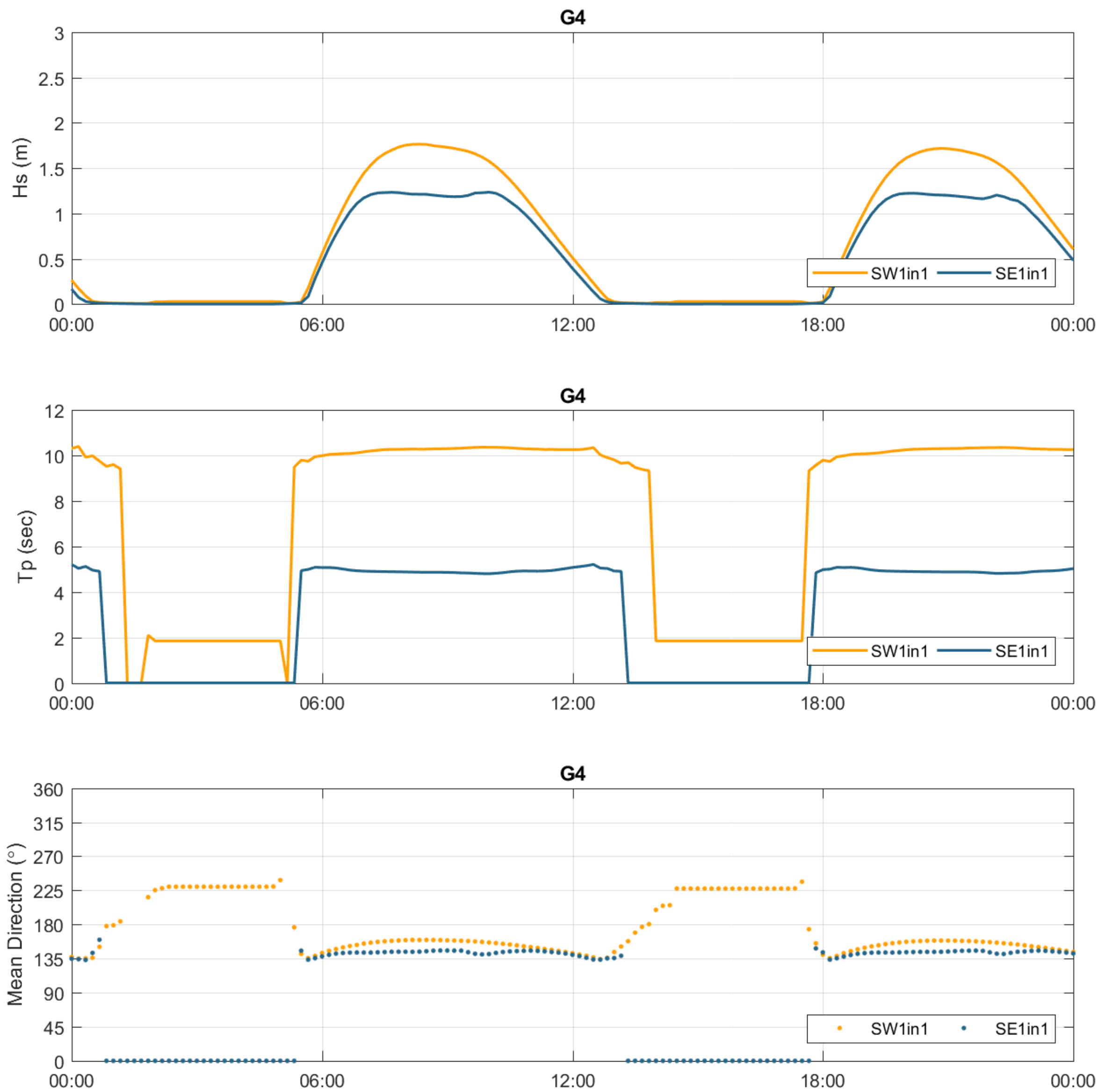

Figure B27. Time series of baseline significant wave height, peak wave period and mean wave direction at G4 - 1 in 1 year event

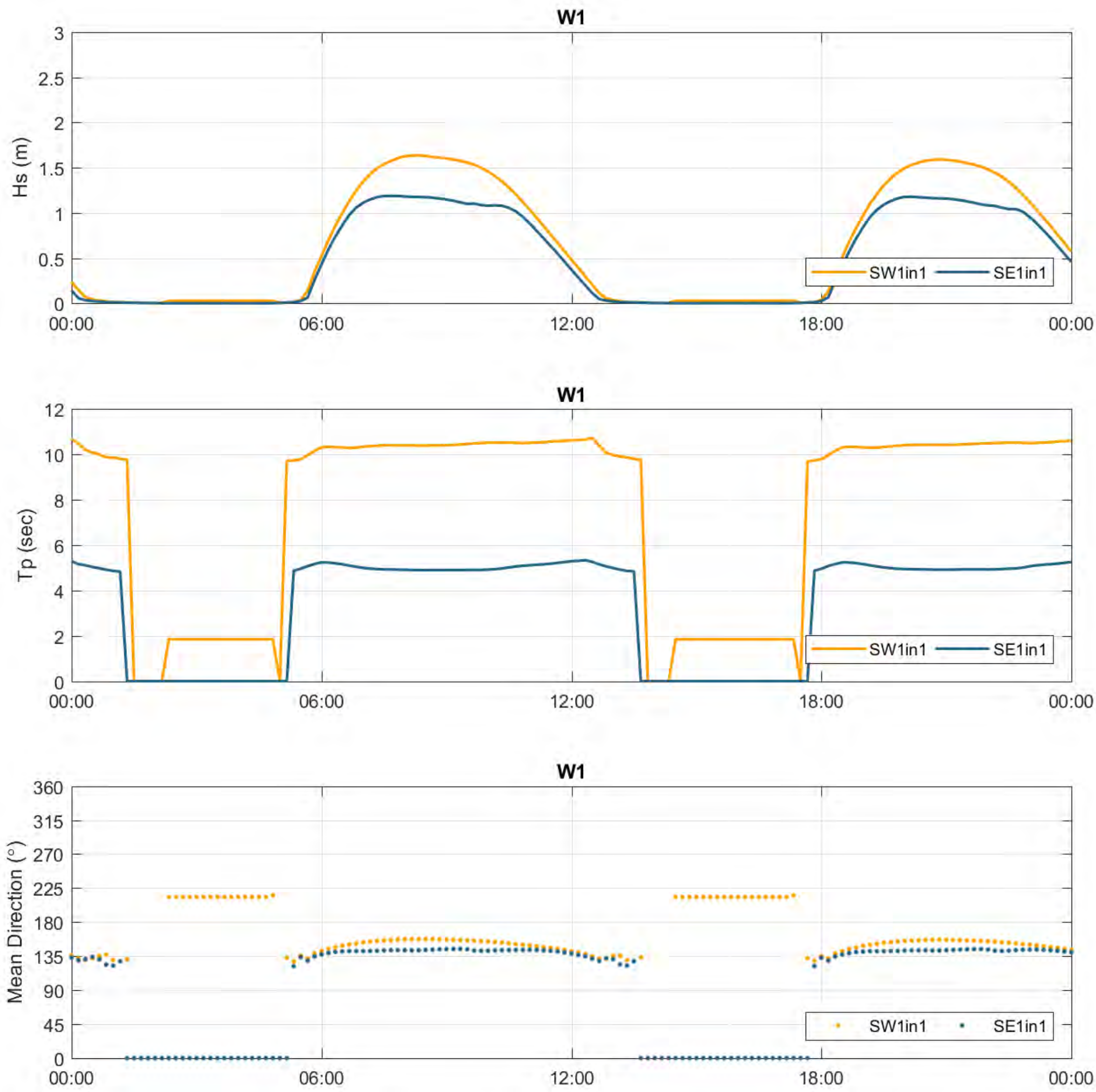

Figure B28. **Time series of baseline significant wave height, peak wave period and mean wave direction at W1 - 1 in 1 year event**

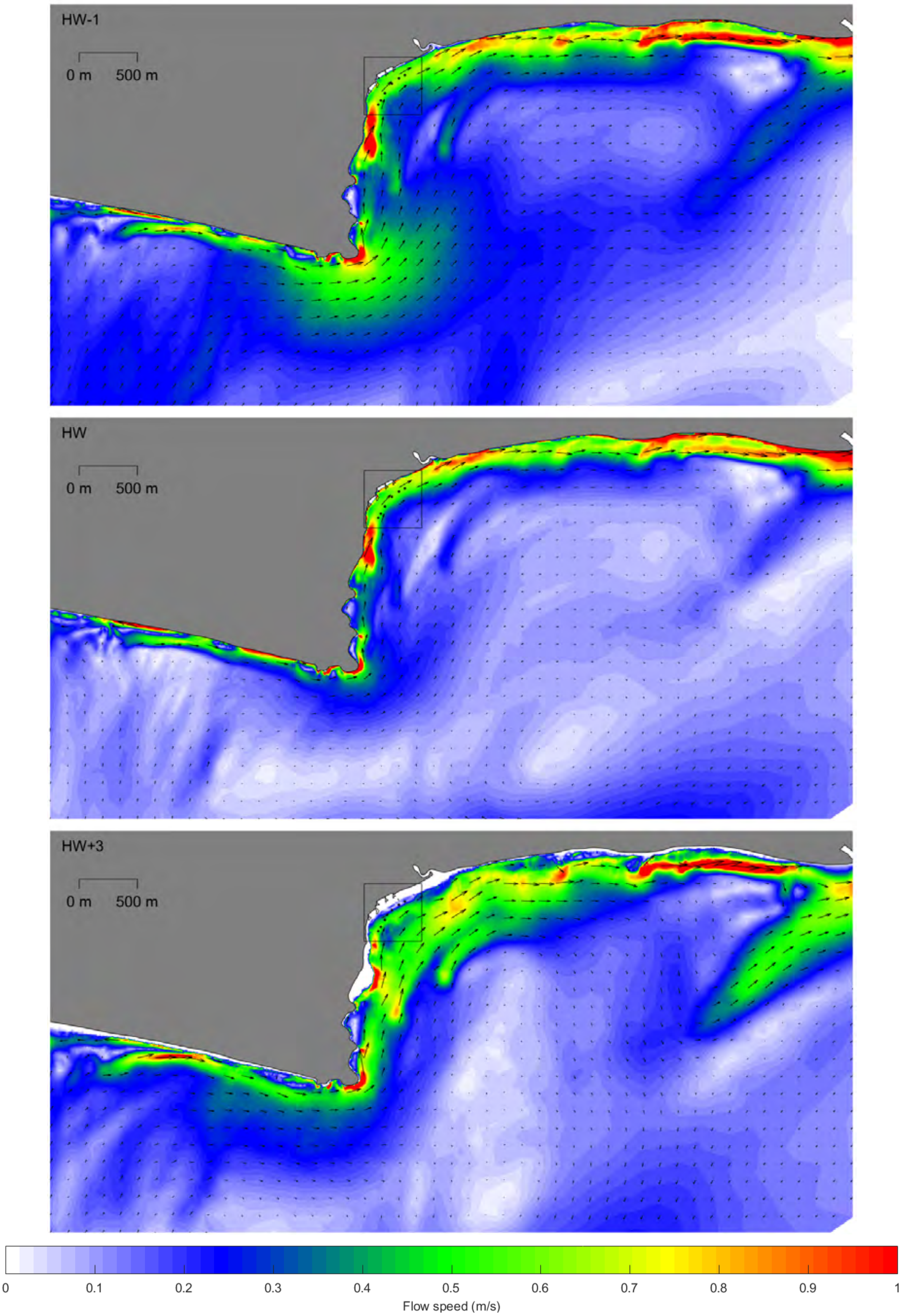

Figure B29. Baseline wave and tidal flow for 1 in 1 year wave from the southwest

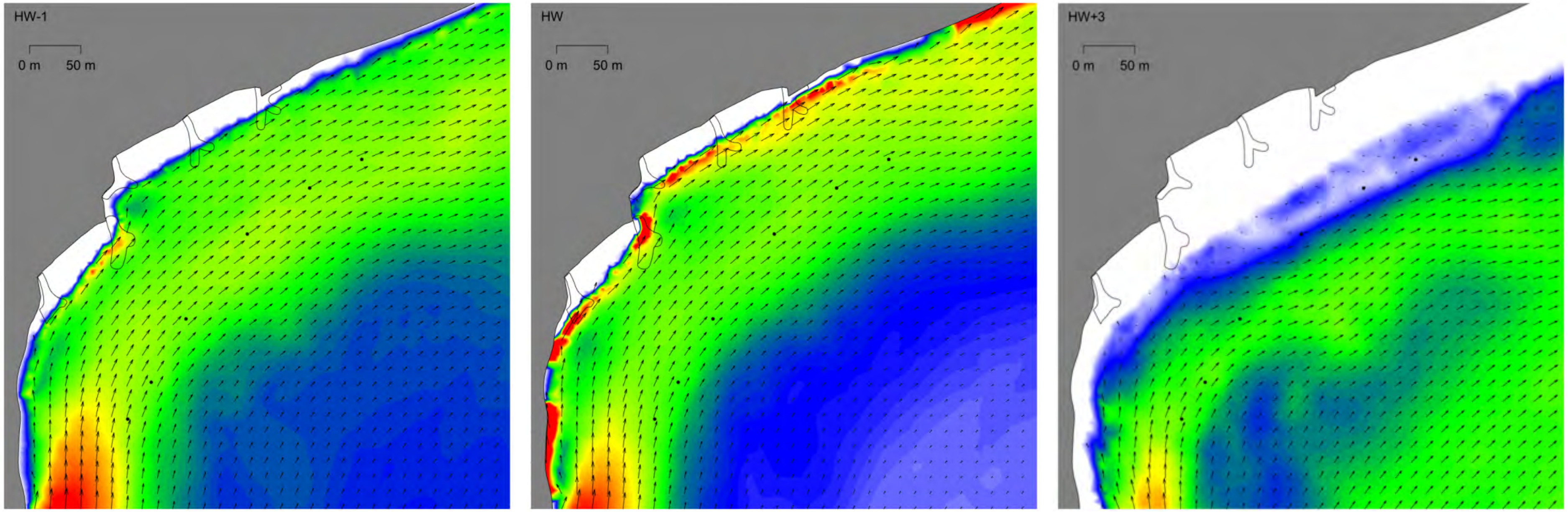

Groynes are not included in the model and are shown only for indicative purposes.
Extraction points are marked for reference but not labelled, see Figure 1 for labels.

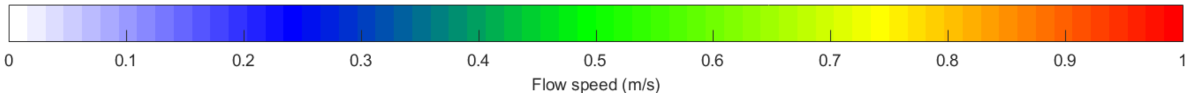

Figure B30. Baseline wave and tidal flow for 1 in 1 year wave from the southwest – local area

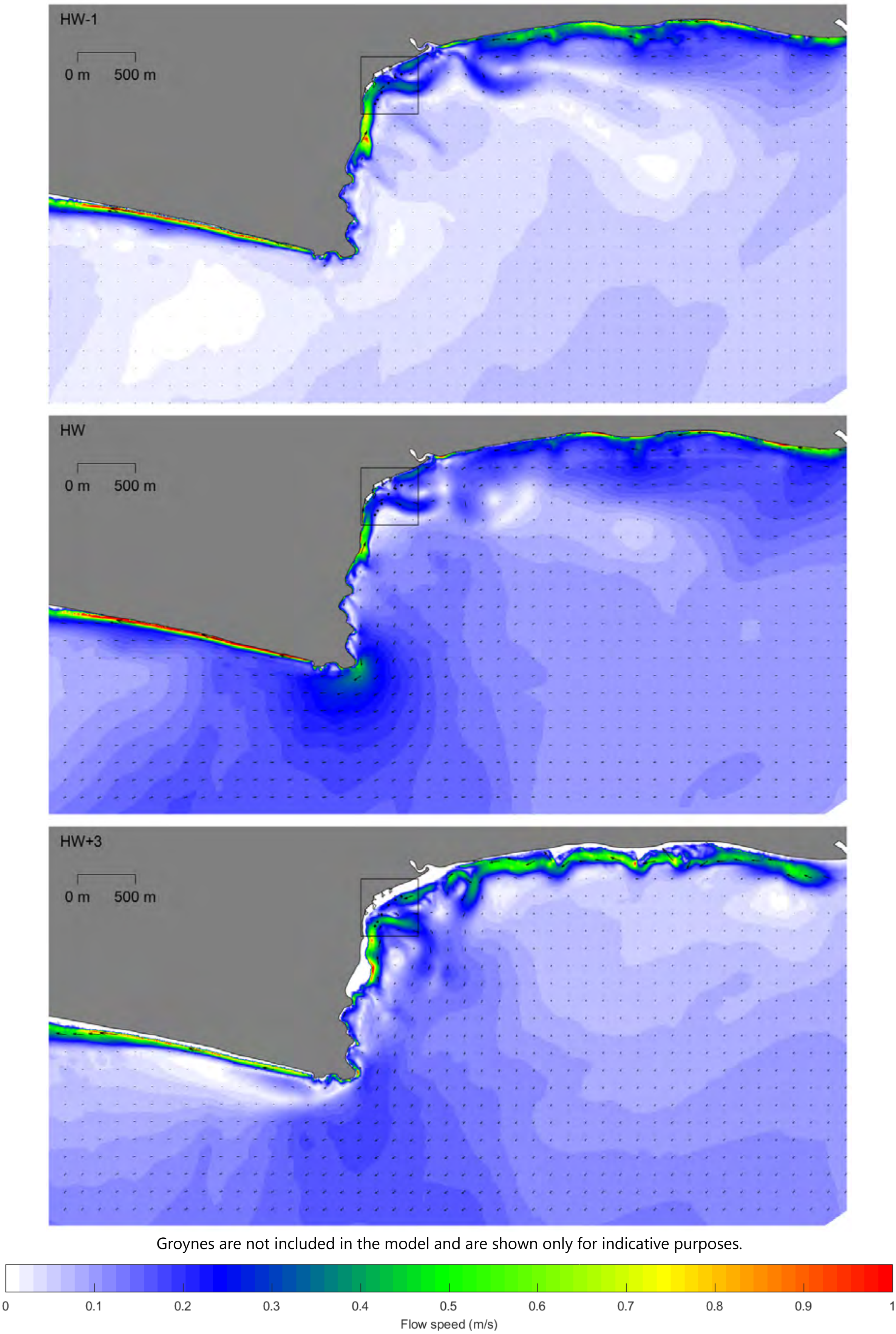

Figure B31. Baseline wave and tidal flow for 1 in 1 year wave from the southeast

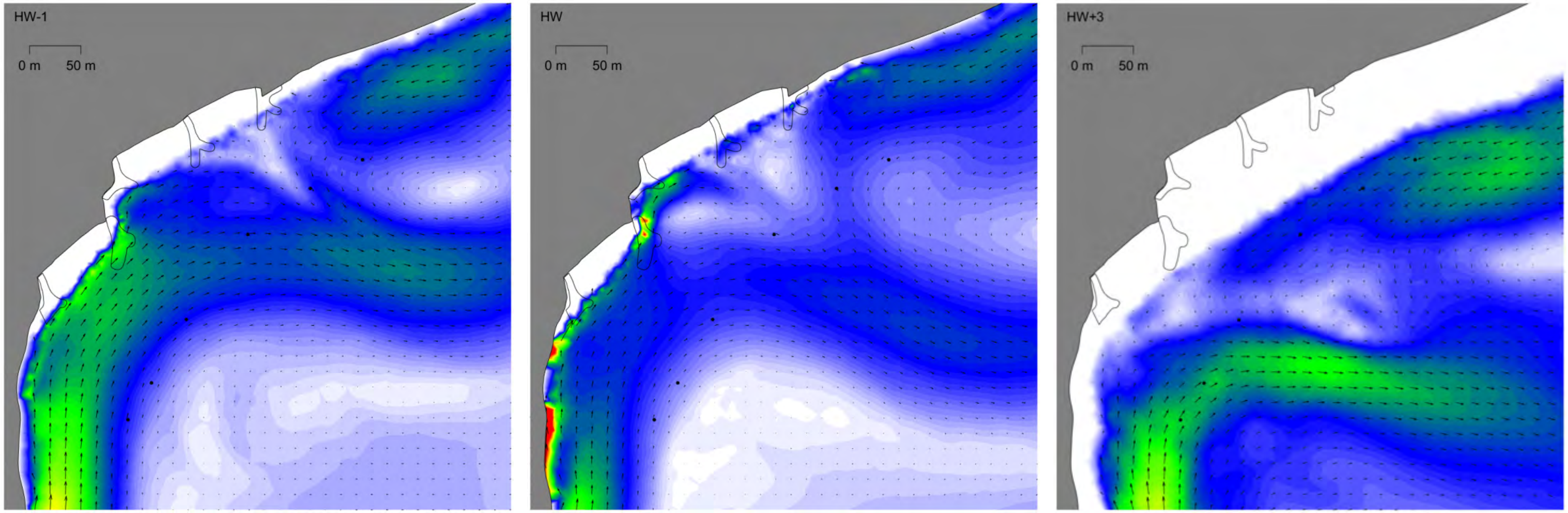

Groynes are not included in the model and are shown only for indicative purposes.
Extraction points are marked for reference but not labelled, see Figure 1 for labels.

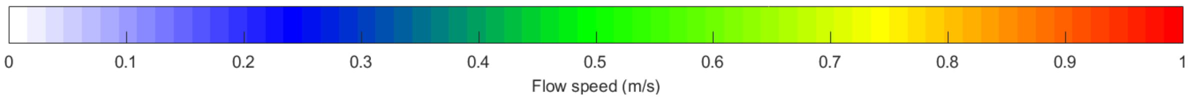

Figure B32. Baseline wave and tidal flow for 1 in 1 year wave from the southeast – local area

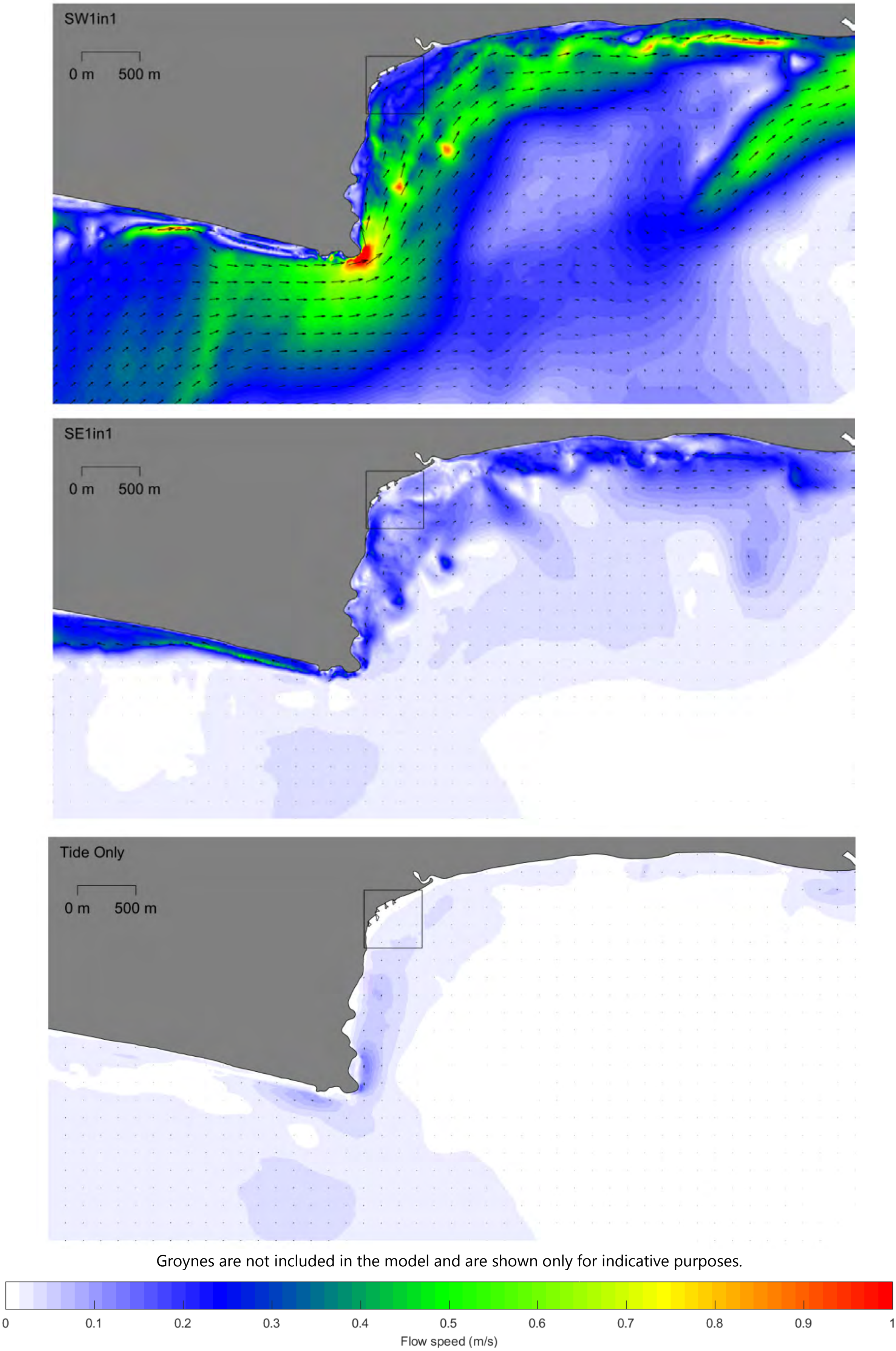

Figure B33. Baseline mean wave and tidal flow throughout tidal cycle during 1 in 1 year events

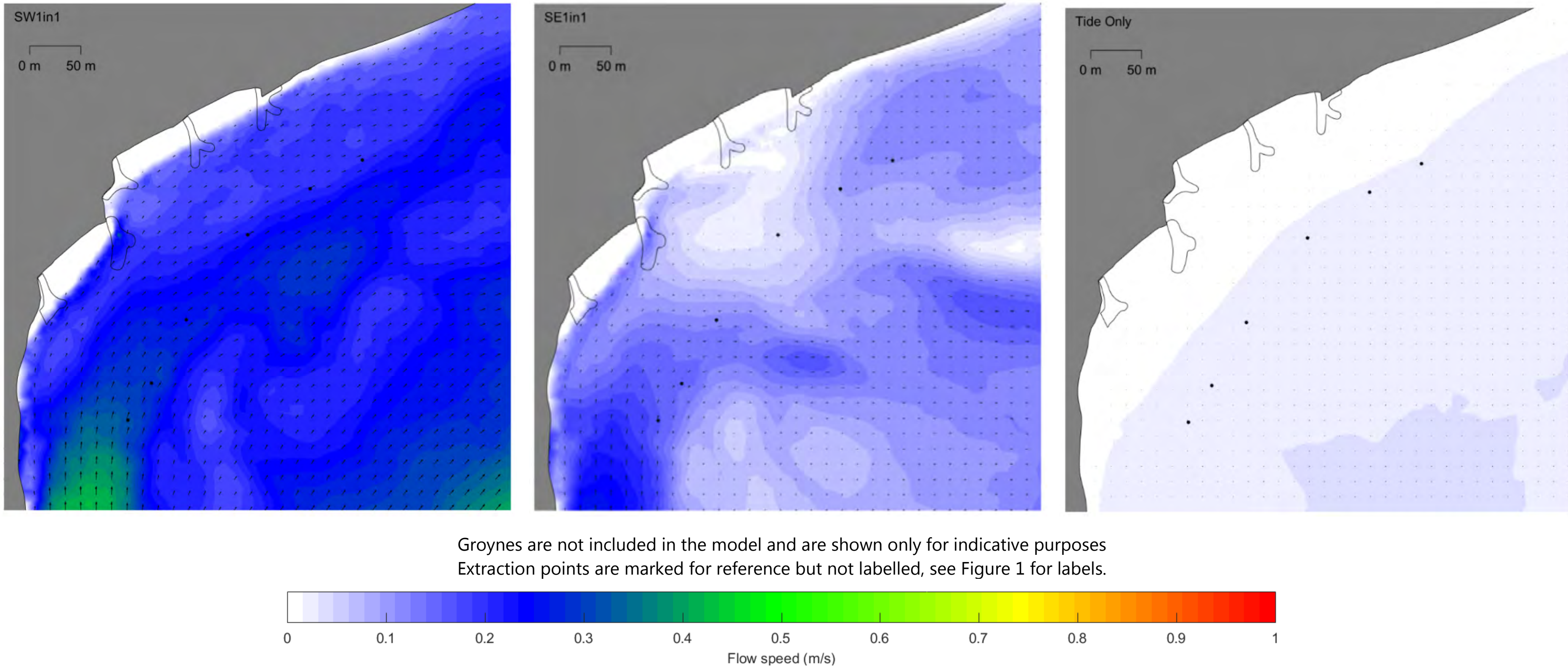

Figure B34. Baseline mean wave and tidal flow throughout tidal cycle for 1 in 1 year events – local area

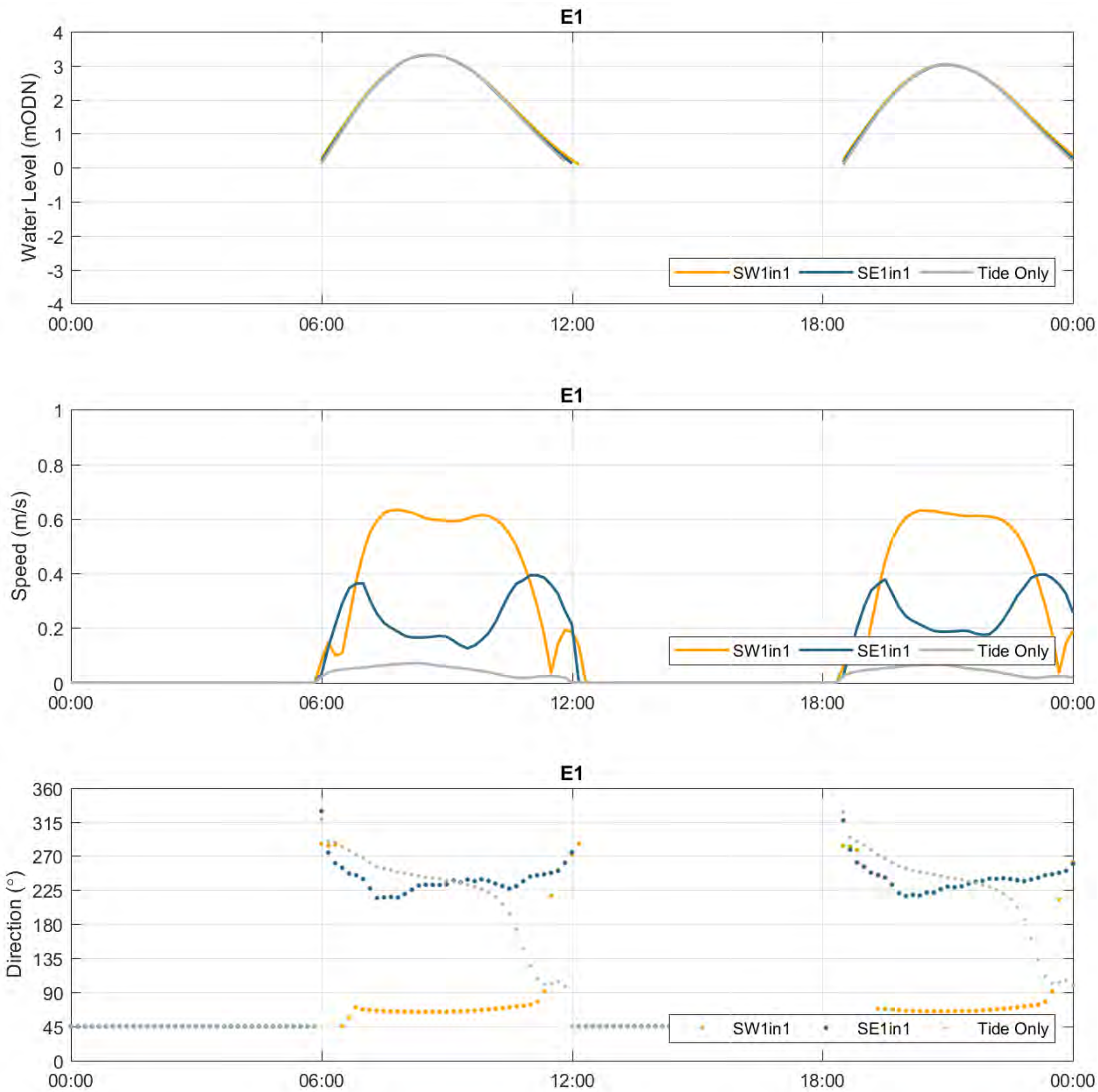

Figure B35. Time series of baseline water level, flow speed and flow direction at E1 for 1 in 1 year events

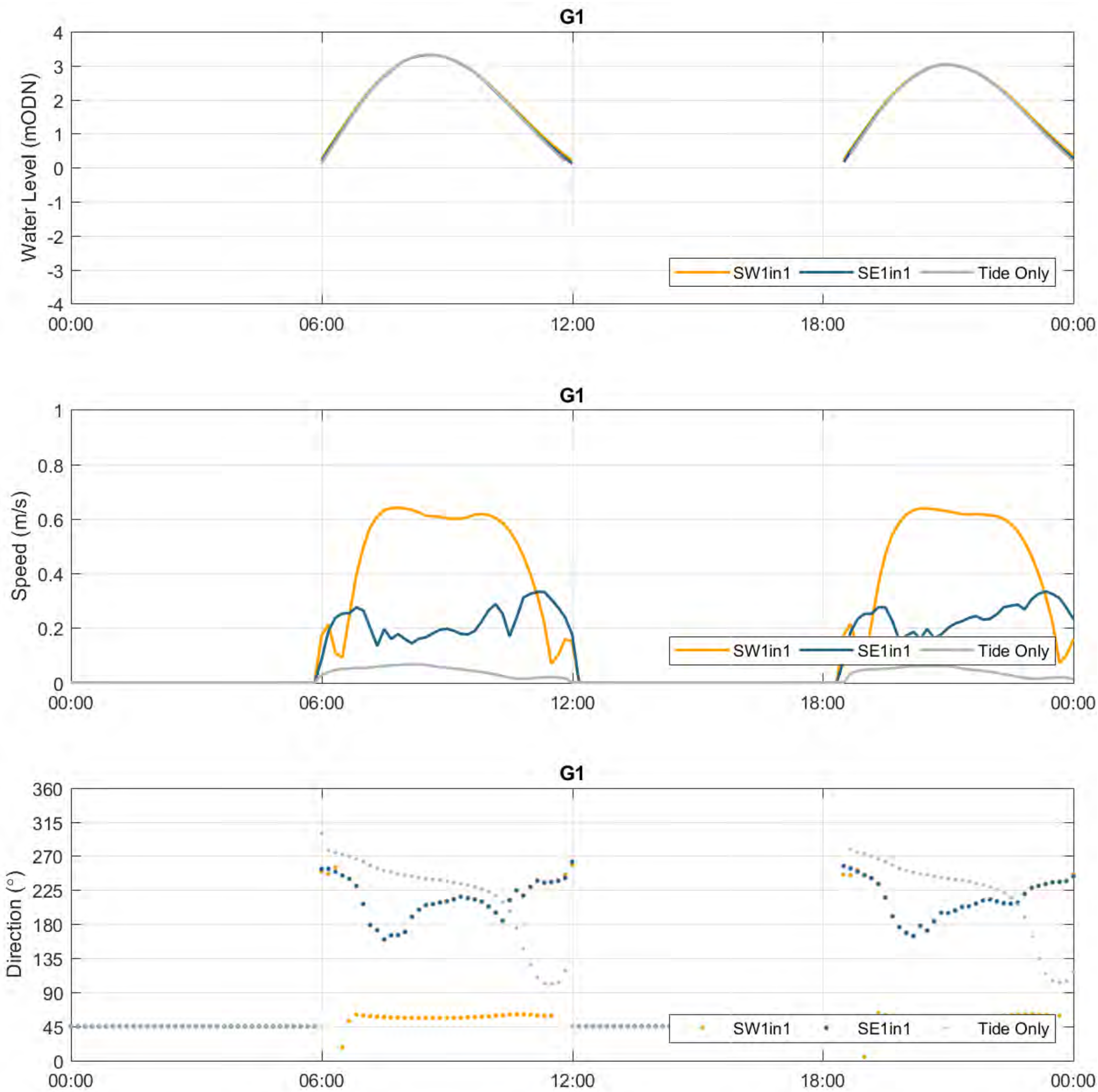

Figure B36. Time series of baseline water level, flow speed and flow direction at G1 for 1 in 1 year events

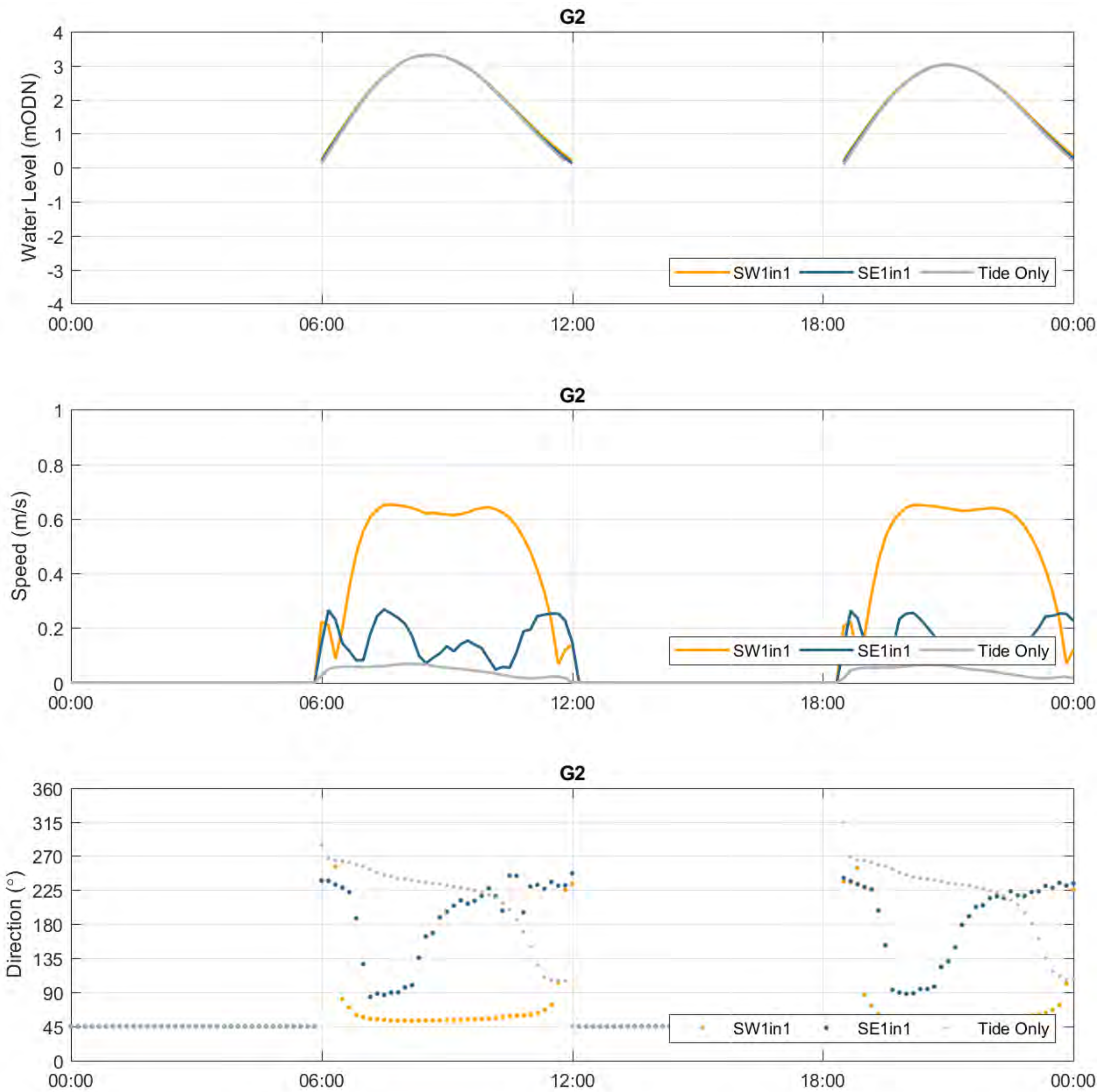

Figure B37. **Time series of baseline water level, flow speed and flow direction at G2 for 1 in 1 year event**

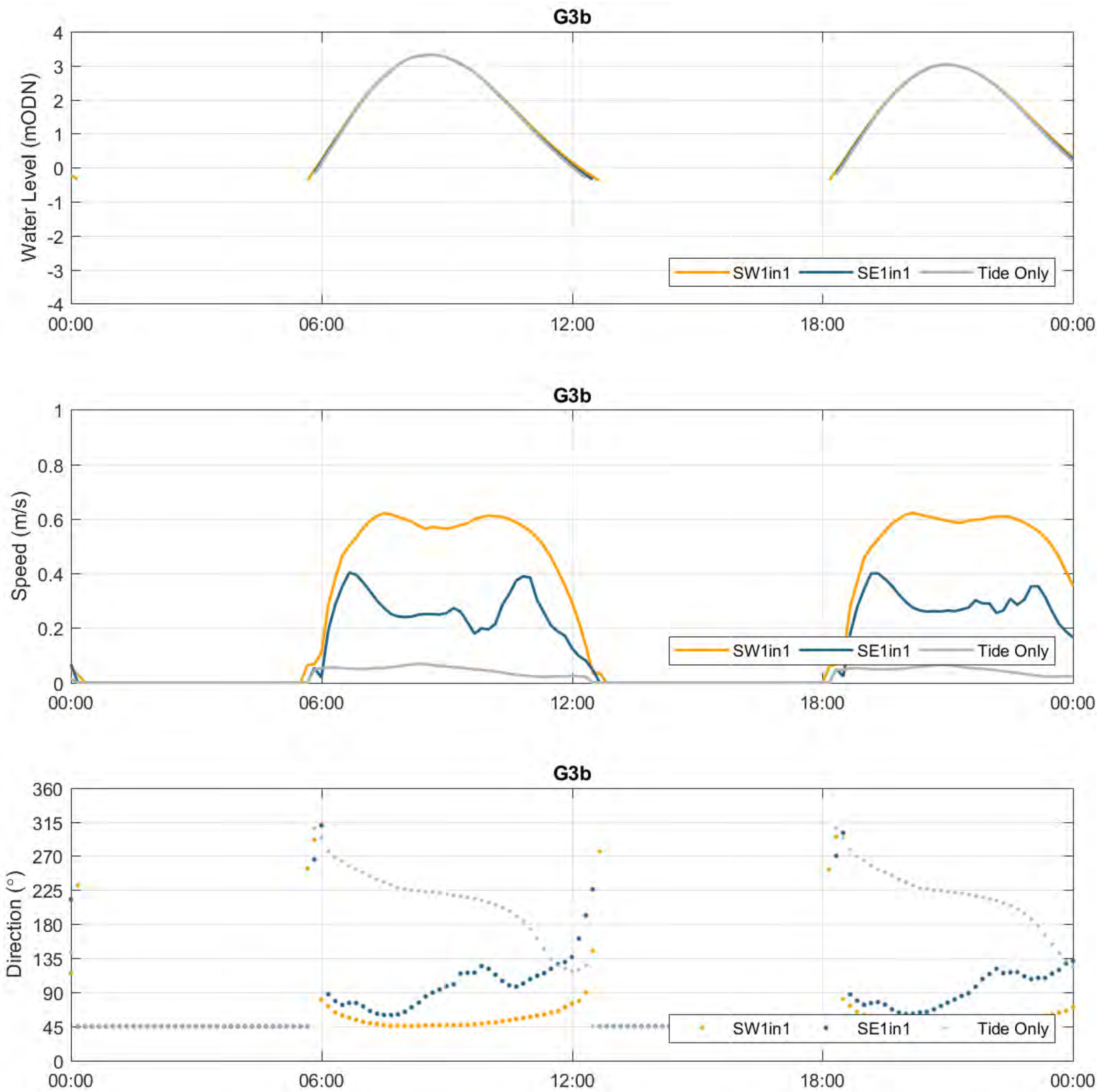

Figure B38. **Time series of baseline water level, flow speed and flow direction at G3b for 1 in 1 year events**

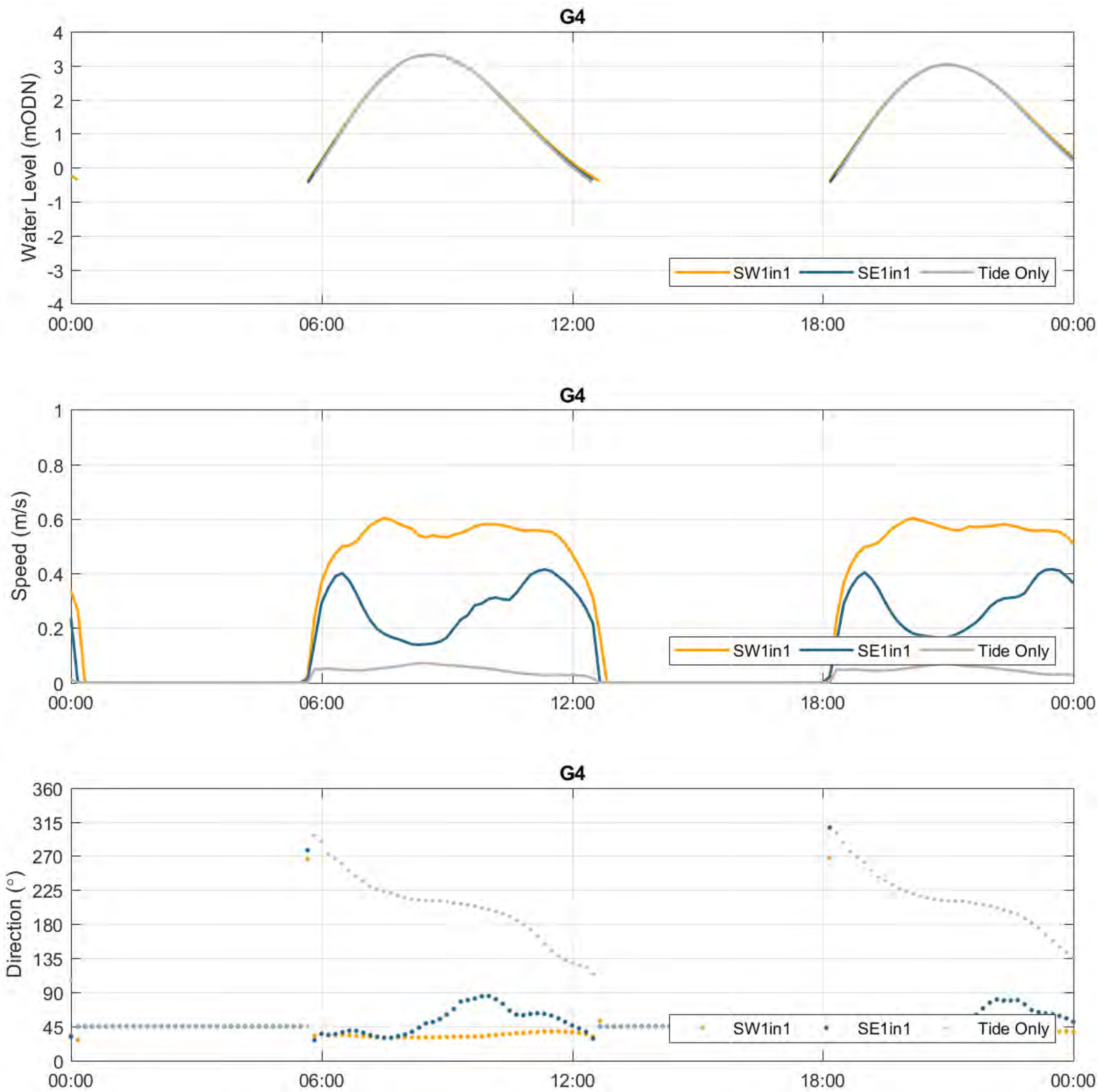

Figure B39. **Time series of baseline water level, flow speed and flow direction at G4 for 1 in 1 year events**

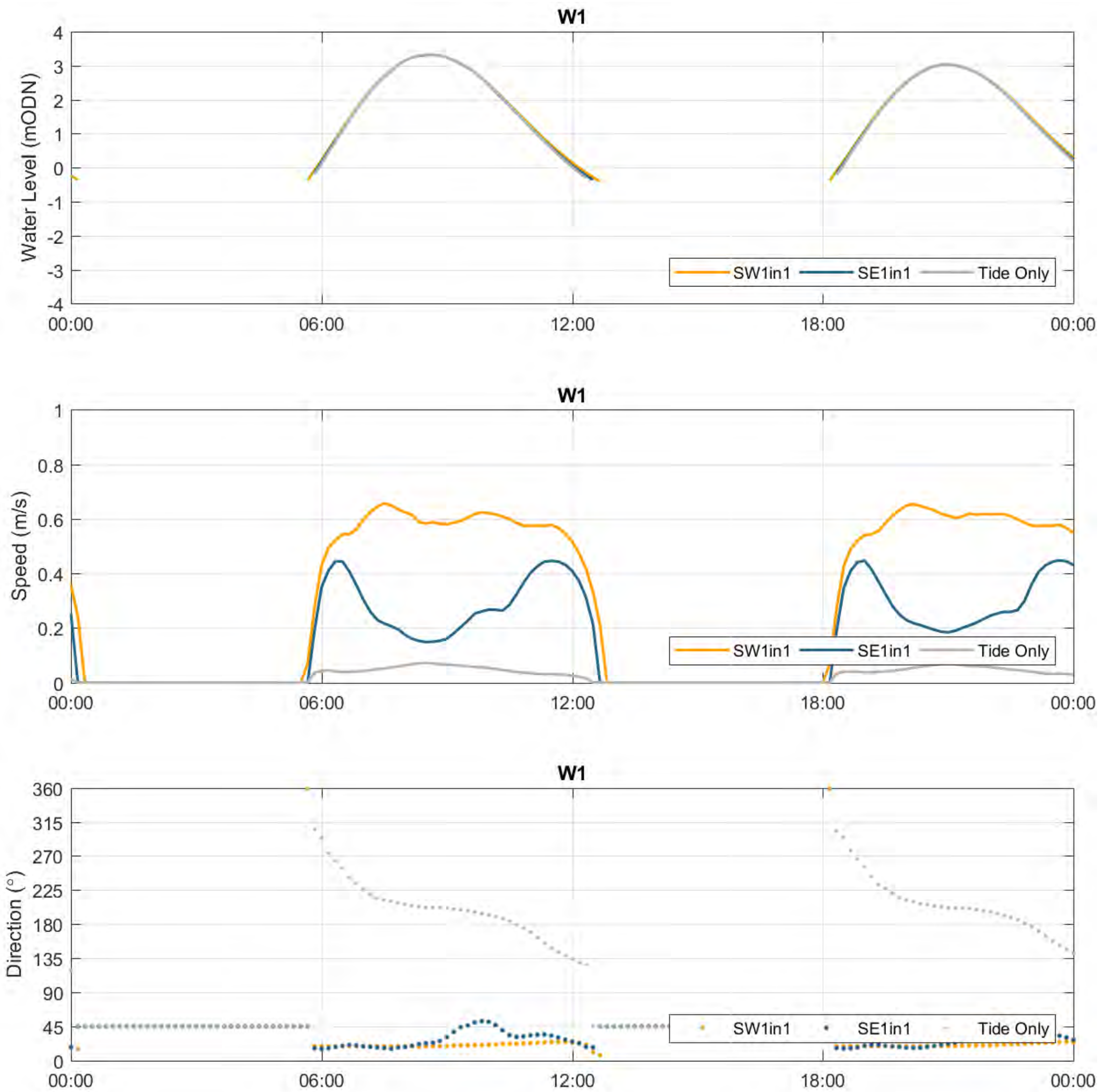

Figure B40. **Time series of baseline water level, flow speed and flow direction at W1 for 1 in 1 year events**

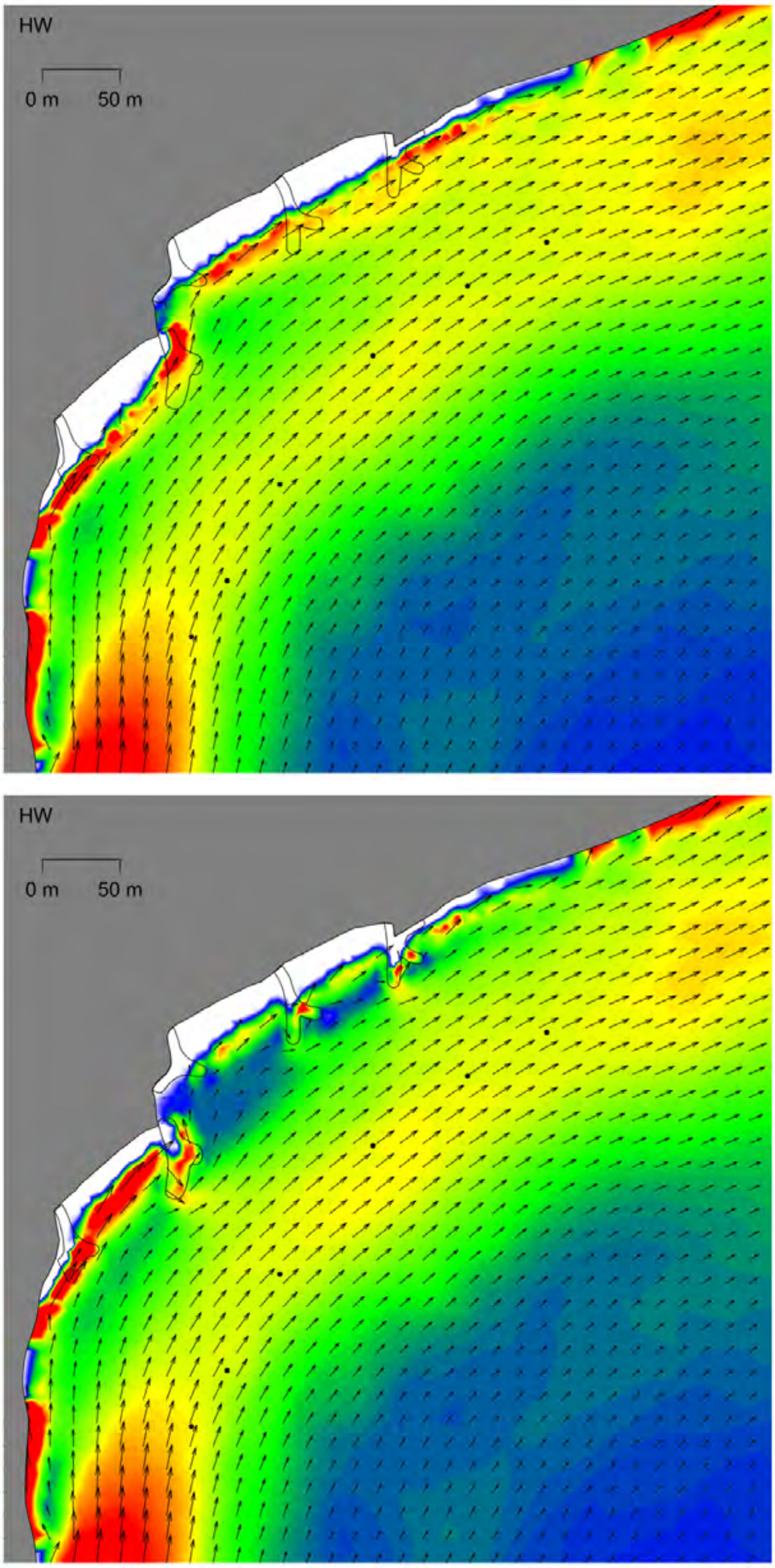

Extraction points are marked for reference but not labelled, see Figure 1 for labels.

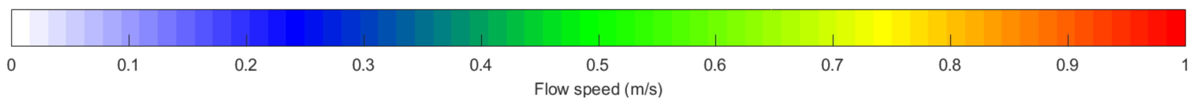

Figure B41. Flows from the 1 in 35 wave from the southwest for baseline (upper) and scheme (lower)

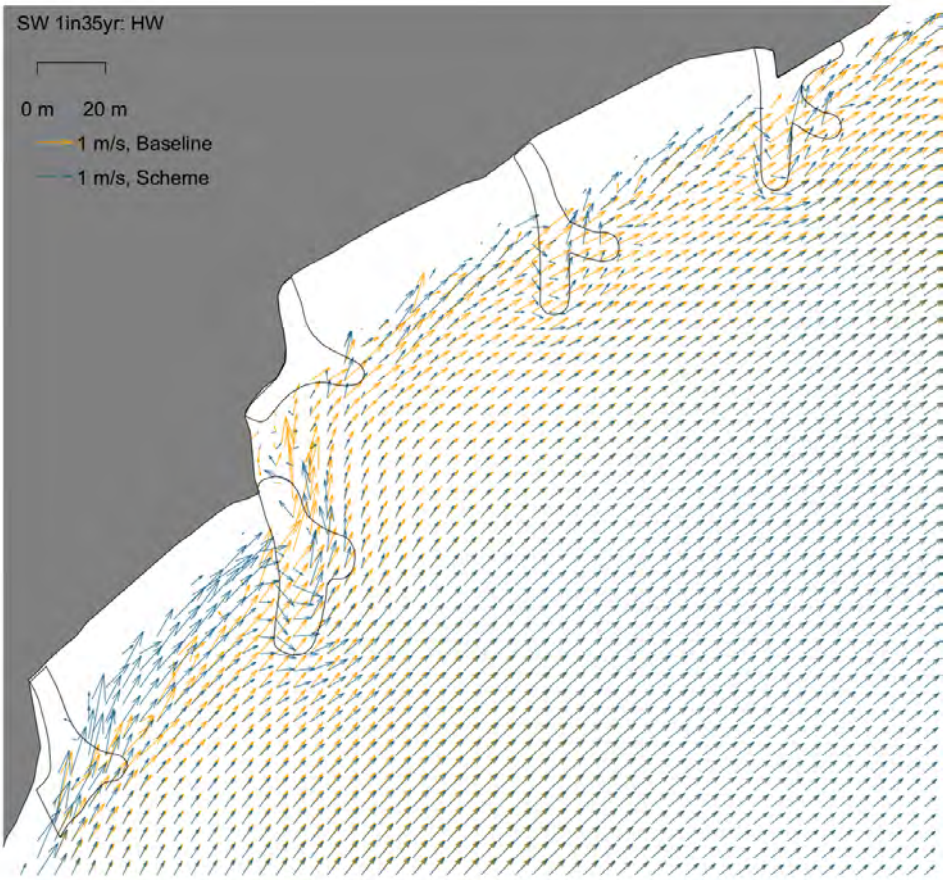

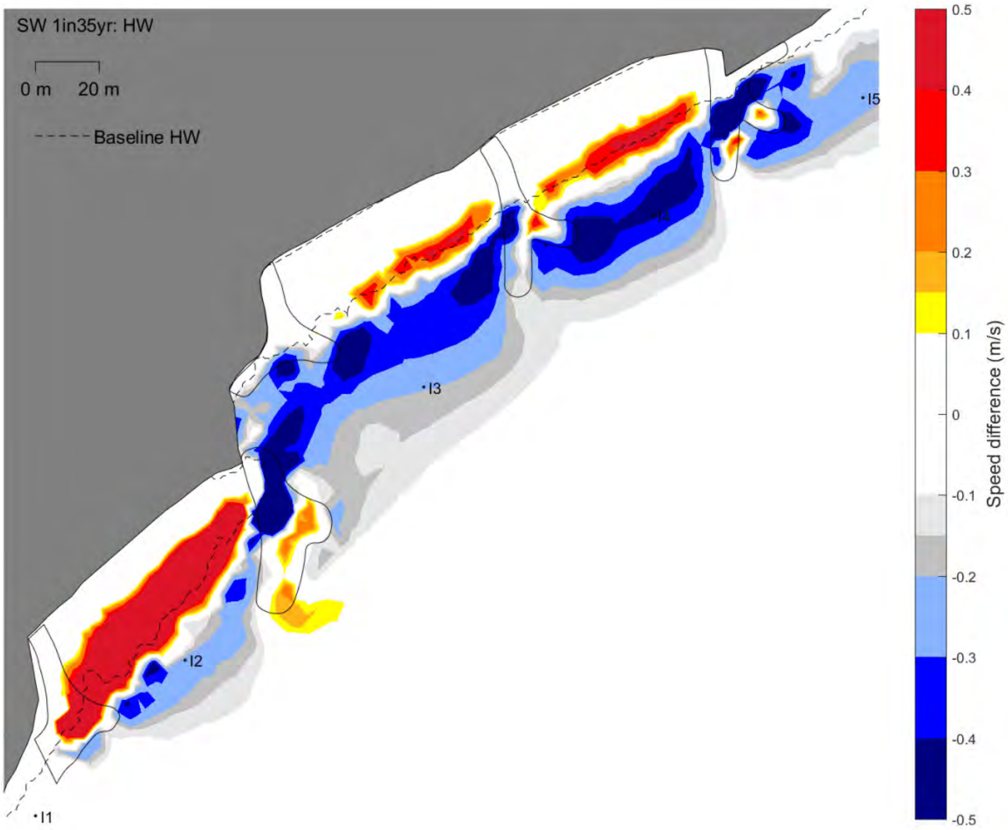

Figure B42. **Baseline and Scheme flows (upper) and the difference in flow (scheme minus baseline) (lower) from the 1 in 35 wave from the southwest**

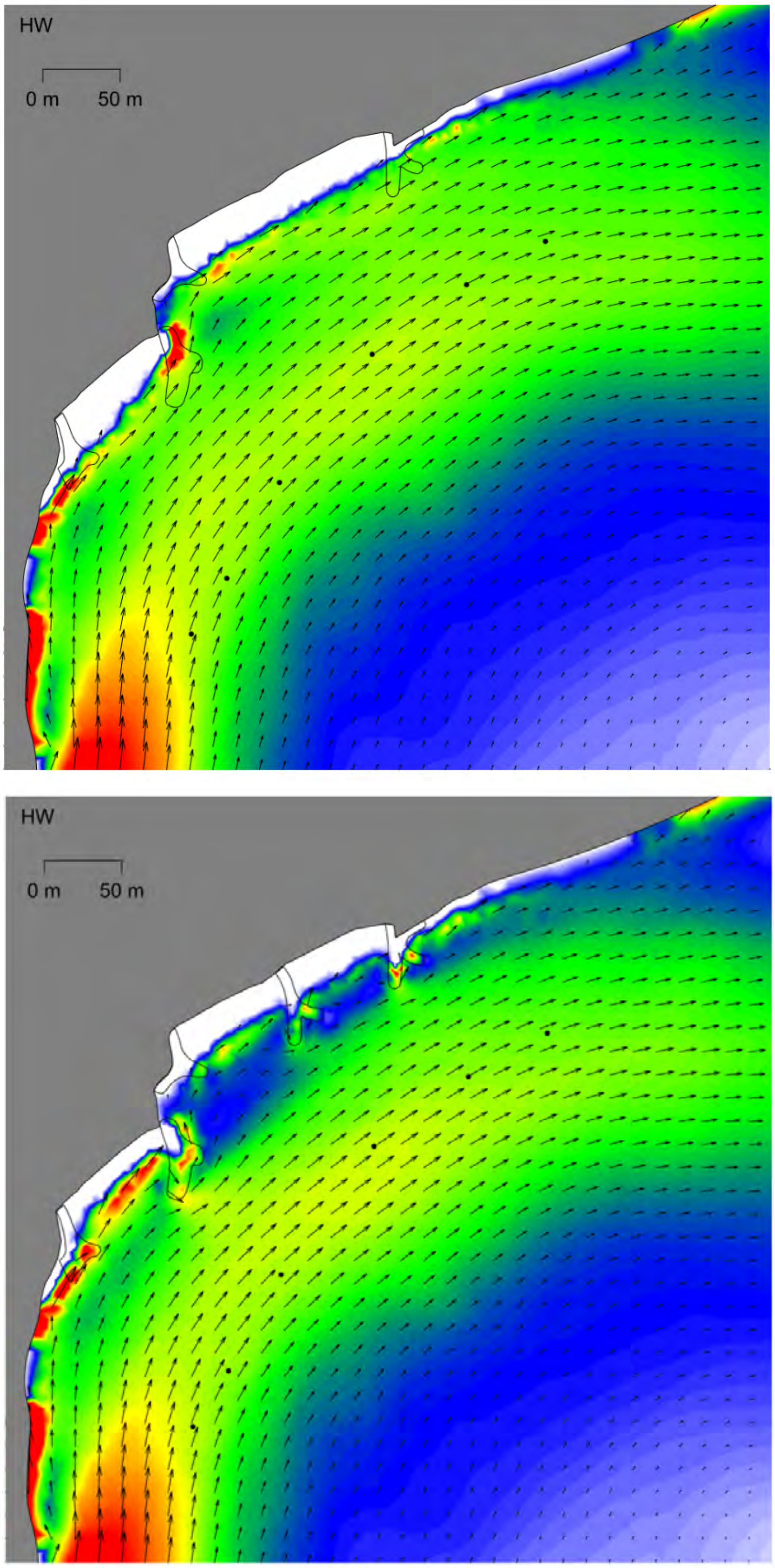

Extraction points are marked for reference but not labelled, see Figure 1 for labels.

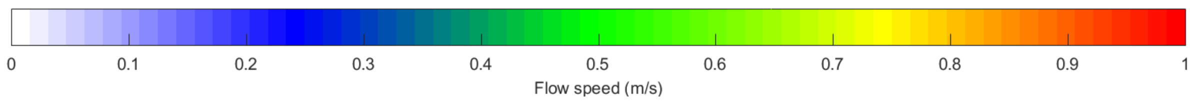

Figure B43. Flows from the 1 in 35 wave from the SE for baseline (upper) and scheme (lower)

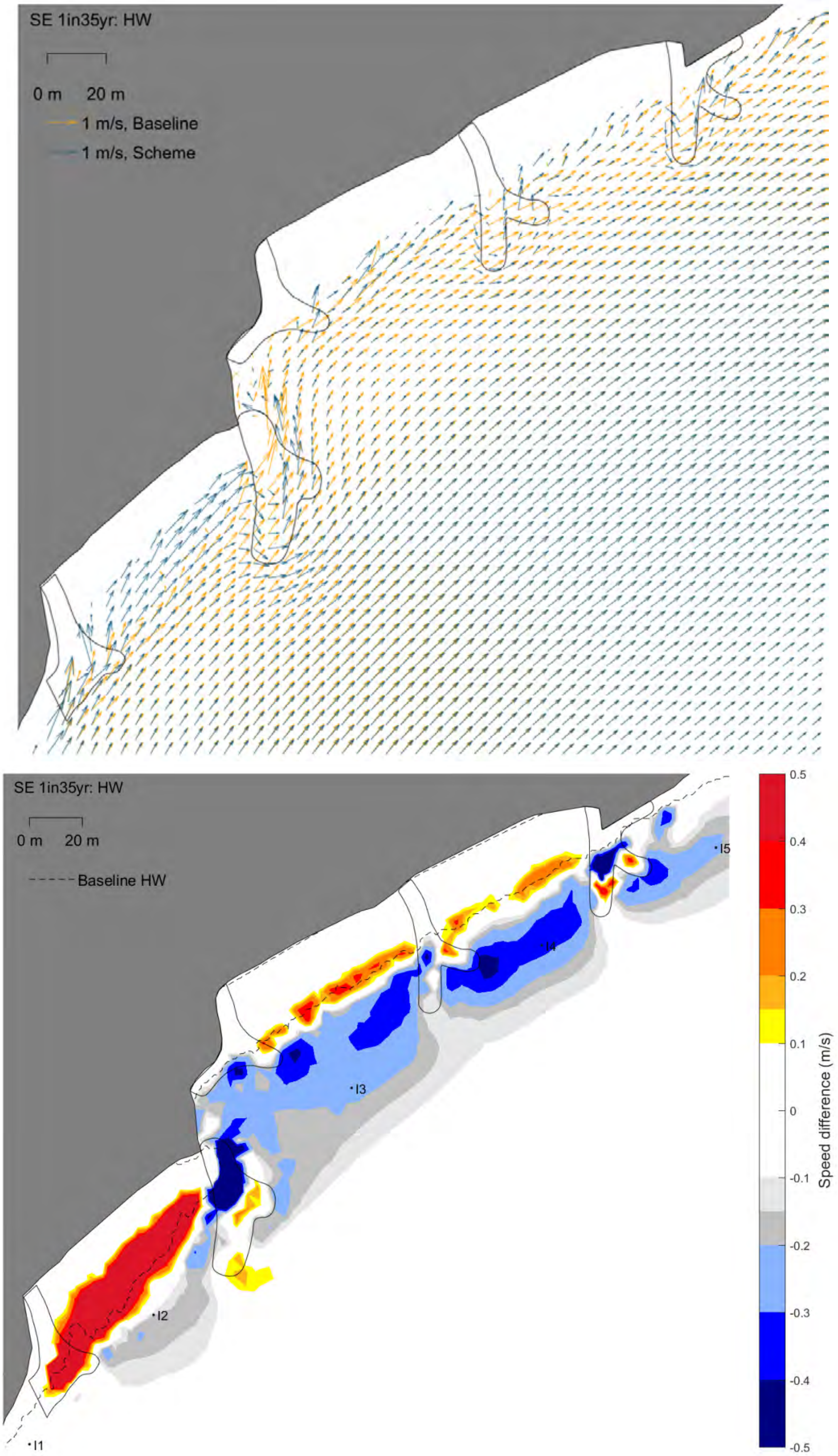

Figure B44. **Baseline and Scheme flows (upper) and the difference in flow (scheme minus baseline) (lower) from the 1 in 35 wave from the SE**

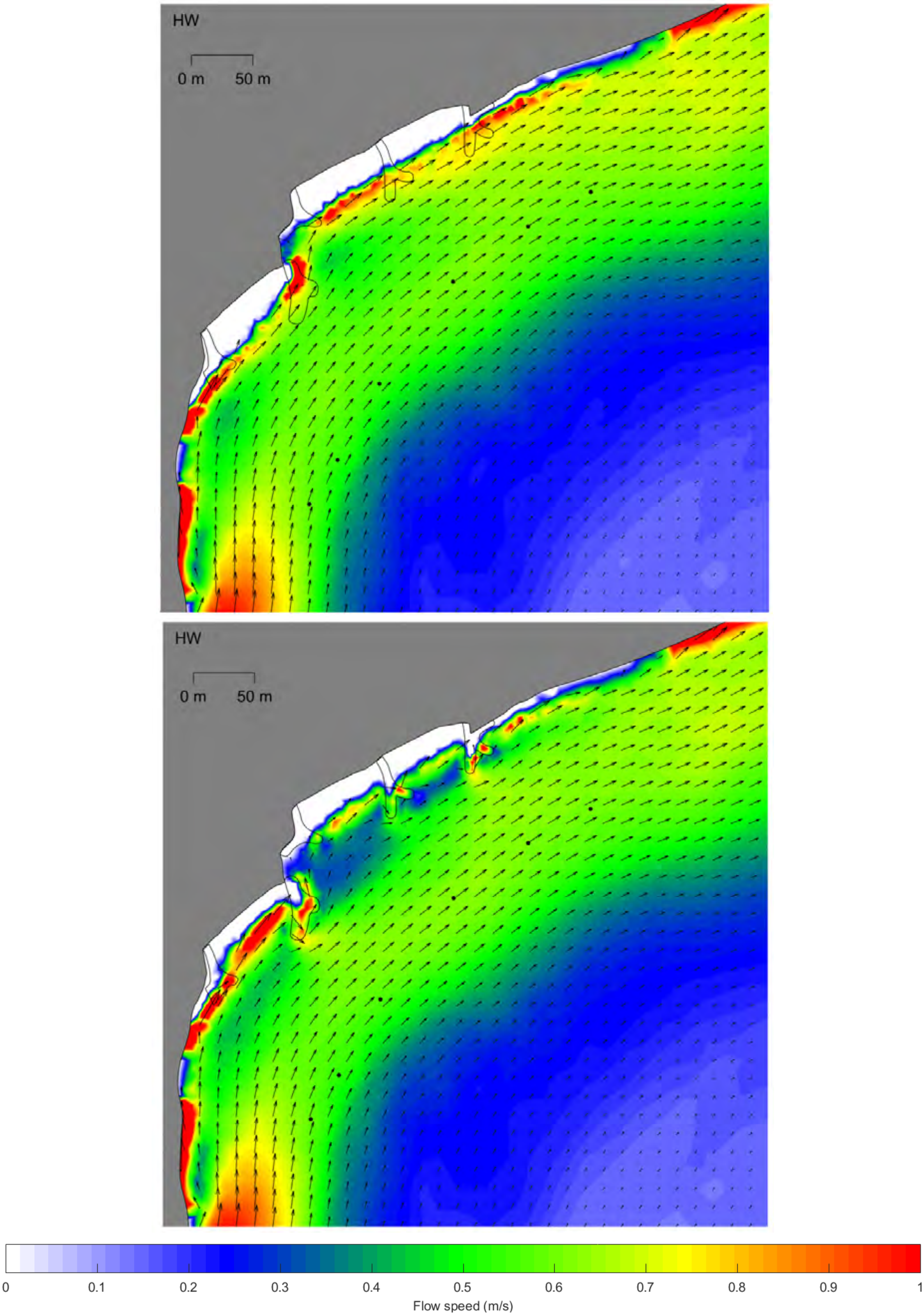

Extraction points are marked for reference but not labelled, see Figure 1 for labels

Figure B45. Flows from the 1 in 1 wave from the SW for baseline (upper) and scheme (lower)

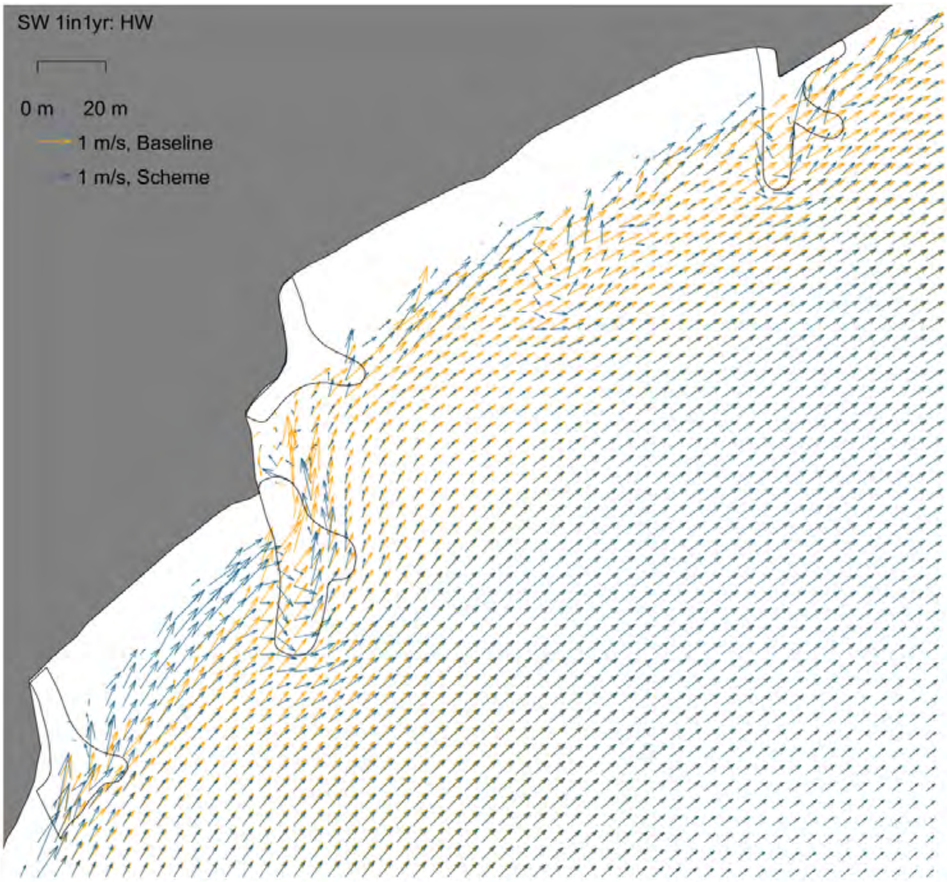

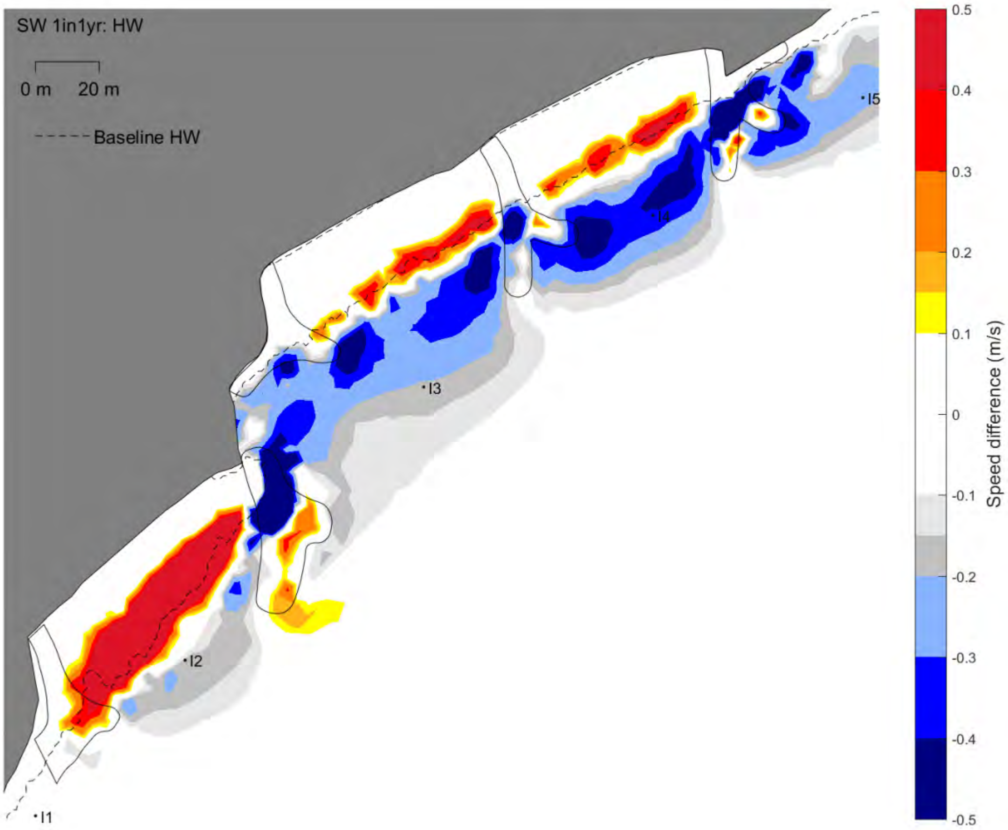

Figure B46. **Baseline and Scheme flows (upper) and the difference in flow (scheme minus baseline) (lower) from the 1 in 1 wave from the SW**

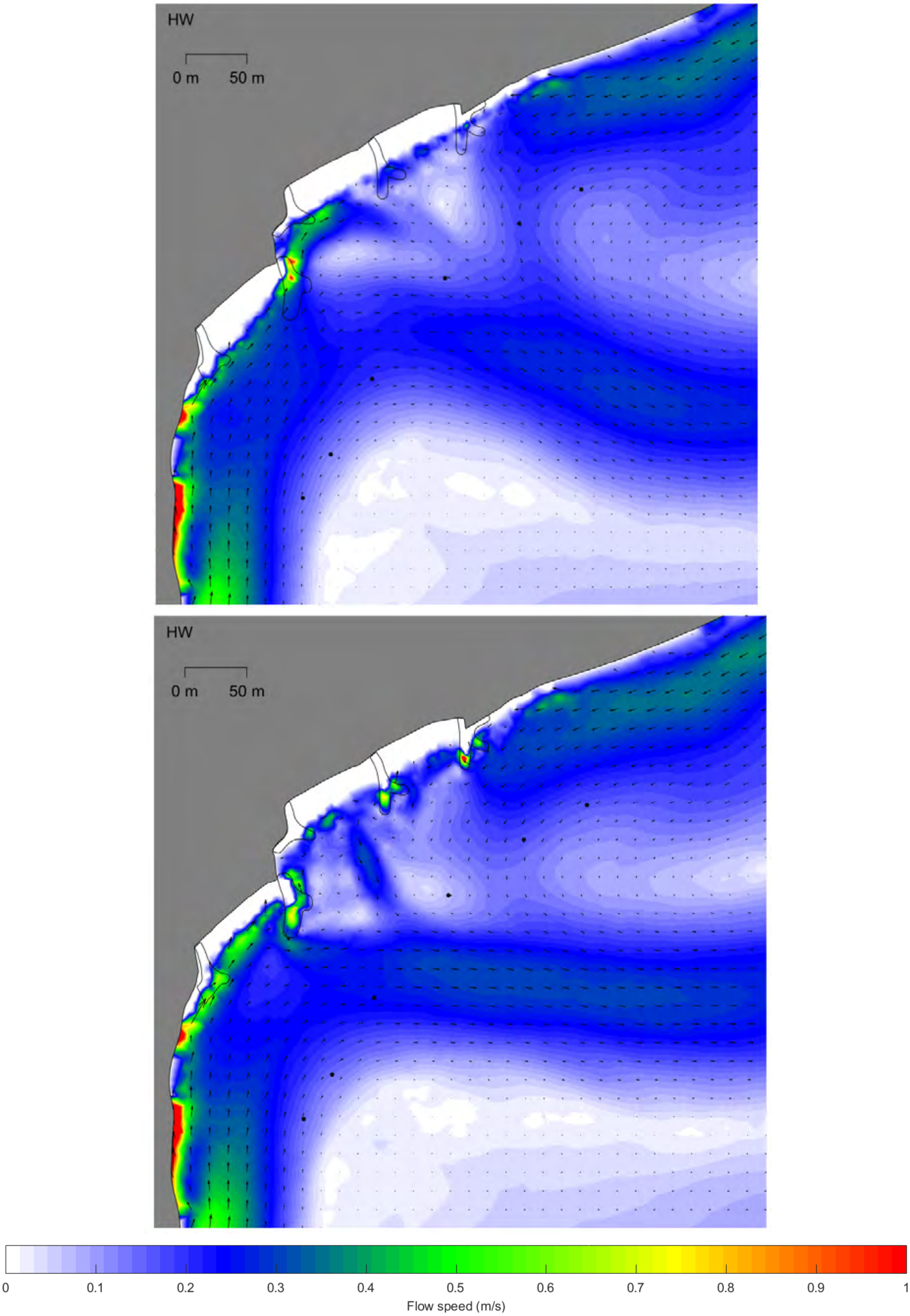

Extraction points are marked for reference but not labelled, see Figure 1 for labels.

Figure B47. Flows from the 1 in 1 wave from the SE for baseline (upper) and scheme (lower)

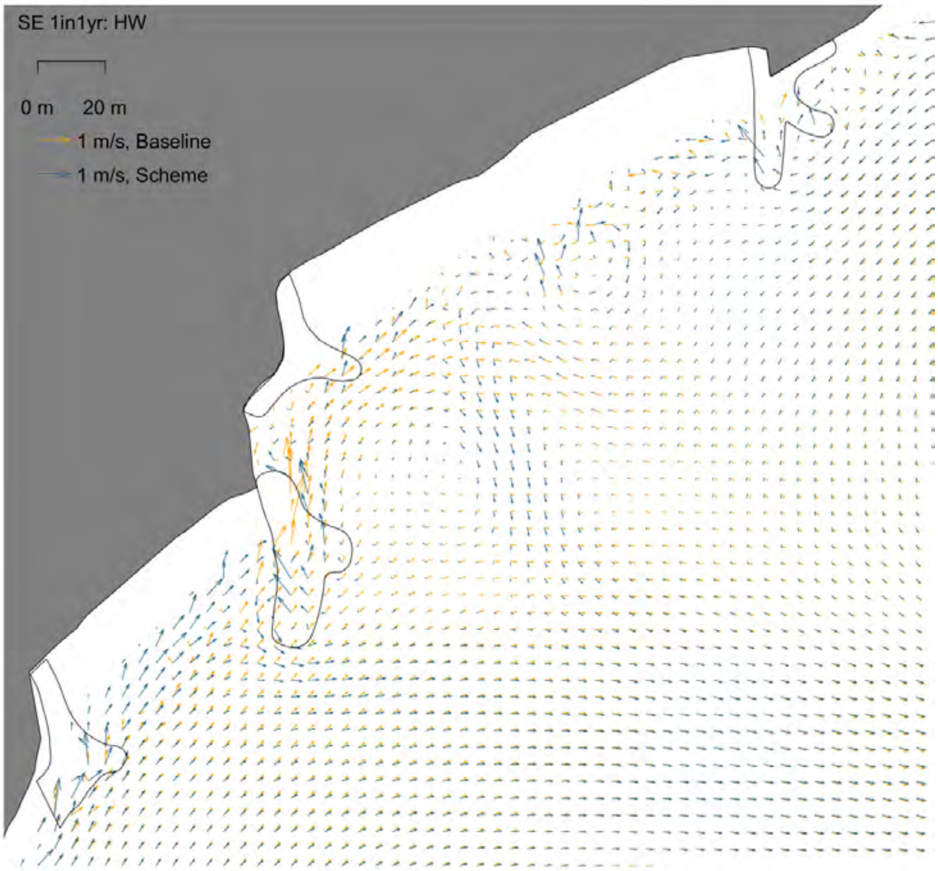

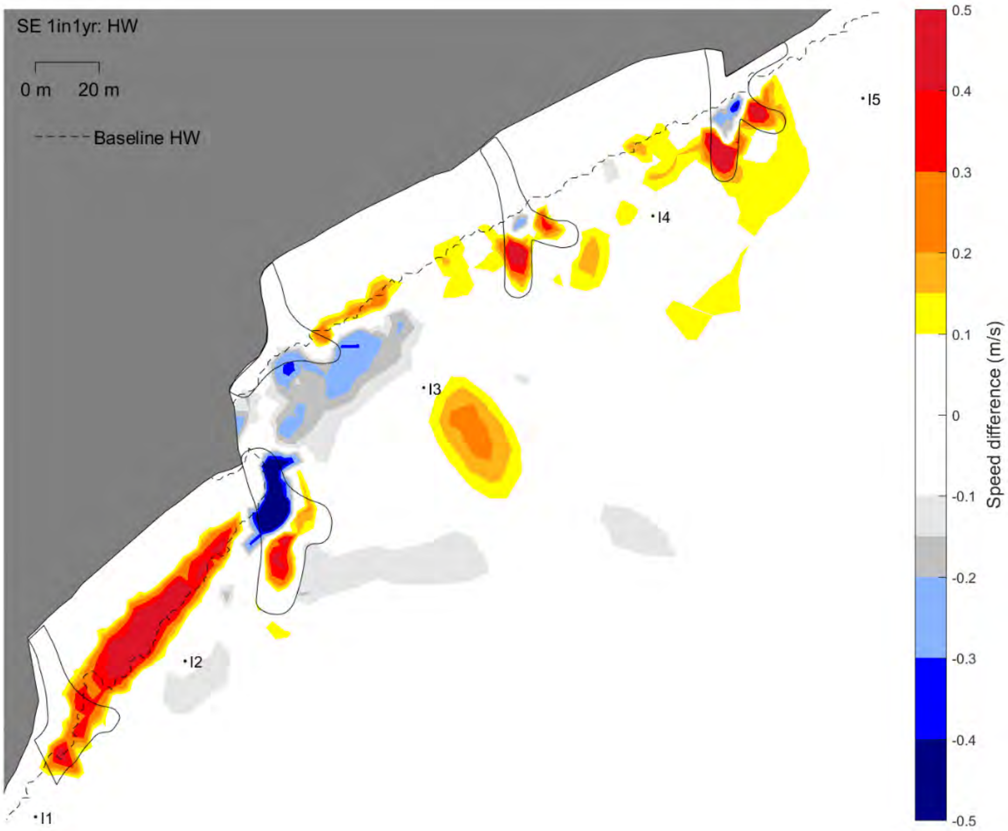

Figure B48. **Baseline and Scheme flows (upper) and the difference in flow (scheme minus baseline) (lower) from the 1 in 1 wave from the SE**

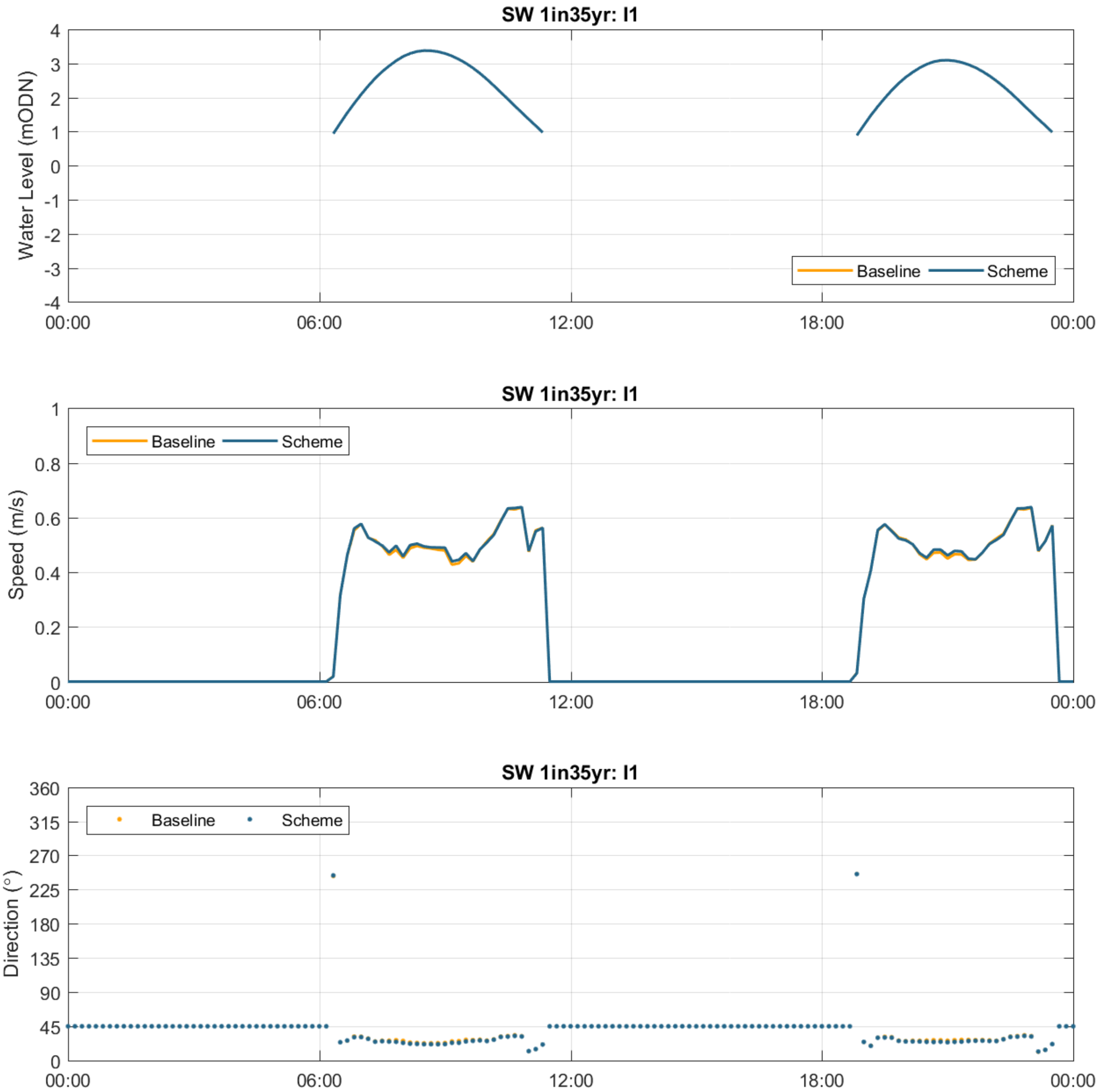

Figure B49. **Time series of water level, flow speed and flow direction at I1 for the baseline and scheme runs for the 1 in 35 year wave from the southwest**

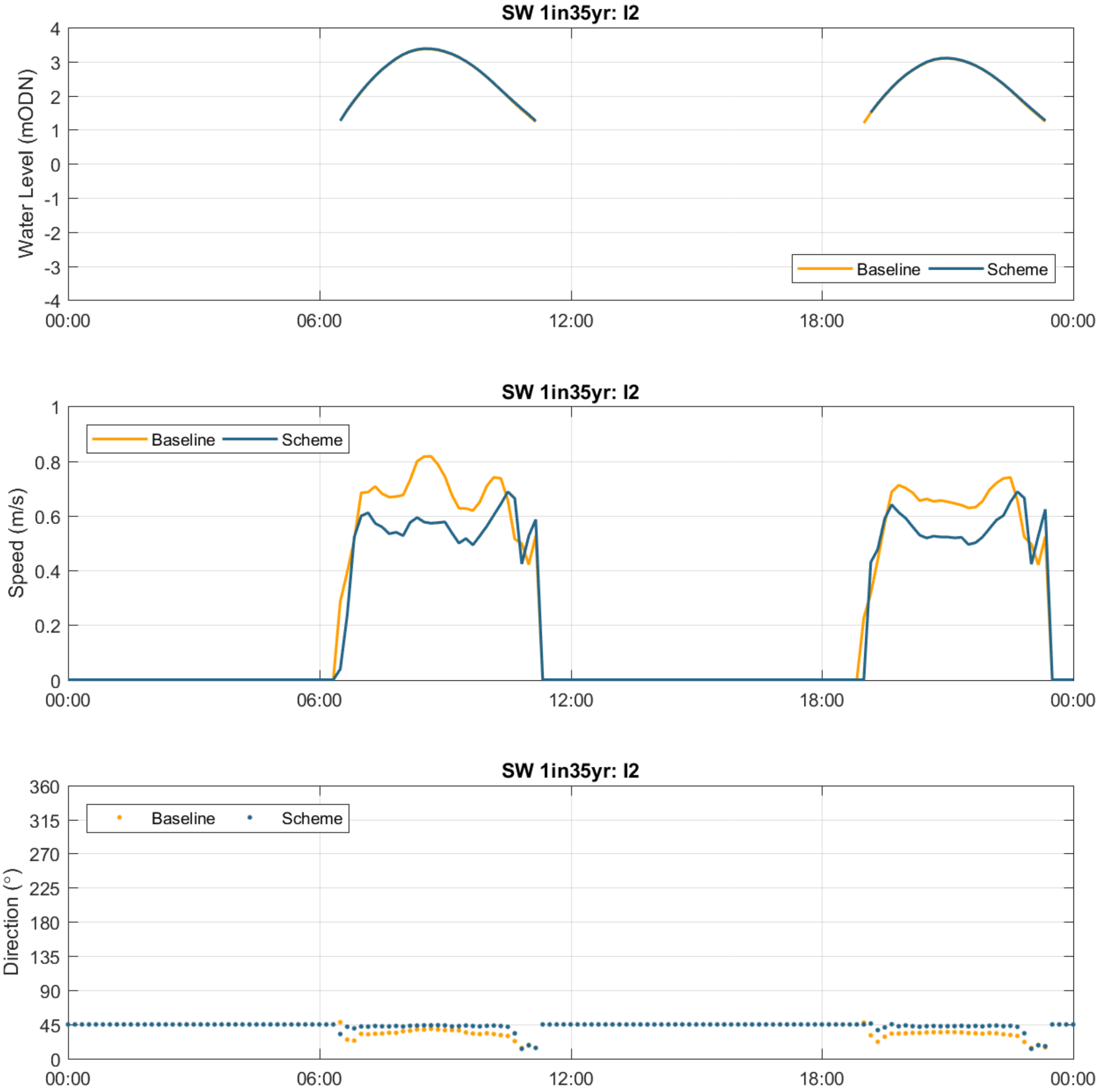

Figure B50. **Time series of water level, flow speed and flow direction at I2 for the baseline and scheme runs for the 1 in 35 year wave from the southwest**

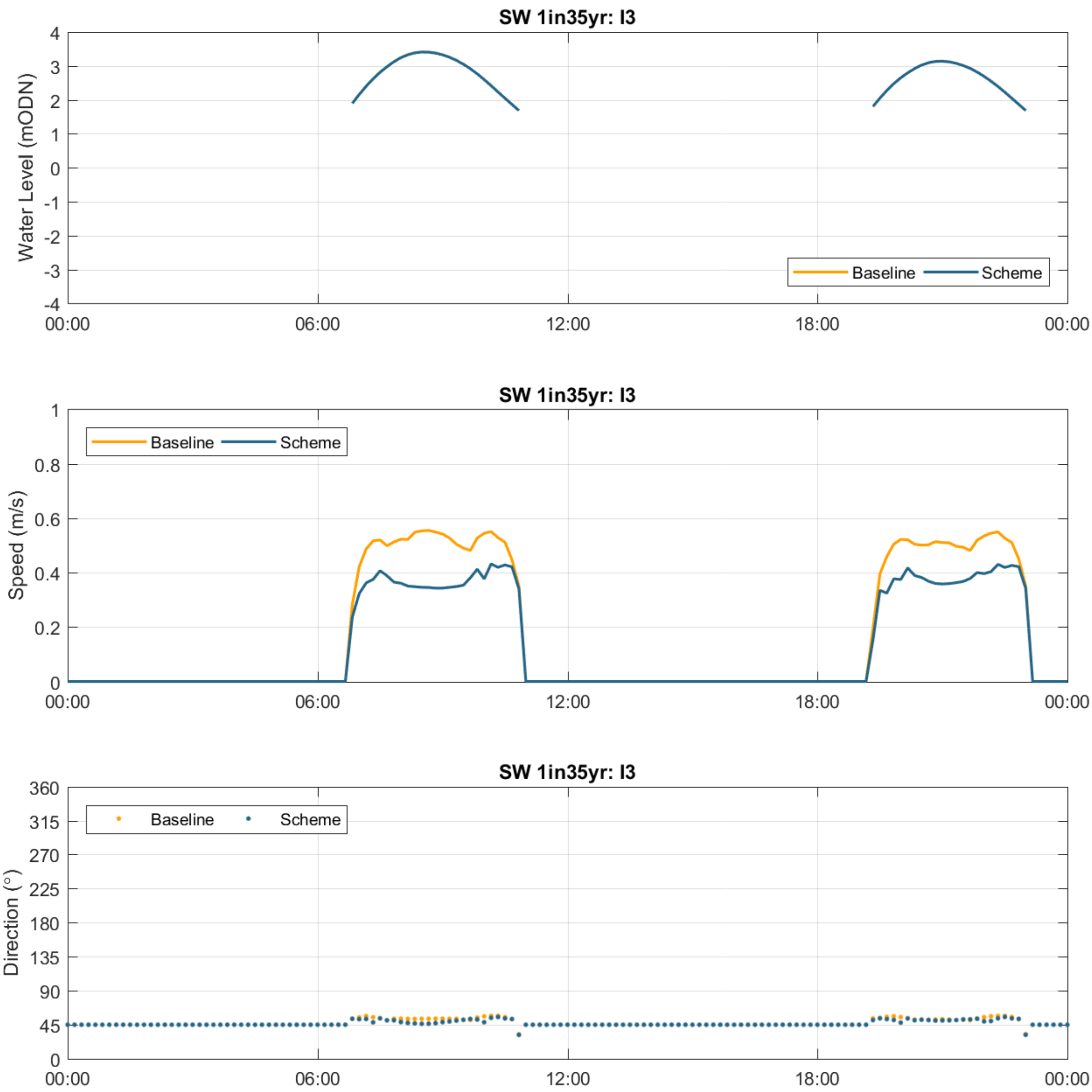

Figure B51. Time series of water level, flow speed and flow direction at I3 for the baseline and scheme runs for the 1 in 35 year wave from the southwest

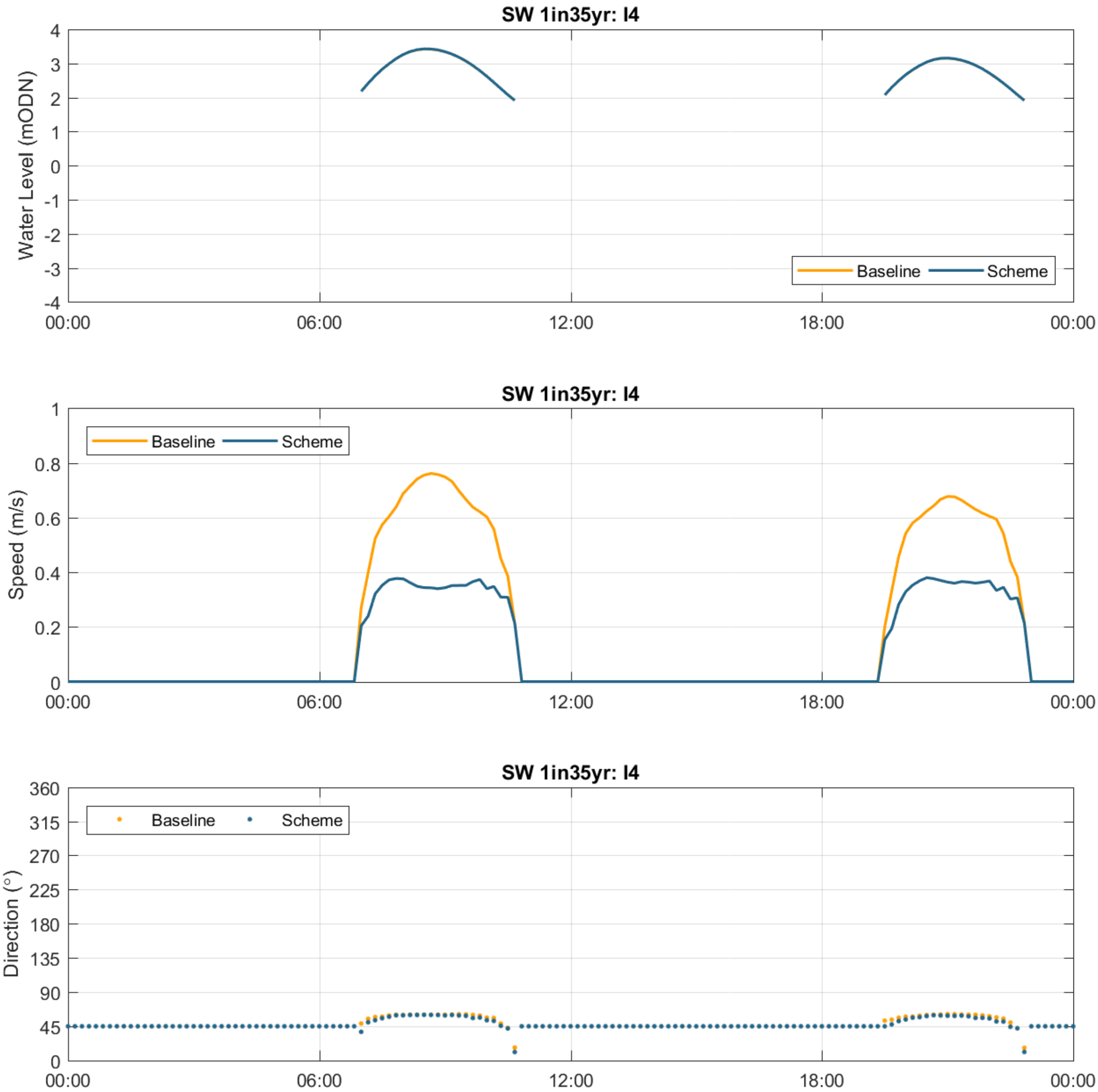

Figure B52. **Time series of water level, flow speed and flow direction at I4 for the baseline and scheme runs for the 1 in 35 year wave from the southwest**

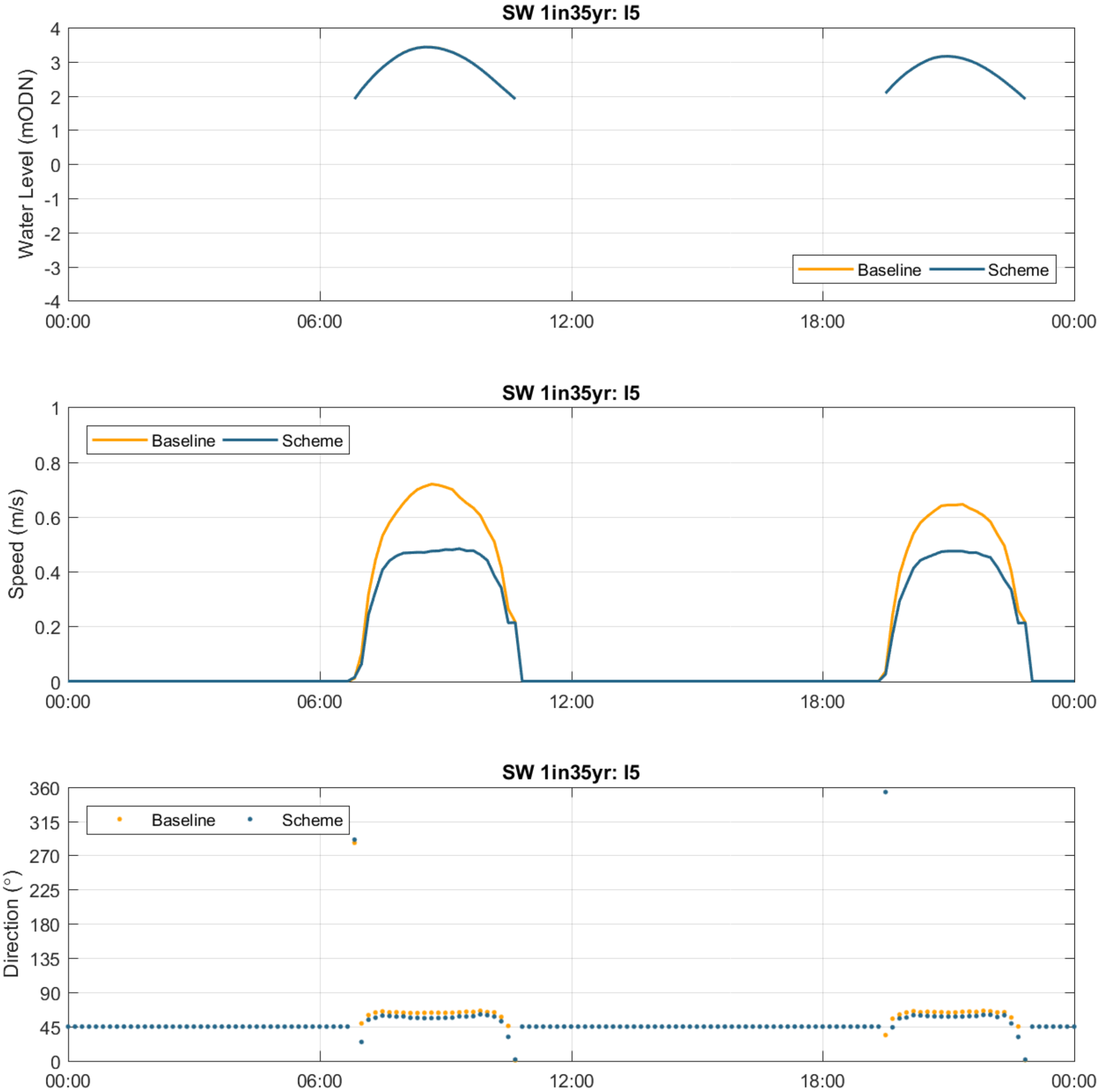

Figure B53. Time series of water level, flow speed and flow direction at I5 for the baseline and scheme runs for the 1 in 35 year wave from the southwest

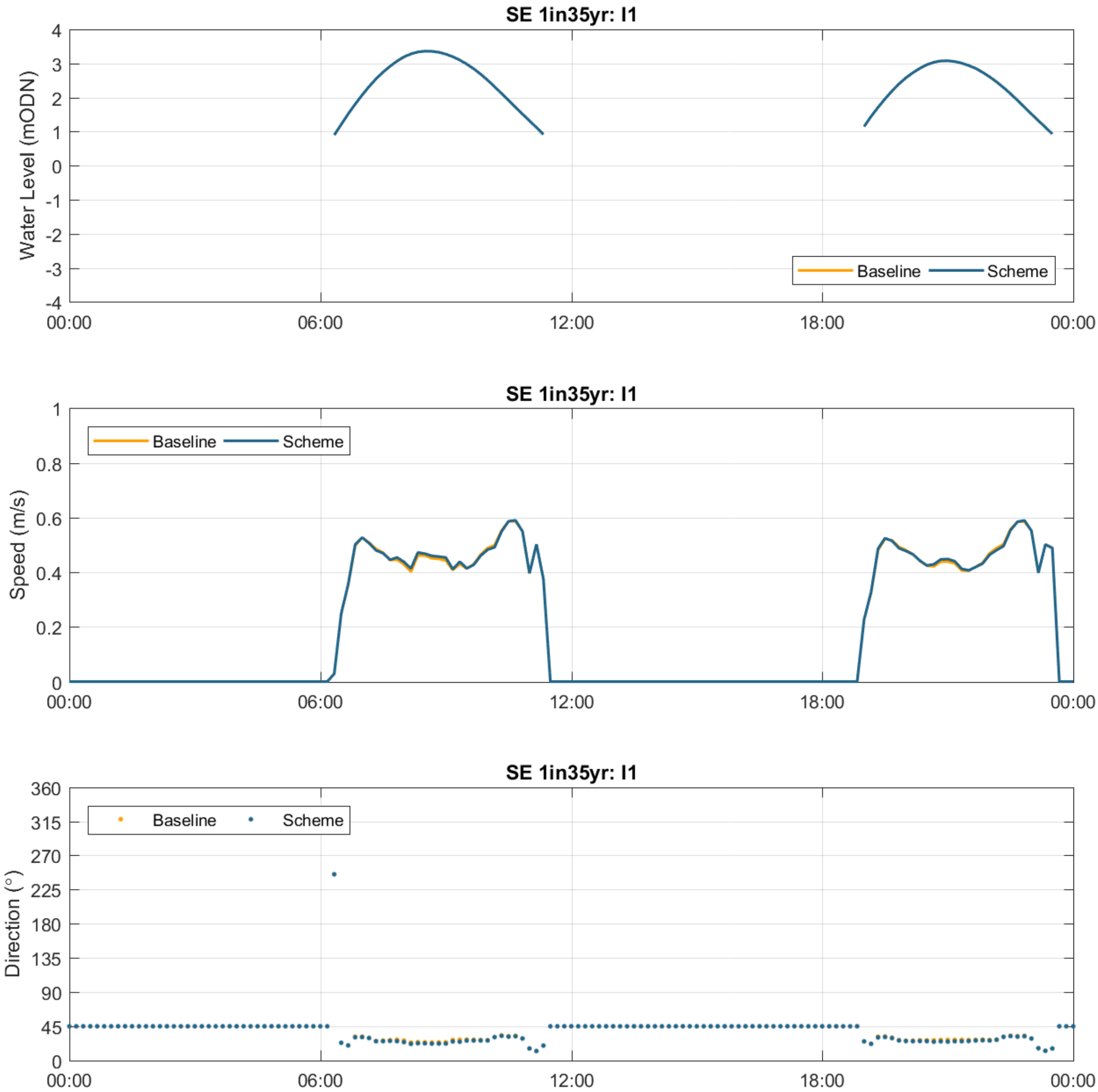

Figure B54. Time series of water level, flow speed and flow direction at I1 for the baseline and scheme runs for the 1 in 35 year wave from the SE

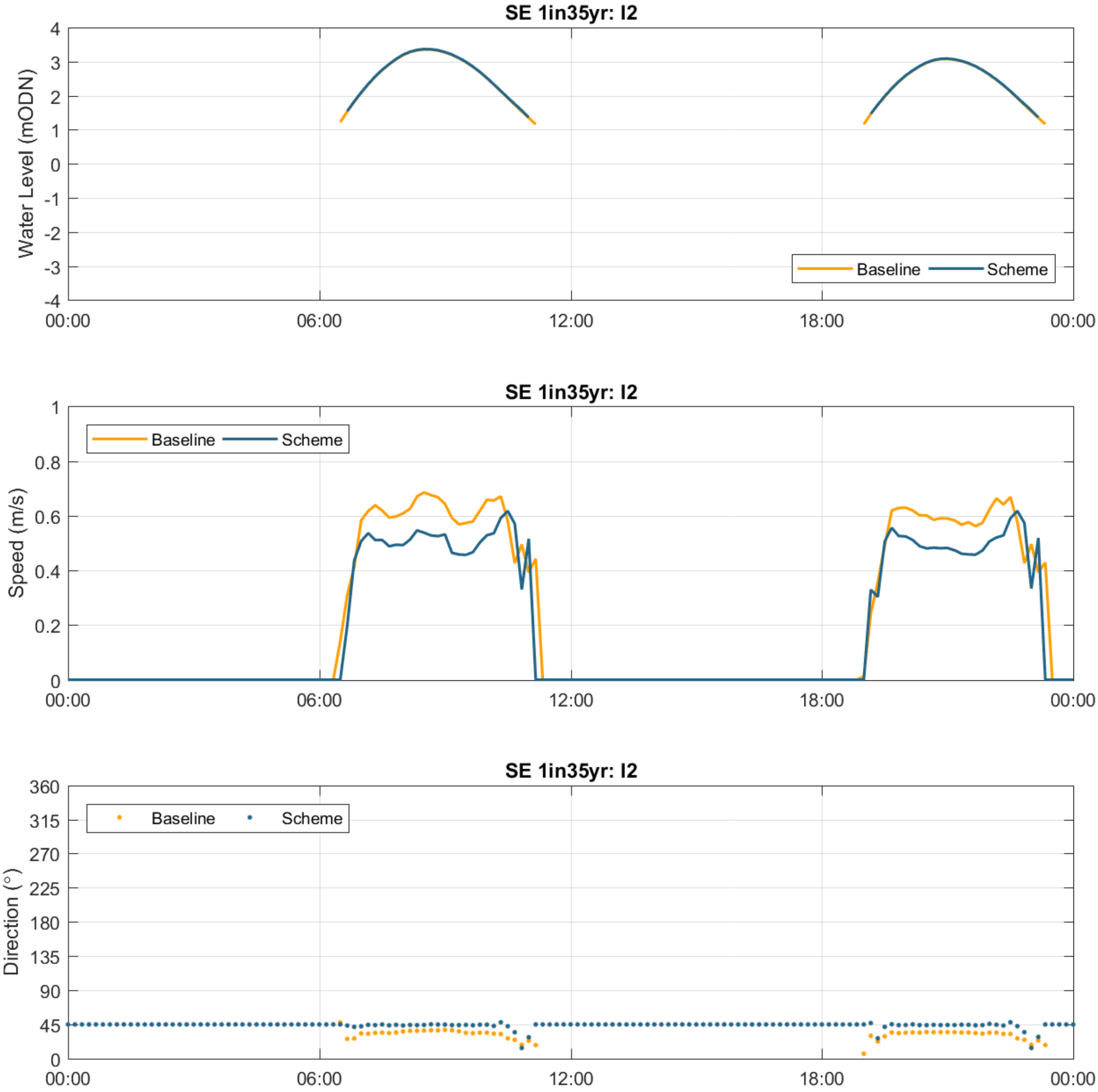

Figure B55. **Time series of water level, flow speed and flow direction at I2 for the baseline and scheme runs for the 1 in 35 year wave from the SE**

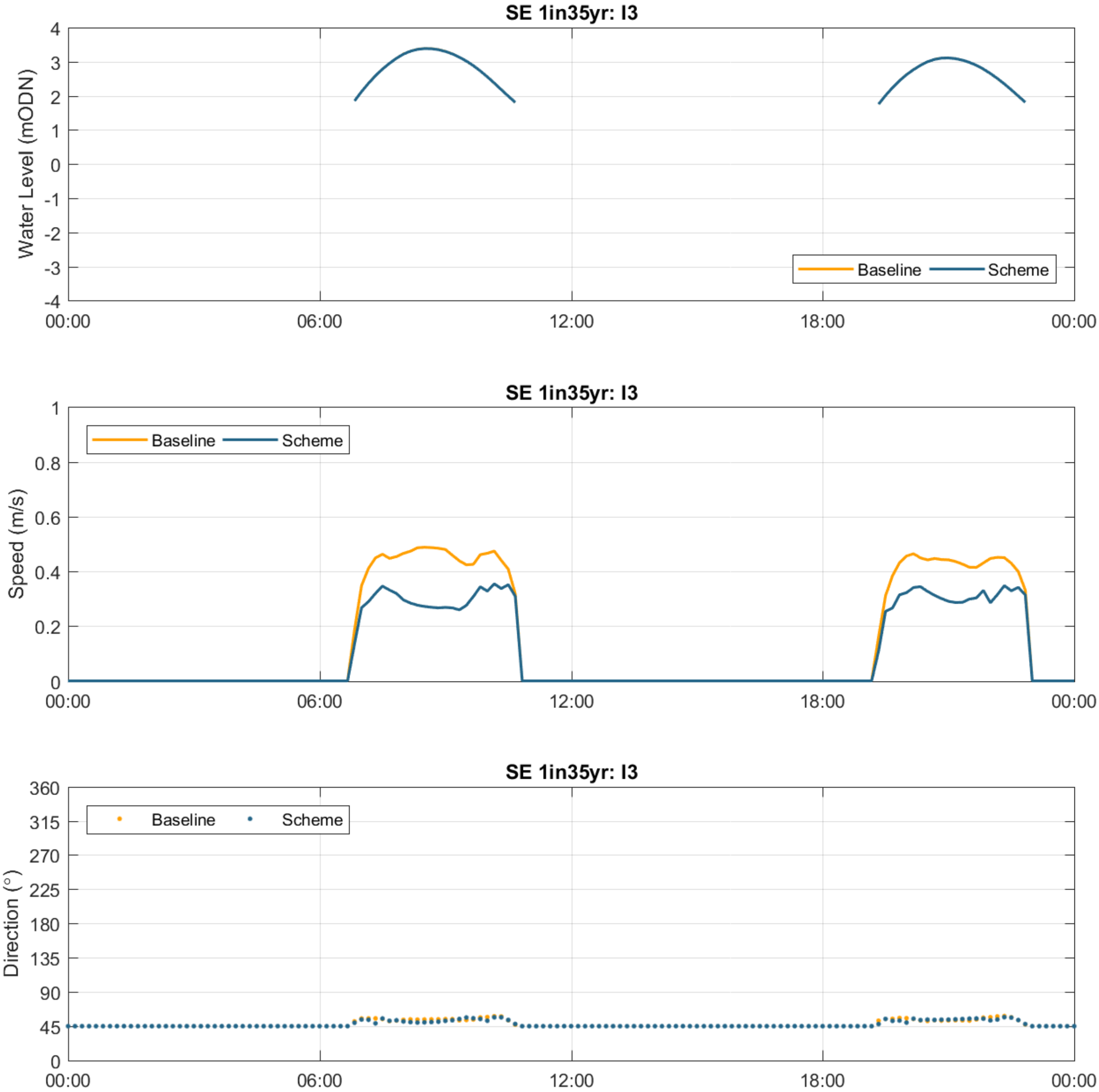

Figure B56. Time series of water level, flow speed and flow direction at I3 for the baseline and scheme runs for the 1 in 35 year wave from the SE

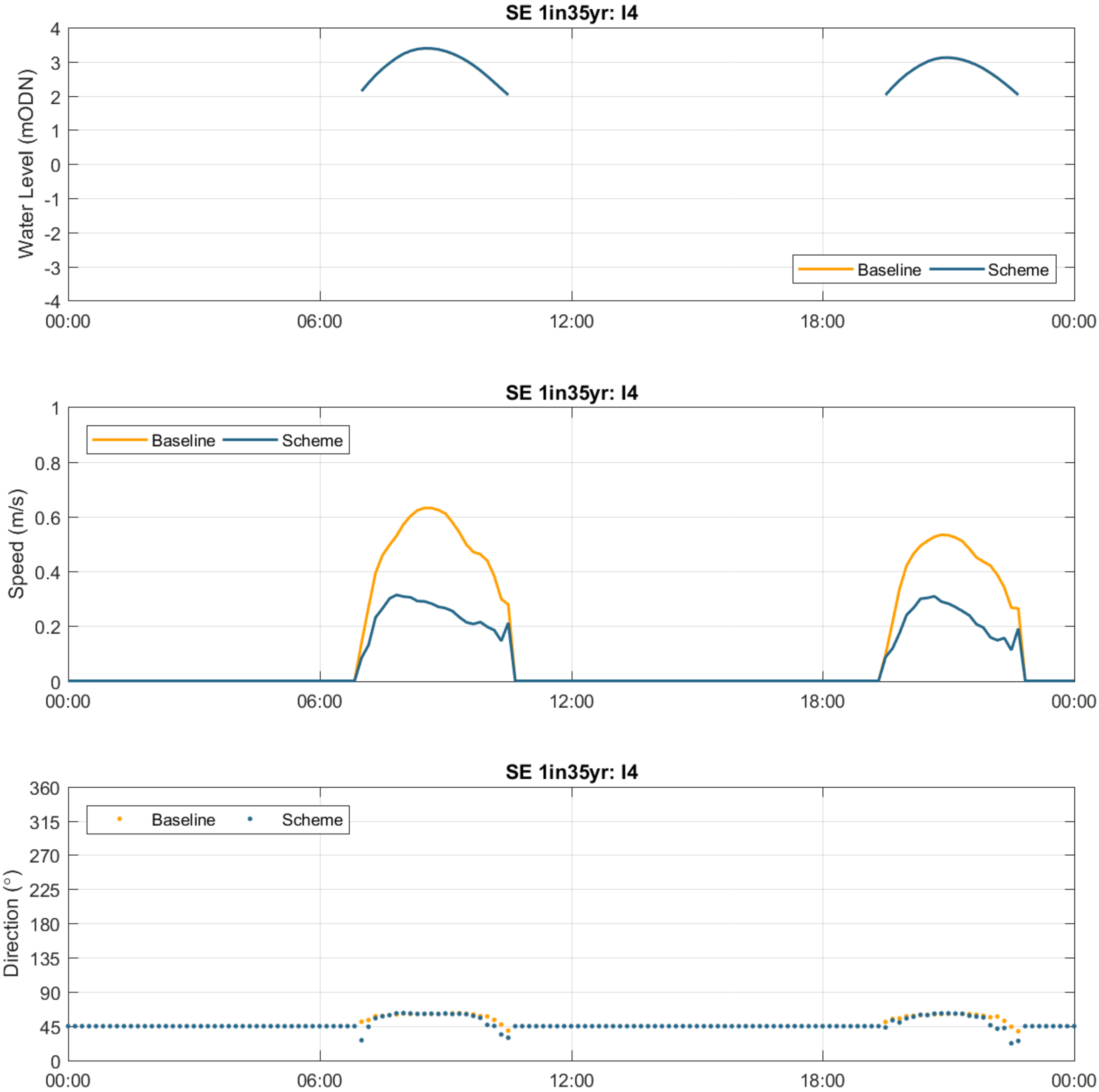

Figure B57. Time series of water level, flow speed and flow direction at I4 for the baseline and scheme runs for the 1 in 35 year wave from the SE

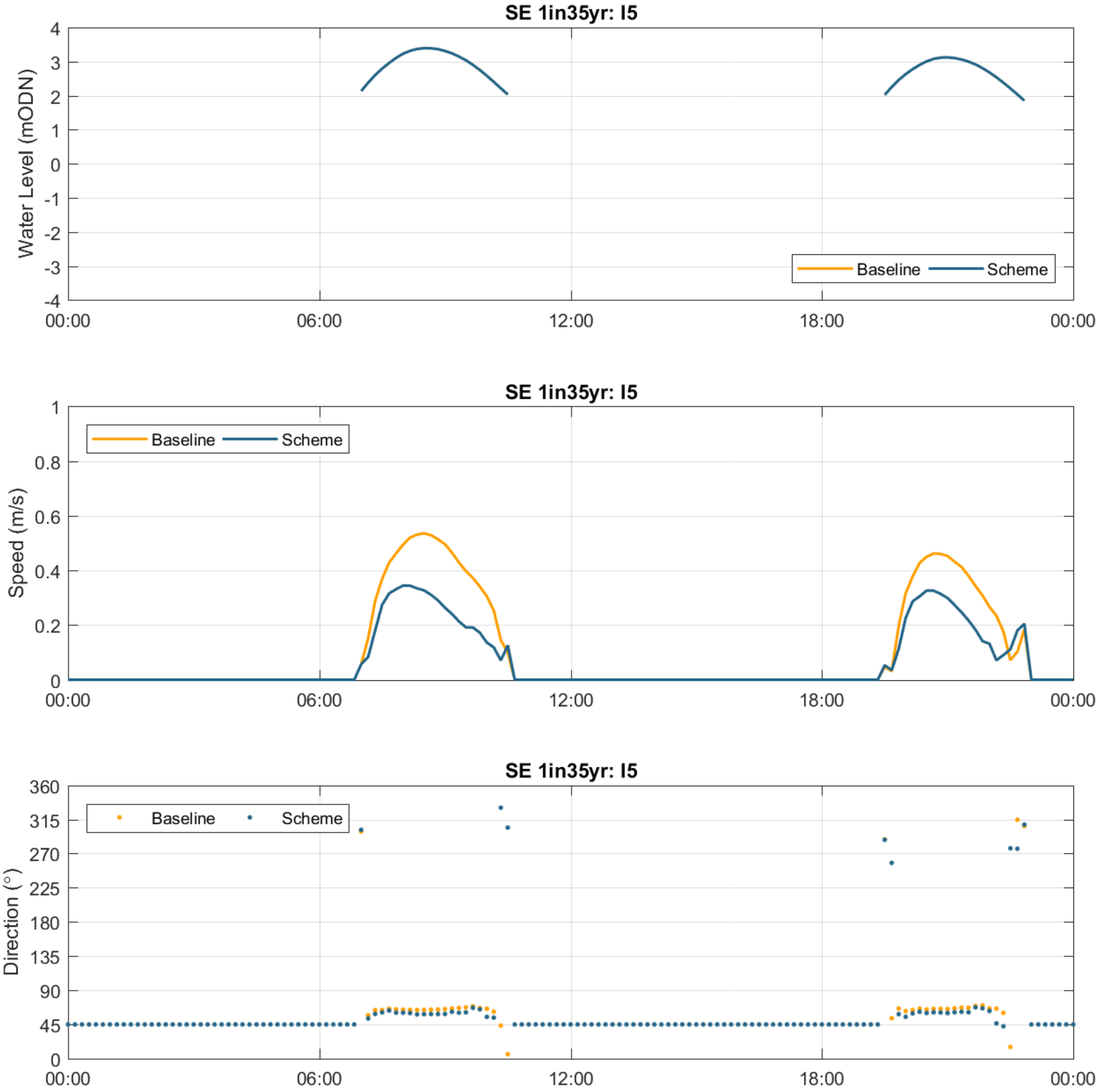

Figure B58. **Time series of water level, flow speed and flow direction at I5 for the baseline and scheme runs for the 1 in 35 year wave from the SE**

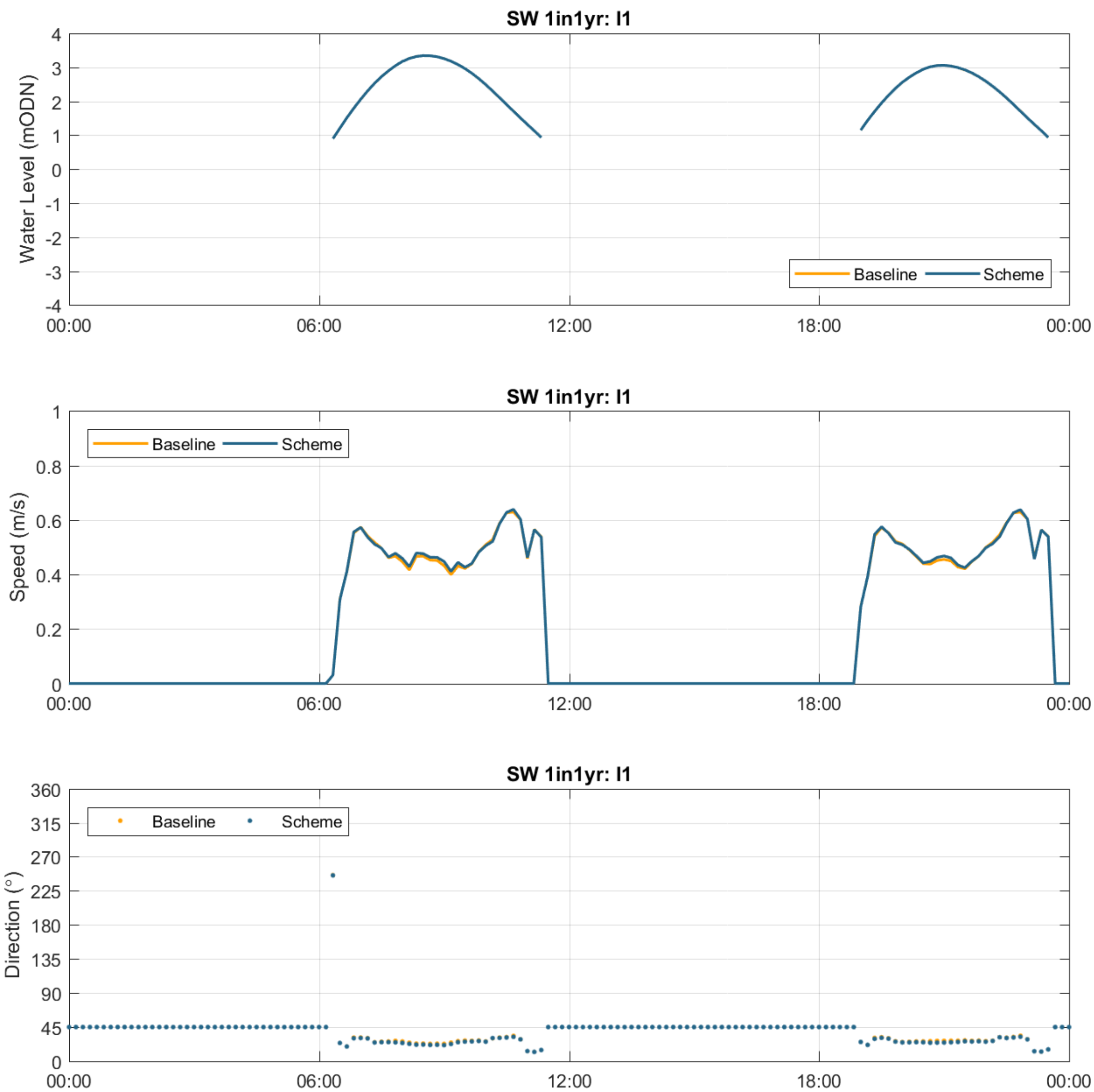

Figure B59. **Time series of water level, flow speed and flow direction at I1 for the baseline and scheme runs for the 1 in 1 year wave from the SW**

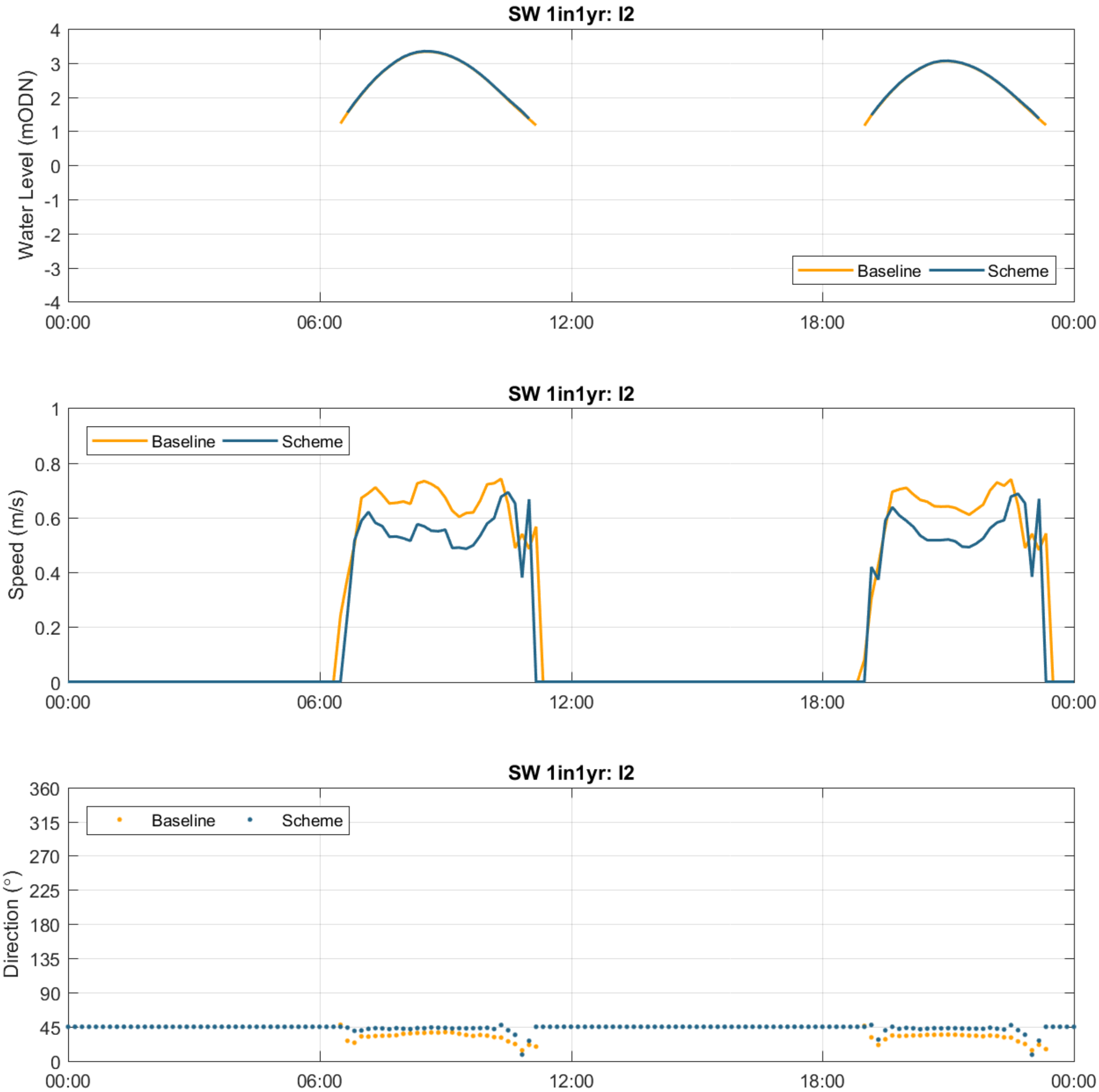

Figure B60. **Time series of water level, flow speed and flow direction at I2 for the baseline and scheme runs for the 1 in 1 year wave from the SW**

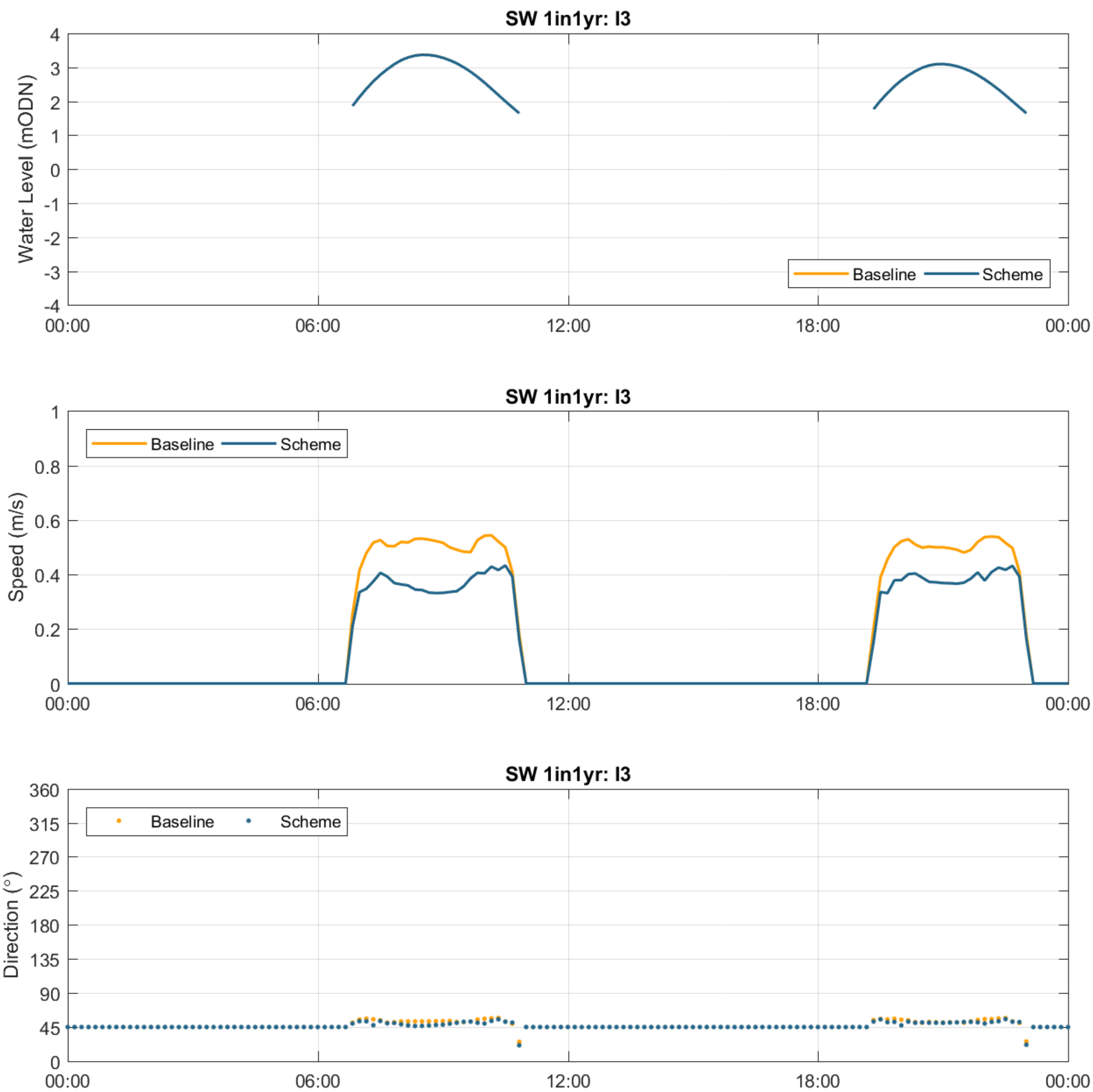

Figure B61. **Time series of water level, flow speed and flow direction at I3 for the baseline and scheme runs for the 1 in 1 year wave from the SW**

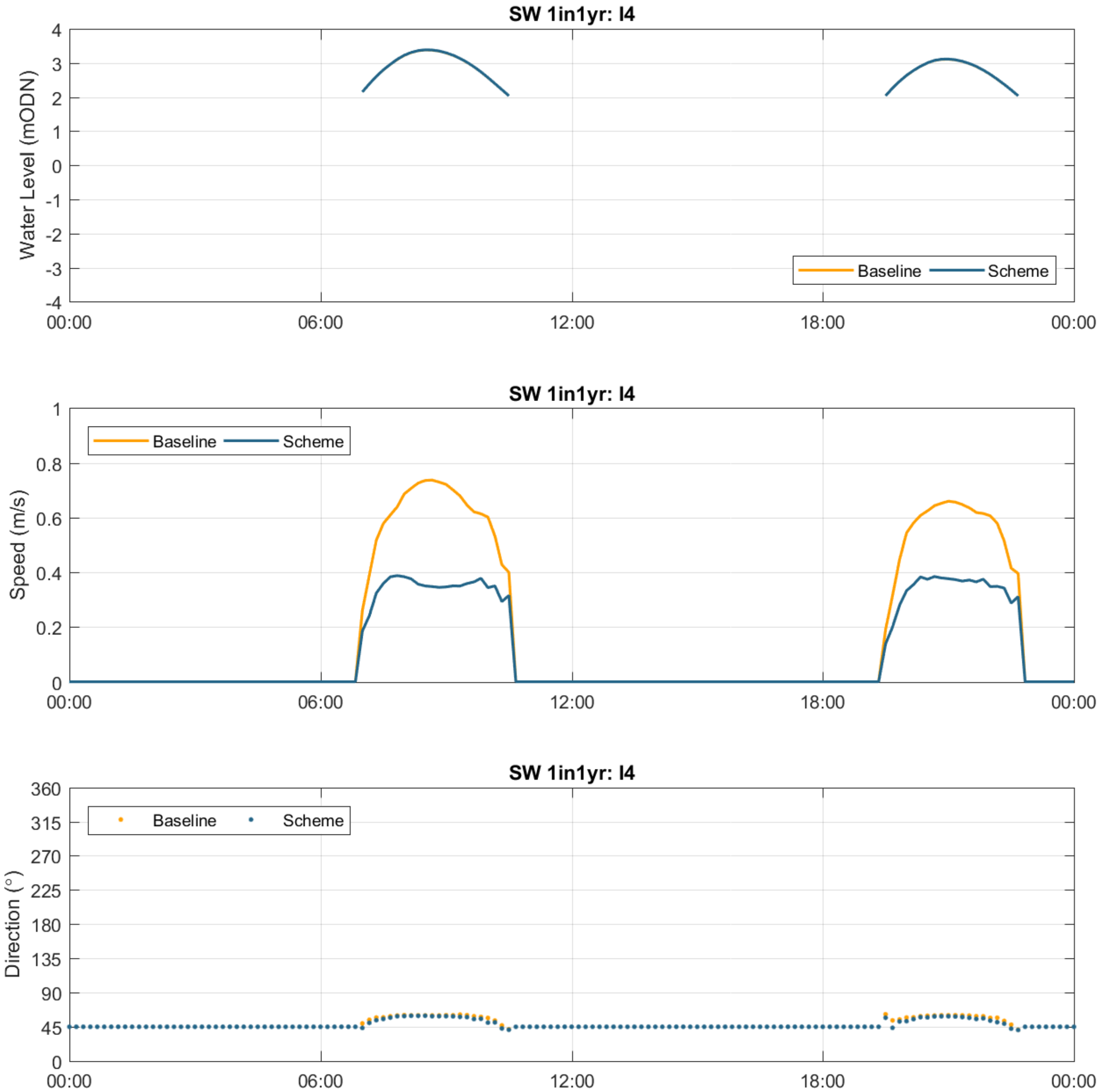

Figure B62. Time series of water level, flow speed and flow direction at I4 for the baseline and scheme runs for the 1 in 1 year wave from the SW

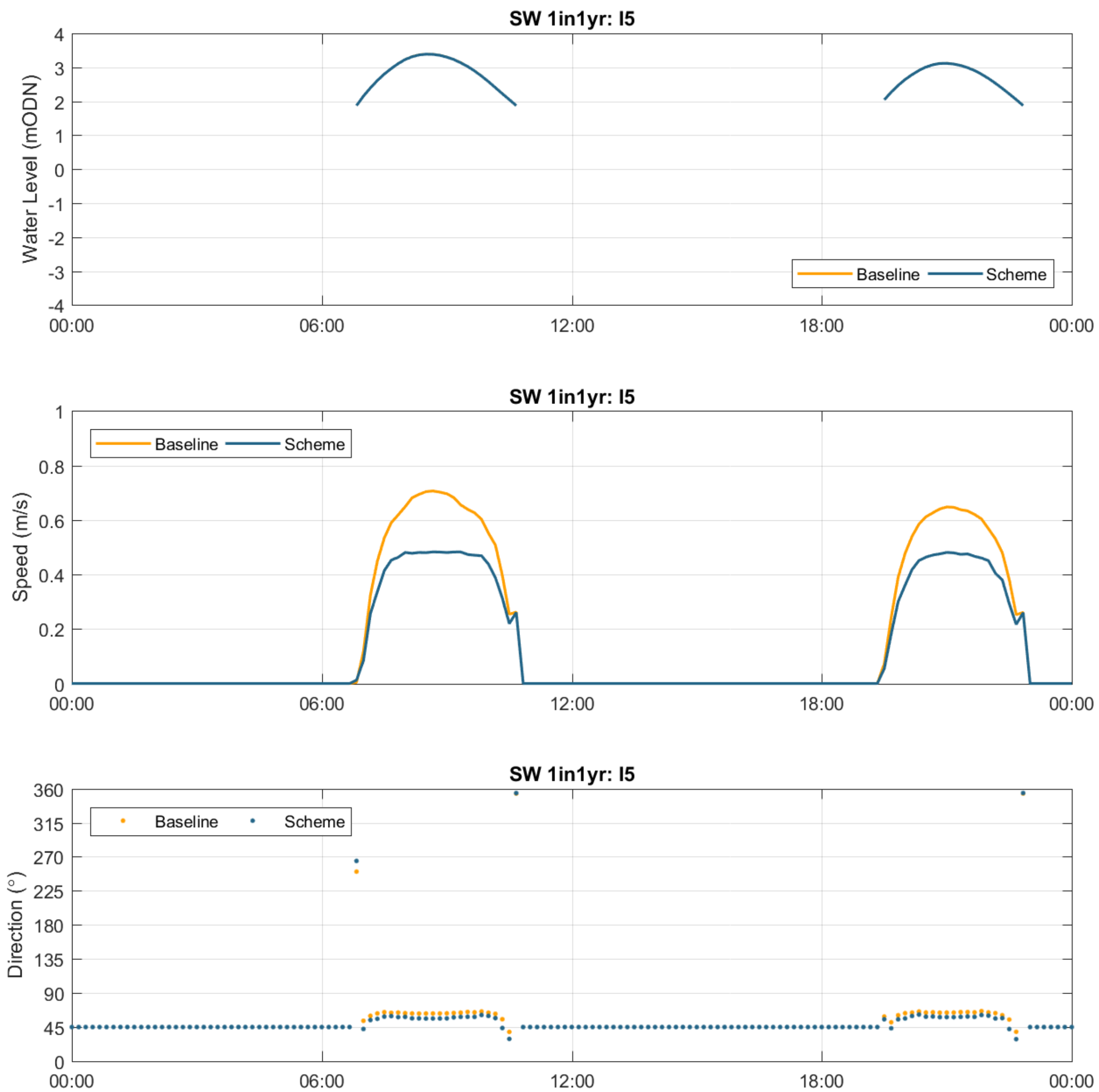

Figure B63. **Time series of water level, flow speed and flow direction at I5 for the baseline and scheme runs for the 1 in 1 year wave from the SW**

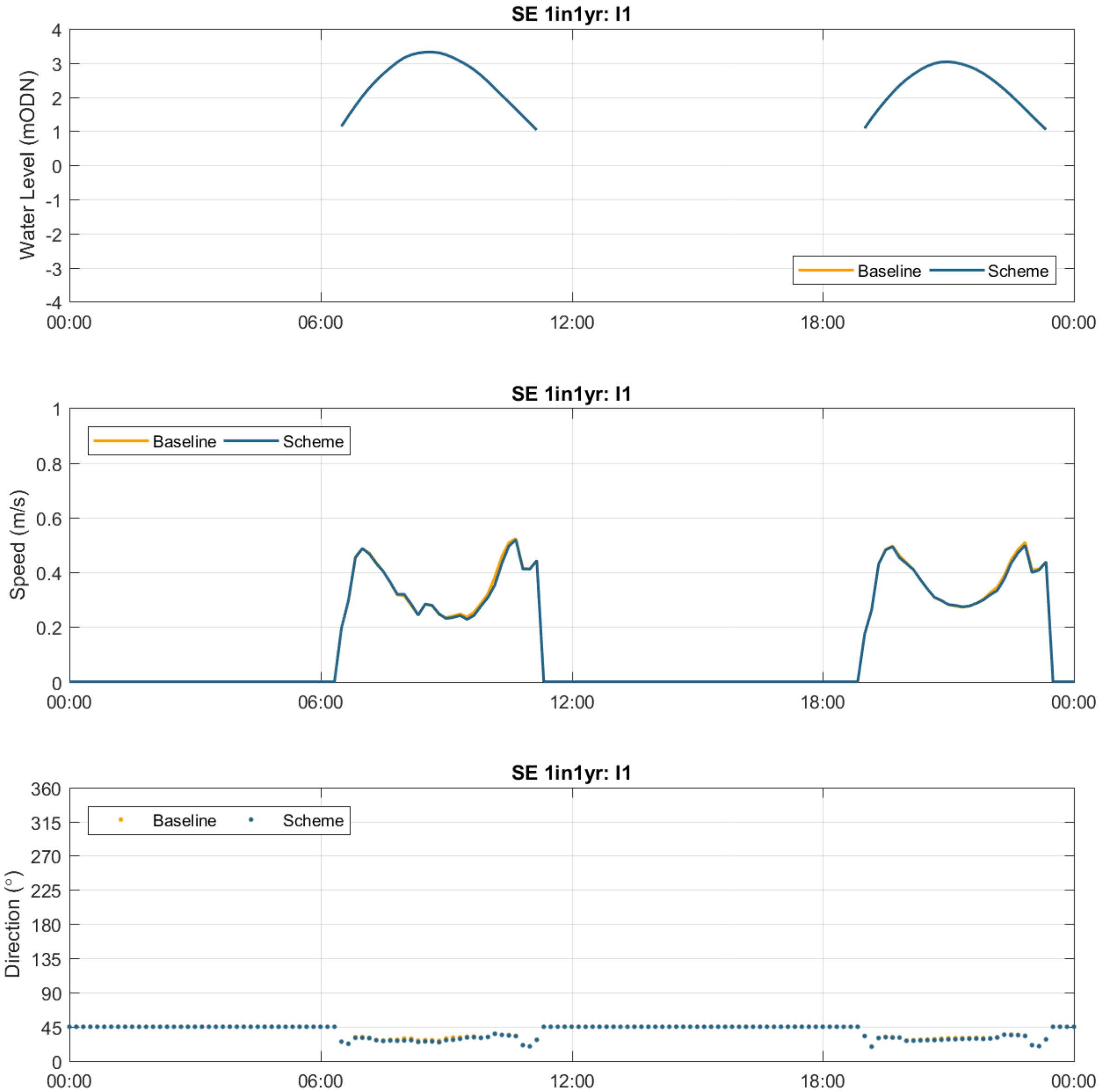

Figure B64. **Time series of water level, flow speed and flow direction at I1 for the baseline and scheme runs for the 1 in 1 year wave from the SE**

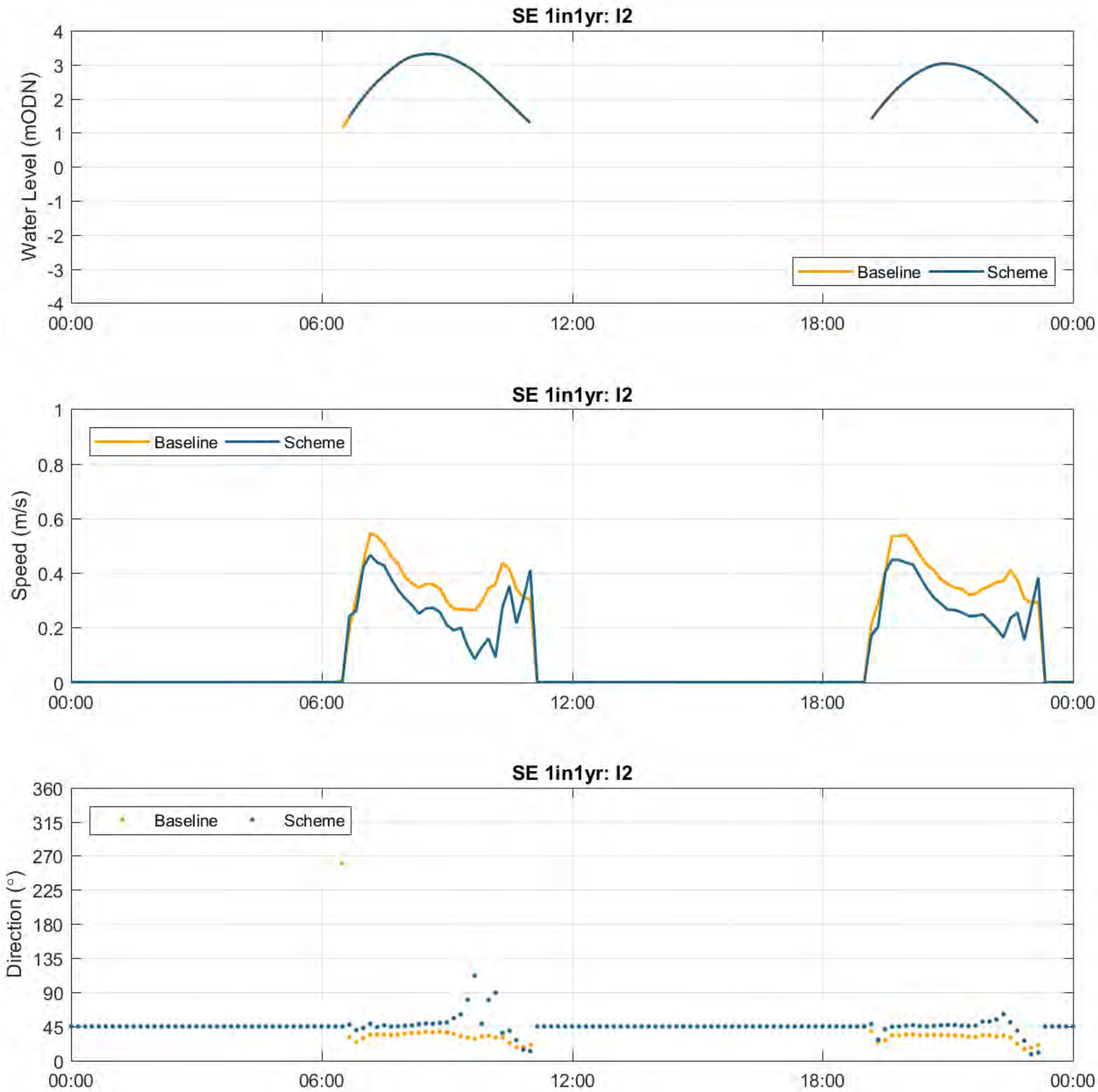

Figure B65. **Time series of water level, flow speed and flow direction at I2 for the baseline and scheme runs for the 1 in 1 year wave from the SE**

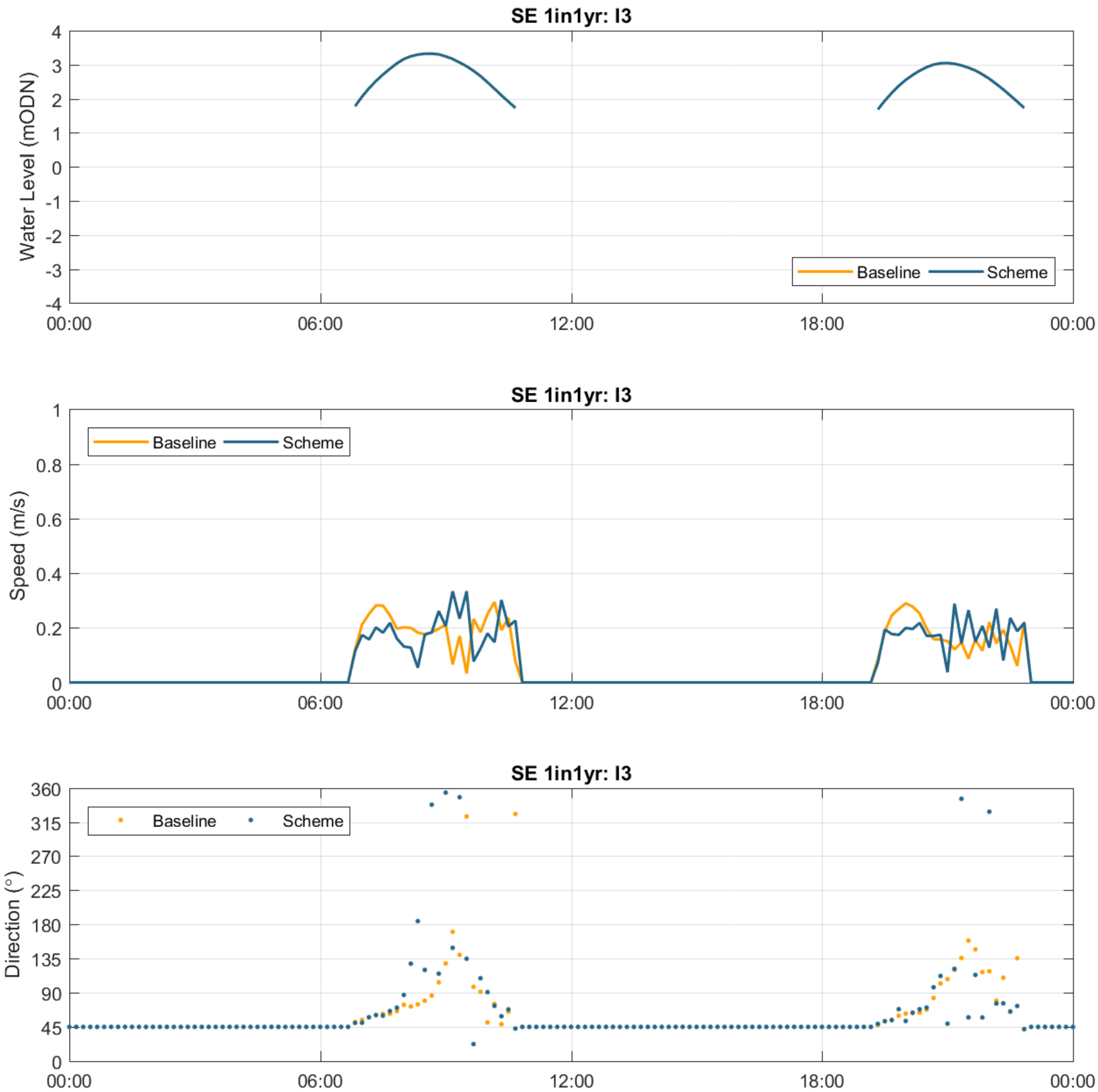

Figure B66. Time series of water level, flow speed and flow direction at I3 for the baseline and scheme runs for the 1 in 1 year wave from the SE

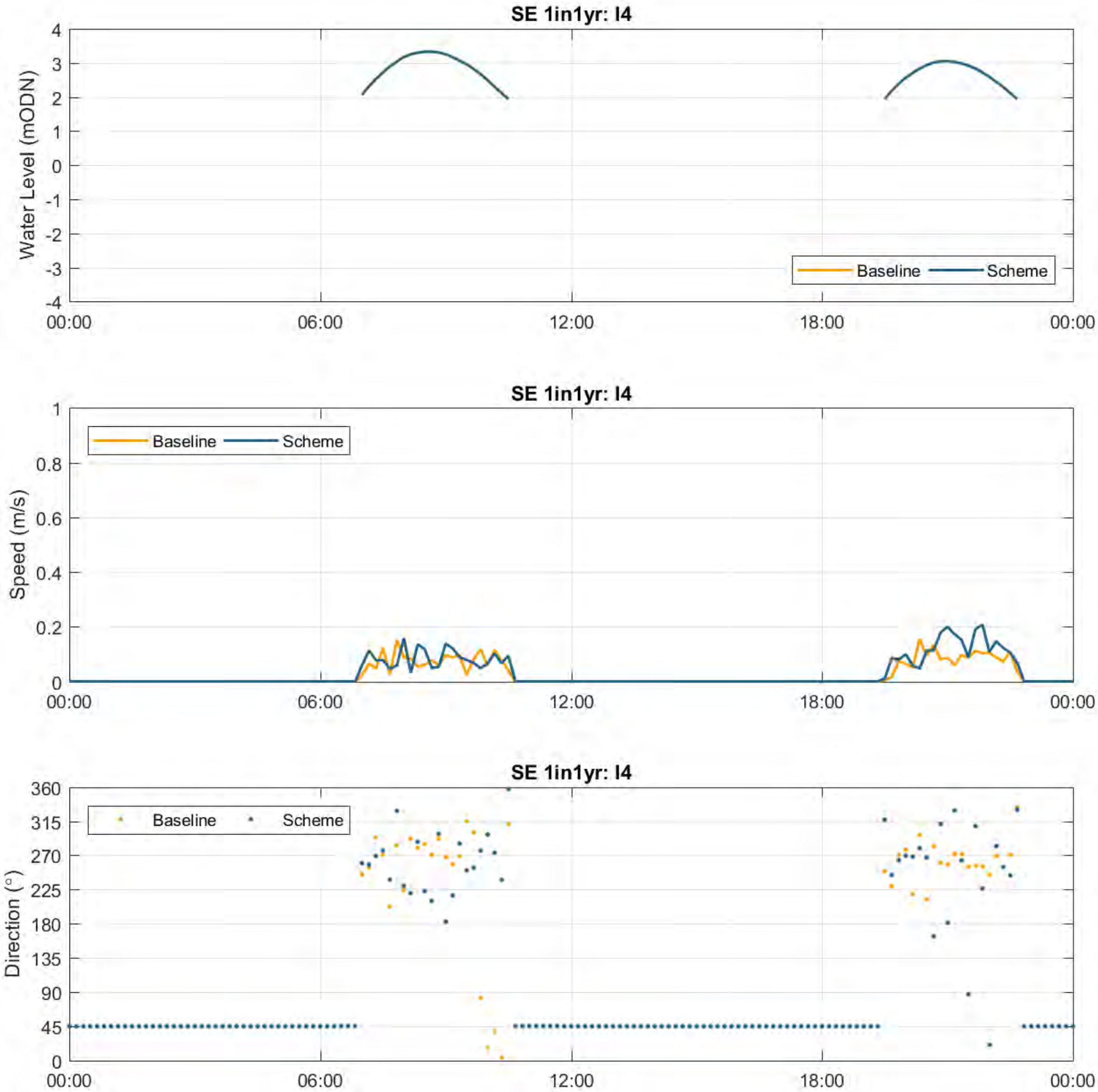

Figure B67. **Time series of water level, flow speed and flow direction at I4 for the baseline and scheme runs for the 1 in 1 year wave from the SE**

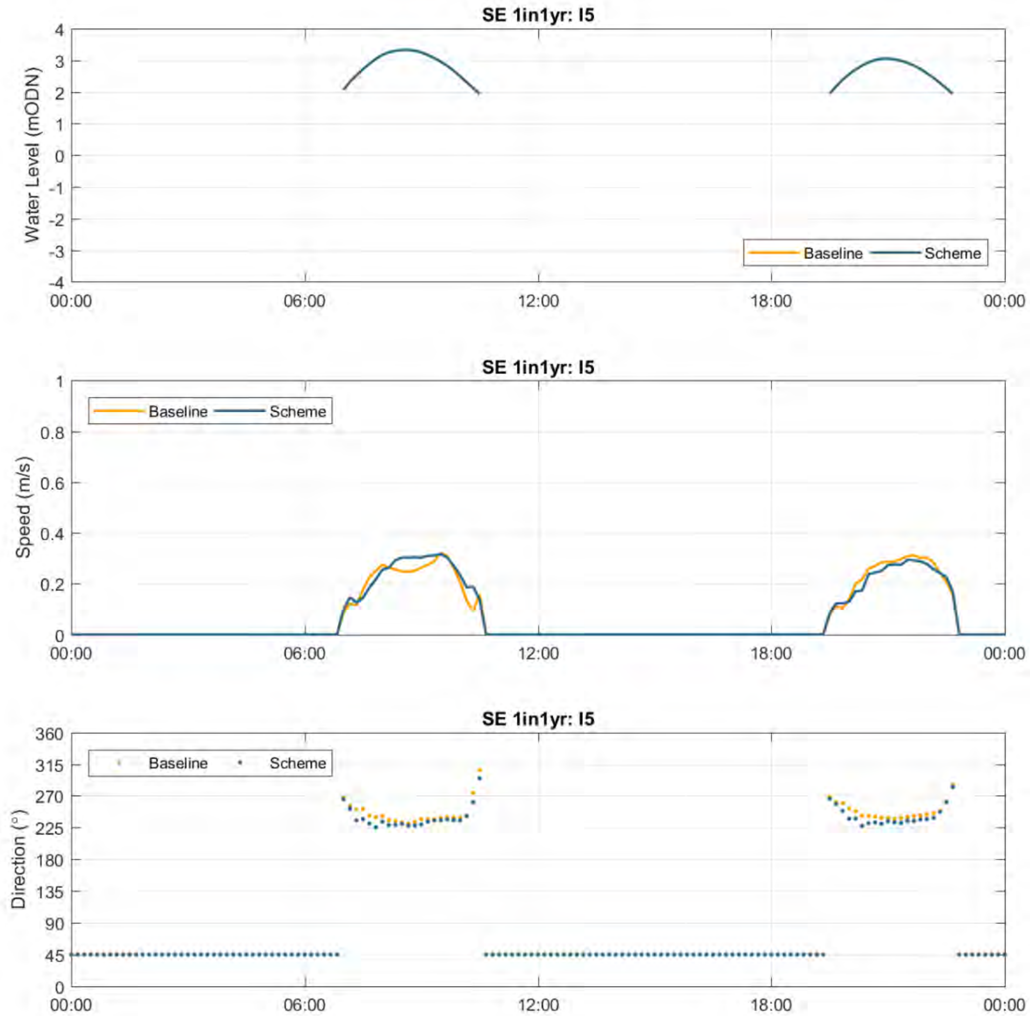

Figure B68. **Time series of water level, flow speed and flow direction at I5 for the baseline and scheme runs for the 1 in 1 year wave from the SE**

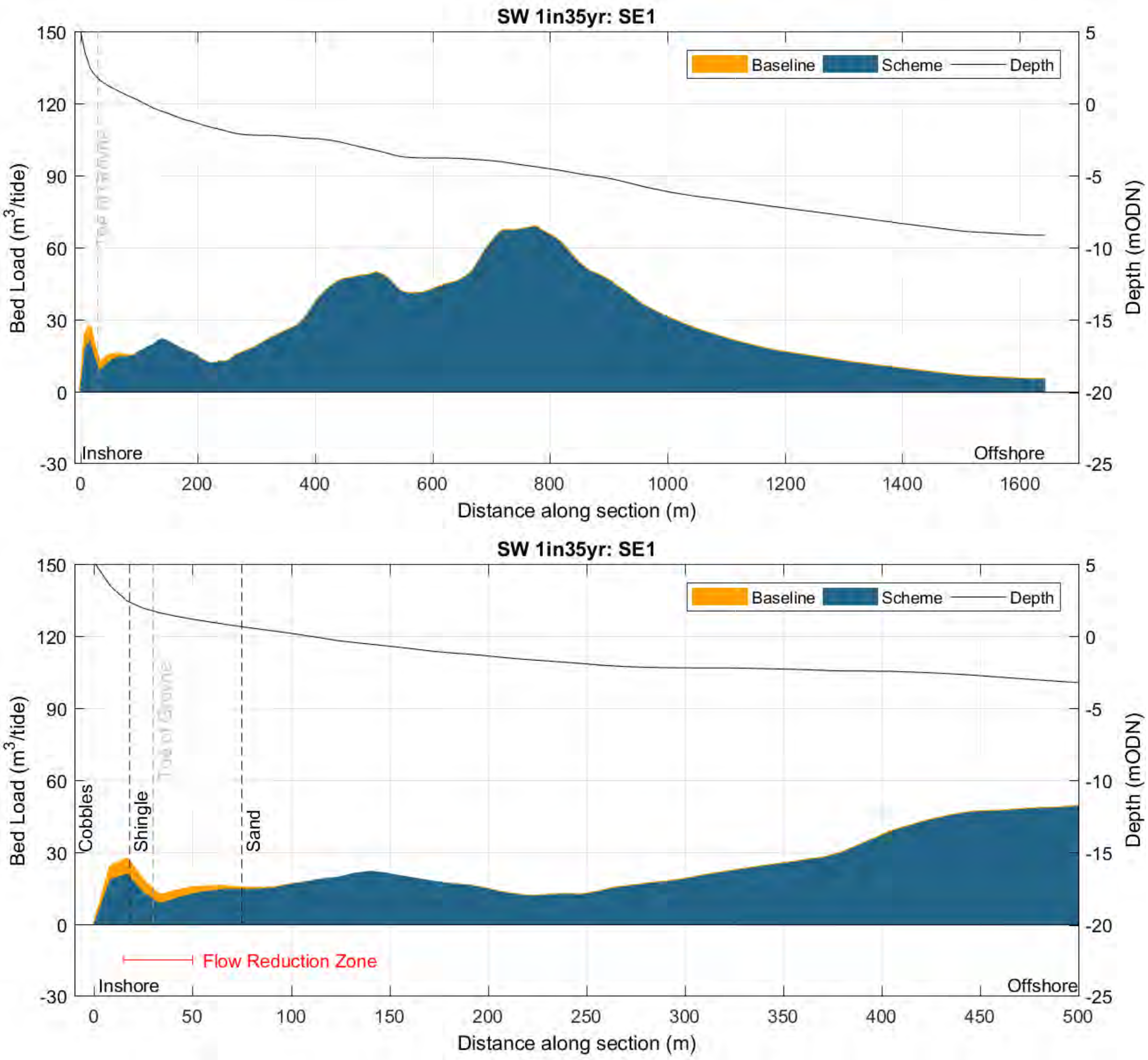

Positive values indicate transport to the northeast and negative values indicated transport to the southwest.
Sediment type i.e. cobbles, shingle and sand are shown for indicative purposes only.
A 0.2 mm sand has been used as the grain size in the model.

Figure B69. Sediment transport across SE1 for 1 in 35 year wave from the southwest

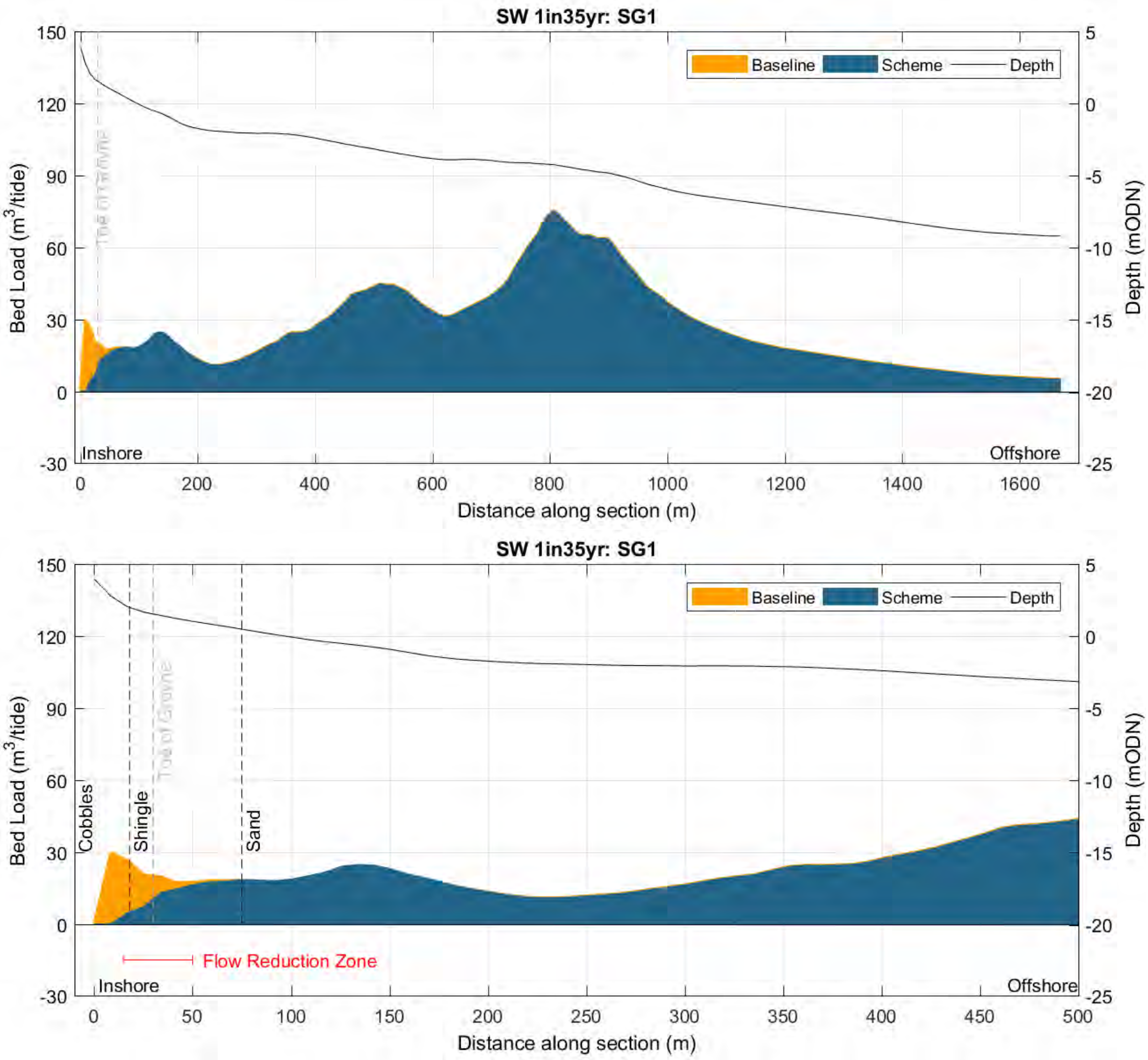

Positive values indicate transport to the northeast and negative values indicated transport to the southwest.
Sediment type i.e. cobbles, shingle and sand are shown for indicative purposes only.
A 0.2 mm sand has been used as the grain size in the model.

Figure B70. Sediment transport across SG1 for 1 in 35 year wave from the southwest

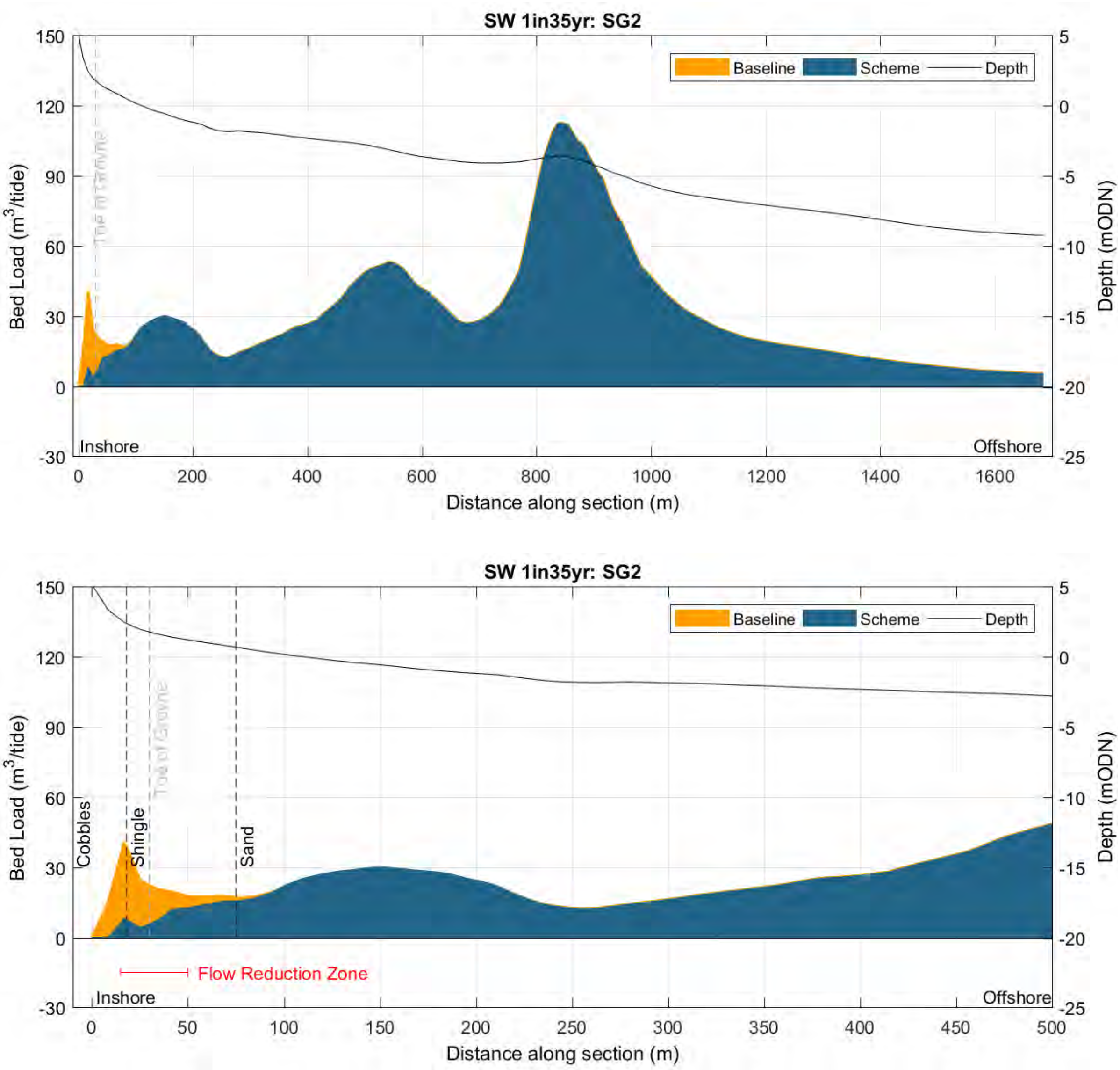

Positive values indicate transport to the northeast and negative values indicated transport to the southwest.
Sediment type i.e. cobbles, shingle and sand are shown for indicative purposes only.
A 0.2 mm sand has been used as the grain size in the model.

Figure B71. Sediment transport across SG2 for 1 in 35 year wave from the southwest

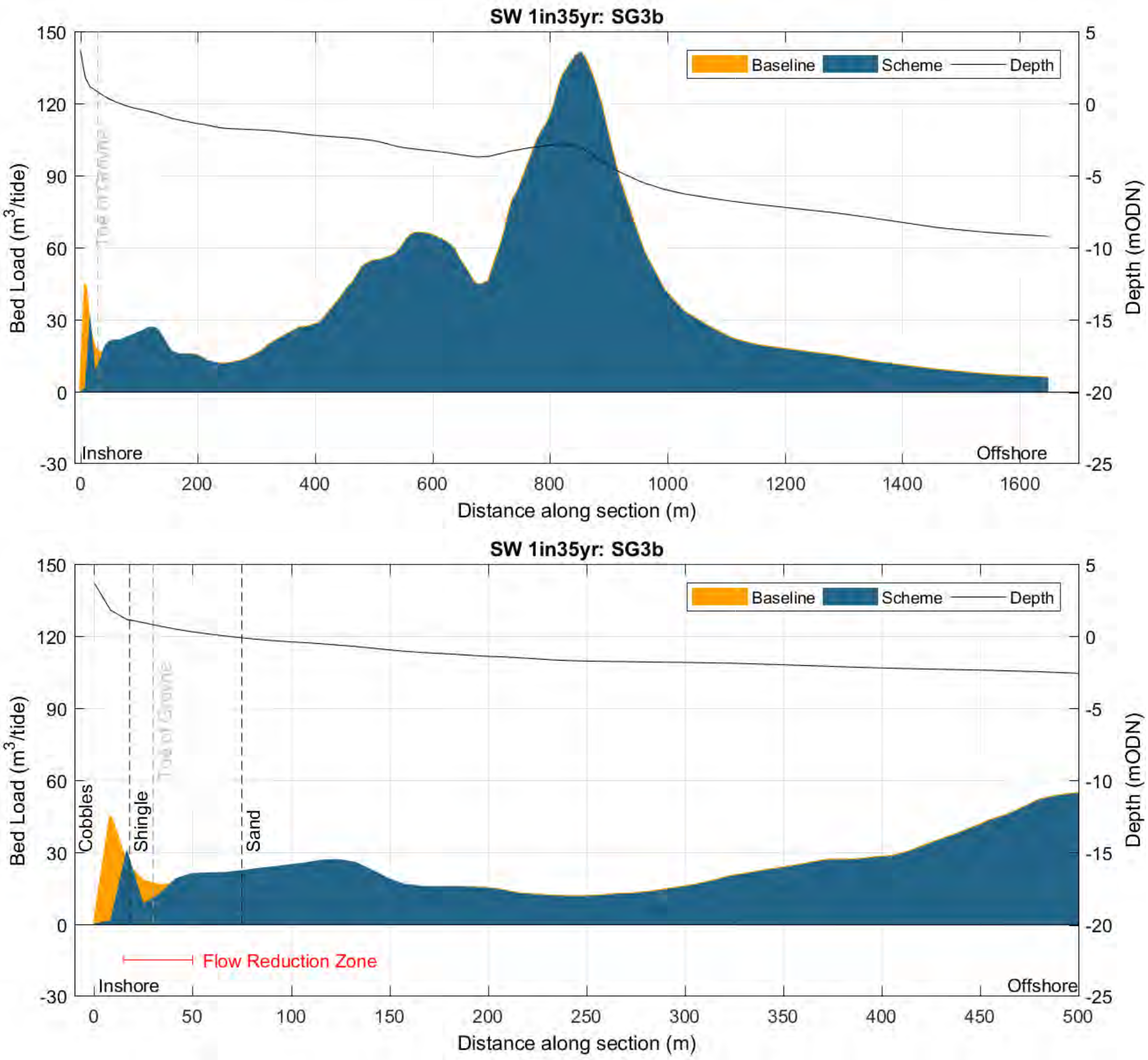

Positive values indicate transport to the northeast and negative values indicated transport to the southwest.
Sediment type i.e. cobbles, shingle and sand are shown for indicative purposes only.
A 0.2 mm sand has been used as the grain size in the model.

Figure B72. Sediment transport across SG3b for 1 in 35 year wave from the southwest

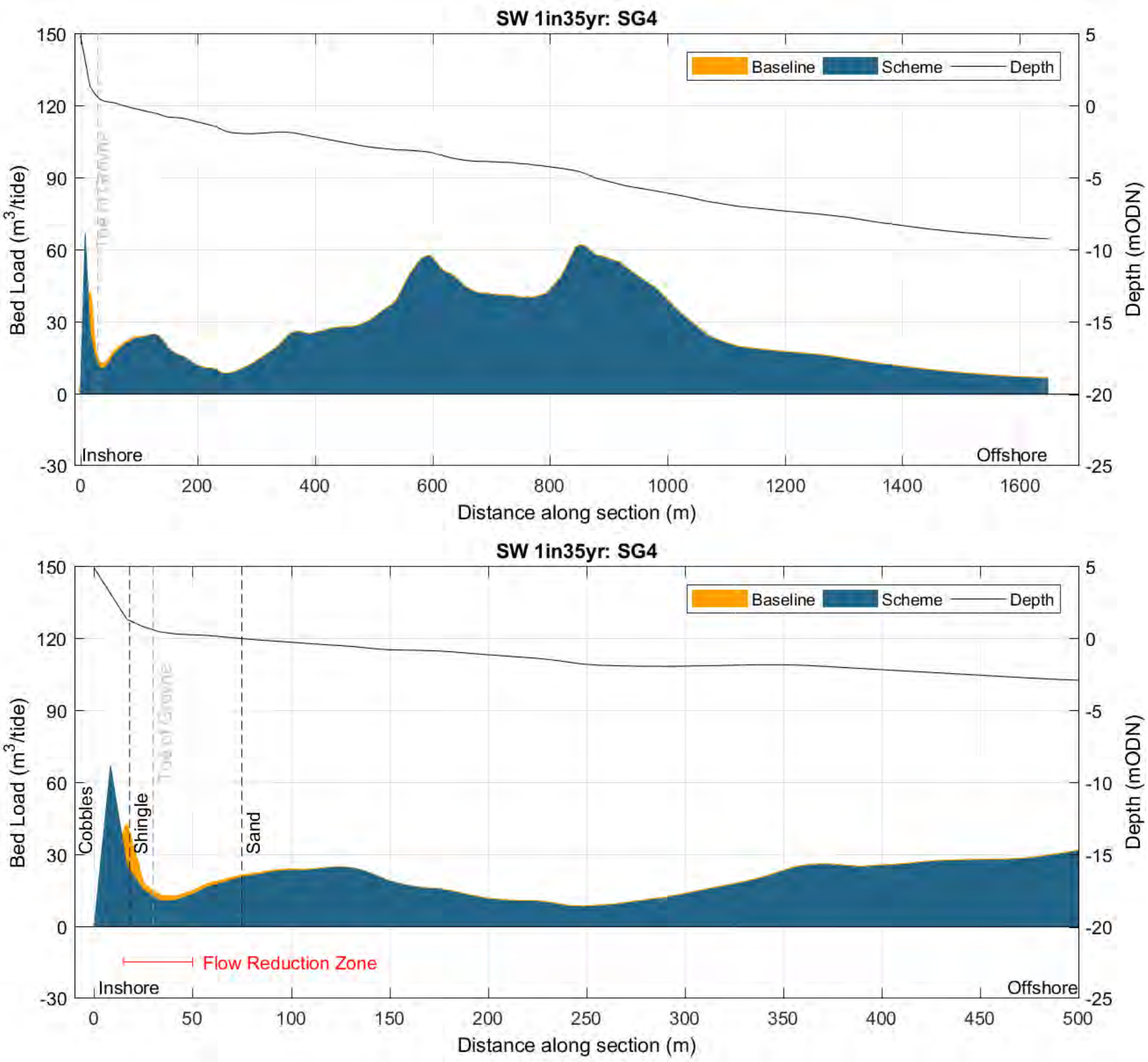

Positive values indicate transport to the northeast and negative values indicated transport to the southwest.
Sediment type i.e. cobbles, shingle and sand are shown for indicative purposes only.
A 0.2 mm sand has been used as the grain size in the model.

Figure B73. Sediment transport across SG4 for 1 in 35 year wave from the southwest

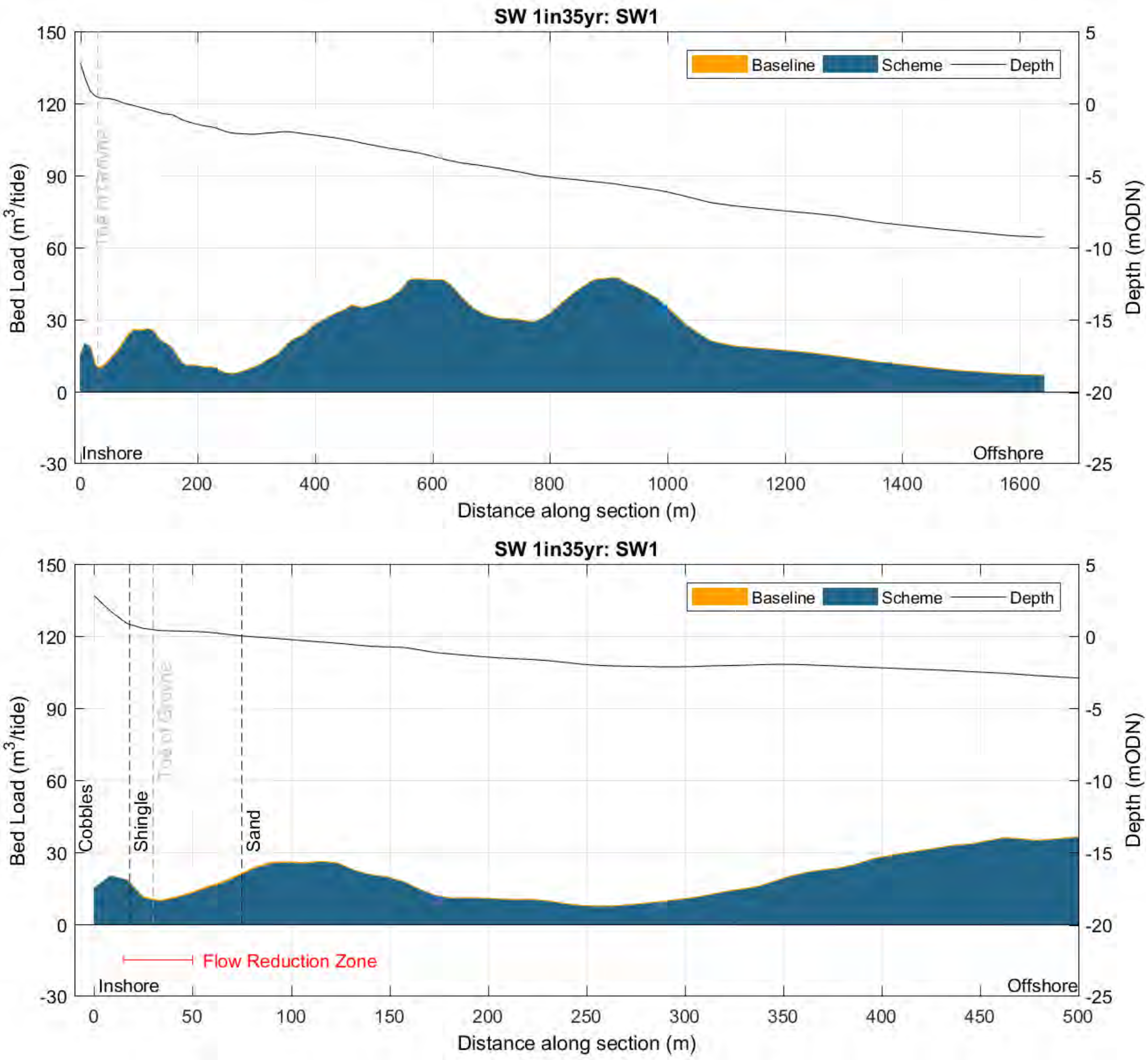

Positive values indicate transport to the northeast and negative values indicated transport to the southwest.
Sediment type i.e. cobbles, shingle and sand are shown for indicative purposes only.
A 0.2 mm sand has been used as the grain size in the model.

Figure B74. Sediment transport across SW1 for 1 in 35 year wave from the southwest

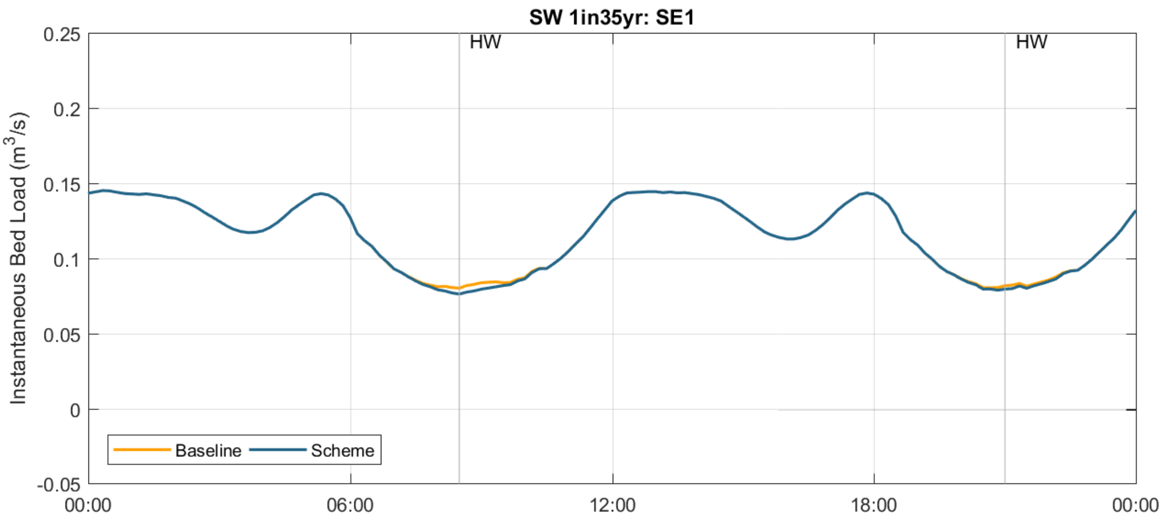

Positive values indicate transport to the northeast and negative values indicated transport to the southwest.

Figure B75. Time series of instantaneous sediment transport across SE1 for 1 in 35 year wave from the southwest

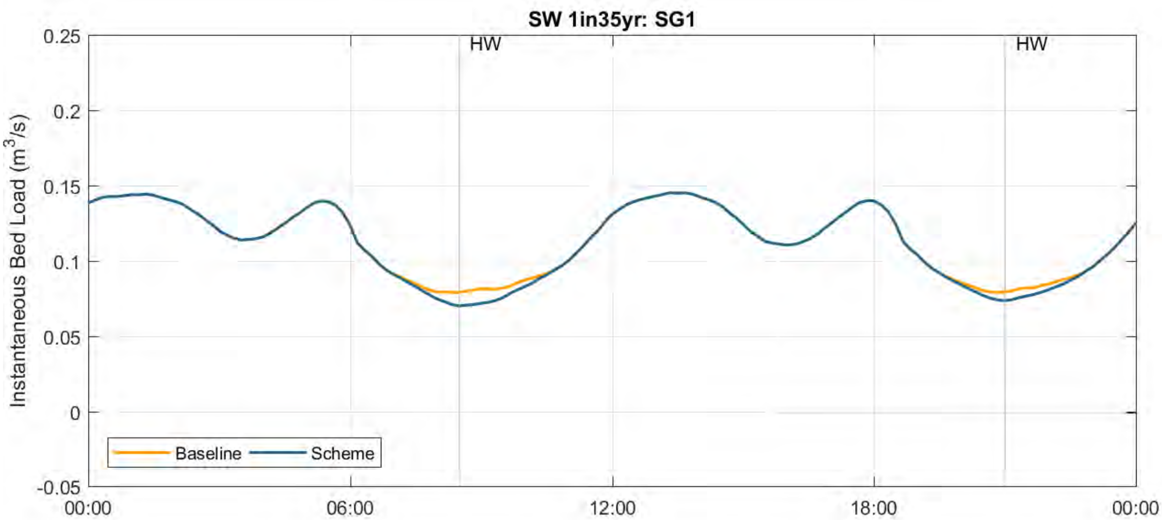

Positive values indicate transport to the northeast and negative values indicated transport to the southwest.

Figure B76. Time series of instantaneous sediment transport across SG1 for 1 in 35 year wave from the southwest

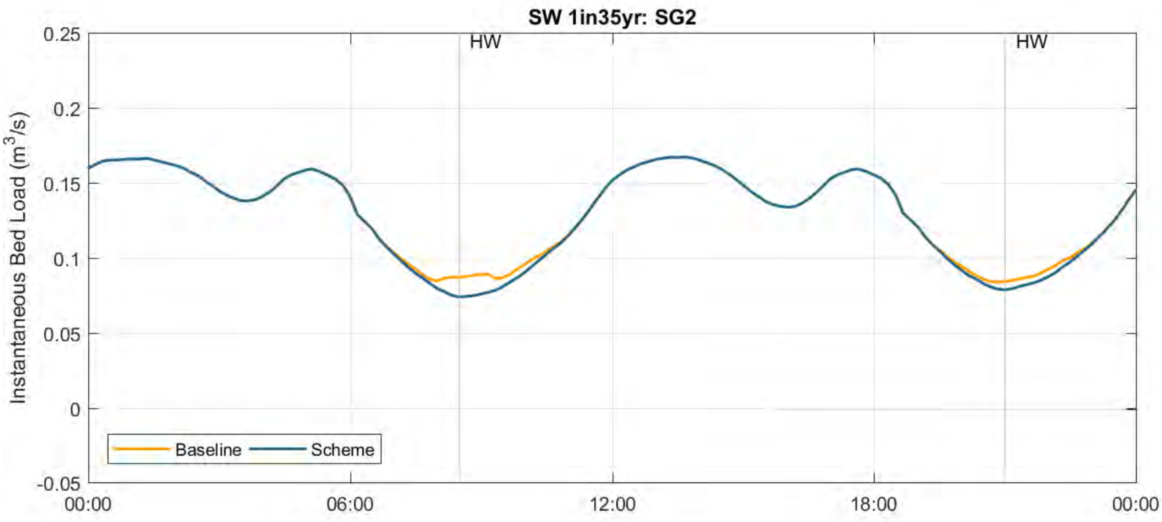

Positive values indicate transport to the northeast and negative values indicated transport to the southwest.

Figure B77. Time series of instantaneous sediment transport across SG2 for 1 in 35 year wave from the southwest

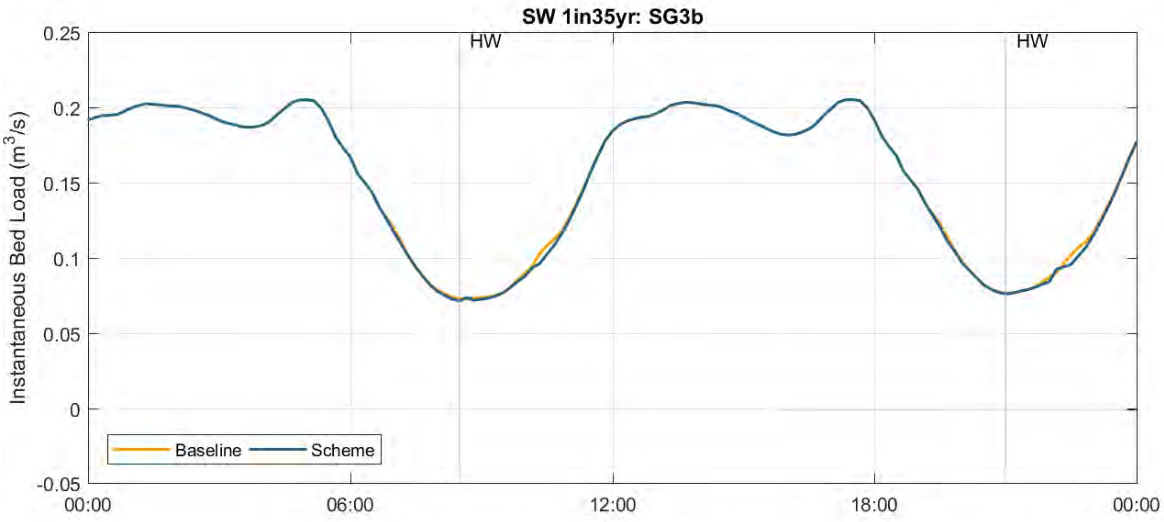

Positive values indicate transport to the northeast and negative values indicated transport to the southwest.

Figure B78. Time series of instantaneous sediment transport across SG3b for 1 in 35 year wave from the southwest

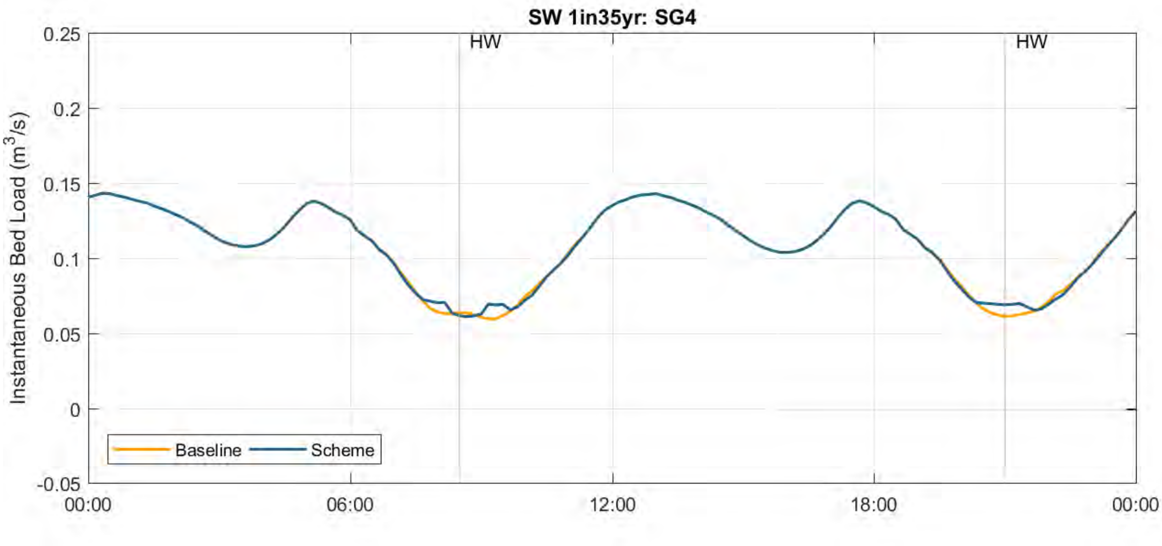

Positive values indicate transport to the northeast and negative values indicated transport to the southwest.

Figure B79. Time series of instantaneous sediment transport across SG4 for 1 in 35 year wave from the southwest

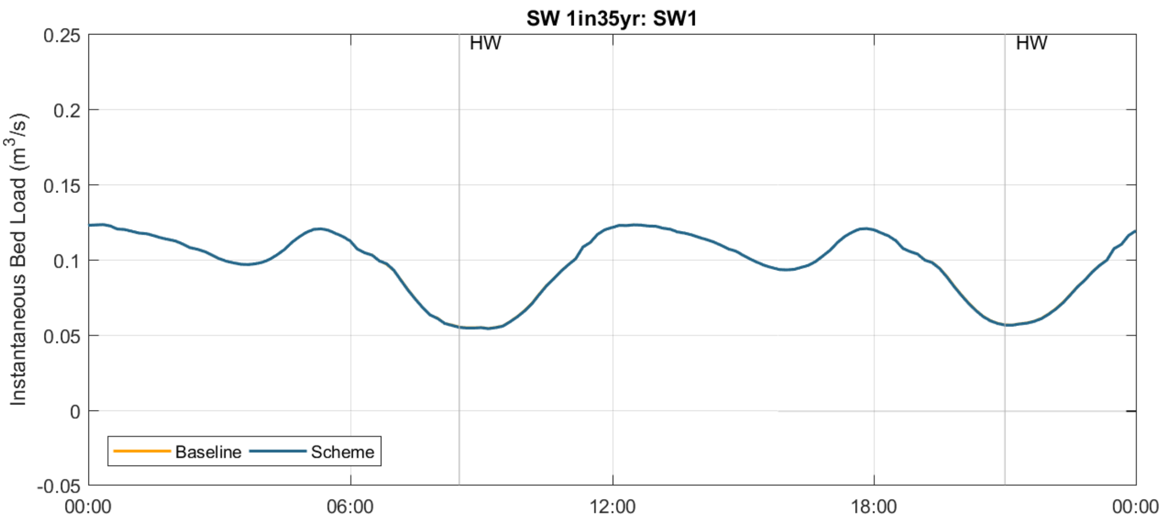

Positive values indicate transport to the northeast and negative values indicated transport to the southwest.

Figure B80. Time series of instantaneous sediment transport across SW1 for 1 in 35 year wave from the southwest

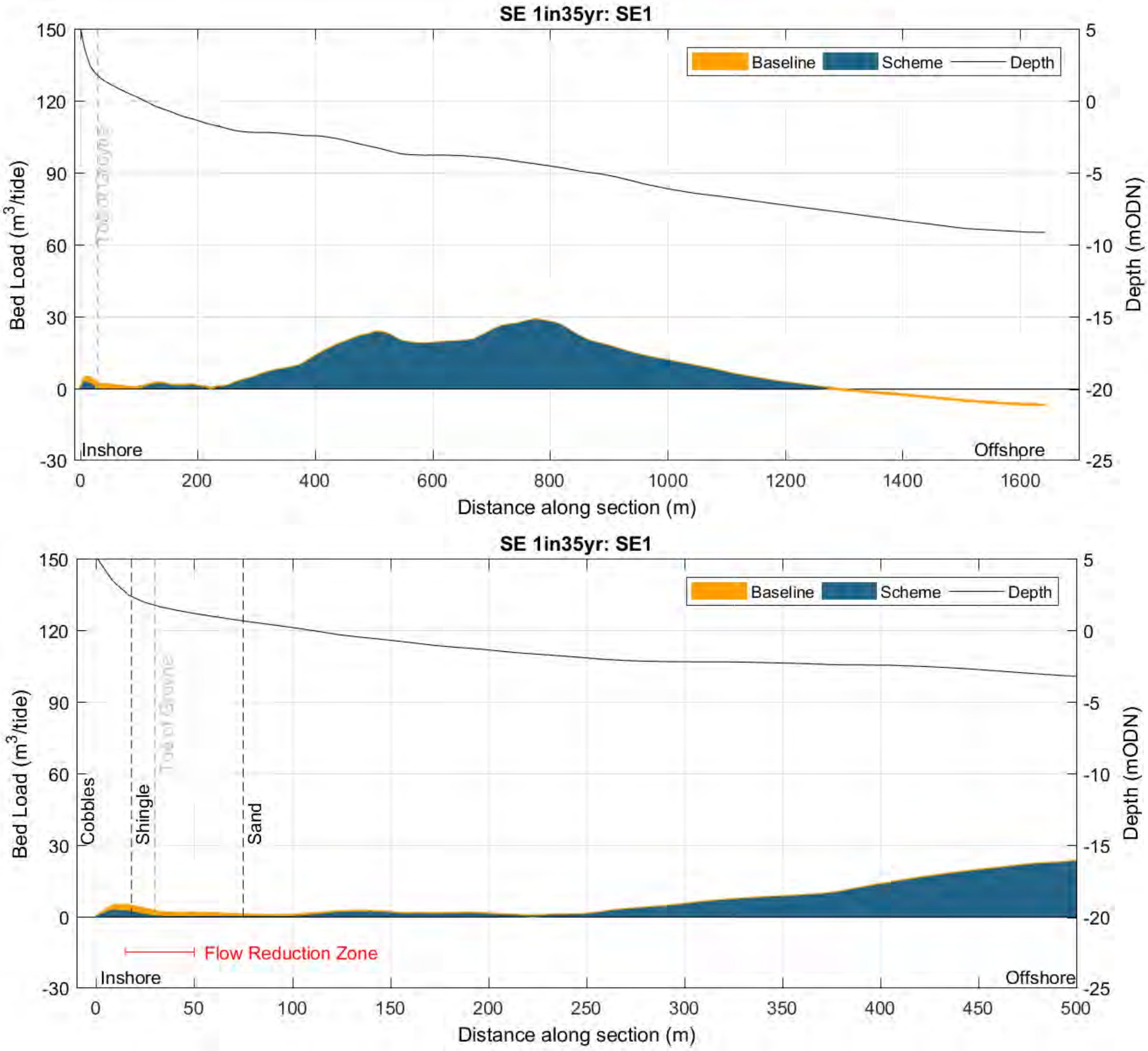

Positive values indicate transport to the northeast and negative values indicated transport to the southwest.
Sediment type i.e. cobbles, shingle and sand are shown for indicative purposes only.
A 0.2 mm sand has been used as the grain size in the model.

Figure B81. Sediment transport across SE1 for 1 in 35 year wave from the southeast

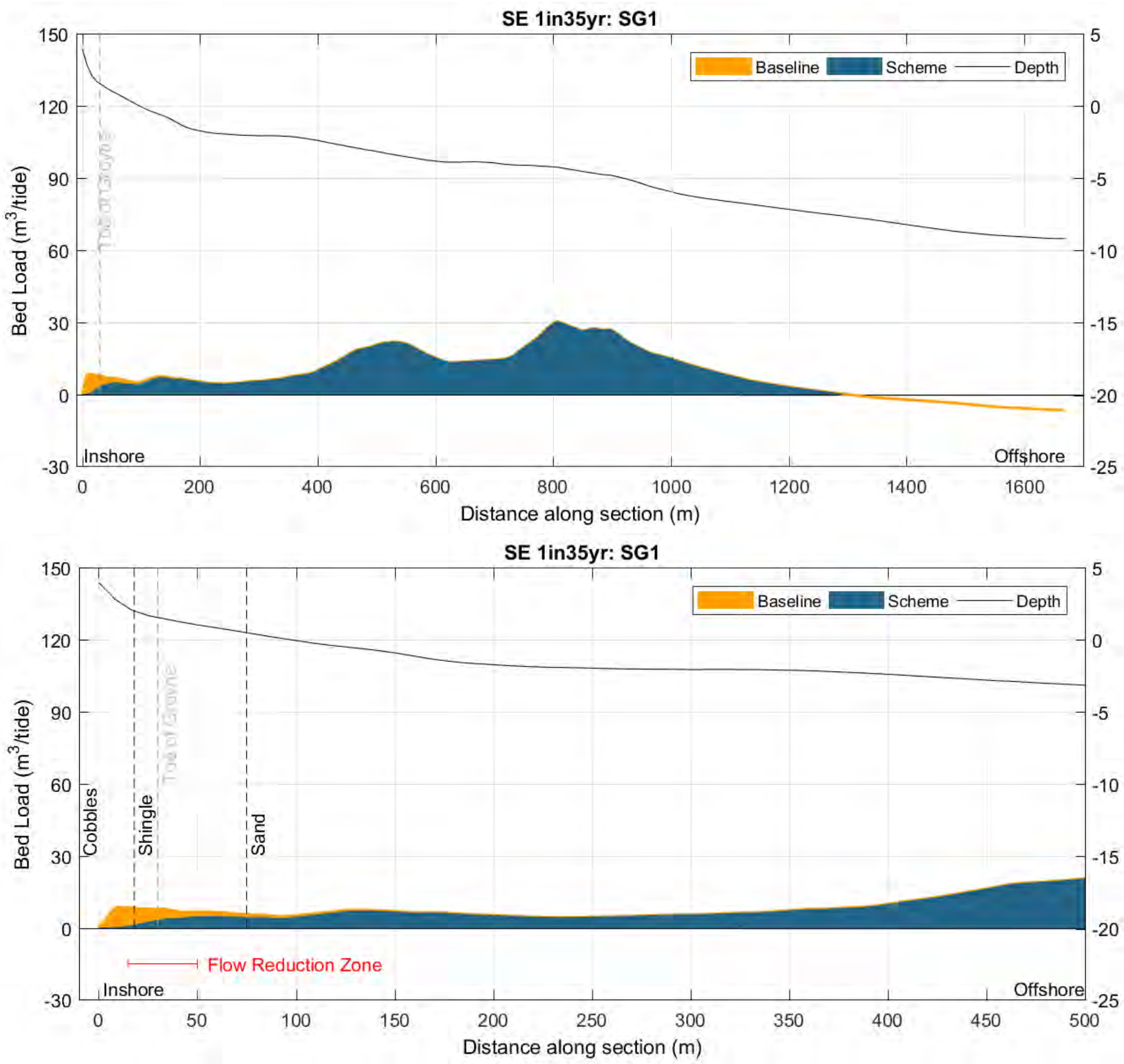

Positive values indicate transport to the northeast and negative values indicated transport to the southwest.
Sediment type i.e. cobbles, shingle and sand are shown for indicative purposes only.
A 0.2 mm sand has been used as the grain size in the model.

Figure B82. Sediment transport across SG1 for 1 in 35 year wave from the southeast

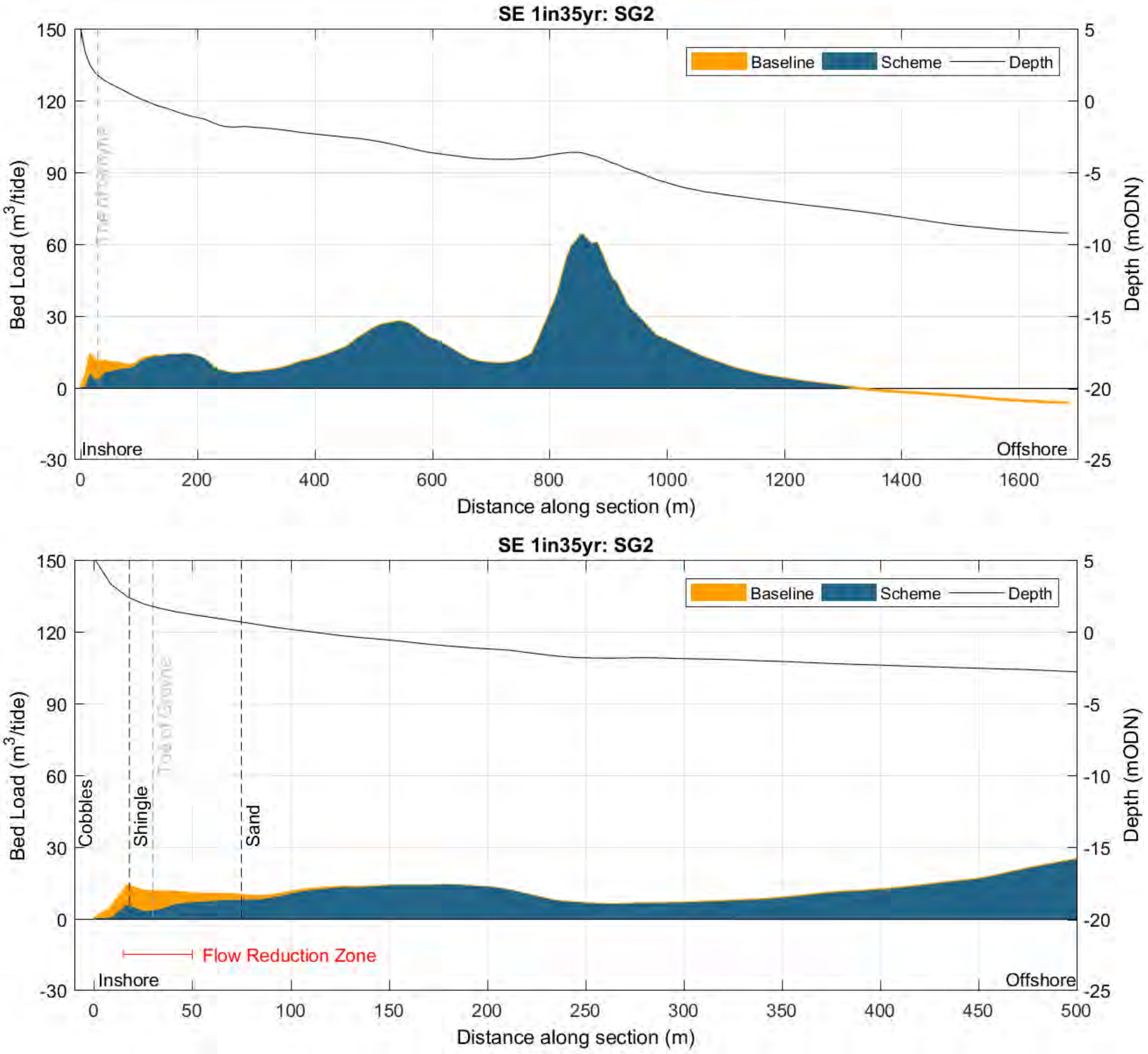

Positive values indicate transport to the northeast and negative values indicated transport to the southwest.
Sediment type i.e. cobbles, shingle and sand are shown for indicative purposes only.
A 0.2 mm sand has been used as the grain size in the model.

Figure B83. Sediment transport across SG2 for 1 in 35 year wave from the southeast

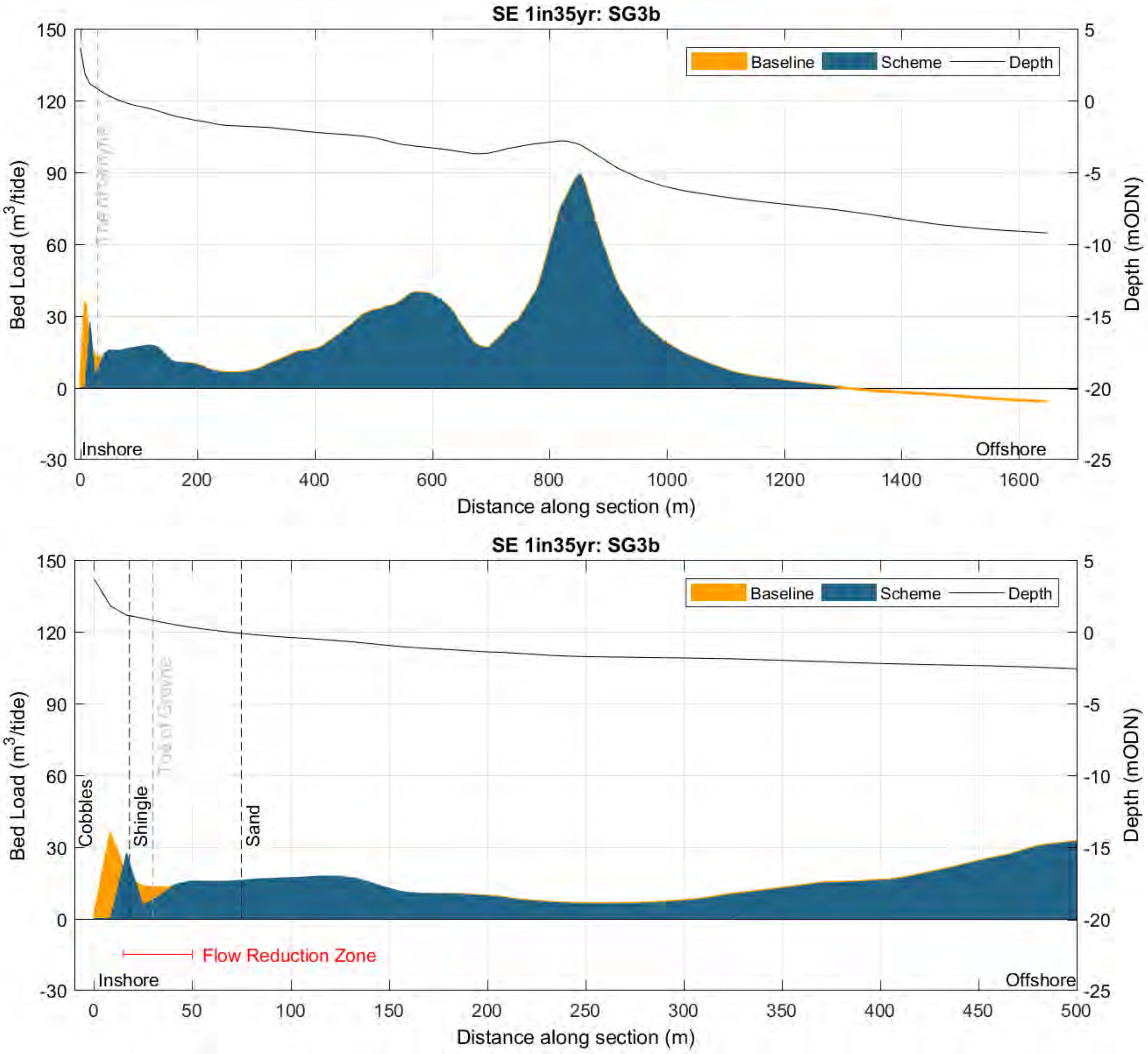

Positive values indicate transport to the northeast and negative values indicated transport to the southwest.
Sediment type i.e. cobbles, shingle and sand are shown for indicative purposes only.
A 0.2 mm sand has been used as the grain size in the model.

Figure B84. Sediment transport across SG3b for 1 in 35 year wave from the southeast

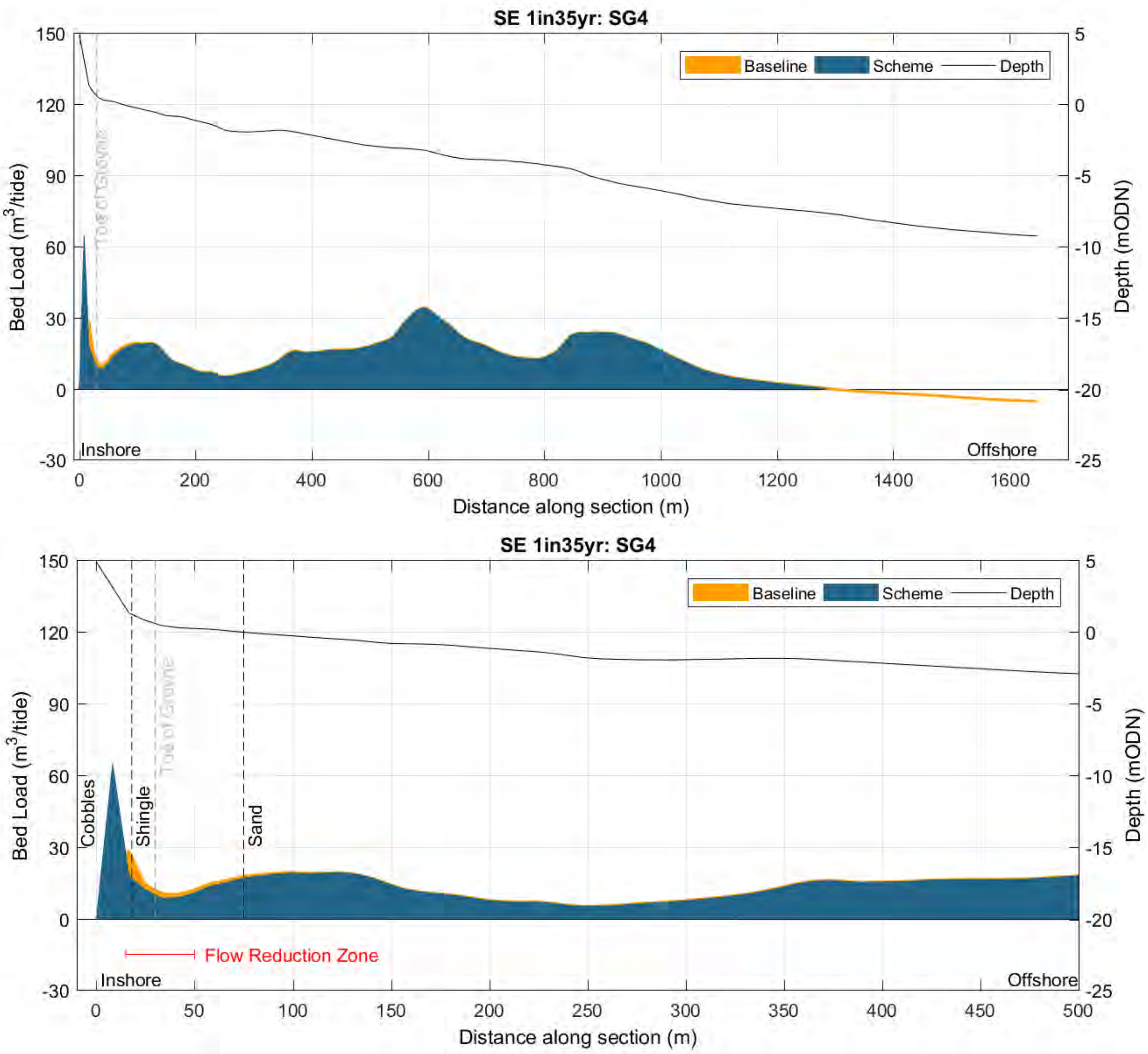

Positive values indicate transport to the northeast and negative values indicated transport to the southwest.
Sediment type i.e. cobbles, shingle and sand are shown for indicative purposes only.
A 0.2 mm sand has been used as the grain size in the model.

Figure B85. Sediment transport across SG4 for 1 in 35 year wave from the southeast

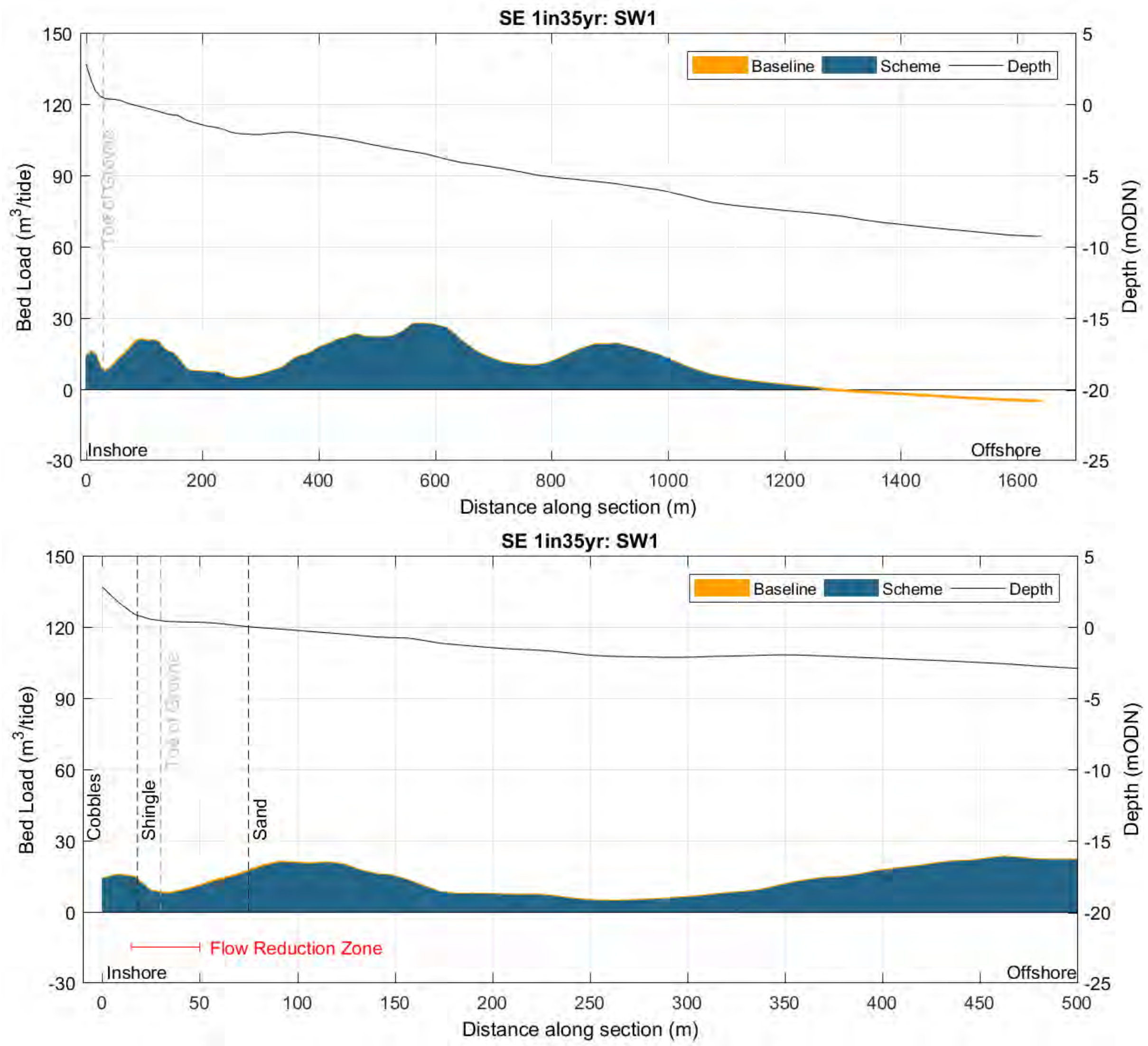

Positive values indicate transport to the northeast and negative values indicated transport to the southwest.
Sediment type i.e. cobbles, shingle and sand are shown for indicative purposes only.
A 0.2 mm sand has been used as the grain size in the model.

Figure B86. Sediment transport across SW1 for 1 in 35 year wave from the southeast

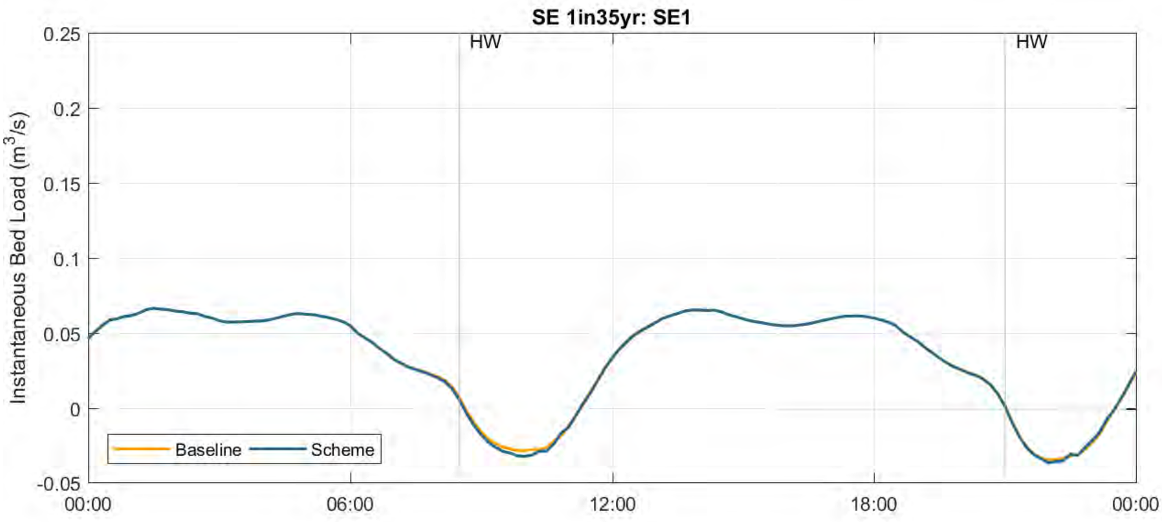

Positive values indicate transport to the northeast and negative values indicated transport to the southwest.

Figure B87. Time series of instantaneous sediment transport across SE1 for 1 in 35 year wave from the southeast

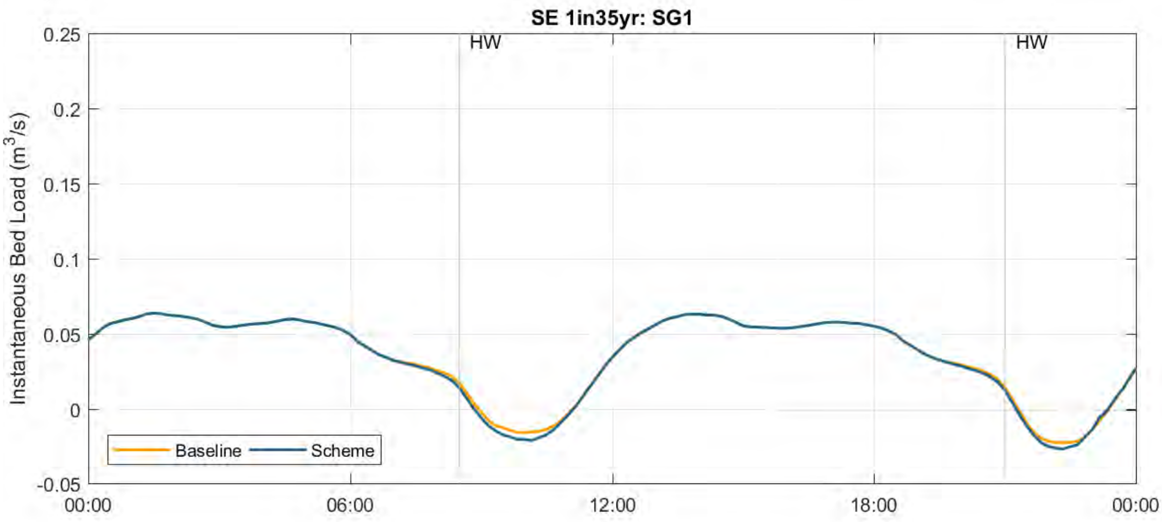

Positive values indicate transport to the northeast and negative values indicated transport to the southwest.

Figure B88. Time series of instantaneous sediment transport across SG1 for 1 in 35 year wave from the southeast

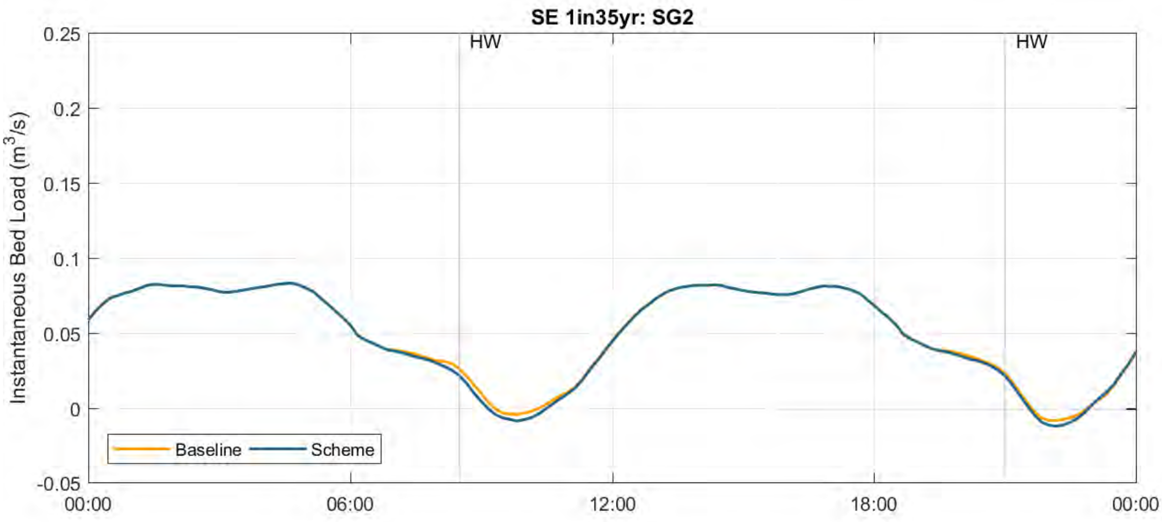

Positive values indicate transport to the northeast and negative values indicated transport to the southwest.

Figure B89. Time series of instantaneous sediment transport across SG2 for 1 in 35 year wave from the southeast

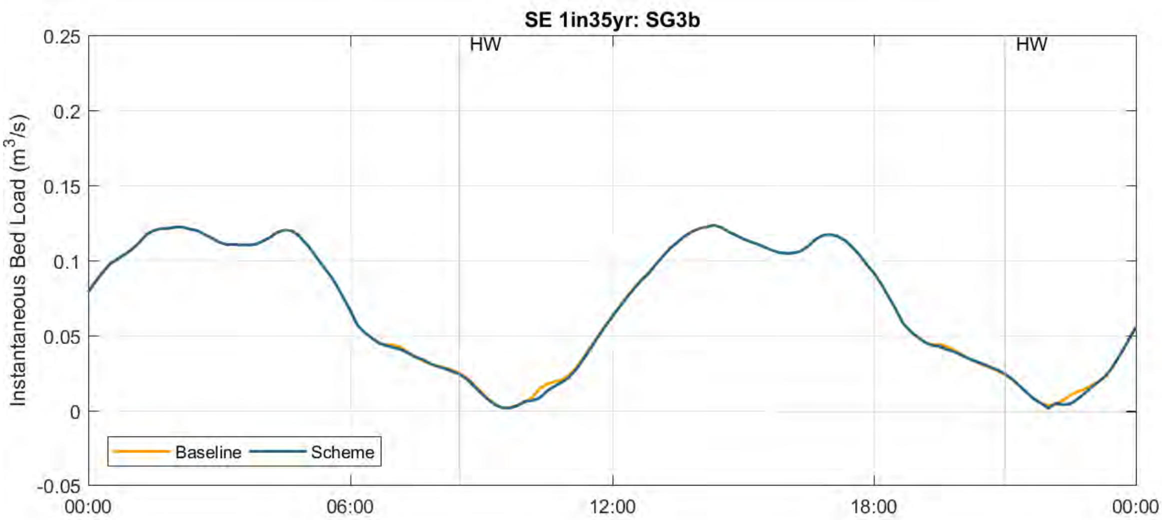

Positive values indicate transport to the northeast and negative values indicated transport to the southwest.

Figure B90. Time series of instantaneous sediment transport across SG3b for 1 in 35 year wave from the southeast

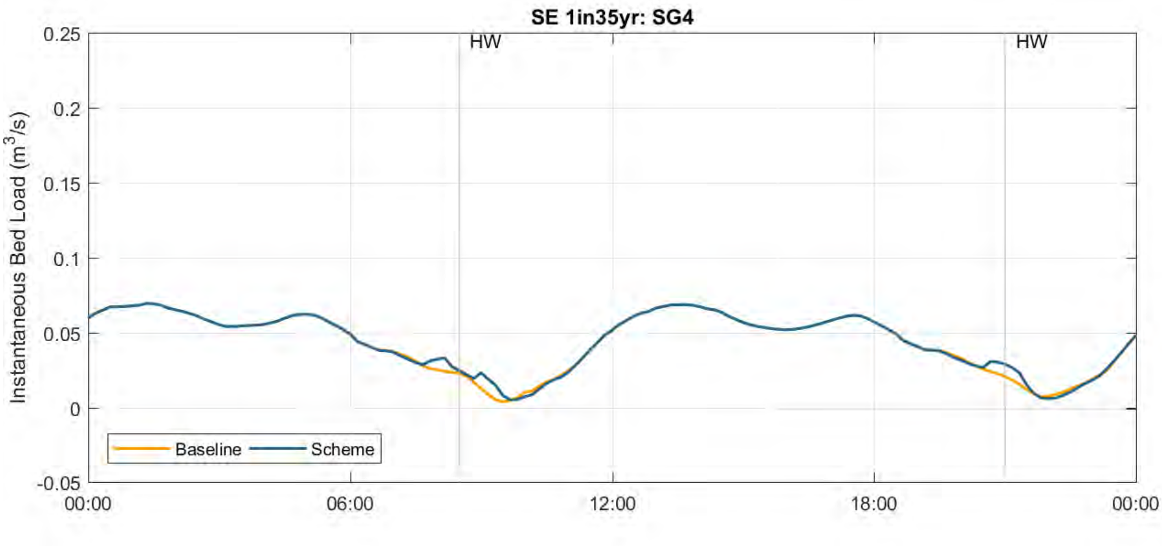

Positive values indicate transport to the northeast and negative values indicated transport to the southwest.

Figure B91. Time series of instantaneous sediment transport across SG4 for 1 in 35 year wave from the southeast

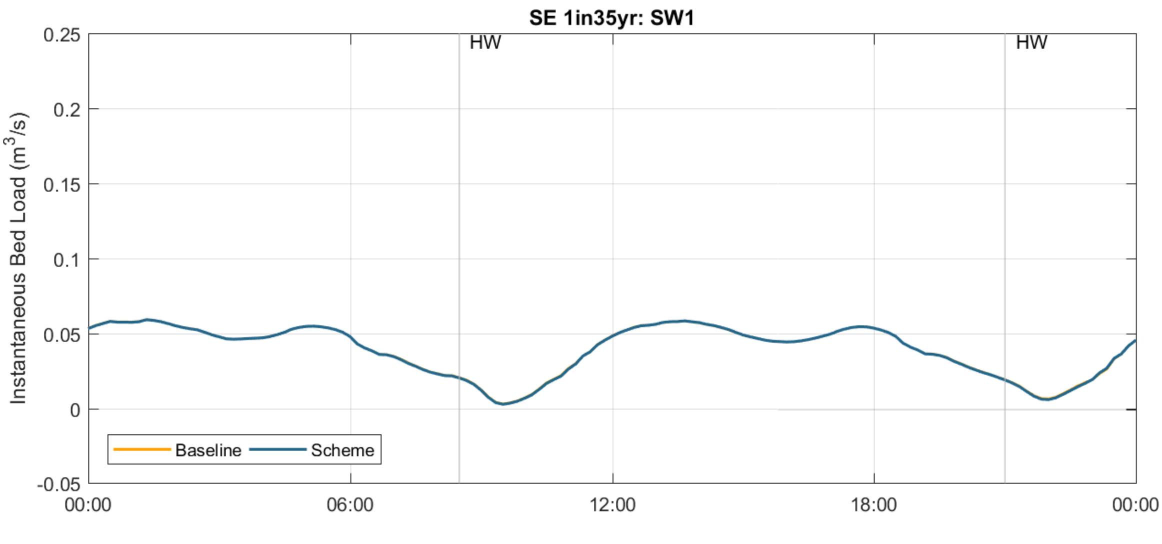

Positive values indicate transport to the northeast and negative values indicated transport to the southwest.

Figure B92. Time series of instantaneous sediment transport across SW1 for 1 in 35 year wave from the southeast

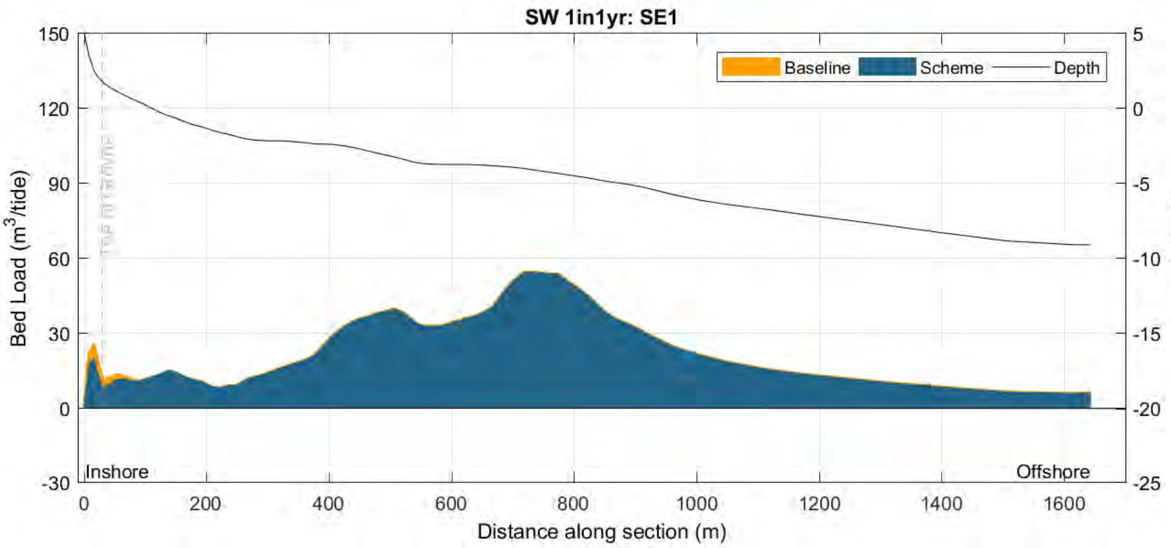

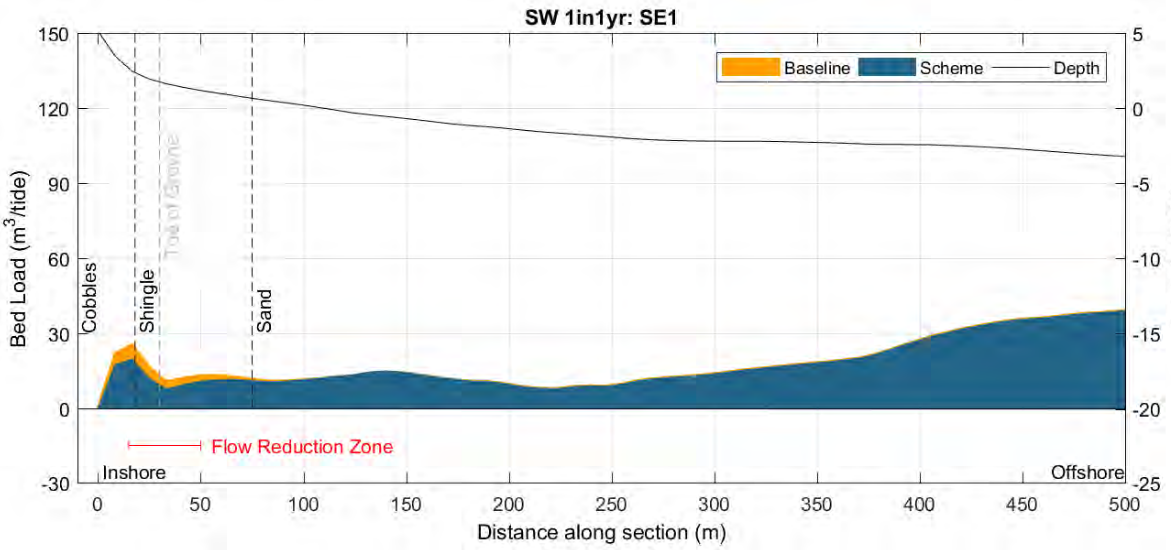

Positive values indicate transport to the northeast and negative values indicated transport to the southwest.
Sediment type i.e. cobbles, shingle and sand are shown for indicative purposes only.
A 0.2 mm sand has been used as the grain size in the model.

Figure B93. Sediment transport across SE1 for 1 in 1 year wave from the southwest

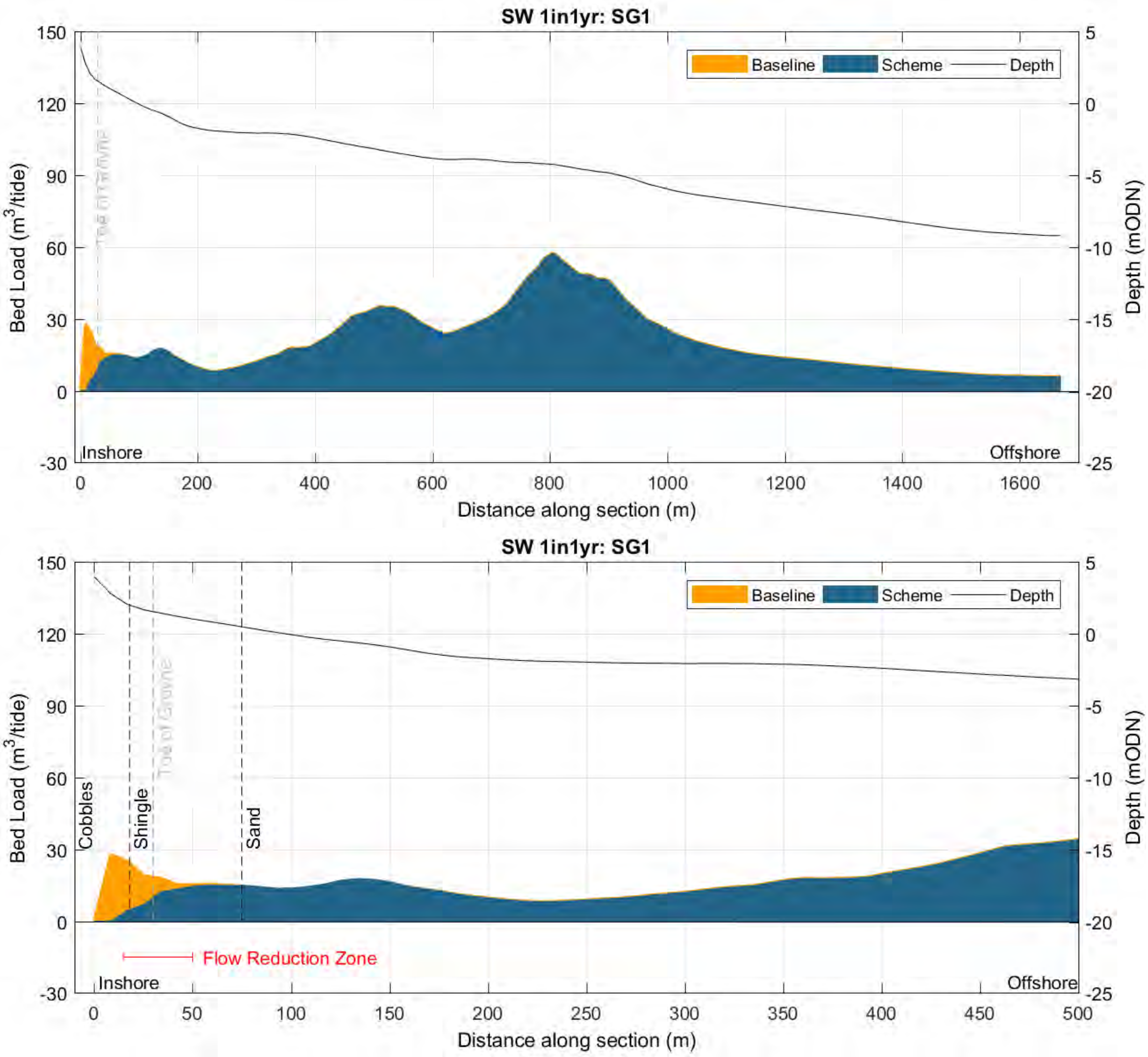

Positive values indicate transport to the northeast and negative values indicated transport to the southwest.
Sediment type i.e. cobbles, shingle and sand are shown for indicative purposes only.
A 0.2 mm sand has been used as the grain size in the model.

Figure B94. Sediment transport across SG1 for 1 in 1 year wave from the southwest

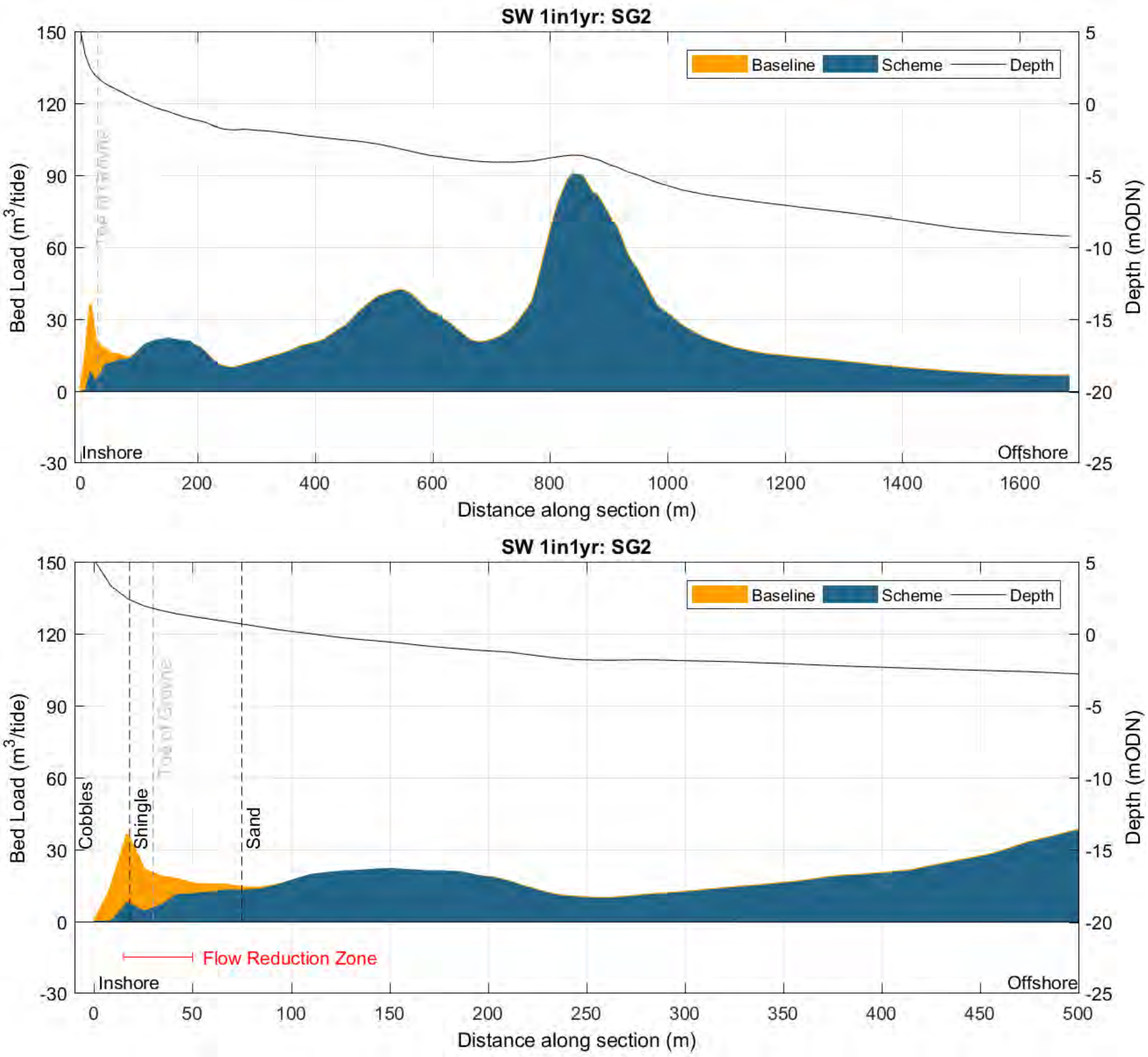

Positive values indicate transport to the northeast and negative values indicated transport to the southwest.
Sediment type i.e. cobbles, shingle and sand are shown for indicative purposes only.
A 0.2 mm sand has been used as the grain size in the model.

Figure B95. Sediment transport across SG2 for 1 in 1 year wave from the southwest

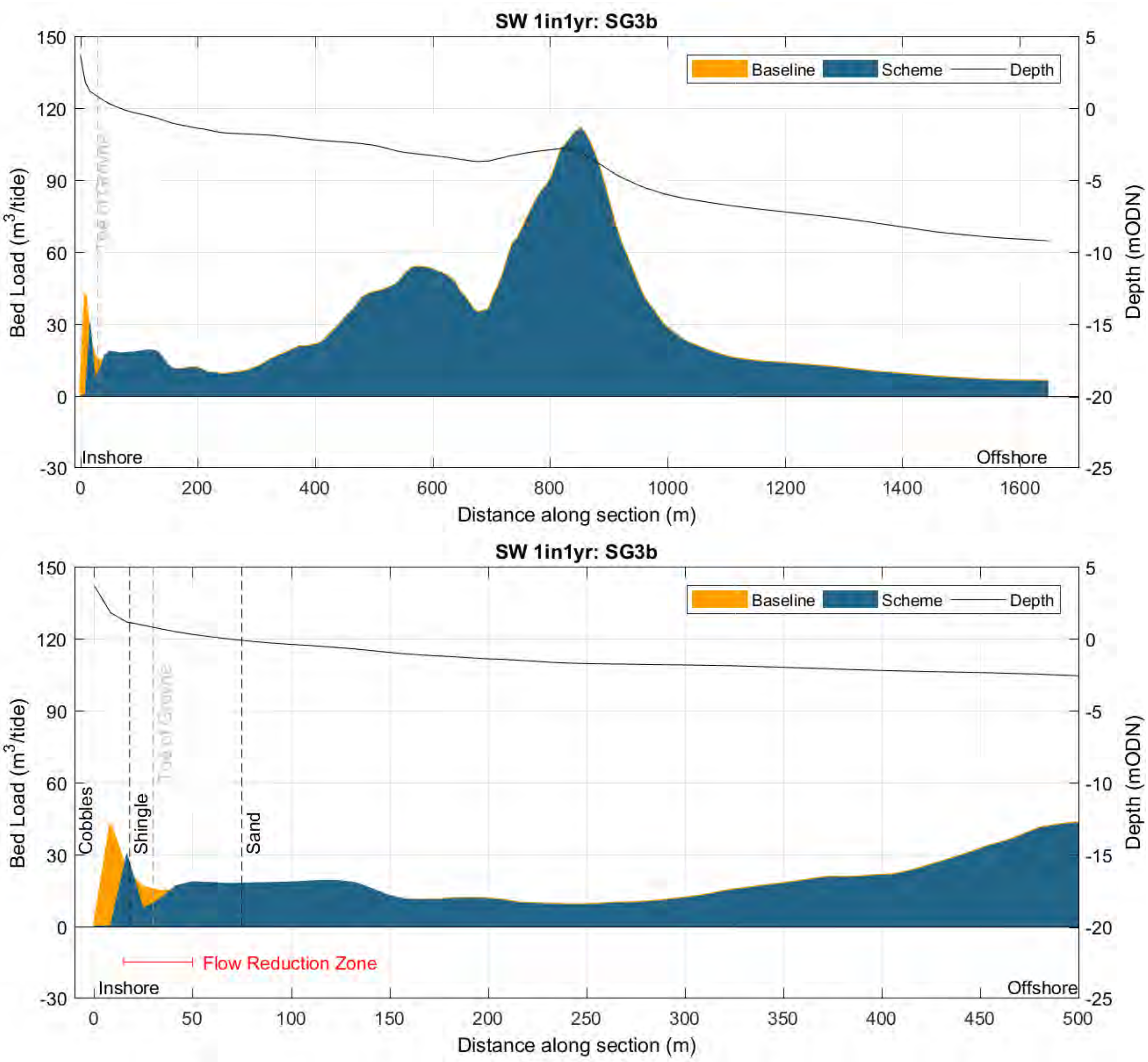

Positive values indicate transport to the northeast and negative values indicated transport to the southwest.
Sediment type i.e. cobbles, shingle and sand are shown for indicative purposes only.
A 0.2 mm sand has been used as the grain size in the model.

Figure B96. Sediment transport across SG3b for 1 in 1 year wave from the southwest

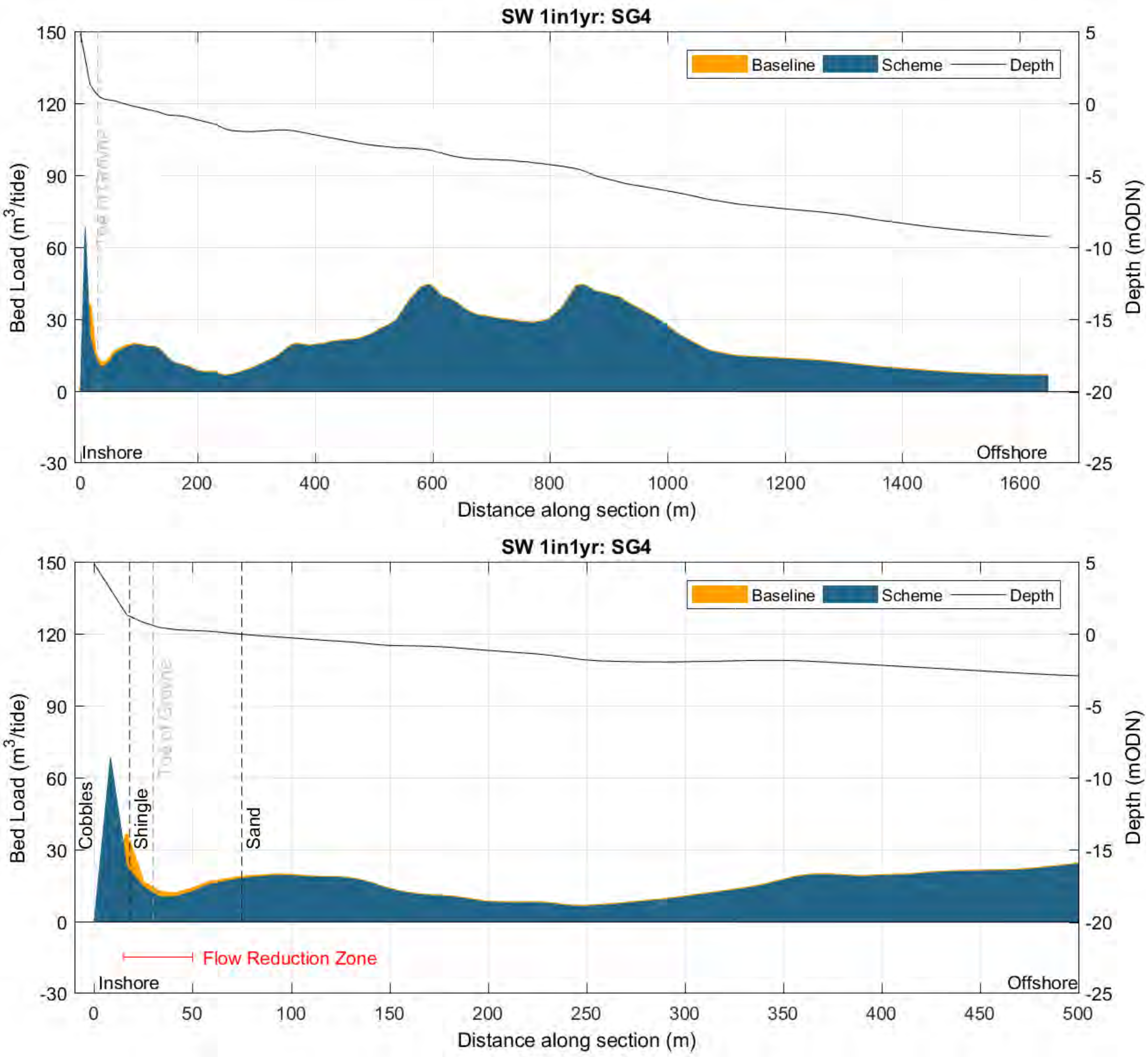

Positive values indicate transport to the northeast and negative values indicated transport to the southwest.
Sediment type i.e. cobbles, shingle and sand are shown for indicative purposes only.
A 0.2 mm sand has been used as the grain size in the model.

Figure B97. Sediment transport across SG4 for 1 in 1 year wave from the southwest

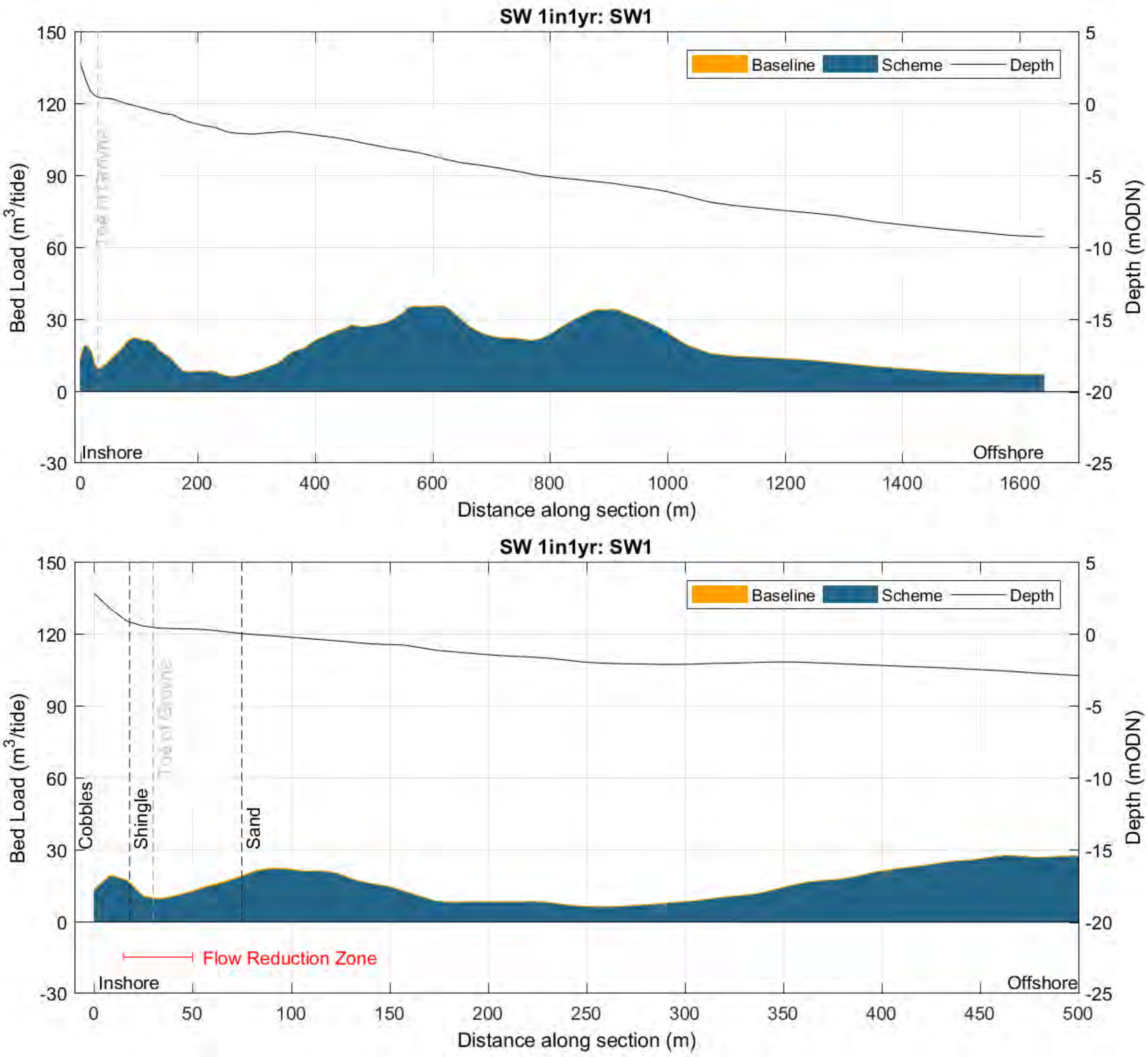

Positive values indicate transport to the northeast and negative values indicated transport to the southwest.
Sediment type i.e. cobbles, shingle and sand are shown for indicative purposes only.
A 0.2 mm sand has been used as the grain size in the model.

Figure B98. Sediment transport across SW1 for 1 in 1 year wave from the southwest

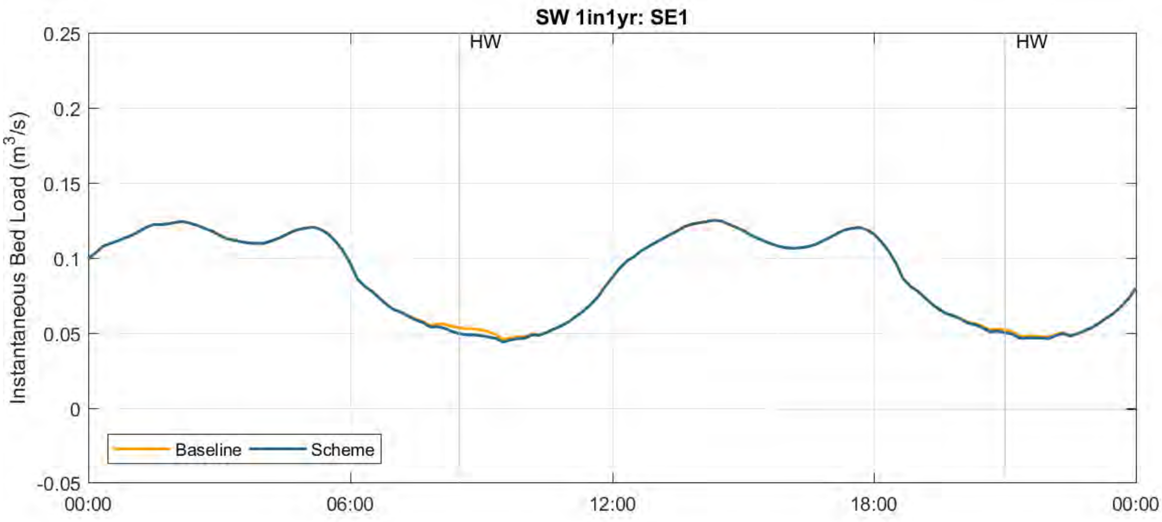

Positive values indicate transport to the northeast and negative values indicated transport to the southwest.

Figure B99. Time series of instantaneous sediment transport across SE1 for 1 in 1 year wave from the southwest

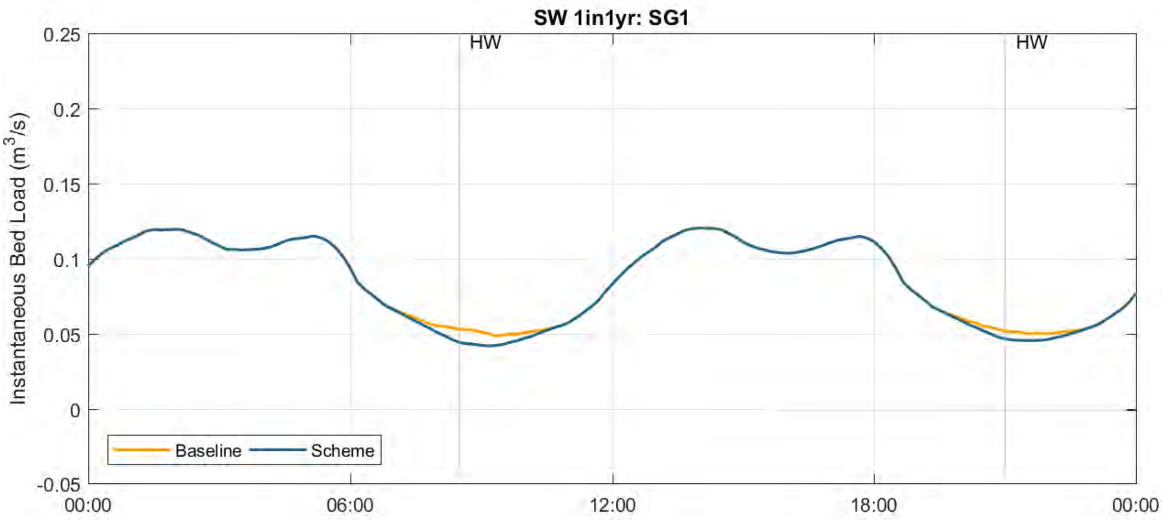

Positive values indicate transport to the northeast and negative values indicated transport to the southwest.

Figure B100. Time series of instantaneous sediment transport across SG1 for 1 in 1 year wave from the southwest

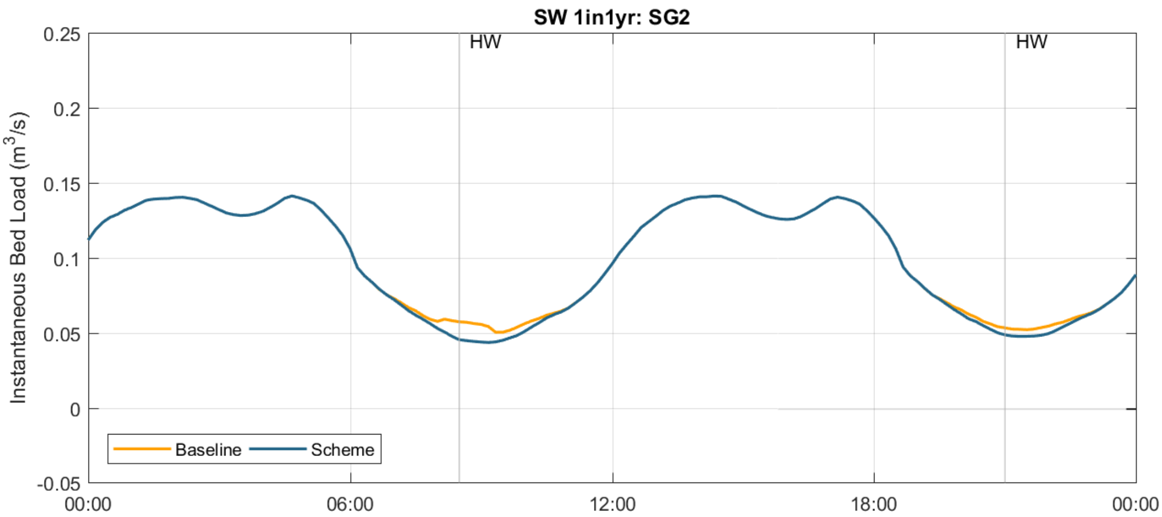

Positive values indicate transport to the northeast and negative values indicated transport to the southwest.

Figure B101. Time series of instantaneous sediment transport across SG2 for 1 in 1 year wave from the southwest

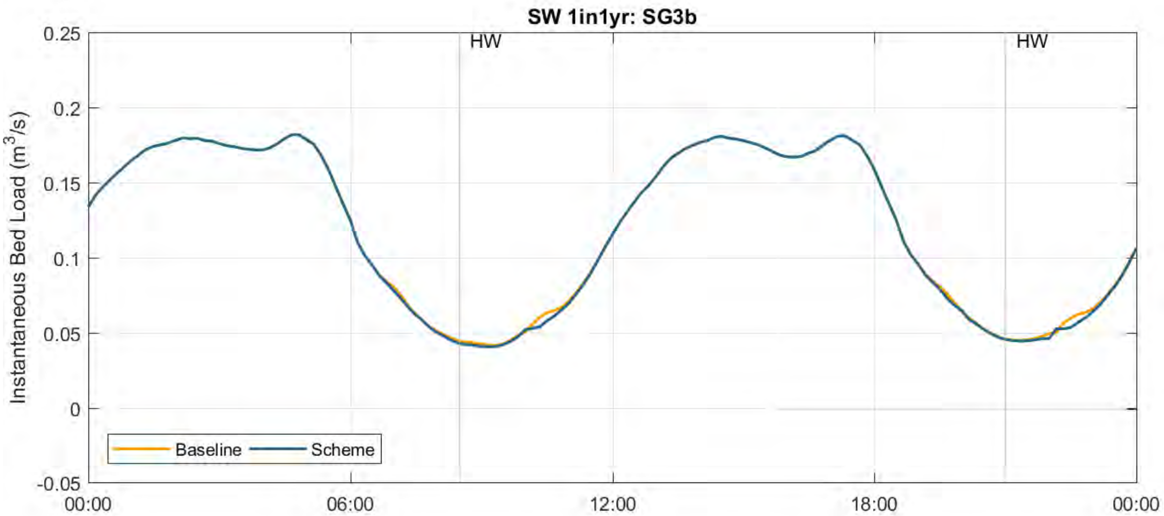

Positive values indicate transport to the northeast and negative values indicated transport to the southwest.

Figure B102. Time series of instantaneous sediment transport across SG3b for 1 in 1 year wave from the southwest

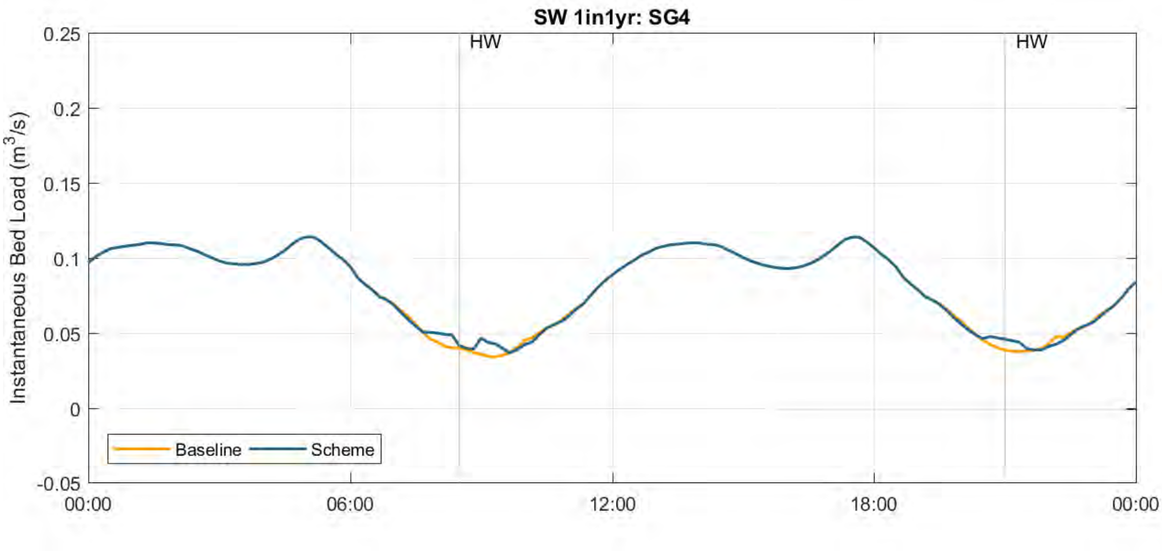

Positive values indicate transport to the northeast and negative values indicated transport to the southwest.

Figure B103. Time series of instantaneous sediment transport across SG4 for 1 in 1 year wave from the southwest

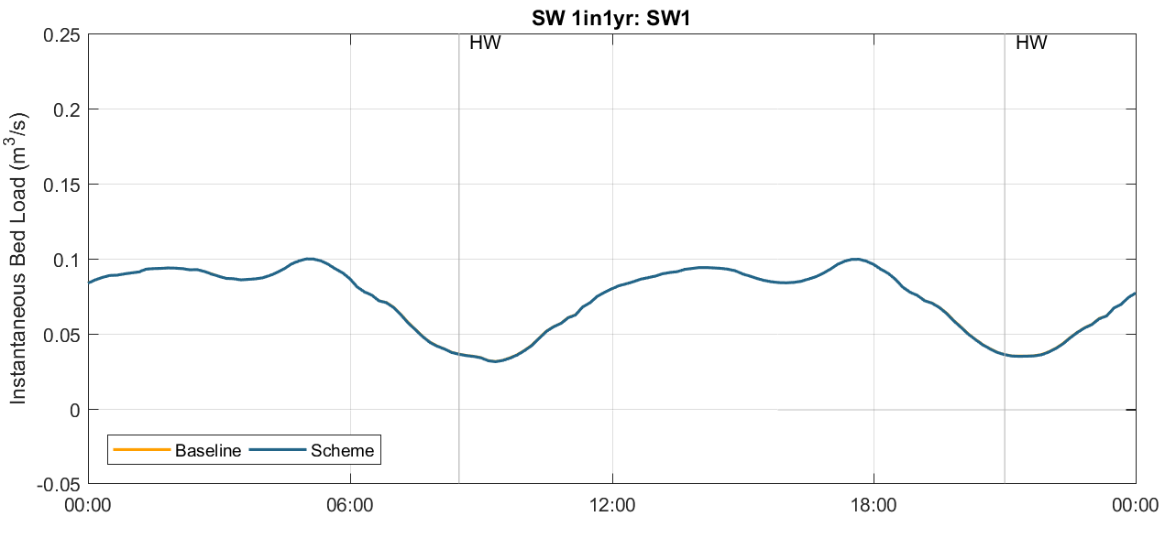

Positive values indicate transport to the northeast and negative values indicated transport to the southwest.

Figure B104. Time series of instantaneous sediment transport across SW1 for 1 in 1 year wave from the southwest

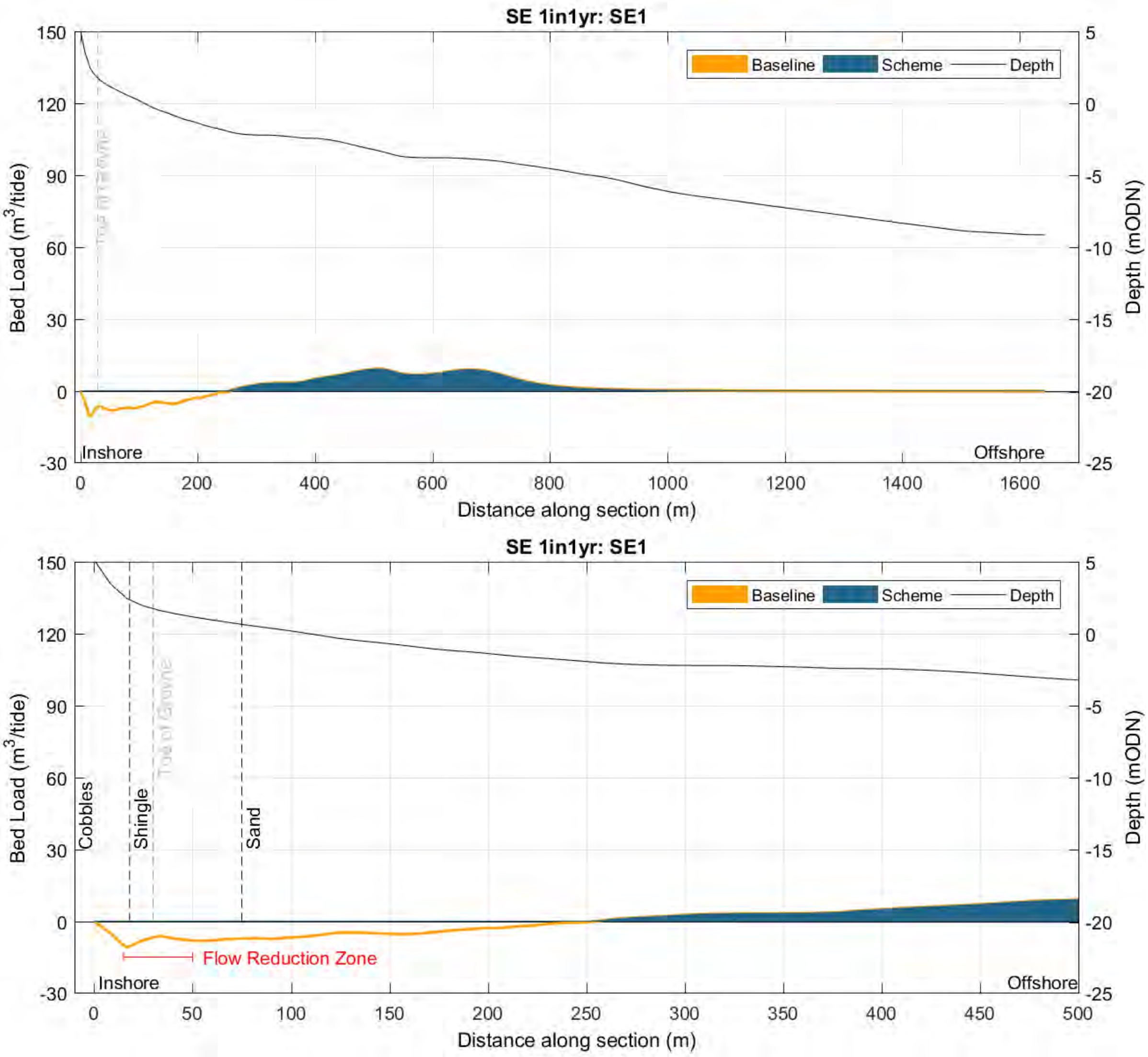

Positive values indicate transport to the northeast and negative values indicated transport to the southwest.
Sediment type i.e. cobbles, shingle and sand are shown for indicative purposes only.
A 0.2 mm sand has been used as the grain size in the model.

Figure B105. Sediment transport across SE1 for 1 in 1 year wave from the southeast

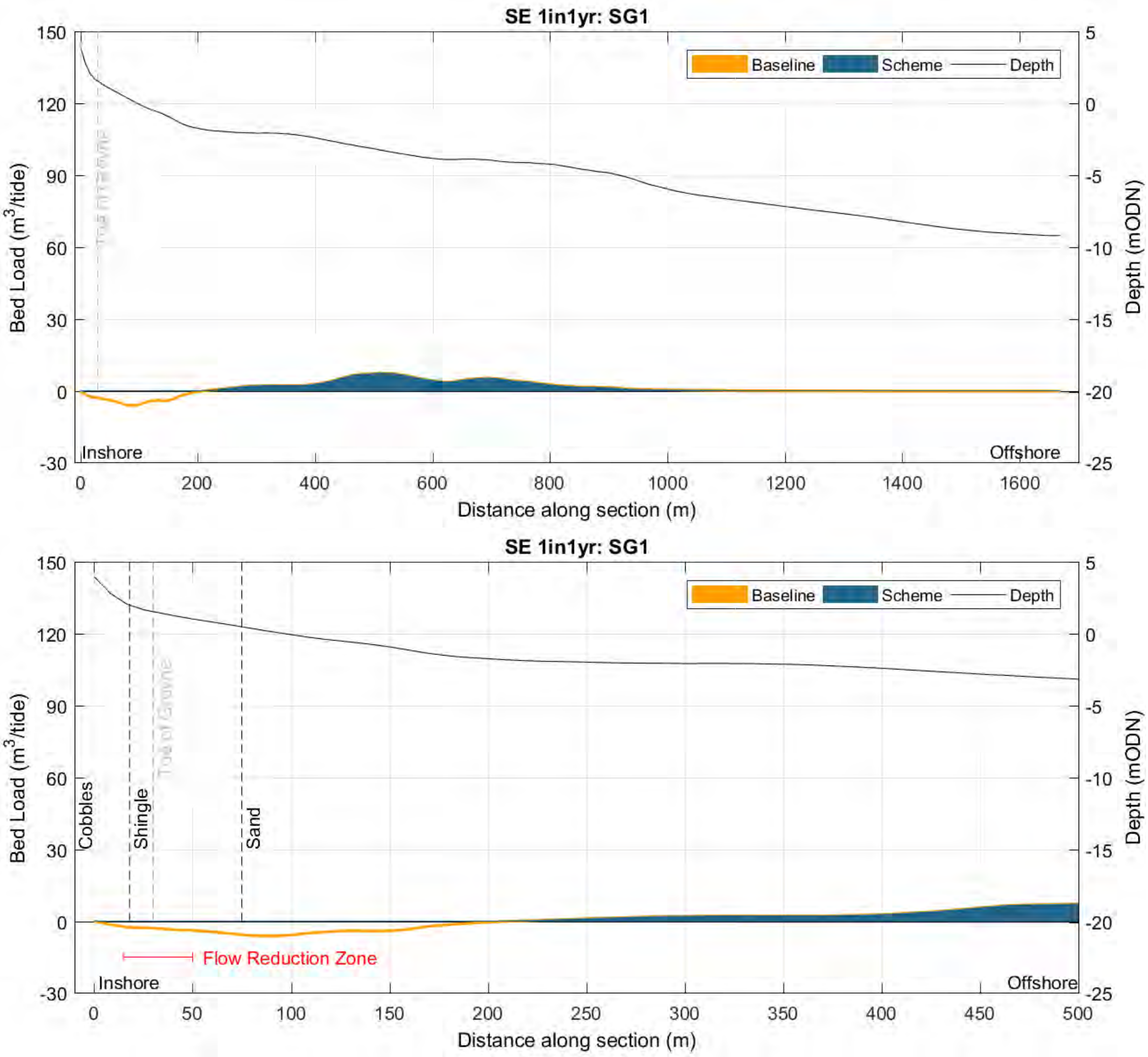

Positive values indicate transport to the northeast and negative values indicated transport to the southwest.
Sediment type i.e. cobbles, shingle and sand are shown for indicative purposes only.
A 0.2 mm sand has been used as the grain size in the model.

Figure B106. Sediment transport across SG1 for 1 in 1 year wave from the southeast

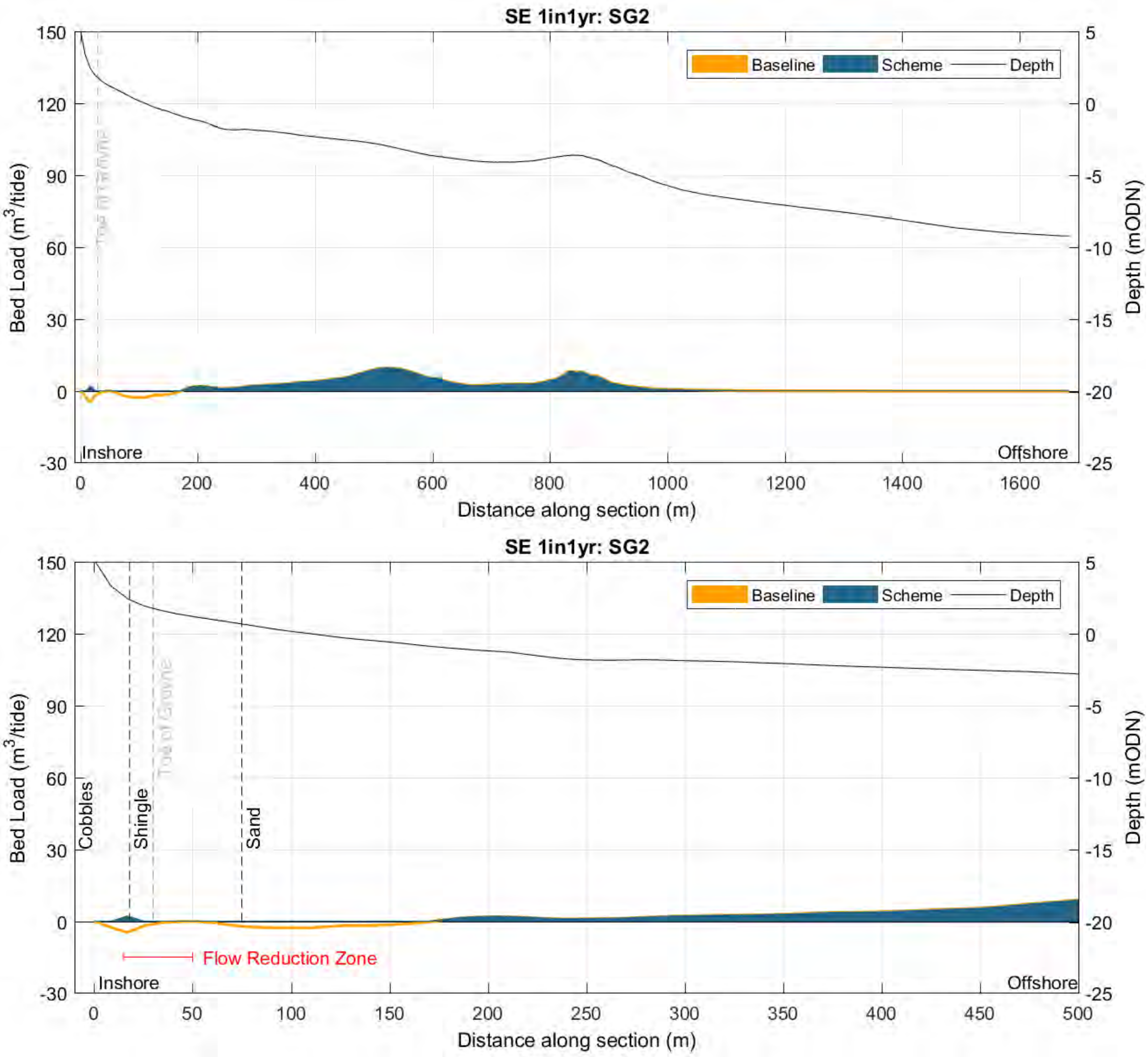

Positive values indicate transport to the northeast and negative values indicated transport to the southwest.
Sediment type i.e. cobbles, shingle and sand are shown for indicative purposes only.
A 0.2 mm sand has been used as the grain size in the model.

Figure B107. Sediment transport across SG2 for 1 in 1 year wave from the southeast

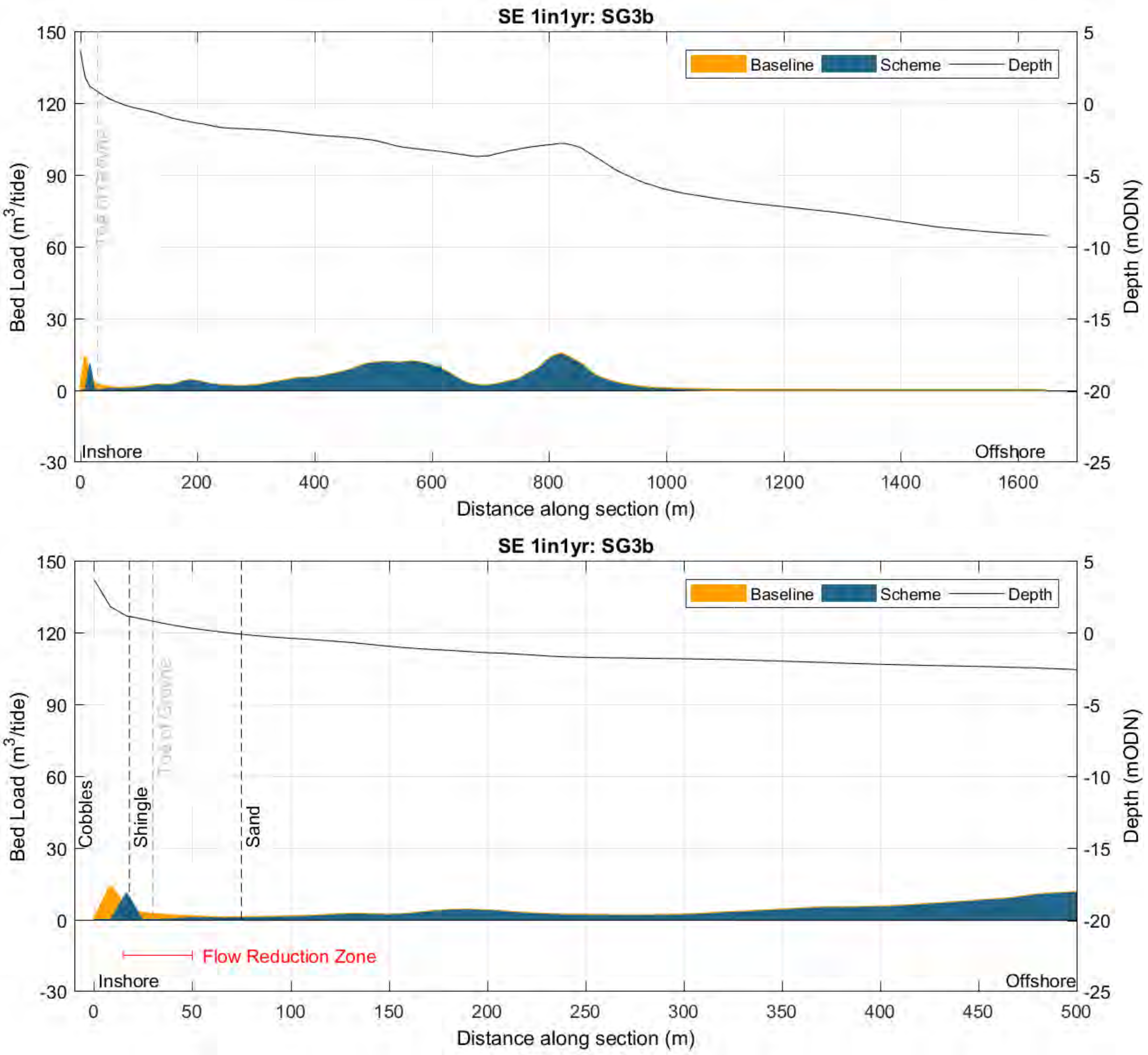

Positive values indicate transport to the northeast and negative values indicated transport to the southwest.
Sediment type i.e. cobbles, shingle and sand are shown for indicative purposes only.
A 0.2 mm sand has been used as the grain size in the model.

Figure B108. Sediment transport across SG3b for 1 in 1 year wave from the southeast

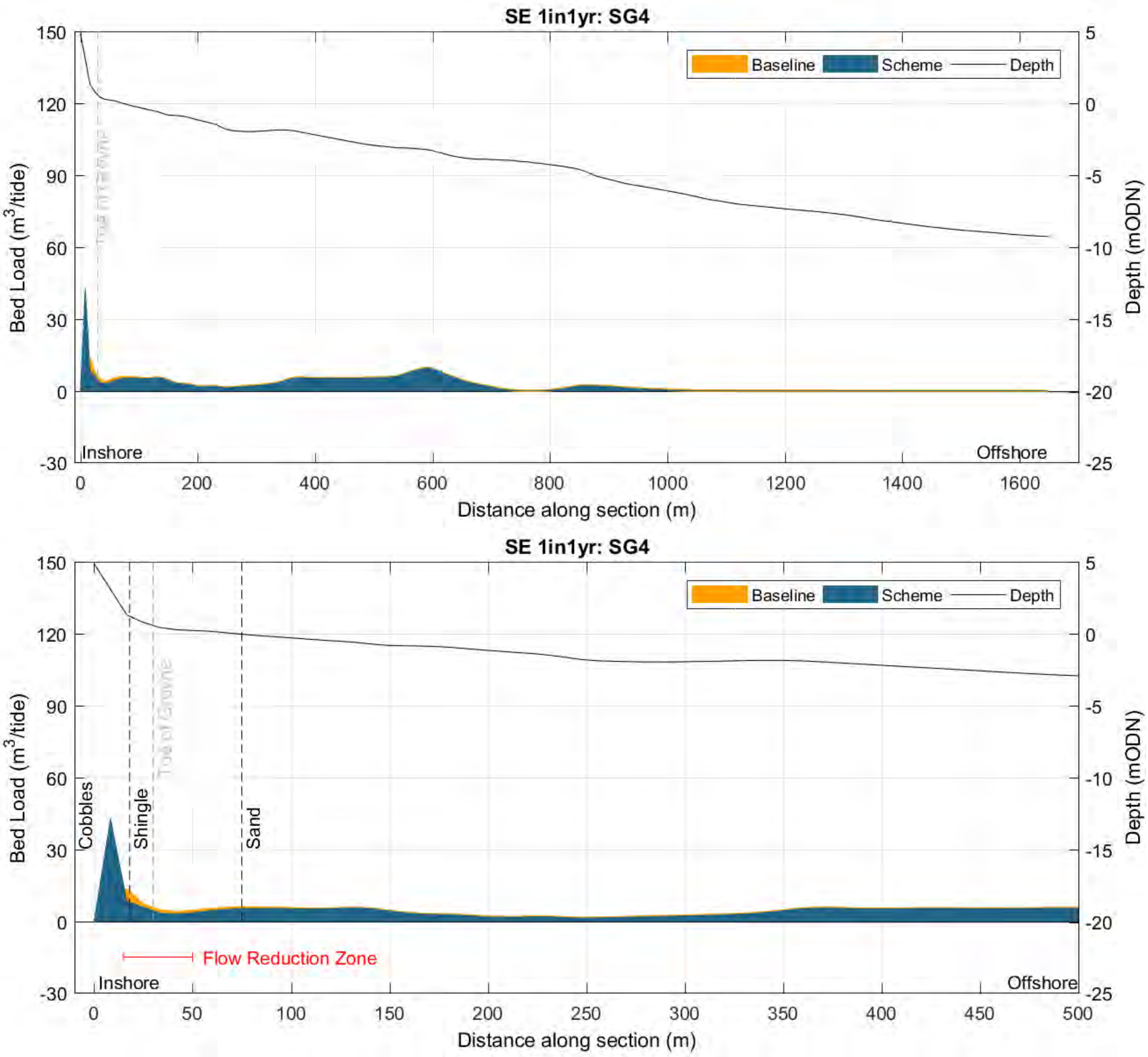

Positive values indicate transport to the northeast and negative values indicated transport to the southwest.
Sediment type i.e. cobbles, shingle and sand are shown for indicative purposes only.
A 0.2 mm sand has been used as the grain size in the model.

Figure B109. Sediment transport across SG4 for 1 in 1 year wave from the southeast

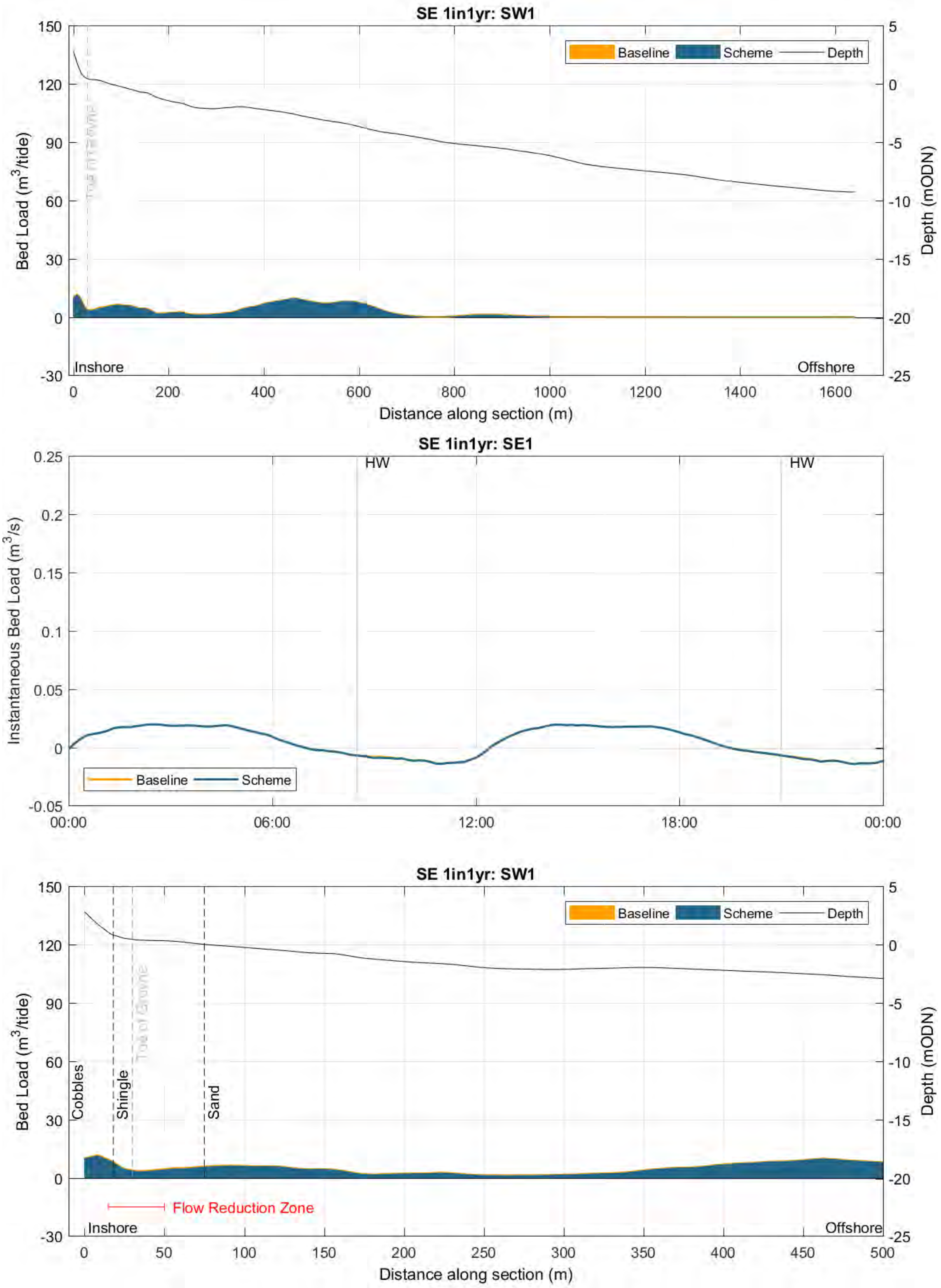

Positive values indicate transport to the northeast and negative values indicated transport to the southwest.
Sediment type i.e. cobbles, shingle and sand are shown for indicative purposes only.
A 0.2 mm sand has been used as the grain size in the model.

Figure B110. Sediment transport across SW1 for 1 in 1 year wave from the southeast

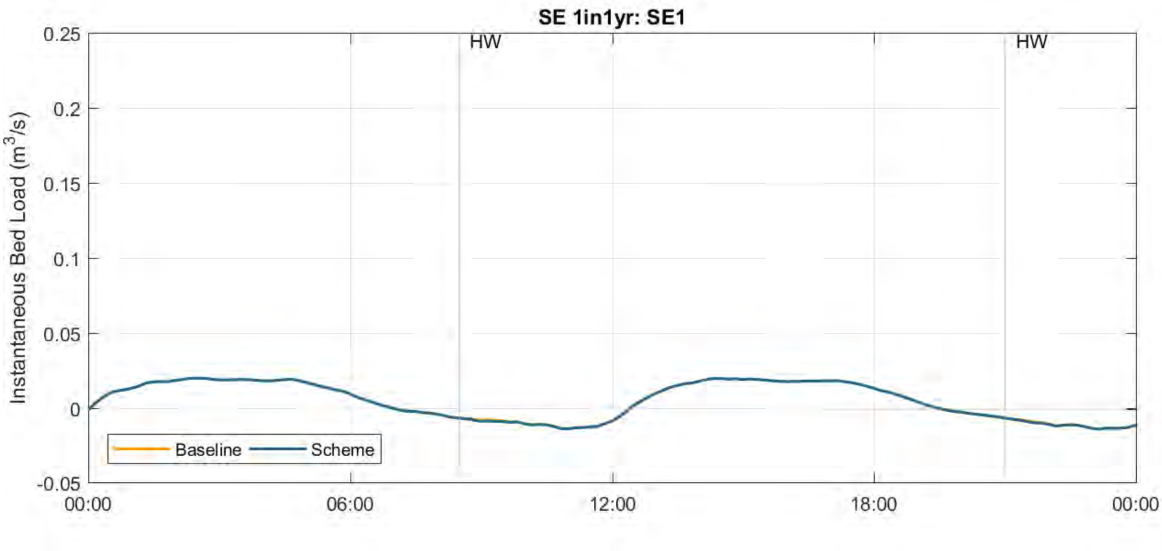

Positive values indicate transport to the northeast and negative values indicated transport to the southwest.

Figure B111. Time series of instantaneous sediment transport across SE1 for 1 in 1 year wave from the southeast

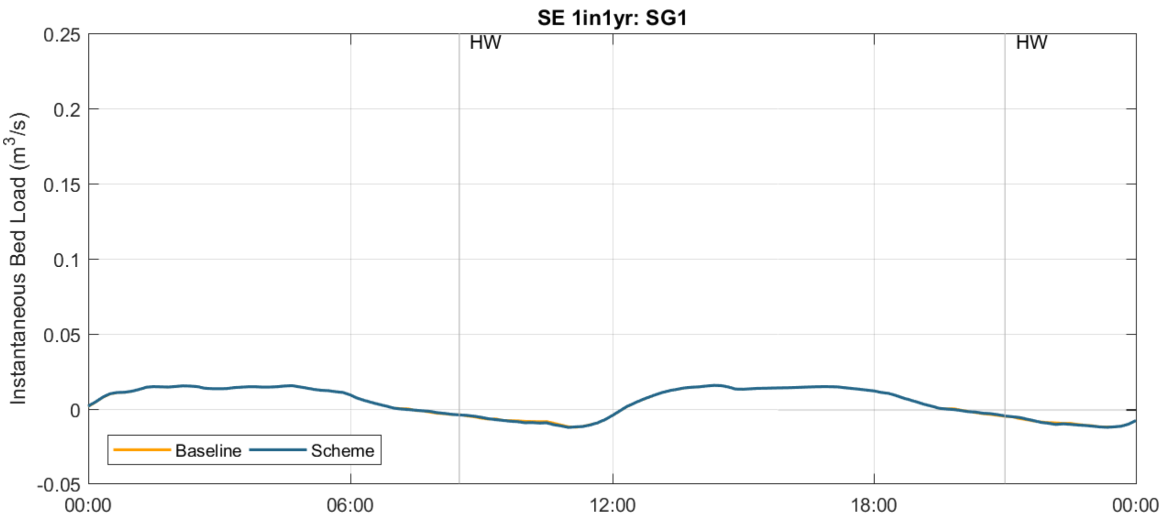

Positive values indicate transport to the northeast and negative values indicated transport to the southwest.

Figure B112. Time series of instantaneous sediment transport across SG1 for 1 in 1 year wave from the southeast

Positive values indicate transport to the northeast and negative values indicated transport to the southwest.

Figure B113. Time series of instantaneous sediment transport across SG2 for 1 in 1 year wave from the southeast

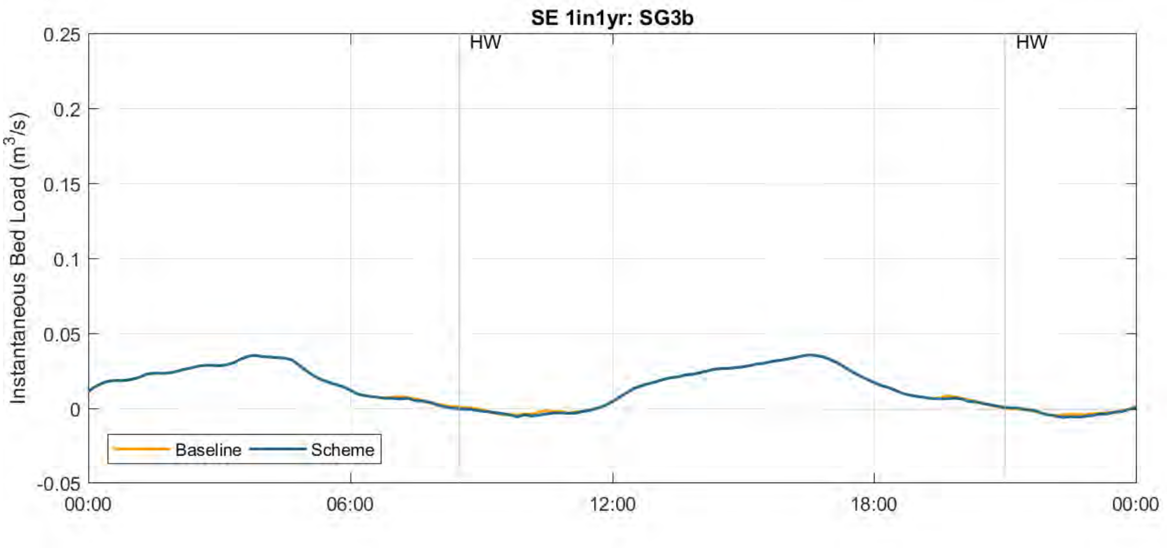

Positive values indicate transport to the northeast and negative values indicated transport to the southwest.

Figure B114. Time series of instantaneous sediment transport across SG3b for 1 in 1 year wave from the southeast

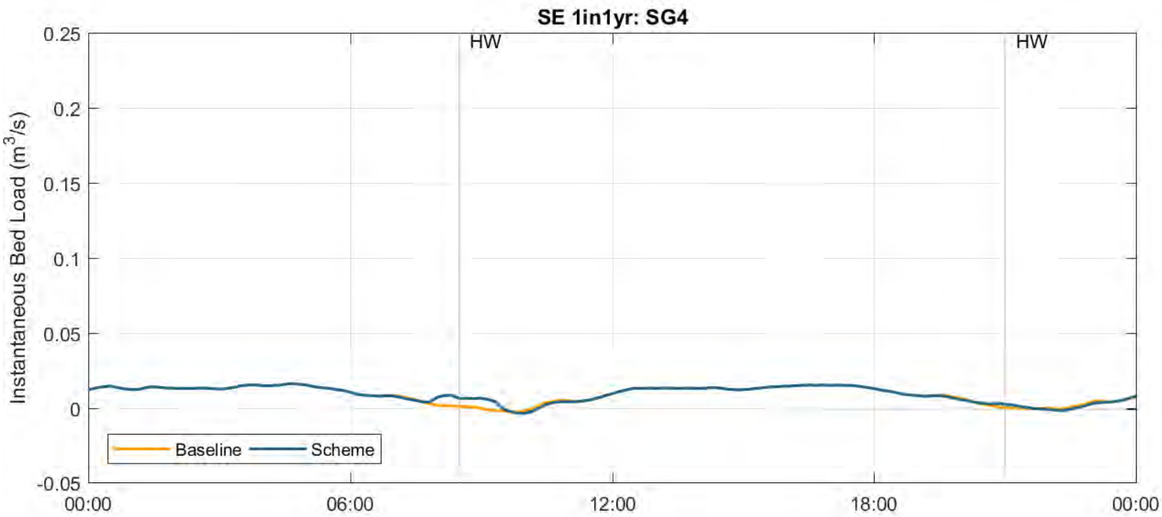

Positive values indicate transport to the northeast and negative values indicated transport to the southwest.

Figure B115. Time series of instantaneous sediment transport across SG4 for 1 in 1 year wave from the southeast

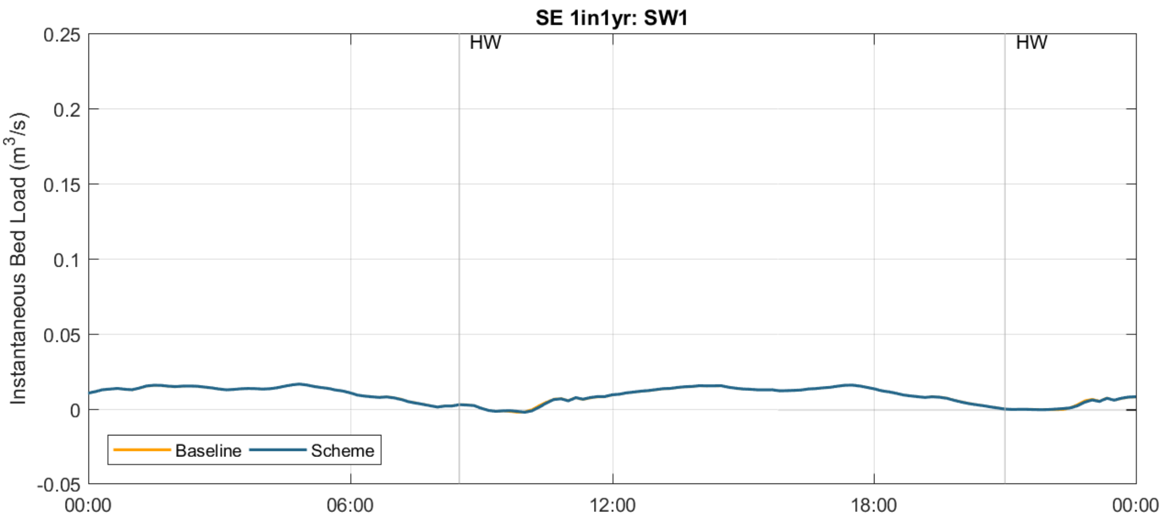

Positive values indicate transport to the northeast and negative values indicated transport to the southwest.

Figure B116. Time series of instantaneous sediment transport across SW1 for 1 in 1 year wave from the southeast

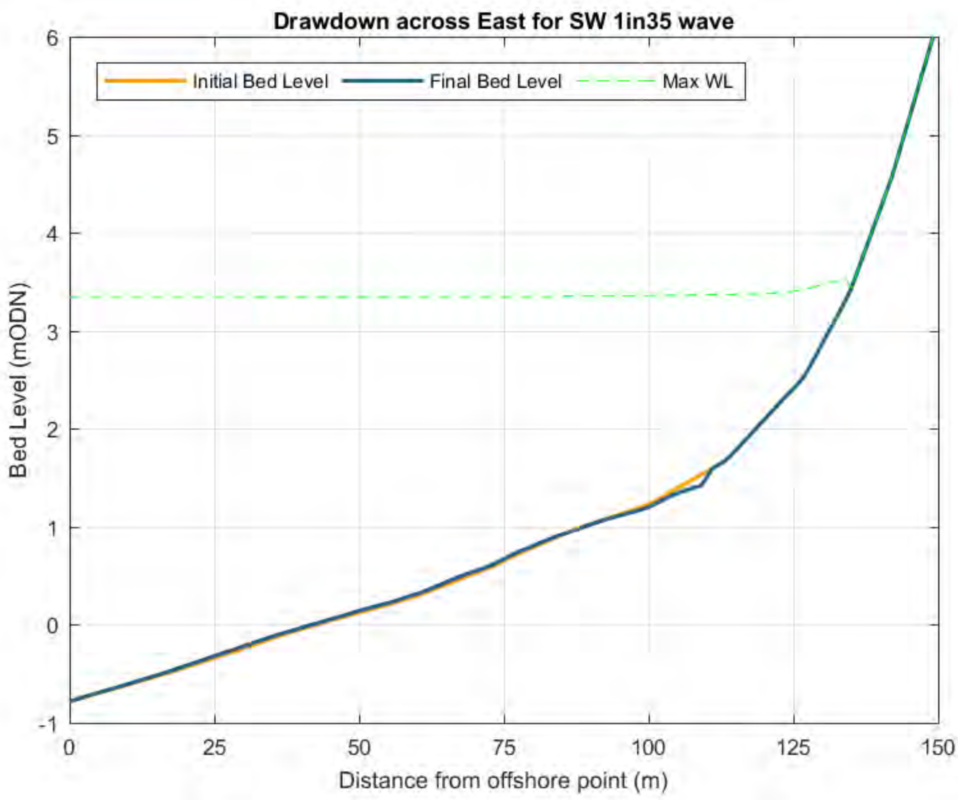

The dotted blue line shows the results for the smaller roughness length

Figure B117. Beach drawdown on East profile during 1 in 35 year wave event from the southwest

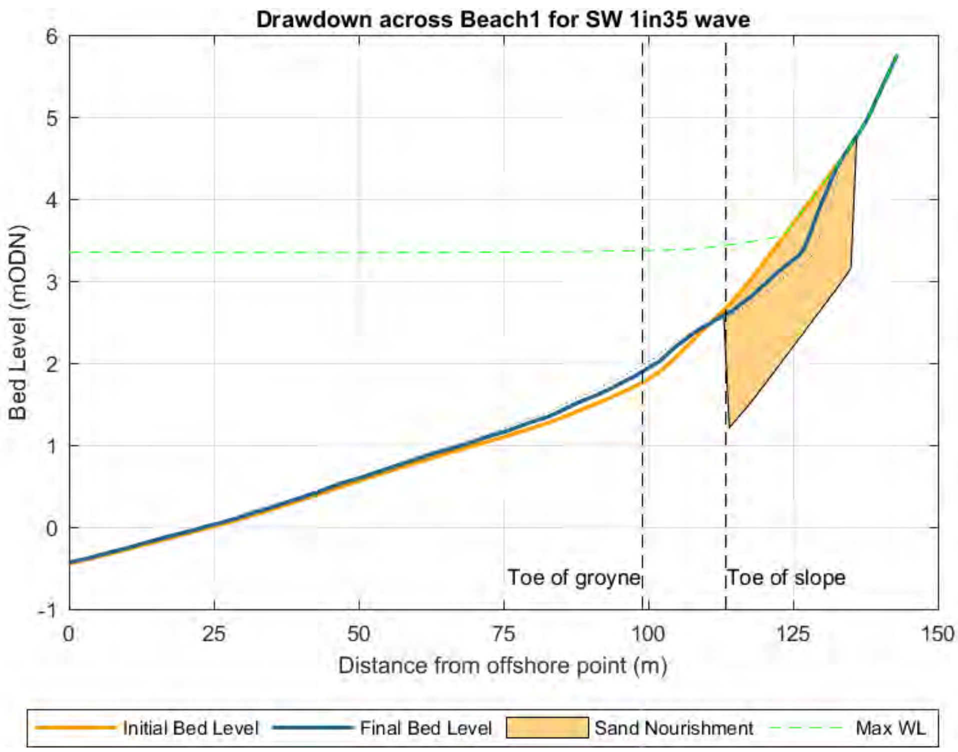

The dotted blue line shows the results for the smaller roughness length.

Figure B118. Beach drawdown on Beach 1 during 1 in 35 year wave event from the southwest

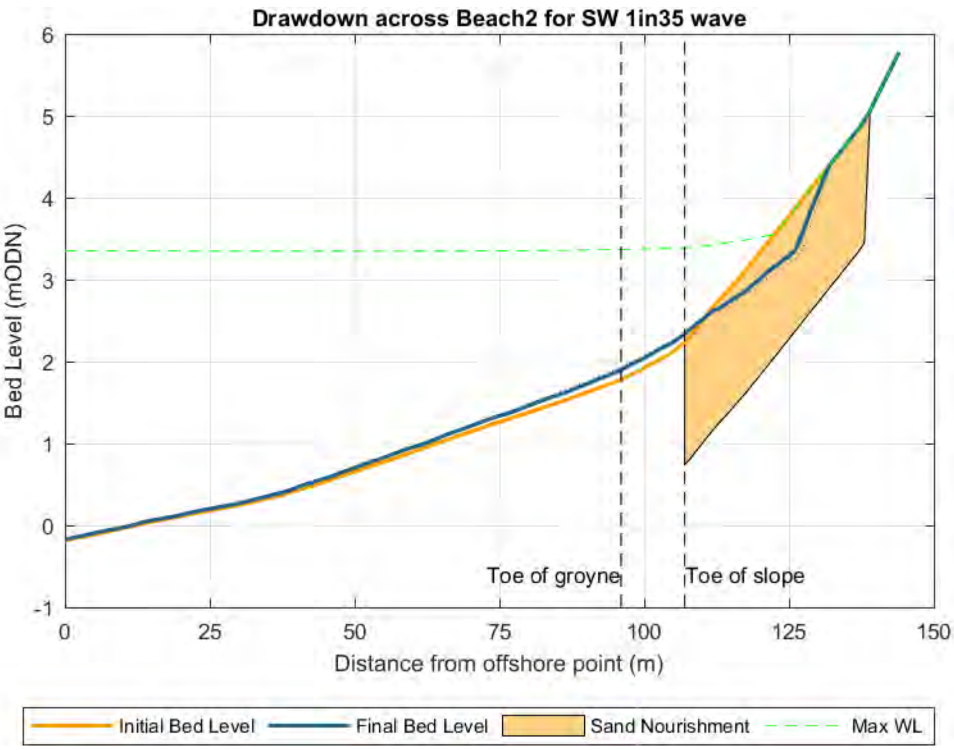

The dotted blue line shows the results for the smaller roughness length.

Figure B119. Beach drawdown on Beach 2 during 1 in 35 year wave event from the southwest

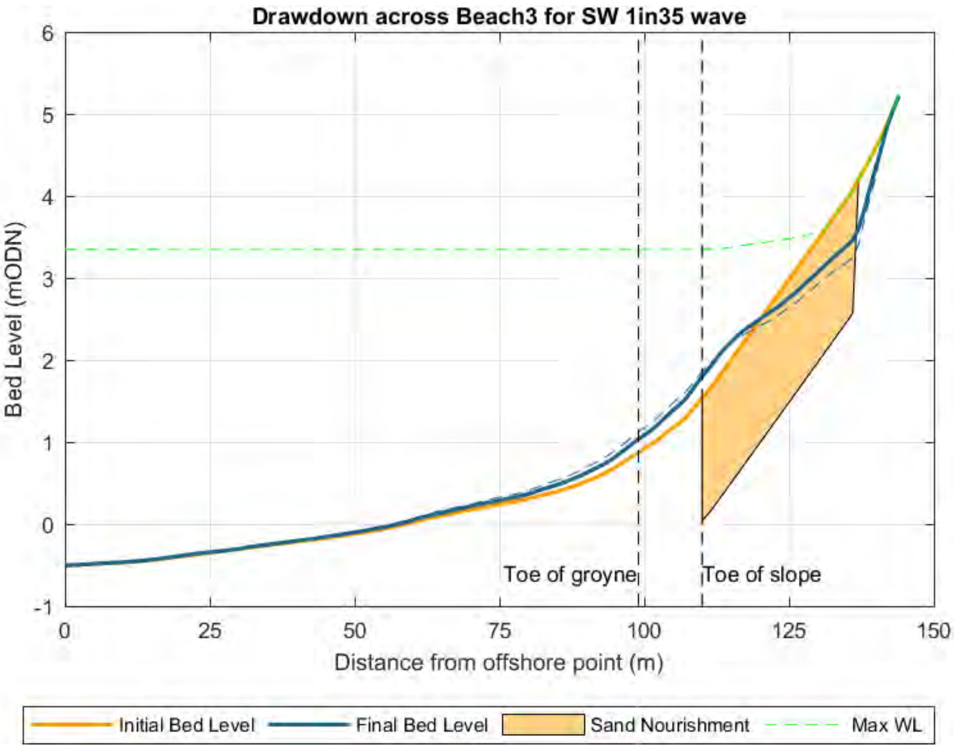

The dotted blue line shows the results for the smaller roughness length.

Figure B120. Beach drawdown on Beach 3 during 1 in 35 year wave event from the southwest

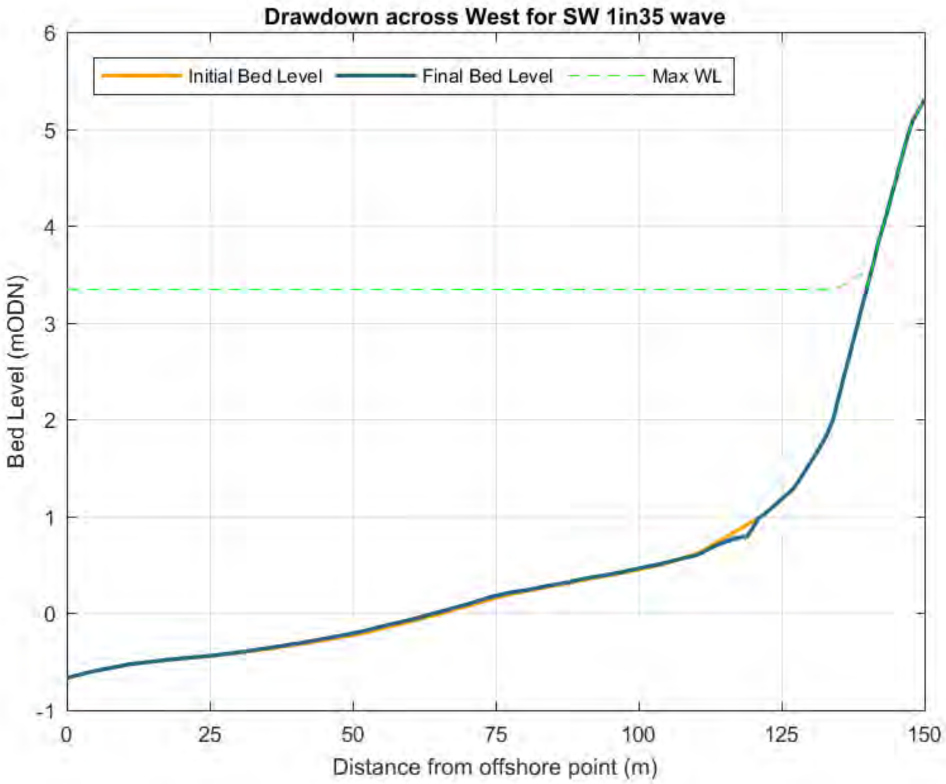

The dotted blue line shows the results for the smaller roughness length.

Figure B121. Beach drawdown on West profile during 1 in 35 year wave event from the southeast

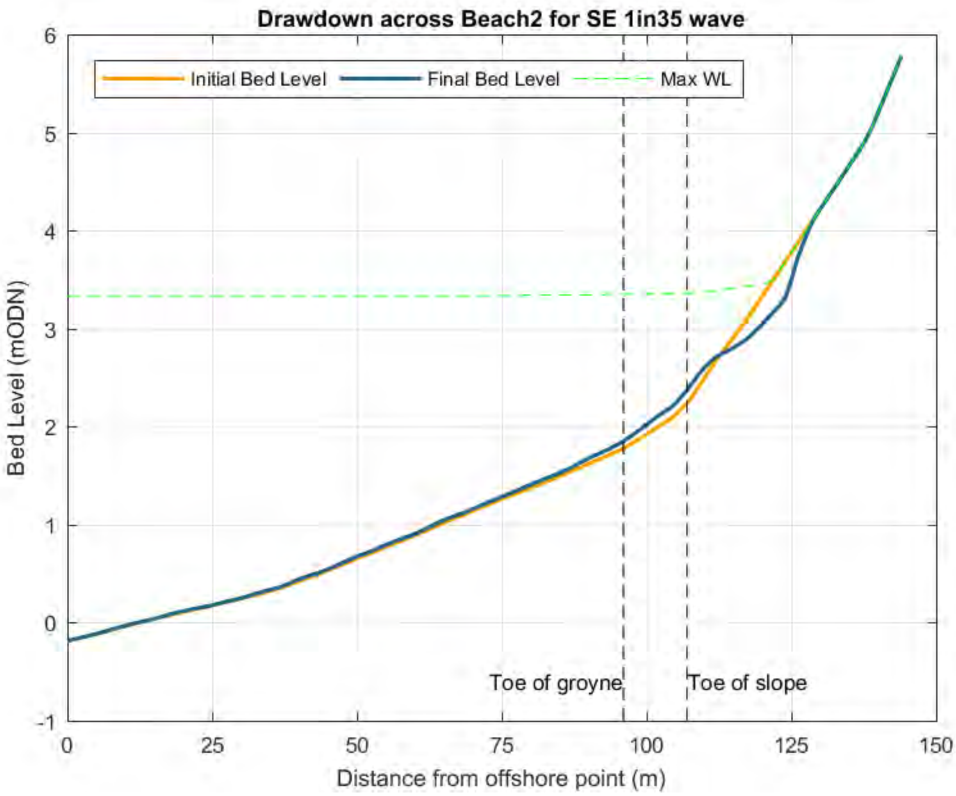

The dotted blue line shows the results for the smaller roughness length.

Figure B122. Beach drawdown on Beach 2 during 1 in 35 year wave event from the southeast

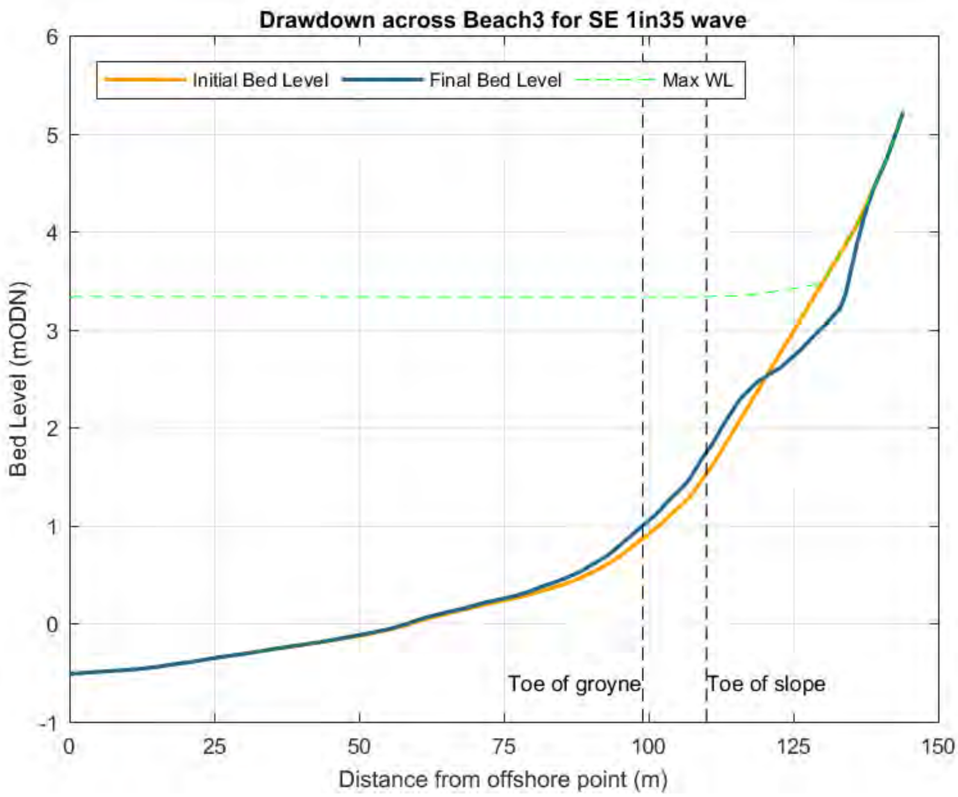

The dotted blue line shows the results for the smaller roughness length

Figure B123. Beach drawdown on Beach 3 during 1 in 35 year wave event from the southeast

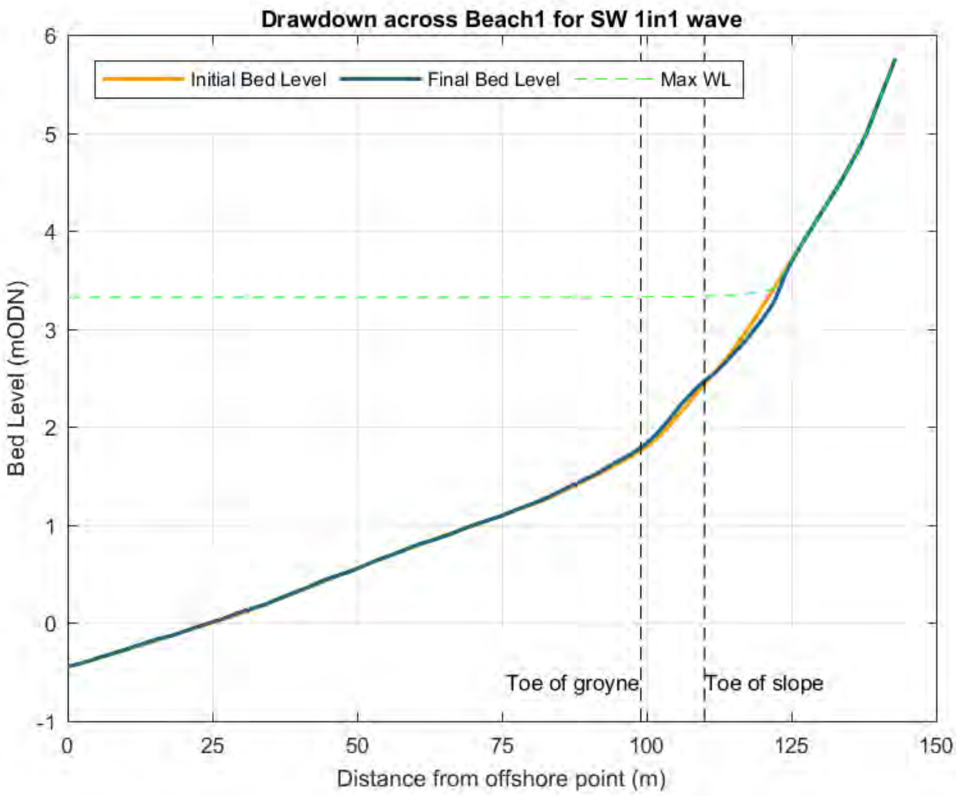

The dotted blue line shows the results for the smaller roughness length.

Figure B124. Beach drawdown on Beach 1 during 1 in 1 year wave event from the southwest

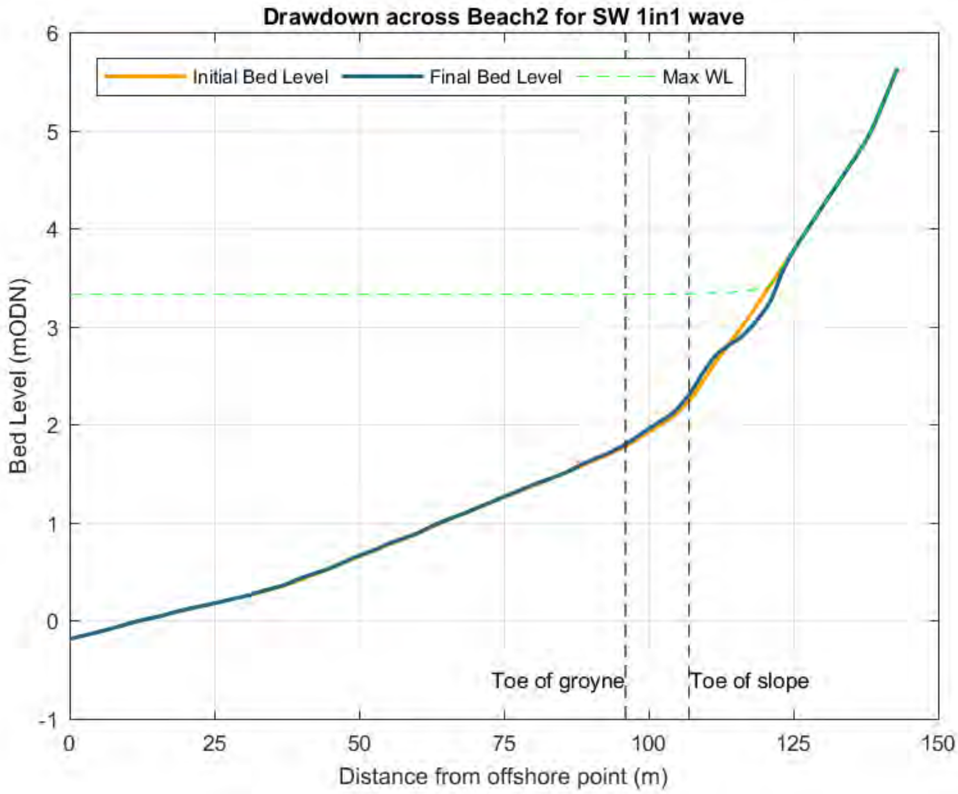

Figure B125. **Beach drawdown on Beach 2 during 1 in 1 year wave event from the southwest**

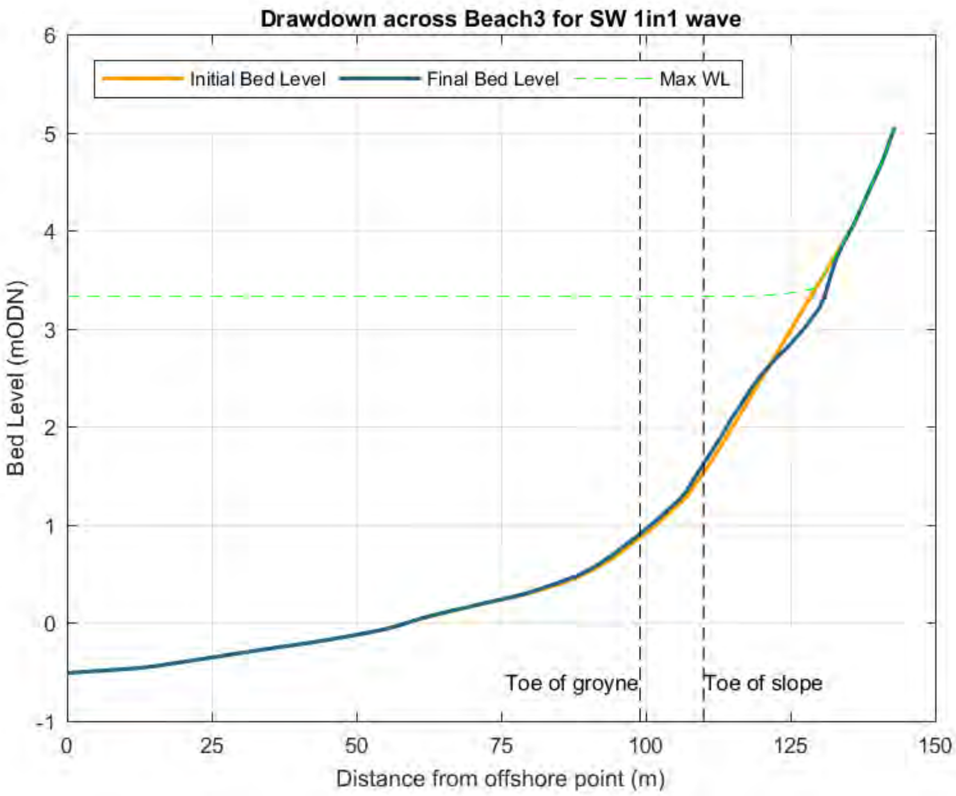

The dotted blue line shows the results for the smaller roughness length.

Figure B126. **Beach drawdown on Beach 3 during 1 in 1 year wave event from the southwest. The dotted blue line shows the results for the smaller roughness length**

Scheme 2 Sensitivity Test: 1 in 35 year Southwest

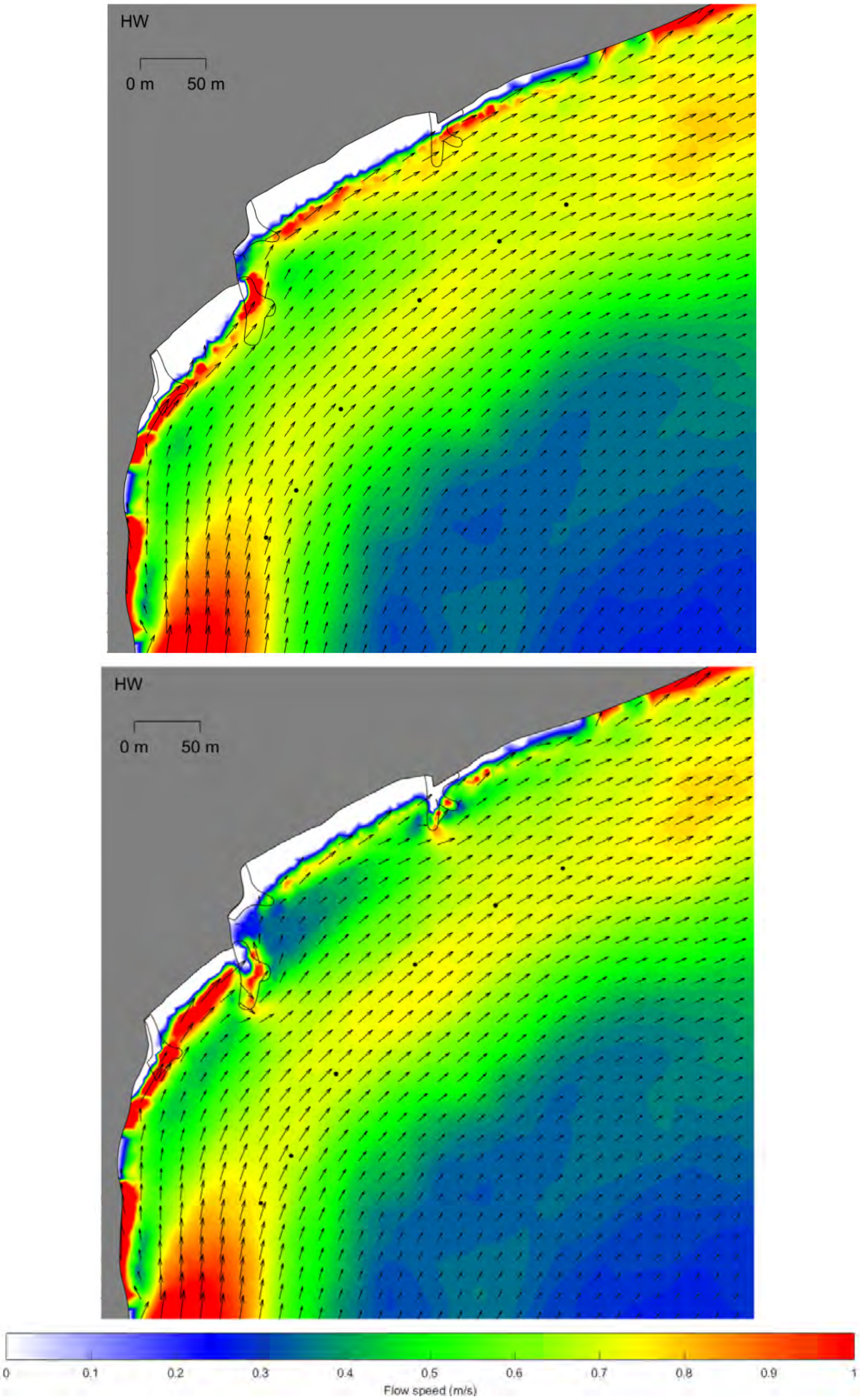

Extraction points are marked for reference but not labelled, see Figure 1 for labels.

Figure B127. Flows from the 1 in 35 wave from the SW for baseline (upper) and scheme 2 (lower)

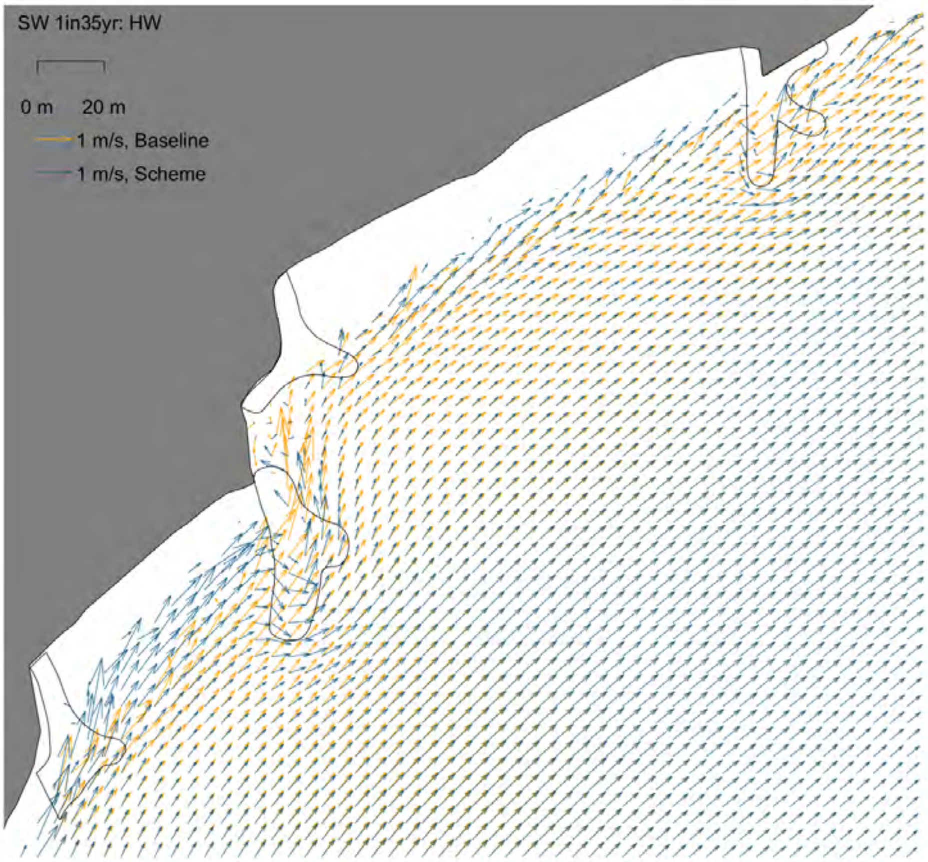

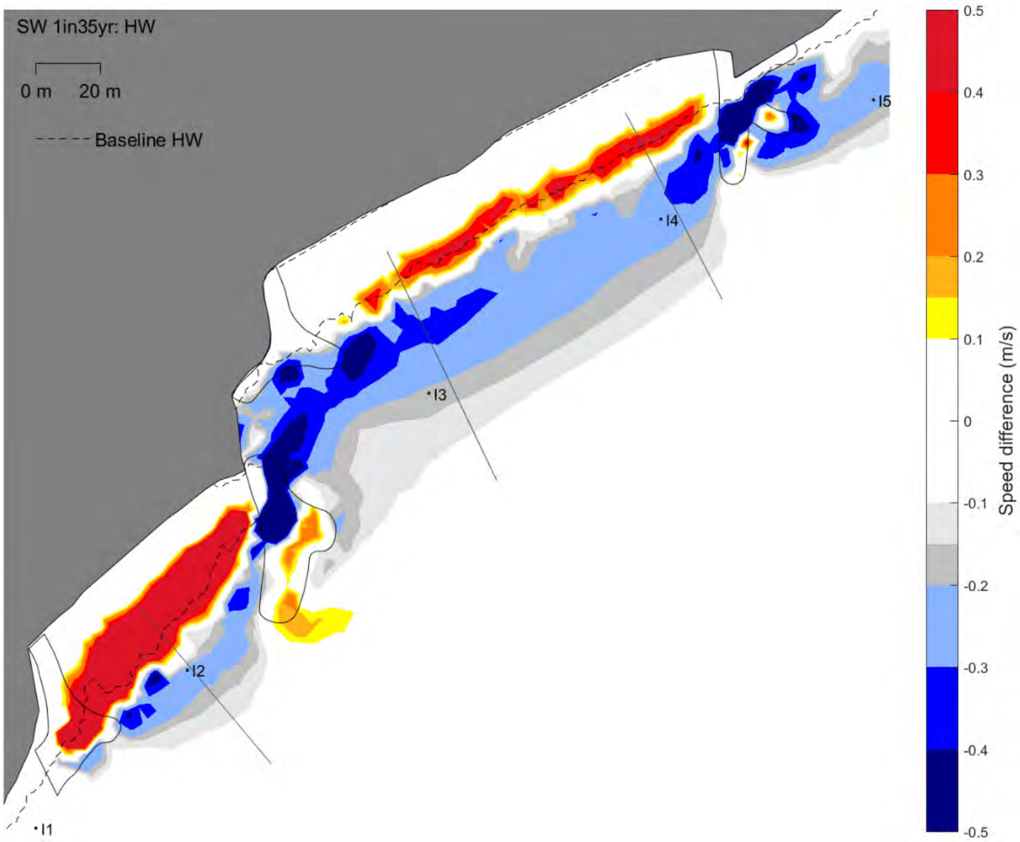

Figure B128. Baseline and Scheme 2 flows (upper) and the difference in flow (scheme 2 minus baseline) (lower) from the 1 in 35 wave from the SW

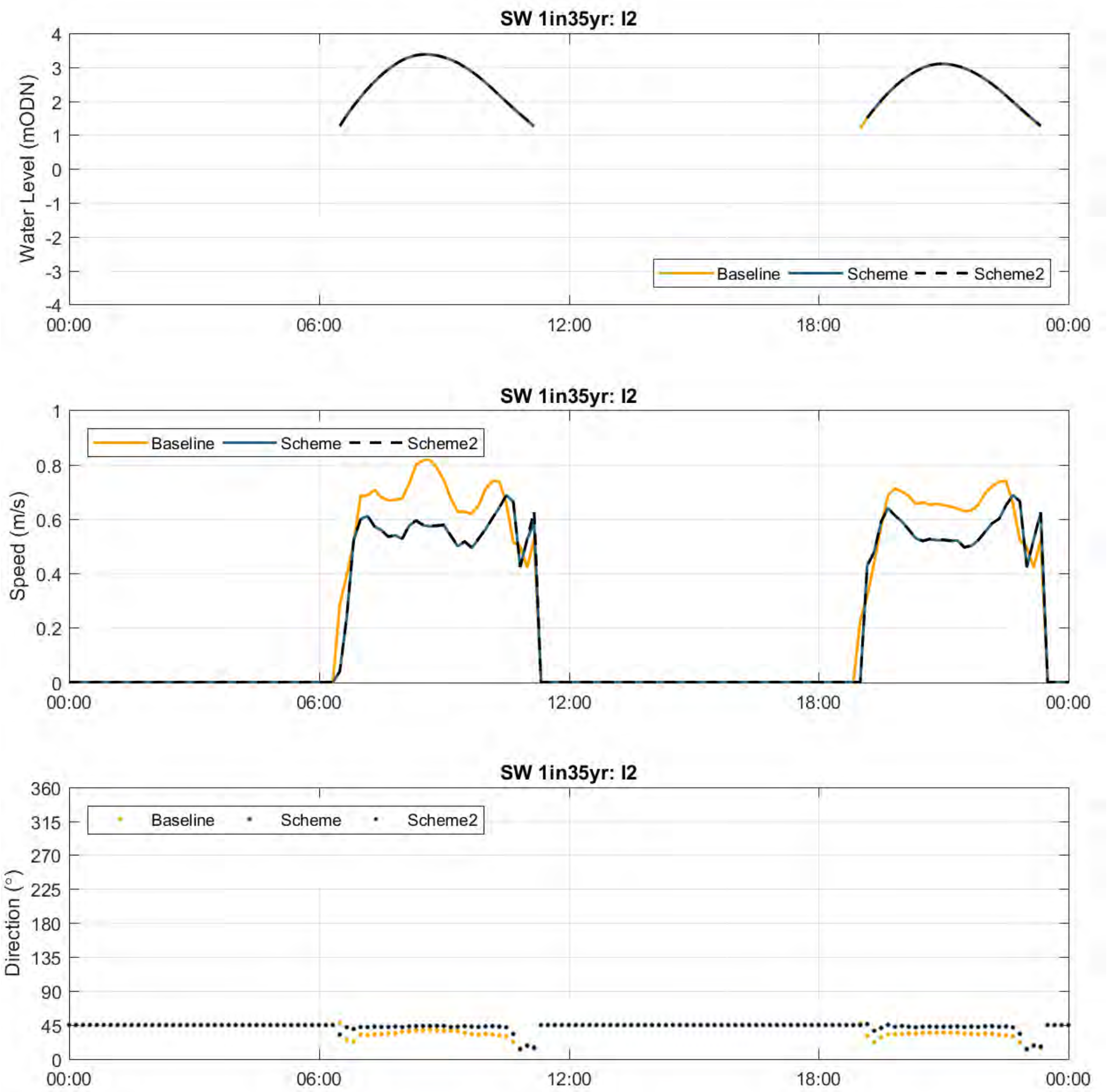

Figure B129. Time series of water level, flow speed and flow direction at I2 for the baseline and scheme runs for the 1 in 35 year wave from the SW

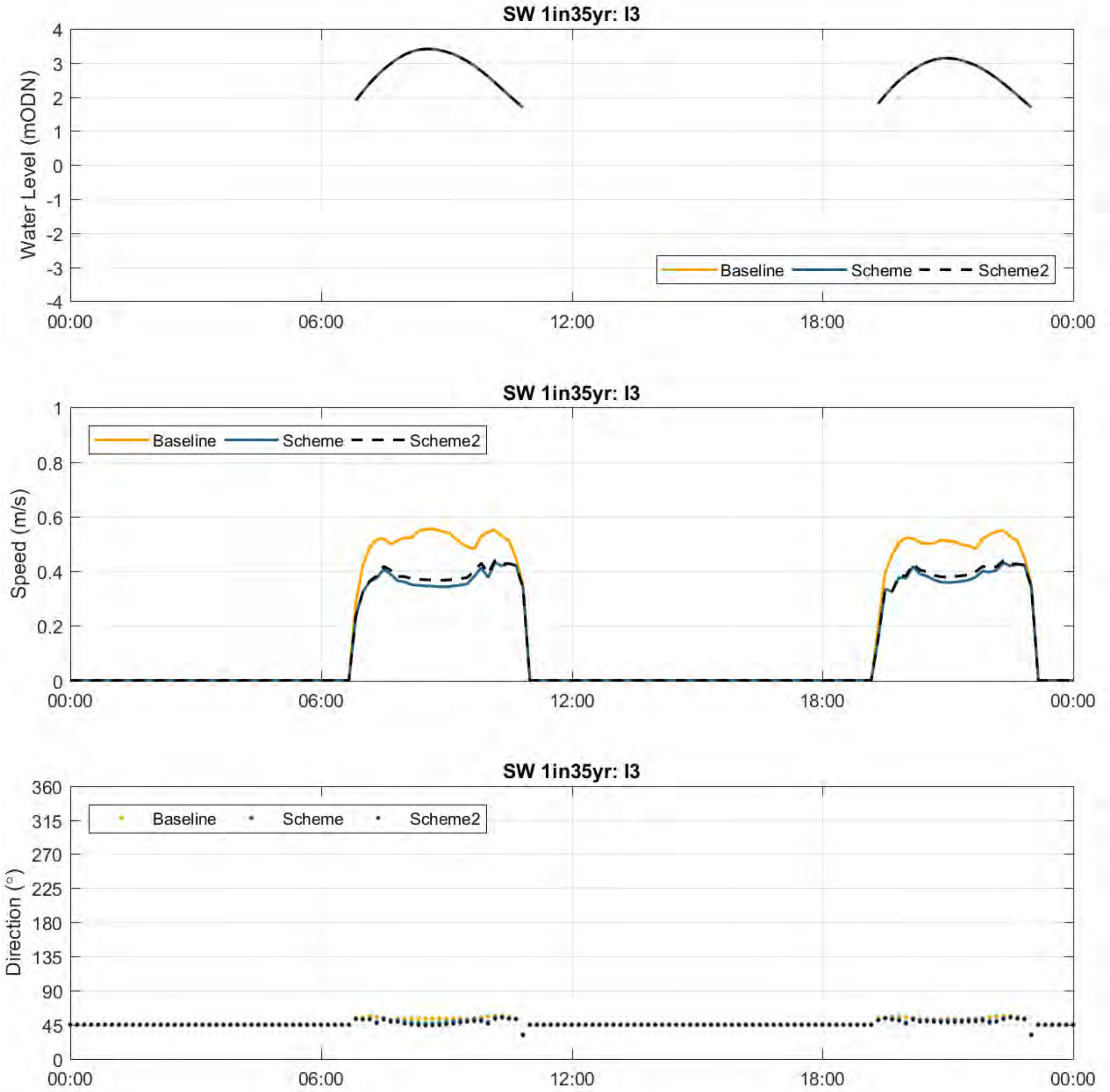

Figure B130. **Time series of water level, flow speed and flow direction at I3 for the baseline and scheme runs for the 1 in 35 year wave from the SW**

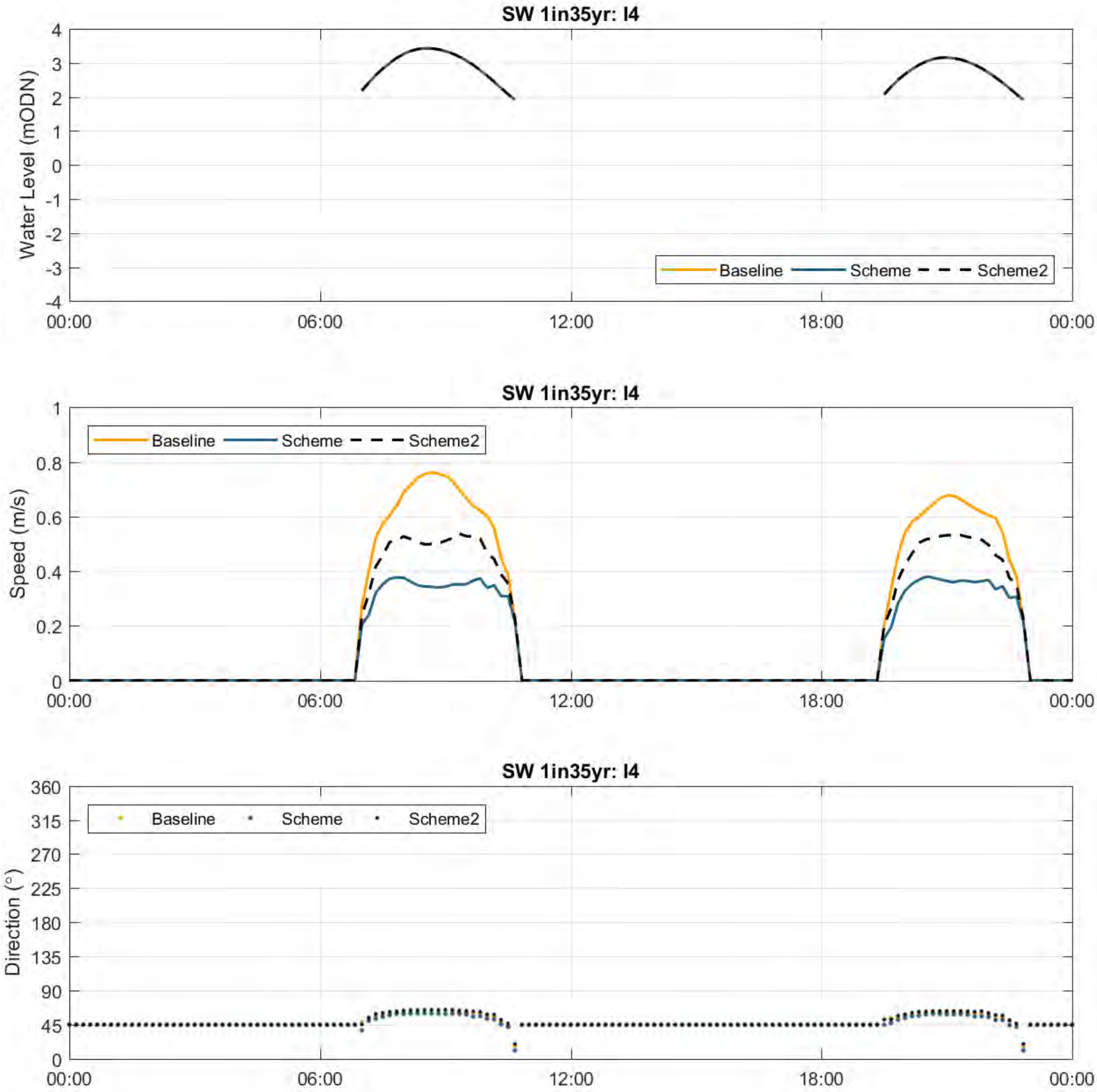

Figure B131. **Time series of water level, flow speed and flow direction at I4 for the baseline and scheme runs for the 1 in 35 year wave from the SW**

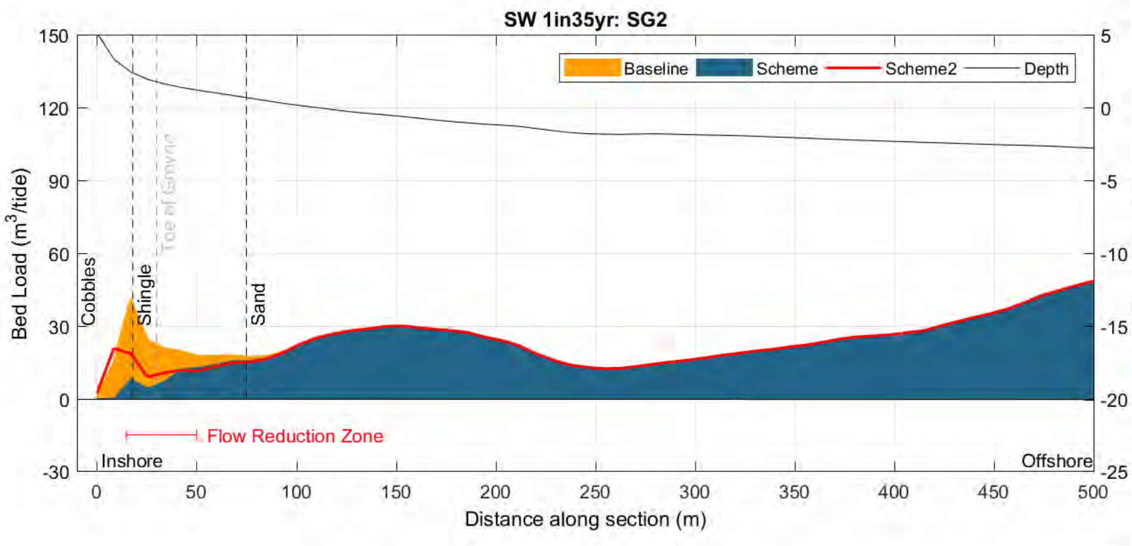

Sediment type i.e. cobbles, shingle and sand are shown for indicative purposes only.
A 0.2 mm sand has been used as the grain size in the model.

Figure B132. Sediment transport across SG2 for 1 in 35 year wave from the southwest

Scheme 2 Sensitivity Test: 1 in 35 year Southeast

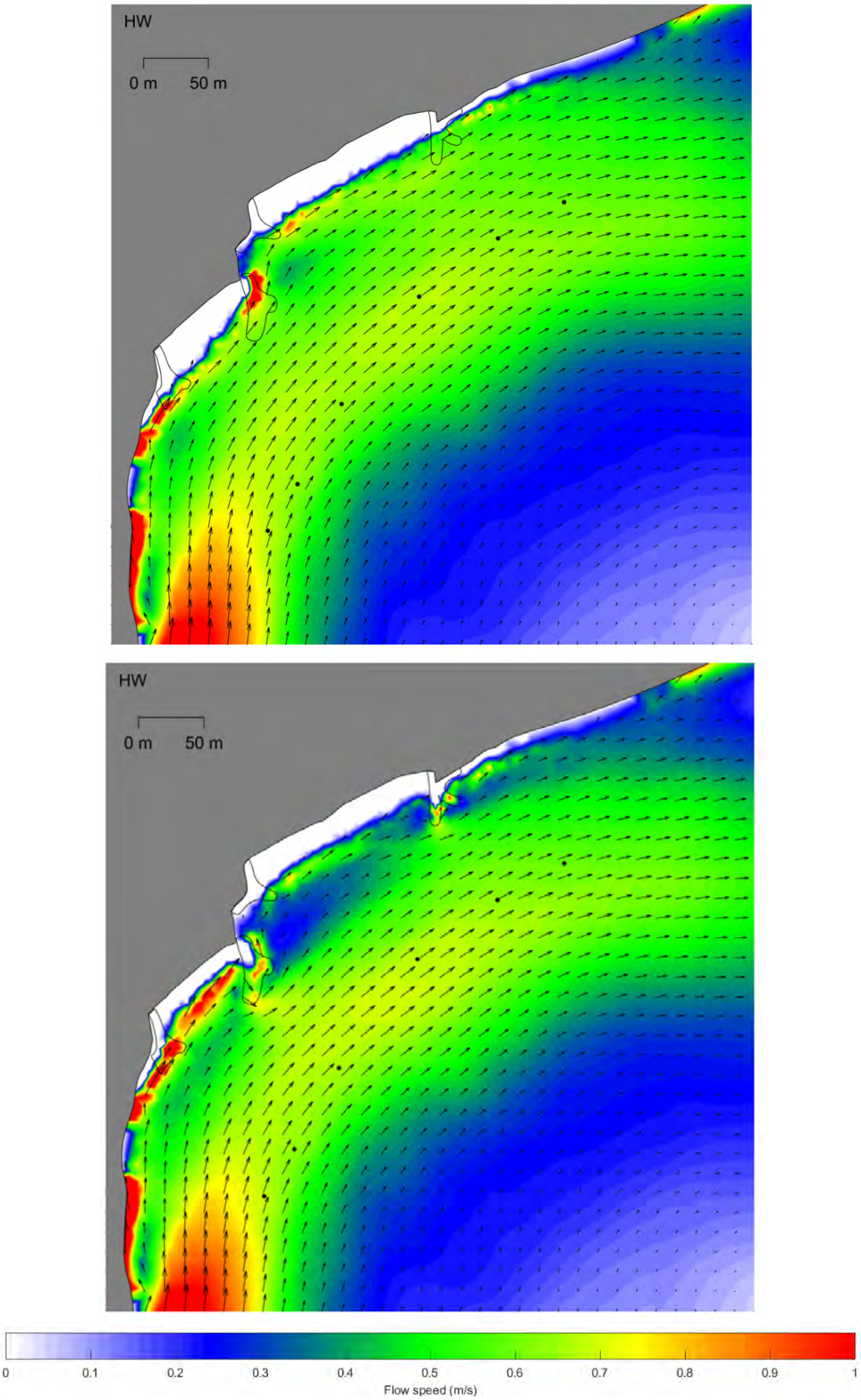

Figure B133. **Flows from the 1 in 35 wave from the SE for baseline (upper) and scheme 2 (lower). Extraction points are marked for reference but not labelled, see Figure 1 for labels**

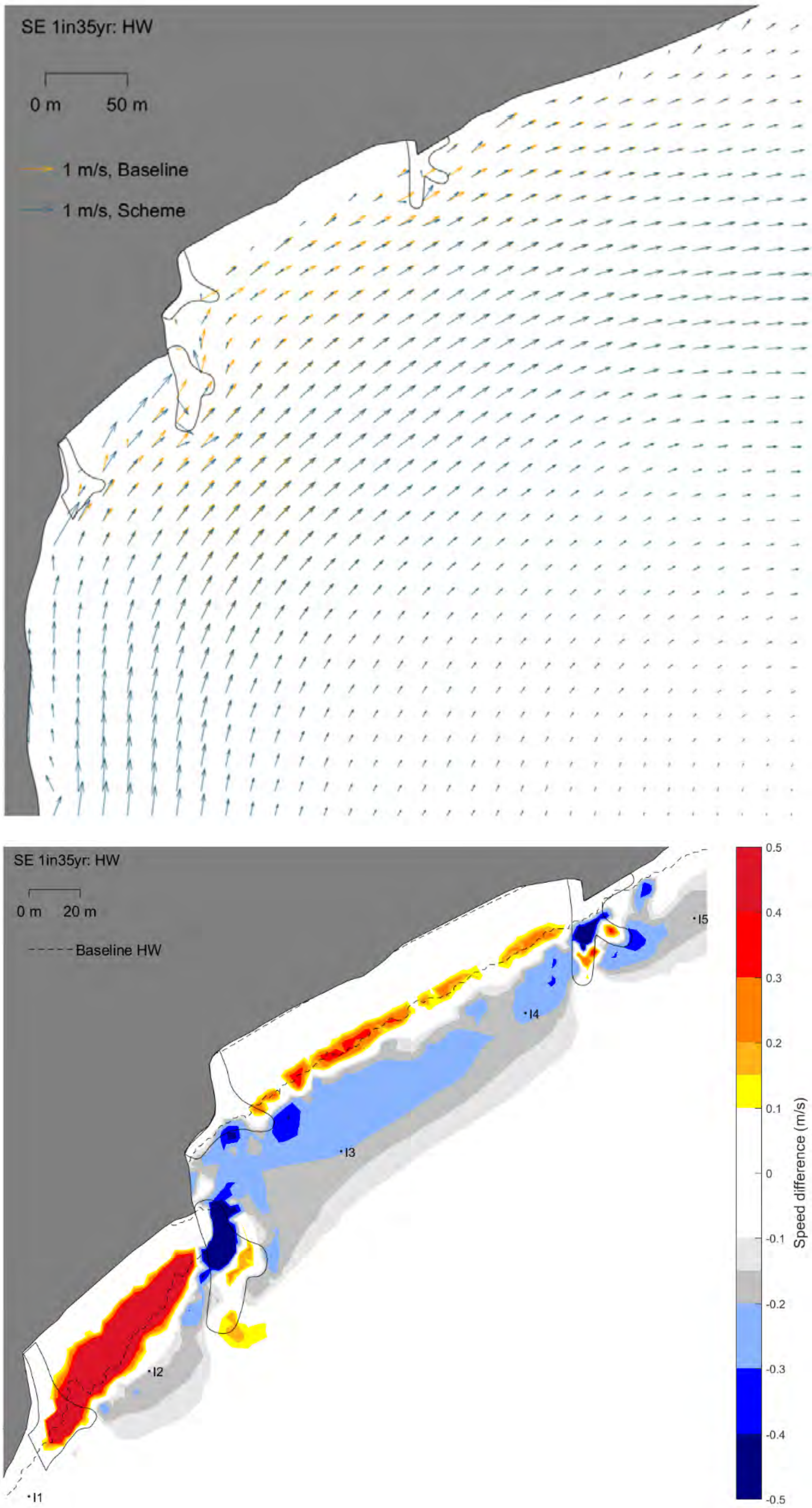

Figure B134. Baseline and Scheme 2 flows (upper) and the difference in flow (scheme 2 minus baseline) (lower) from the 1 in 35 wave from the SE

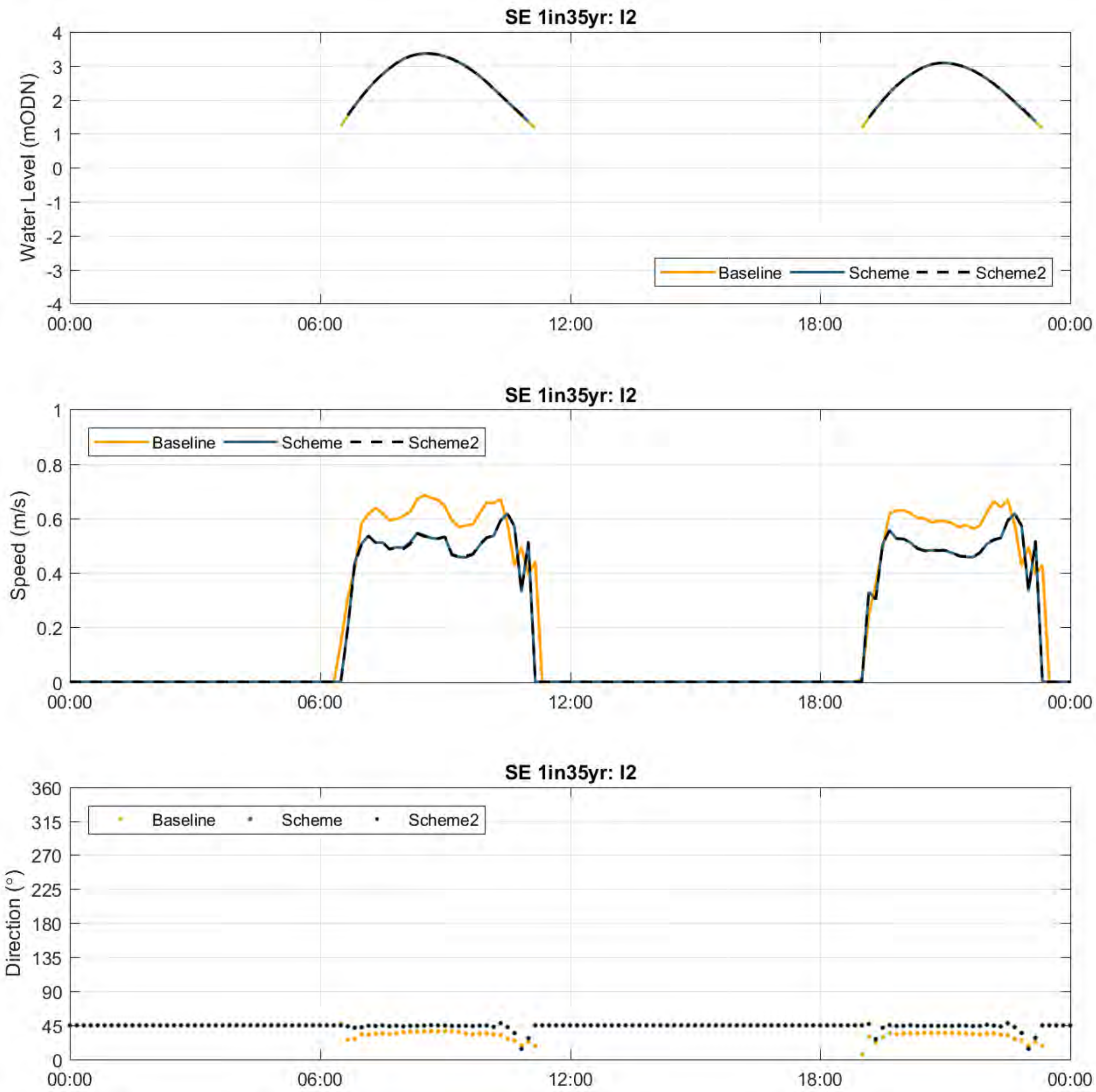

Figure B135. Time series of water level, flow speed and flow direction at I2 for the baseline and scheme runs for the 1 in 35 year wave from the SE

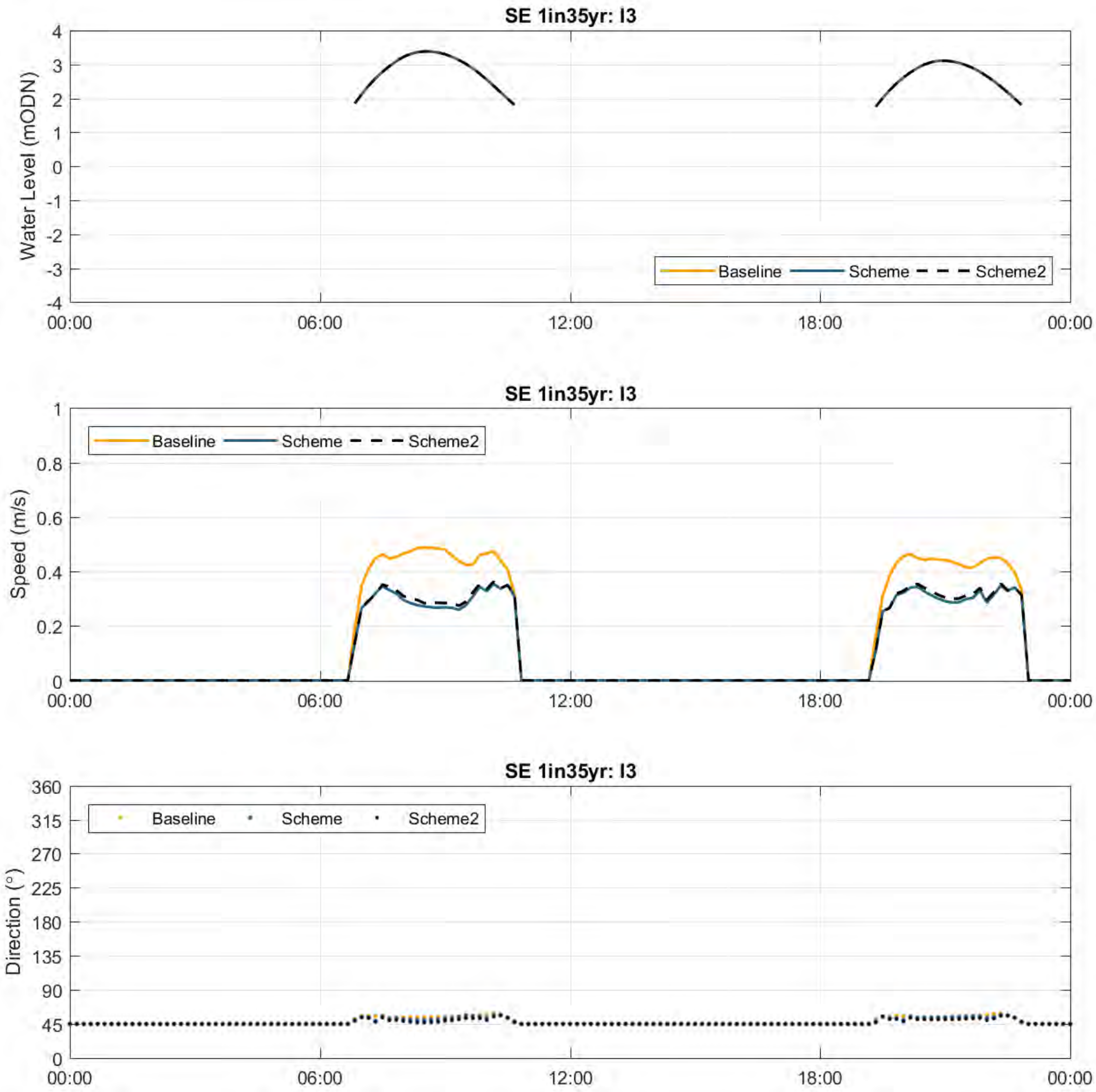

Figure B136. Time series of water level, flow speed and flow direction at I3 for the baseline and scheme runs for the 1 in 35 year wave from the SE

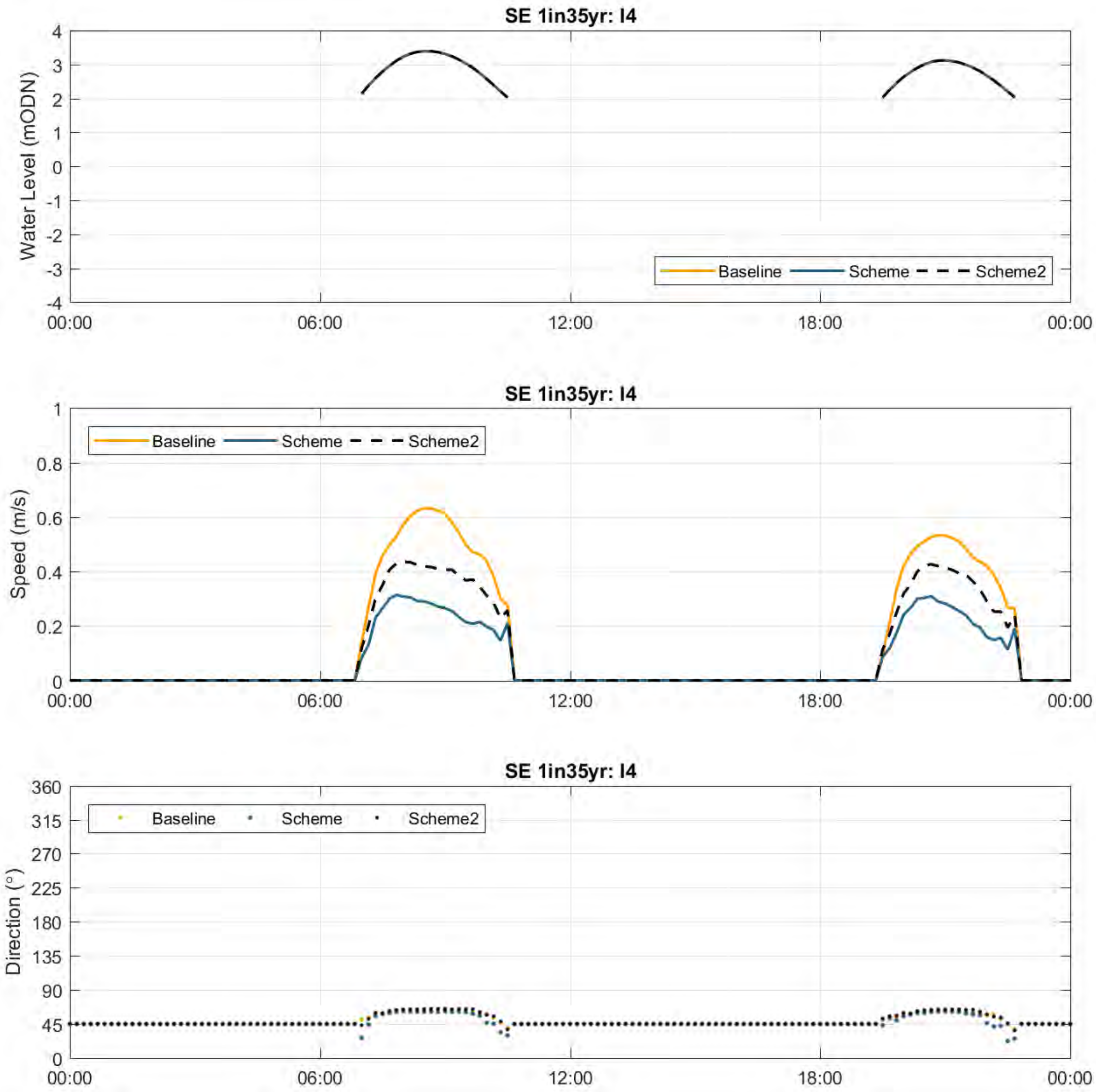

Figure B137. Time series of water level, flow speed and flow direction at I4 for the baseline and scheme runs for the 1 in 35 year wave from the SE

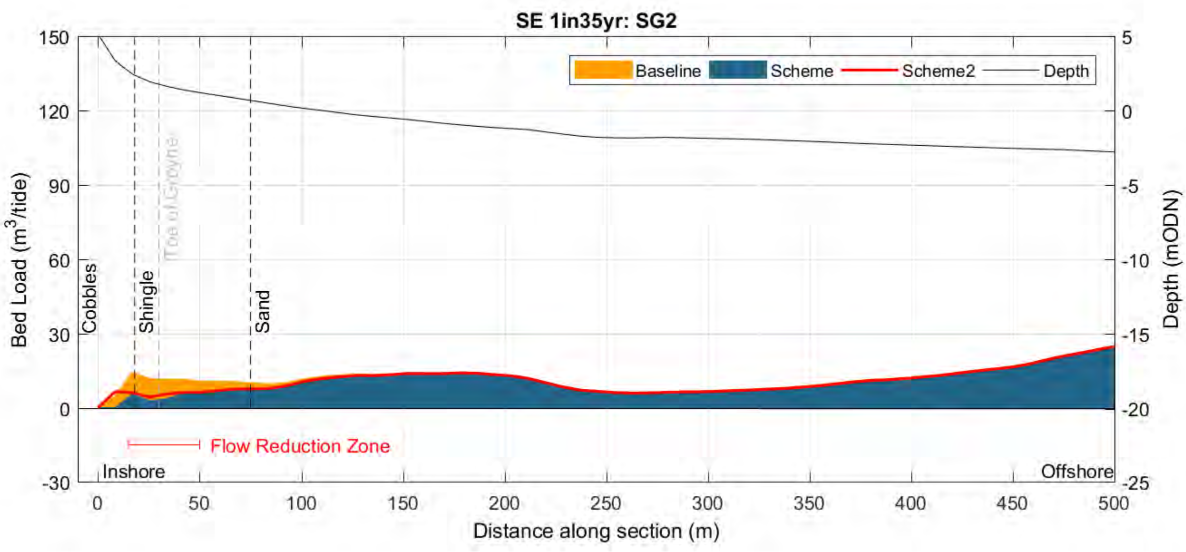

Sediment type i.e. cobbles, shingle and sand are shown for indicative purposes only.
A 0.2 mm sand has been used as the grain size in the model.

Figure B138. Sediment transport across SG2 for 1 in 35 year wave from the southeast

Contact Us

ABPmer

Quayside Suite,
Medina Chambers
Town Quay, Southampton
SO14 2AQ

T +44 (0) 23 8071 1840
F +44 (0) 23 8071 1841
E enquiries@abpmer.co.uk

www.abpmer.co.uk